Modeling, Estimation, and Control of Indoor Climate in Livestock Buildings

Ph.D. thesis

Zhuang Wu

Department of Electronic Systems
Section for Automation and Control
Aalborg University
Fredrik Bajers Vej 7, 9220 Aalborg East, Denmark

April 16^{th}, 2009

Modeling, Estimation, and Control of Indoor Climate in Livestock Buildings
Ph.D. thesis

ISBN 978-87-92328-22-9
April 2009

Copyright 2004–2009 © Zhuang Wu

This thesis was typeset using LaTeX 2$_\varepsilon$ in `report` document class.

Preface

This thesis is submitted to the Aalborg University, Denmark, in partial fulfillment of the requirements for the degree of Doctor of Philosophy (Ph.D.) in the Section of Automation and Control, Department of Electronic Systems.

The research reported in this thesis has been carried out in the period September 2004 to March 2008 under the supervision of Professor Jakob Stoustrup and Associate Professor Klaus Trangbaek from the Section of Automation and Control, Department of Electronic Systems, and Professor Per Heiselberg from the Department of Building Technology and Structure Engineering, at Aalborg University.

Aalborg University, April 2009
Zhuang Wu

Acknowledgments

I am very grateful to my supervisor, Professor Jakob Stoustrup, for giving me a rich and rewarding graduate experience. A sincerely thanks for his invaluable and inspiring guidance, encouragement and support through out my study.

I feel very grateful to Professor Per Heiselberg, for his expertise advice on hybrid ventilation systems and airflow dynamics.

I am also very grateful to Professor James. B. Rawlings during my four months staying at University of Wisconsin Madison. I strongly appreciate Jim and his research group for sharing their profound knowledge and several inspiring discussions. I will miss the priceless time spent together with them.

I am also deeply appreciating for the financial support from Center for Model Based Control (CMBC) and the project directing from the committee. Especially I would extend my gratitude to Mr. Martin Riisgaard Jensen, my industry supervisor from SKOV A/S, who has given me so much consideration in my work; Associate Professor John Bagterp Jorgensen, from Technical University of Denmark, whose constructive help provided me further understanding and realization in my research. I enjoyed hearing instructions from Professor Sten Bay Jorgensen and Mr. Jorgen K.H. Knudsen. Their wisdom and humor are so impressive.

I also would like to express my deepest gratitude to Associate Professor Klaus Trangbaek, my co-supervisor, for his professional insight and patience all the time; Brian Solberg, my office mate, for the intellectual interactions and fun conversations we had. I really appreciate Jan Jakob Jensen, the experiment lab trouble-shooter, with his knowledge on embedded software design and the students from Esbjerg, for their excellent work in Syvsten. Further more, I will say thanks to Morten Bisgard, for his great help on my Latex writing and formatting. I would express my gratitude to the support and friendship of all the staff in our section for making my three and a half year study so enjoyable.

Finally, I am grateful most of all to my parents and my husband. Their endless love and support have made it possible and all the effort worthwhile.

Abstract

Modeling, Estimation, and Control of Indoor Environment for Livestock Buildings

The main objective of this research is to design an efficient control system for the indoor climate of a large-scale partition-less livestock building, in order to maintain a healthy, comfortable and economically energy consuming indoor environment for the agricultural animals and farmers. The mathematical models are analyzed and developed based on a real scale laboratory stable, where the building is equipped with hybrid ventilation system, which mainly consists of a inlet system controlled through adjustable bottom-hanged flaps, and a exhaust unit manipulated with axial-type fans and swivel shutters. The advanced control theories are applied based on the process models, to better determine the optimal ventilation operation, increase the actuator's utilization, guarantee the pleasant indoor thermal comfort and the reasonable indoor air quality, lower cost (energy) and improve the quality (productivity).

In this thesis, a conceptual multi-zone climate model is proposed according to the knowledge about the hybrid ventilation theory. The method is to compartmentalize the building into some well-mixed macroscopic homogeneous zones, with the major emphasizes on the occupied spaces where the animals confined in. With necessary assumptions and simplifications, the dominant air flow distributions are investigated and the phenomenon of horizontal variations are well depicted. The nonlinear models for manipulators are derived from the characteristic analysis, and the parameters are identified through the time series data collected from the experiments. The comparative simulation results show reasonable agreement between theory and practice.

The designed entire control system consists of an outer feedback closed-loop dynamic controller and an inner feed-forward redundancy optimization. The dynamic control is implemented through Model Predictive Control (MPC) algorithm based on linearized time invariant state space representations. The application of moving horizon approach for estimation and regulation, accompanied with target calculation and disturbance modeling, demonstrate the significant advantages of MPC on performance improvement, tracking reference, rejecting disturbance, compensating model/plant mismatch, and naturally dealing with constraints. An auto-covariance least-square method is applied to increase the estimation quality through recovering the unknown covariances entering the system.

Energy consumption, actuator saturation and disturbances in wide spectrum of frequencies are crucial issues in designing an applicable and utilizable indoor climate control system for modern livestock buildings. The redundancy optimization is applied through exploiting the nonlinearities of the actuators to passively attenuate the high frequency disturbance (wind gust), to accommodate the limitation of the bandwidth of the closed-loop system as well as pursuit of an optimum energy solution. By assigning different weights in the objective function which is based on energy consumption considerations and the covariance of the high frequency component disturbances, the optimal control command generated from the dynamic controller are reallocated to the end effectors. This strategy enhances the resilience of the control system to disturbances beyond its bandwidth, increases the manipulators utilization efficiency, and reduces energy consumption by solving a constrained convex optimization.

Through comparative simulation results analysis, the proposed modeling and control technique is proved to be able to capture the salient of the indoor climate dynamics, refine the individual operation of manipulators, and realize the attenuation of different zonal disturbances. This technique is expected to be feasible in the similar real scale livestock buildings, and could be considered as an alternative solution to the current used decentralized PID controller. Therefore, the aim of this research is achieved.

Synopsis

Modellering, estimation, og regulering af indeklima i staldbygninger

Hovedformålet med dette forskningsarbejde er at udforme et effektiv reguleringssystem til indeklimaet i en mindre husdyrbygning uden opdelinger, med henblik på at opretholde et sundt, komfortabelt og økonomisk energiforbrugende indendørs miljø for dyrene og landmændene. De matematiske modeller analyseres og udvikles baseret på en fuldskala laboratore-stald, hvor bygningen er udstyret med et hybridt ventilationssystem, som hovedsagelig består af et indsugningssystem styret via justerbare bundhængte ventiler, og en udsugningsenhed aktueret af aksial-type ventilatorer og lukkeventil. Avanceret reguleringsteori baseret på proces-modeller anvendes for bedre at kunne afgøre den optimale ventilationsdrift, øge aktuator's udnyttelse, garantere en rimelig indendørs termisk komfort og indendørs luftkvalitet, lavere omkostninger (energi) og forbedre kvaliteten (produktivitet).

I denne afhandling, foreslås en begrebsmæssig multi-zone klima model baseret på teori om hybrid ventilation. Den metode baserer sig på at inddele bygningen i nogle godt blandede makroskopisk homogene zoner med de særlig fokus på de områder, hvor dyrenes færd er begrænset til. Den dominerende luftindsugningsdistribution undersøgt og fænomenet horisontale variationer er beskrevet, med nødvendige antagelser og forenklinger. De ikke-lineære modeller for manipulatorer er udledt fra karakteristik-analyse, og de tilhørende parametre er identificeret gennem tidsrække data indsamlet fra forsøgene. Sammenlignende simuleringsresultater viser rimelig overensstemmelse mellem teori og praksis.

Det samlede reguleringssystem består af en ydre feedback dynamisk controller og en indre feed-forward optimering, der benytter aktuator-redundancs. Dimensionering af den dynamiske kontrol er gennemført ud fra Model Predictive Control (MPC) algoritmer baseret på lineariserede tidsinvariante tilstands repræsentationer. Anvendelsen af glidende-horisont tilgangen til estimering og regulering, ledsaget af target beregning og forstyrrelsesmodellering, demonstrerer betydelige fordele af MPC mht. performance-forbedringer, reference-følge, undertrykkelse af forstyrrelser, kompensation for model / system afvigelser, og naturligvis håndtering af begrænsninger. En auto-kovarians mindste kvadraters metode anvendes til at øge estimationskvaliteten ved at genskabe de ukendt kovarianser af forstyrrelser, der kommer ind i systemet.

Energiforbrug, aktuatormætning og forstyrrelser i et bredt spektrum af frekvenser er afgørende spørgsmål i forbindelse med udformningen af et praktisk og implementerbar-levant reguleringssystem for indeklimaetstyring af moderne husdyrbrug bygninger. Optimeringsmetoderne baseret på aktuator redundans bygger på en udnyttelse af aktuatorernes ikke-lineære karakteristikker til passivt at dæmpe høj-frekvente forstyrrelser (vindstød), idet der tages hensyn til begrænsning af båndbredden af det lukkede kredsløb. Dette sker i afvejning med at finde en energimæssigt hensigtsmæssig løsning. Ved at tildele forskellige vægte i en kostfunktion, som er baseret på energiforbrugsbetragtninger og kovariansen af de højfrekvente komponenter af forstyrrelserne, bliver det optimale styresignal genereret fra det dynamiske regulator omfordelt til udsugningsaktuatorerne. Denne strategi øger reguleringssystemets evne til at undertrykke forstyrrelser ud over sin båndbredde, øger manipulatorernes udnyttelseseffektivitet, og reducerer energiforbruget ved at løse et konvekst optimeringsproblem med sidebetingelser.

Gennem komparativ analyse af simuleringsresultater, har de foreslåede modelleringsog reguleringsmetoder vist sig at være i stand til at indfange den væsentligste del af indeklimaets dynamik, finjustere den individuelle brug af manipulatorer og realisere dæmpningen af forstyrrelser i forskellige zoner af stalden. Denne teknik forventes at være muligt i lignende fuldskala staldbygninger, og kan derfor anses som en alternativ løsning til den aktuelle, hvor der anvendes decentrale PID regulatorer. Derfor er målet med dette forskningsprojekt opnået.

Contents

List of Figures

List of Tables

Nomenclature

Acronyms and Abbreviations

TNZ	Thermal Neutral Zone
LCT	Lower Critical Temperature
UCT	Upper Critical Temperature
ECT	Evaporative Critical Temperature
NPL	Neutral Pressure Level
TC	Thermal Comfort
IAQ	Indoor Air Quality
AMV	Active Mixing Volume
CFD	Computer Fluid Dynamics
CMZCM	Conceptual Multi-Zone Climate Model
ARX	Auto Regressive with eXogenous input
ARMAX	Auto Regressive Moving Average with eXogenous input
LTI	Linear Time Invariant
SISO	Single Input Single Output
MIMO	Multiple Input Multiple Output
PID	Proportional Integral Derivation
PIP	Proportional Integral Plus
LQ	Linear Quadratic
MPC	Model Predictive Control
MHE	Moving Horizon Estimation
ALS	Auto-covariance Least-Square
COTS	Commercial Off The Shelf system
ACM	Auto-Covariance Matrix

System Modeling Nomenclature

T	Temperature
$\dot{Q}$	Heat transfer rate

C_r	Air Contaminant gas concentration
g	Gravitational acceleration
M	Air mass
A	Area
V	Volume
H	Height
U	Heat transfer coefficient of building construction material
c_p	Heat capacity at constant pressure
ρ	Density
$\dot{m}$	Mass flow rate
$\dot{q}$	Air volume flow rate
$\dot{n}$	Air exchange rate
$\dot{G}$	Contaminant gas generation rate from animals
M_a	Animal activity level
C_d	Discharge coefficient of inlet valve system
P	Pressure
ΔP	Pressure difference
P_i	Internal Pressure at reference height
C_p	Surface pressure coefficient
V_{ref}	Wind speed at reference level
V_{volt}	Supplied voltage to the axial fan
θ	Opening angle of swivel shutter

Subscript

i	Indoor zonal numbers
o	Outdoor
in	Input to the building
out	Output from the building
$water$	Water flow in the heating pipe
$wall$	Building envelope
$transmission$	Heat transfer through convection, conduction and radiation
$source$	Production or generation source
$inlet$	Inlet valve system
fan	The exhaust unit
w	Windward
l	Leeward

Part I

Extended Summary

This part gives a comprehensive overview of the entire project. The content is organized logically, from the motivation of the research, through the literature review, the methodology description, and the solution analysis, to the conclusions and perspective. This part displays the exposition of the major achieved results and represents the main contributions of this thesis.

Chapter 1

Introduction

This chapter presents the background and motivation of this research, provides an overview on the indoor climate comfort for living animal, virtually depicts the assessment for animal comfort zones with experimental data, and describes the working principle and application of modern hybrid ventilation strategy. The previous work on the environmental control for livestock buildings are investigated. The objectives of the research are summarized. The thesis outline is given in the end.

1.1 Background and Motivation

Healthy, comfortable, and economically energy consuming housing for happy agricultural animals and the farmers, is always the popular topic and major purpose for designers and producers. There are many factors that influence the health and productivity of those animals, including temperature, humidity, air movement and contaminant level, physical activity, bedding condition, body mass, group size and so on. The change of the livestock housing condition - the indoor climate, is of particular importance for the animal's well-being and production performances. Effective and efficient ventilation control system plays crucial role on providing a comfort indoor environment which could enhance voluntary feed intake, alleviate thermal strain and humidity, as well as maintain an acceptable indoor air quality. Failure to provide the adequate environment will reduce profitability, growth rate and development, poorer feed conversion, and increase disease, condemnation and mortality, and eventually affect the animal product quality.

In Denmark, Skov A/S (founded back in 1954 by the Danish brothers Kristen and Kjeld Skov), an international company for developing and manufacturing the ventilation equipments and climate control system for pig and poultry stables, in collaboration with Aalborg University, has funded research into improving the welfare of farming animals as well as the farmers, and increasing the energy consumption efficiency.

1.2 Overview of Animal Comfort Indoor Climate

A proper indoor climate is indispensable in maintaining an optimum animal performances, and it is required for all ages and classes of living stock who live in the highly constrained farming environment. Analysis from [der Hel *et al.*, 1986],[Rinaldo *et al.*, 2000],[Beattie *et al.*, 2000] illustrate the direct influence of the indoor environment on the animals. This section is dedicated to defining the animal's comfort zones which will be the objective and set-point of the environmental control system.

The understanding of the needs of the animals can be derived from physiological, physical and behavioral studies ([Baldwin and Ingram, 1967], [Ingram and Legge, 1974], [Geers *et al.*, 1991], [Xin, 1999]). The conventional way of assessing the thermal comfort is by the Thermo-Neutral Zone (TNZ), which is defined as the zone of environmental temperature in which metabolic rate is at a minimum and from that follows that the Lower (LCT) and Upper Critical Temperature (UCT), respectively. These are the lowest and the highest environment temperatures at which the metabolic rate remains minimal ([Ingram, 1974]). When the air temperature begins to rise from LCT, pigs endeavor to remove heat by increasing their breathing rate and will eventually begin panting. The temperature at which evaporative heat loss increases noticeably occurs is known as the Evaporative Critical Temperature (ECT). At temperatures above ECT, pigs are out of their comfort zone and will further increase respiration to maximize evaporative heat loss which is at UCT. When UCT is exceeded, body temperature increases and as a result so does the metabolic rate and if the heat exposure continues for a prolonged period, body temperature reaches fatal levels and the animal succumbs to the heat stress ([Tauson *et al.*, 1998]). Therefore, the thermal comfort zones are the temperature ranges in which animals feels most comfortable, so does the zones for air contaminant concentration that provides acceptable air quality for animals. These comfort zones vary in relation to the animal's species, the growth stage, the environmental as well as housing conditions. [Pedersen and Sallvik, 1984] and [Poulsen and Pedersen, 2005] have derived some references for different livestock from combination of small-scale laboratory experiments and statical analysis which are mainly based on the Northern Europe climatic conditions.

Except the complex environmental requirement for the living animals, the animals are likely have significant and numerous effects on its physical surroundings. The variation of the animal heat production and contaminant gas generation, according to the living indoor climate and external weather condition are discussed in [Poulsen and Pedersen, 2005], [Pedersen and Sallvik, 2002], [Wachenfelt *et al.*, 2001] and [Milgen *et al.*, 1997]. [Pedersen and Sallvik, 2002] provides the diurnal rhythm of animal heat production values for latent heat as well as sensible heat.

In order to visualize the connection between the indoor climate and the animal well-being, to have further realization about the definition and assessment of animal living comfort zone, a series of example figures as shown in Fig. 1.1 reflect the influence of indoor climate such as the temperature, humidity and ventilation rate, on the growing pig's feeding status, water consumption and body mass gain. Approximately 8000 data were

collected in a real scale pig stable during September, 2004 at Research Center Bygholm in Horsens city, Denmark. The stable is equipped with roof inlet hybrid ventilation system regulated by a classical PI controller. The approximate thermal comfort zone for growers

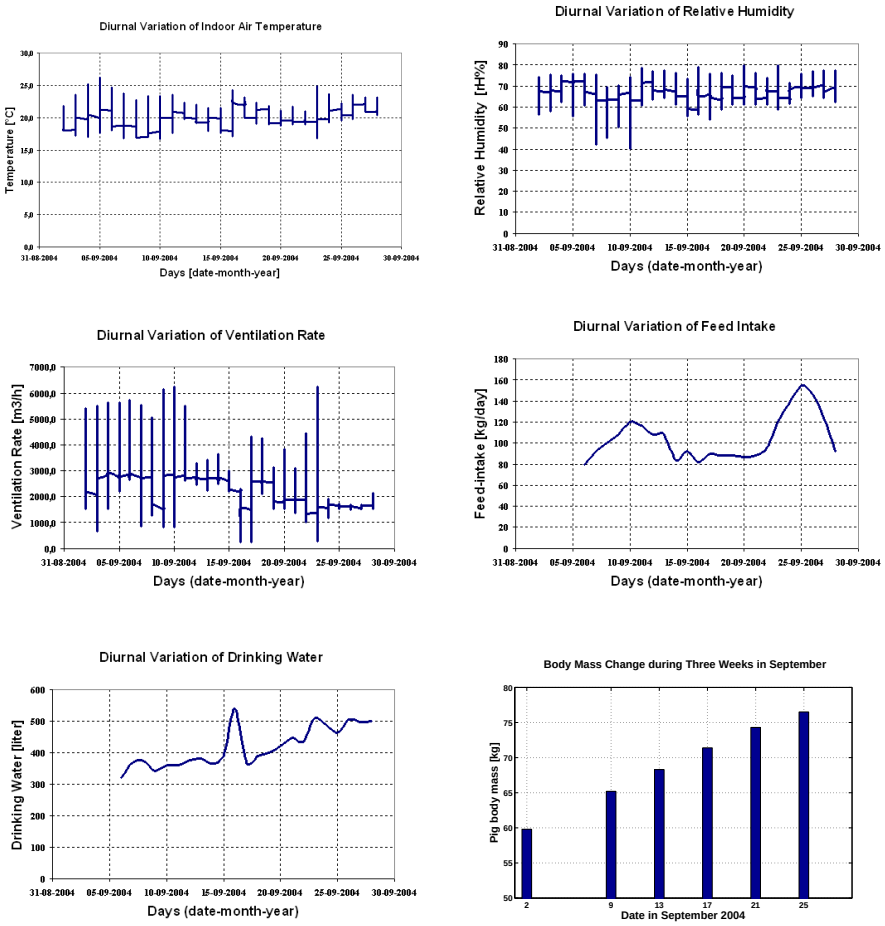

Figure 1.1: The Diurnal Variation of Indoor Climate and Pig Behavior and Production

is from 19 to 22 ^{o}C and the comfort relative humidity is from 60% to 80% with the ventilation rate from 1000 to 3500 m^3/h. On average, the growers are raised within a relatively comfort living environment and have positive production tendency, except during September, from 12th to 22th, the growers are sick with arthritis which directly leads to the low feed intake and increase of water consumption.

Concluded from the above analysis, farming animals' well-being are directly related with their living indoor climate, and ventilation is one of the most important tools for controlling the livestock building indoor climate. Even though, the current used climate control system is performing relatively fine, the oscillated system response can not be ignored, and its weakness on maintaining system stability, rejecting large disturbances and saving energy are obvious. Therefore, a more reliable and optimal control system deserves to be investigated.

1.3 Hybrid Ventilation for Livestock Buildings

For livestock, ventilation is concerned with comfort interpreted through animal welfare, behavior and health, and most importantly, it is concerned with qualifiable factors such as conversion ratio, growth rate and mortality ([Carpenter, 1981]). The purpose of livestock ventilation system is to provide oxygen, remove moisture and odors, prevent heat buildup and dilute air-contained disease organisms. Through controlling the air exchange rate and air flow pattern, the optimum indoor environment conditions, such as the Thermal Comfort (TC) defined by temperature and Indoor Air Quality (IAQ) characterized by contaminant gas concentration are guaranteed within the ventilated structure.

Traditionally, ventilation is accomplished by either natural or mechanical means, and for many years, these two methods have been developed separately. Natural ventilation makes the most use of the natural forces such as the thermal buoyancy and wind, and the effectiveness greatly depends on the design process. Its passiveness in use appears limited and the uncertainties in performance results in risk. Mechanical ventilation could be designed independent of the building and have flexibility for modification. The primary disadvantage of mechanical ventilation is the energy consumption cost. Hybrid ventilation, which has access to both the natural and mechanical ventilation in one system, being as an comprehensive and efficient ventilation strategy have been widely used for livestock buildings. Hybrid ventilation system utilizes and combines the best features of each system in a two-mode system where the operating mode varies according to the season and within individual days. Therefore, the hybrid ventilation system is able to fulfill the requirements on indoor environmental performance, the increasing need for energy savings and sustainable development by optimizing the balance between indoor air quality, thermal comfort, energy efficiency and outdoor environmental impact [Heiselberg, 2004b].

The main hybrid ventilation principles are catalogued with three: Natural and mechanical ventilation which is based on two fully autonomous systems where the control strategy switches between two modes; Fan-assisted natural ventilation which combines a natural ventilation with an extract fan to generate pressure difference (low pressure) to meet the increased demands or during periods of weak natural driving forces; Stack- and Wind-assisted mechanical ventilation where the natural driving forces account for a considerable part of the necessary pressure. The currently researched ventilation strategy in the livestock stable is the fan assisted natural (low pressure) ventilation, which uses the exhaust fans to mechanically generate a relatively low internal pressure, by pulling out

warm indoor air and inhaling outdoor fresh air into the building in order to create demand air exchange rate. Depending on the local climate, building tradition and installation condition, there are four types in use: wall inlet; roof inlet; diffuse; and tunnel ventilation as depicted in Fig. 1.2

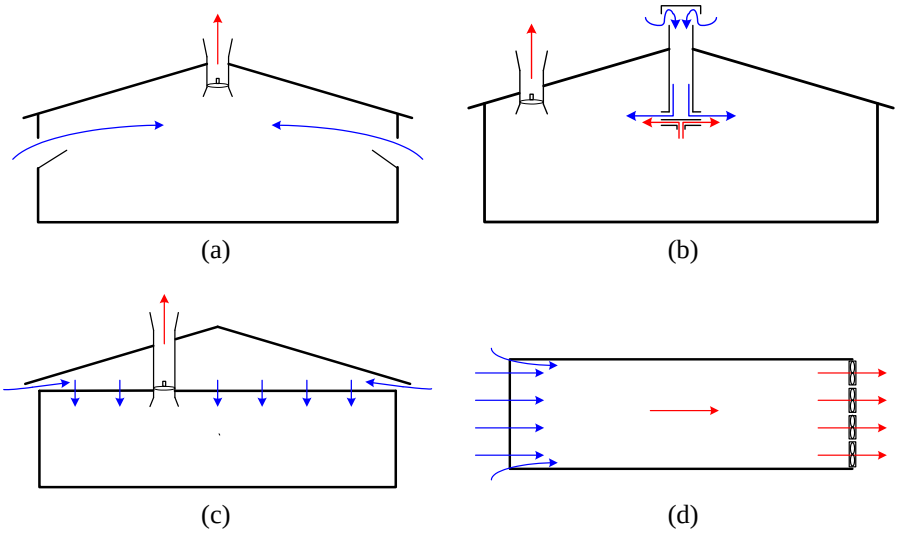

Figure 1.2: The Negative Pressure Ventilation Type Normally Used in Livestock Buildings (a) Wall Inlet (b) Roof Inlet (c) Diffuse Ceiling (d) Tunnel

During winter, ventilation must remove the excess contaminant gas in order to provide a good indoor air quality inside the livestock stable; while during summer, the main reasons for ventilation are for cooling. Humidity is necessary to be removed as well depending on the indoor climate conditions. [Jessen, 2007] provides analysis of the possible ventilation scenarios in mild weather countries such as Denmark.

1.4 Previous Work on Livestock Environmental Control

Due to the similarity on the indoor environmental condition and the principle of ventilation control, the general modeling/control methods applied in horticulture is also studied.

Environmental control is of substantial importance in maintaining good indoor climate. Several discussions and researches applications involving environmental control of animal building or greenhouse have been performed ([Barber and Feddes, 1994], [Zhang and Barber, 1995], [Timmons *et al.*, 1995], [Tchamitchian and Tantau, 1996], [Chao and Gates, 1996], [Linker *et al.*, 1997]). Recent research leads to the application of more sophisticated methods for the design of the control for indoor climate systems. It has

been shown, e.g. the fuzzy logic control strategy ([Chao *et al.*, 2000] and [Gates *et al.*, 2001]); the model-based Proportional-Integral-Plus (PIP) control scheme ([Taylor *et al.*, 2004]). Mainly concerning the disturbance rejection, uncertainties compensation and reference tracking, [Soldatos *et al.*, 2005], [Daskalov *et al.*, 2006] and [Arvanitis *et al.*, 2007] proposed a robust adaptive nonlinear control algorithms consisting of the feedback and feed-forward linearization, the nonlinear robust compensator and the adaptive integral control. Their results show advantages compared with conventional Multiple Input and Multiple Output (MIMO) PID controller, but its ability for handling constraints don't appear obvious. The Model-based Predictive Control (MPC) algorithm, with more efficiency and flexibility in dealing with system nonlinearities and constraints, together with its economic optimal operation, has increasingly attracted attentions in application for the agricultural buildings. The relevant experiences with MPC have been reported such as in [Moor and Berckmans, 1996a], [Nielsen and Madsen, 1996], [Brecht *et al.*, 2005] and [Wagenberg *et al.*, 2005]. However, the discussion in most of the research works are mainly on applying MPC scheme for single zone model, that in fact the advantages of MPC in dealing with MIMO system and handling constraints are not clearly demonstrated, and the output performance are far enough from the climate requirement for a large scale livestock building.

Most of the studies on analysis and control of the environment inside the animal house have been based on some models. These models include the first principle model which is based on the physical laws of the process, and the grey/black box model which is based on the analysis of the input-output data of the process or the transfer function with some unknown parameters. Some static physical models are proposed in [Schauberger *et al.*, 2000] and [Pedersen *et al.*, 1998]. These models are not applicable for control purpose due to the lack of considering time variant dynamics. A thorough understanding of the dynamics of the thermal environment is needed for the selection of optimized equipments and control strategies. A simulation model is presented which describes the transient thermal responses within a ventilated livestock building in [Y. Zhang, 1992]. [Panagakis and Axaopoulos, 2004] compared the steady state and dynamic model based on the experiment in a swine building and proved the accuracy and efficiency of applying the transient method. [Nielsen and Madsen, 1998] proposes a linear continuous time stochastic model for the heat dynamics of a greenhouse which takes the global radiation, the outdoor air temperature and the heat supply as input variables. A black box model is developed in [Cunha *et al.*, 1997] with a second order dynamic parametric ARX model which is described as a linear system around a operating point. In [Daskalov, 1997], a Dynamic discrete Auto-Regressive Moving Average (ARMAX) models is derived by using recursive prediction error (maximum-likelihood and least-square) method. Other approach has been considered in [Ferreira *et al.*, 2002] where a neural network based model of the climate in greenhouse has been explored. However, the mathematical models developed in the above research works have primarily focused on the simple heat balance based on the single zone method which assumes that the entire building is a homogeneous well-mixed zone where the internal temperature and contaminant gas concentration level are

uniformly distributed. Obviously, for the large enclosures like livestock buildings, this simplification for single zone modeling will lead to a significant deviation from the optimal environmental control. As has been pointed in [Heiselberg, 1996], the design under this simplification suffers both from over-sizing of equipment and from excessive energy requirement, which are usually caused by the lack of knowledge and guidance on the airflow pattern, air flow rate inside the occupied zones, distribution of animals, installation of actuators and so on. There have been some researches which have recognized the imperfect mixing problems in ventilated airspace of agricultural buildings and proposed some approaches, for example, [Moor and Berckmans, 1996b] developed a second order grey box model for the micro-climate in an imperfectly mixing forced ventilated agriculture building with the Active Mixing Volume (AMV) concept, which involves the classical theory of heat transfer into the connection of well-mixed zone and surrounding environment. [Young *et al.*, 2000], [L. Price, 1999], [K. Janssens, 2004] and [Brecht *et al.*, 2005] presented further analysis and implementation on the Data-Based Mechanistic (DBM) modeling approach which is interpreted as a AMV model and is applied to data obtained from ventilation experiments carried out on a laboratory test chamber designed to represent a scale model of a livestock building, at the Katholieke Universiteit Leuven. Even though, the AMV concept is for the imperfect mixing space, it is still applied for single mixing zone, and for solving the problem of large airspace with multiple mixing zones, the ability of this methodology is unclear.

The proposed modeling method in this thesis is more advantageous not only on taking into consideration of the variation of climate variable (temperature etc.) within the large space agricultural building, but also on its simplicity and feasibility for further industry application and academic research. The designed control scheme is advanced with high potential on improving performance of indoor global/local climate, increasing the efficiency of ventilation system, and optimizing the energy consumption for multi-variable dynamic system.

1.5 Objectives

The main objective of this thesis is to investigate the modeling and control methodology applied for the modern livestock hybrid ventilation system. At the beginning, the focus is mainly on the developing a mathematical model which can capture the significant phenomenon of indoor climate, for example, the stratification and horizontal variation of temperature/contaminant gas concentration, the dominant air flow interaction and distribution, and the major dynamic characteristic within a large-scale livestock building. The developed model should be sufficient and accurate, but also simple and applicable for future complex control purposes. Followed by the completion of system modeling, designing an advanced control system which allows for determining the demand ventilation rate and air flow pattern, improving the performance of indoor climate, increasing the utilization of actuators, and optimizing the energy consumption, becomes the most innovative part of this work and proves the most significant improvement. The result of this

research is expected to be an alternative solution for the current used decentralized PID controller. Fig. 1.3 provides an graphical aids for readers to understand the entire idea of this research thoroughly and clearly.

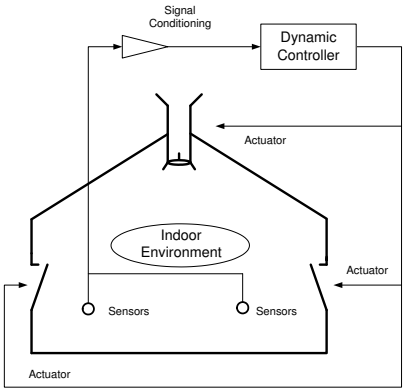

Figure 1.3: The Function Diagram of Livestock Building Indoor Environment Control

1.6 Thesis Outline

The thesis is organized with three major parts: Extended Summary, Contributed Papers and Appendixes. The Extended Summary part provides an comprehensive overview of the achieved major work and fulfilled implementations in a condensed way. The Contributed Papers part consists of six papers which have been published and accepted by the international conferences. In this part, the most important contributions are described and the amount of progress gained during the past three and a half years is displayed. Each paper presented in this thesis has been reproduced based on the original paper, under the conditions of the copyright agreement with the corresponding institutions/organizations. The Appendixes part is a supplementary part, which contains the related work including the formulation and evolvement of equations and matrices in modeling and control process.

Part I Extended Summary :

Chapter 1 Introduction gives the background and motivation of this research. Graphical demonstrations on the topic of thermal comfort and indoor air quality, and the application of modern hybrid ventilation systems are given. The

previous work on environmental control for livestock buildings and the prediction methods are summarized. The objective and the outline of this thesis is presented.

Chapter 2 System Modeling and Verification overviews the whole procedure of developing and verifying the system models for the livestock ventilation systems and associated indoor climate. The validation results manifest the sufficiency and applicability of the developed models for prediction and control purposes.

Chapter 3 Indoor Climate Control emphasizes the control strategy design and performance optimization. The algorithm is stated from both the theoretical point of view and the practical application. The simulation results show the potential of proposed method in realizing the ambitions of improving animal living environment, lowering energy consumption and increasing efficiency of asset utilization.

Chapter 4 Conclusions named the major contributions of the thesis in modeling and control design. Conclusion and perspective are discussed and summarized.

Part II Contributed Papers :

Chapter 5 [Wu *et al.*, 2005]: Modeling and Control of Livestock Ventilation Systems and Indoor Environments, published in the Proceedings of the 26^{th} Air Infiltration and Ventilation Center (AIVC) Conference: in Relation to the Energy Performance of Buildings, pages 335 - 340, 2005.

In this paper, the conceptual multi-zone modeling approach is first proposed, and applied for indoor environment prediction in livestock building. The Linear Quadratic (LQ) optimal control technique is used for this nonlinear multivariable system. The simulation results show the promising perspectives and are prepared for the future design of advanced control strategy.

Chapter 6 [Wu *et al.*, 2006]: Model Predictive Control of the Hybrid Ventilation for Livestock, published in the Proceedings of the 45^{th} IEEE Conference on Decision and Control (CDC), pages 1460 - 1465, 2006.

In this paper, the principle of Model Predictive Control (MPC) is introduced and implemented through the Multi-Parametric Toolbox. The nonlinear process model is linearized, combined and transformed into a state space representation. The Kalman Filter estimation and control system is structured, and the advantages of applying MPC algorithm is demonstrated.

Chapter 7 [Wu *et al.*, 2007b]: Model Predictive Control of Thermal Comfort and Indoor Air Quality in Livestock Stable, published in the Proceedings of the IEEE European Control Conference (ECC), pages 4746 - 4751, 2007.

In this paper, an off-set free control algorithm comprised of target calculation, receding horizon regulation and disturbance modeling is presented. The multiple objectives optimization is implemented for Thermal Comfort (TC) and indoor air quality (IAQ). The actuator constraints and output limitation are take into account.

Chapter 8 [Wu *et al.*, 2007a]: Application of Auto-covariance Least - Squares Method for Model Predictive Control of Hybrid Ventilation in Livestock Stable, published in the Proceedings of the 26^{th} IEEE American Control Conference (ACC), pages 3630 - 3635, 2007.

This paper primarily focuses on the application of a newly introduced auto-covariance least - squares method to recover the unknown noise covariances, determine adaptively the filter gain, for the purpose of increasing the estimation quality. The comparison of simulation results show the advantages of this method in improving process behavior, reducing output variances, and compensating the un-measured disturbances or the model/plant mismatch.

Chapter 9 [Wu *et al.*, 2008b]: Moving Horizon Estimation and Control of Livestock Ventilation Systems and Indoor Climate, published in the Proceedings of the 17^{th} Triennial Event of International Federation of Automatic Control (IFAC) World Congress, 2008.

The content of this paper provides an overview of the entire control strategy, proves the feasibility of using the on-line linear and nonlinear dynamic optimization scheme in moving horizon estimation and control together with actuator redundancy, addresses the superior advantages of the proposed methods in handling constraints, increasing actuator's utilization efficiency and saving energy.

Chapter 10 [Wu *et al.*, 2008a]: Parameter Estimation of Dynamic Multi-zone Models for Livestock Indoor Climate Control, published in the Proceedings of the 29^{th} Air Infiltration and Ventilation Center (AIVC) Conference: Advanced Building Ventilation and Environmental Technology for Addressing Climate Change Issues, 2008.

This paper presents the verification of the parameters which are employed in the process models. The assumption and simplification about the zonal interaction is further investigated. The comparative simulation results show good agreement between theory and practice.

Part III Appendixes :

Appendix A Multi-zone Climate and Ventilation Equipment Model Equations contains the full equations of the multi-zone indoor climate model and ventilation component model in process of carrying out simulation, linearization, coupling and combination. Model scaling is described.

Appendix B Matrices for Estimation and Control provides the evolvement of matrices used for dynamic optimization in estimation and control.

Chapter 2

System Modeling and Verification

Indoor climate model of the livestock building is essential for improving environmental performance and control efficiency. Therefore, before connecting to the control system designing phase, our research focus is mainly on the process modeling. A survey on the existed approaches for predicting the indoor temperature/concentration distribution and stratification for large partition-less building is given. A full-scale livestock building located in Syvsten Denmark, for the purpose of making laboratory experiments is described. A new multi-zone modeling concept for indoor climate involving the thermal comfort and indoor air quality is proposed and the model is developed based on a energy balance equation. The significant parameters employed in the system models are described and identified. The relevant assumptions and simplifications are provided. Finally, a conclusion is given at the end of this Chapter.

2.1 Modeling Methodology

2.1.1 Method Introduction

For livestock, the alleviation of thermal strain and the maintenance of a good indoor air quality, significantly depend on the measurement and control of indoor temperature and contaminant gas concentration level. However, performing accurate measurement and control is still uncertain due to the lack of appropriate model that could unite the simplicity on the parameter level and the ability of capturing the salient feature of dominant airflow distribution and characteristic of temperature/concentration variation. For the large scale partition-less livestock building with long dimensional size, neglecting the horizontal variation could obviously result in the significant deviations from the optimal

environment for the sensitive pigs and chickens. Therefore, it is necessary and significant to study more specifically the mass transfers of the compartmentalized local zonal climate, the associated airflow interaction and the zonal energy transmission, so that a good control system for not only maintaining the entire environment, but also control more specifically the local zonal heating and ventilation rate could be established, and a high quality production could be guaranteed.

The method proposed for indoor climate modeling is called Conceptual Multi-Zone Climate Model (CMZCM) which compartmentalize the building into some macroscopic homogeneous well mixed zones, with the major emphasizes on the occupied spaces where the animals confined in. With some necessary assumption and simplifications, individual zones are analyzed based on the mass and heat balance equations, and the dominant air flow distributions including the inter-zonal flow interaction are investigated. The previous research works on relevant analysis and methods are reviewed as follows.

Assuming that in the researched laboratory livestock building, an advanced waste-handling system equipped and the manure storage units are frequently cleaned, then if the ventilation rate are adequate to remove heat and contaminant organisms or gas, the moisture is usually well diluted and present no problem. Further more, humidity has little effect on thermal comfort sensation at or near comfortable temperatures unless it is extremely low or high. Therefore the humidity is not considered in this work.

2.1.2 Literature Review

Conventional multi-zone modeling (or multi-room modeling) method is often appropriate for average size buildings with physical walls for partition, and each room may act like a well-mixed compartment ([Sohn and Small, 1999],[O'Neill, 1991]). For partitionless livestock building with localized ventilation and source locations, with persistent spatial temperature/concentration gradient, the single well-mixed compartment approach may be inappropriate. Using Computer Fluid Dynamic (CFD) codes [Berckmans *et al.*, 1993], though proves to give detailed information on inter-zonal flow and temperature distribution as demonstrated in [Svidt and Bjerg, 1996], [Harral and Boon, 1997], [Svidt *et al.*, 1998] and [Bjerg *et al.*, 2000], the analysis are based on the steady state models formulated with Navier-Stokes equations. The CFD technique numerically solves these equations and is able to calculate physical parameters which are not measurable, but its requirements for high cost, huge computational effort and time consuming make it difficult for implementation and design within a general building simulation program and control technology field. A new so-called Conceptual Multi-Zone Climate Model (CMZCM) method is proposed in this work, that the principle consists of breaking up the entire indoor air volume into macroscopic homogeneous conceptual zones in which mass and energy conservation must be obeyed. This zonal model concept within a partitionless enclosure is not new, and has been previously investigated in several works ([Gagneau and Allard, 2001], [Haghighat *et al.*, 2001] and [Riederer *et al.*, 2002]). However, in these works, only the accuracy of the proposed method compared with CFD on steady state

cases are proved. Because the airflows with plume, jet and boundary layers are taken into account and the correlation of convective phenomenon is integrated into the inter-zonal flow connection which obviously influenced the model simplicity, therefore, the finalized highly coupled zonal models still remain questionable on whether it is capable and realistic of making dynamic analysis or not. The new CMZCM method is able to satisfy the necessary precision for evaluating the active local climate within a large scale building in order to reach the desired controlling objectives, but most importantly, it also maintains the simplicity of the first order model for describing the dynamic properties of zonal climate and for the purpose of applying advanced control strategies.

2.2 System Description

The laboratory of livestock stable which is used to be a broiler house is located in Syvsten, Denmark. It is a large scale concrete building, with the floor area of $753m^2$, the length of $64.15m$, the width of $11.95m$, and the approximate volume of $2890m^3$ (see Fig. 2.1). Hybrid ventilation system is equipped in the building with five exhaust units which are

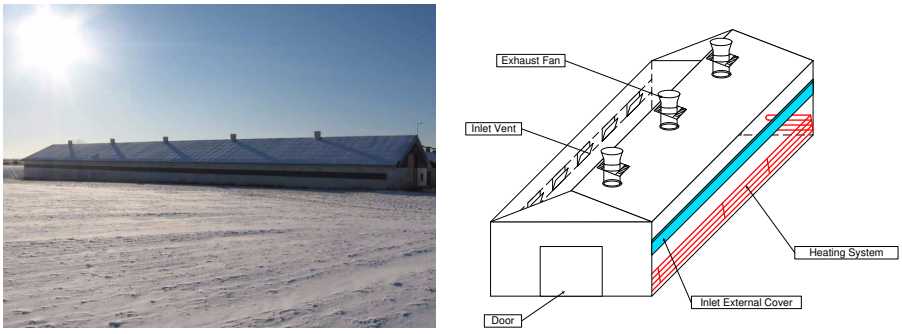

Figure 2.1: A Full Scale Poultry Stable Located in Syvsten, Denmark

evenly distributed on the ridge of the roof with the total maximum flow rate of $17.8m^3/h$, and sixty-two inlet valves controlled by winch motors mounted on the side walls with the whole maximum opening area of $6.45m^2$, as shown in Fig. 2.2. The heating system consists of two major heat sources, one for heating up the indoor temperature through the steel pipes installed under the inlet system when ventilation is not adequate to satisfy the animals comfort requirement, and the other for physically simulating the animal heat production with six water heating radiators equipped near the floor. They are both coupled to an oil furnace placed in the monitor room which could provide warm water with temperature ranging from 15^oC to 55^oC.

The exhaust units are the most important link in the ventilation system. They are the driving forces that provide needed air exchange and guarantee a low pressure ventilation

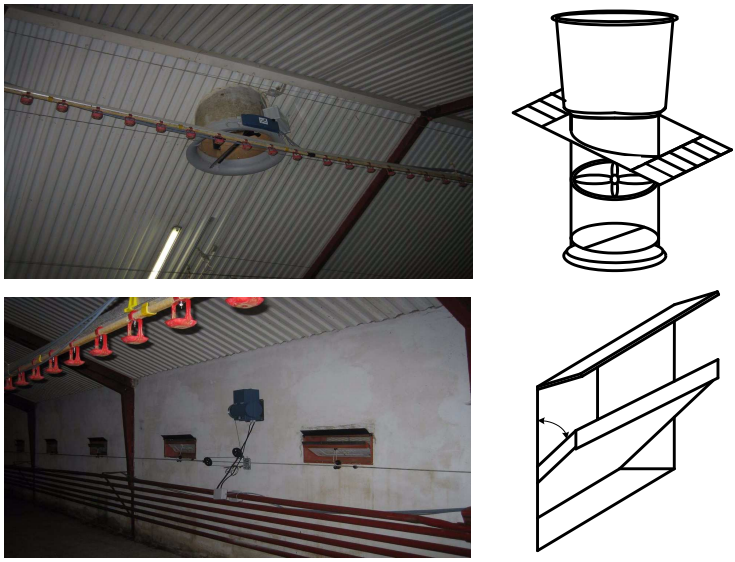

Figure 2.2: The Exhaust and Inlet System

strategy. Each exhaust unit consists of an axial-type fan and a swivel shutter. The airflow capacity is controlled by adjusting the *r.p.m.* of the fan impeller and the angle of the swivel shutter. The inlet system provides variable airflow directions and controls the amount of incoming fresh air by adjusting the bottom hanged flaps. The shutter in fan and the inlet flap play essential role on attenuating the effect of wind gust. Through the inlet system, the incoming fresh cold air mixes with the indoor warm air, and then drops down to the animal environmental zones slowly in order to satisfy the zonal comfort criteria. In autumn and winter, when the outdoor temperature is much lower than the animal comfort temperature, the inlet flap opening angle will be decreased to lead the cold air directly towards the ceiling, to protect against the intrude of the cold air to the animal living zone by slowing down the mixing procedure. The main airflow pattern mostly occurs in spring and summer is depicted in Fig. 2.3.

In order to measure and regulate the indoor climate, a large amount of sensors were installed and connected to an acquisition and control system based on an PC located in the monitor room. The inside air temperatures are measured with temperature sensors which are positioned around one meter above the floor. The exhaust flow rate, inlet valve opening positions and pressure difference across the inlet are measured by flow sensors, position sensors and pressure sensors, respectively. The top view of the positioning and numbering of the hardware and sensors in the test stable are described in Fig. 2.4 and Fig. 2.5, and the functioning are explained in Table 2.1 and Table 2.2.

The control computer in the stable is a Commercial Off-The shelf System (COTS)

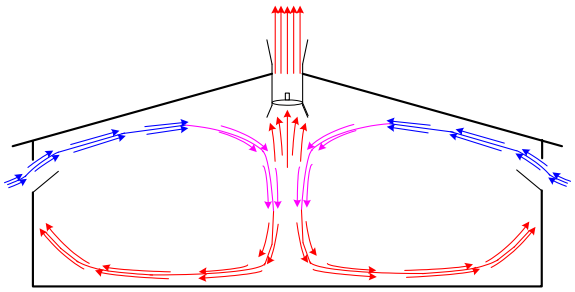

Figure 2.3: The main airflow circulation inside the livestock building

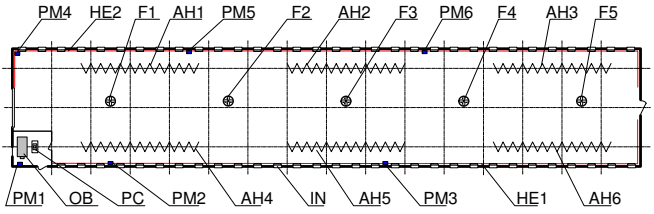

Figure 2.4: Overview of the Hardware Equipped in the Stable

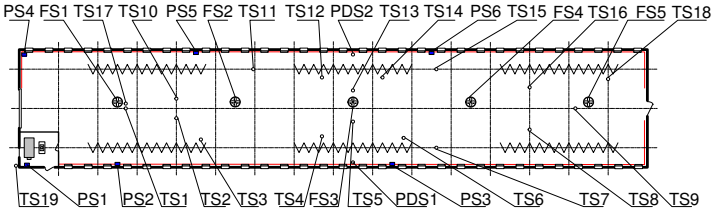

Figure 2.5: Overview of the Sensors Mounted inside the Stable

Symbol	Function
AH1 - AH6	Heat Sources Simulator for Animal Heat Production
SH1 - SH2	Heat Sources Simulator for Stable Heating System
IN	Inlet
OB	Oil Furnace
PC	System Computer
PM1 - PM6	Winch Motor
F1 - F5	Axial Exhaust Fan

Table 2.1: Hardware Equipped in The Livestock Building

Symbol	Function
FS1 - FS5	Flow Sensors (outlet)
PDS1 - PDS2	Pressure Difference Sensors
TS1 - TS19	Temperature Sensors (air)
PS1 - PS6	Position Sensors (inlet)

Table 2.2: Sensors Installed in The Livestock Building

([Jessen *et al.*, 2006a] and [Jessen *et al.*, 2006b]). The computer runs Linux and uses Comedi as an open source library to communicate with the I/O cards, which is used to connect to the sensors and actuators in the stable. The control demand and the sensor values could be accessed and acquired through a network interface card (NIC) over the Internet or a local area network (LAN) to a web browser.

2.3 System Modeling

The entire process mainly constitute four sub-processes including the exhaust unit, inlet unit, heating system, and the indoor climate system, where the dissipated heating energy is simplified into constants.

2.3.1 Multi-zone Climate Model

The schematic diagram of a large scale livestock stable equipped with hybrid ventilation system analyzed with the conceptual multi-zone method is shown in Fig. 2.6(1), Fig. 2.6(2) and Fig. 2.6(3). From the view of direction A and B, Fig. 2.6(a) and Fig. 2.6(b) provide a description of the dominant air flow map of the building including the airflow interaction between each conceptual zones. Basically, the zone partition is made according to the number of the operating exhaust units. The necessary simplifying assumptions for developing process models are as follows:

- An ideal uniform flow process is assumed, which means that the fluid flow at any inlet or outlet is uniform and steady, and thus the fluid properties do not change

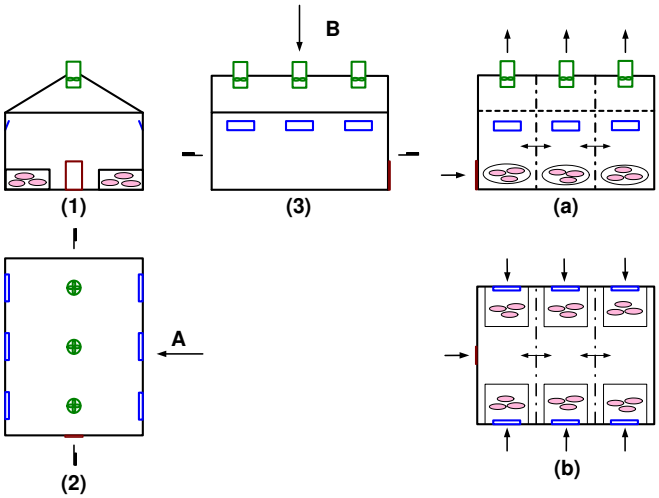

Figure 2.6: Synoptic of Large Scale Livestock Barn and the Dominant Airflow Map of the Barn

with time or position over the cross section of an inlet or outlet.

- The interactive airflow between internal zones, which is influenced by the inlet air jet trajectory, thermal buoyancy forces and convective heat plume are assumed to be constant.
- Heat gain from animals and solar radiation are assumed to be constant.
- The rate of the heat loss by evaporation is neglected.
- The thermal properties of the airflow are assumed to have bulk average values.
- Airflow involves no mass accumulation inside the building.
- The heat transfer coefficient of building envelope is assumed to be constant.
- The pressure is assumed to be constant on each building surface (same value of pressure coefficient C_p is used for all openings on the same side of the building).
- A hydrostatic pressure distribution is assumed in the space.
- Opening characteristics are assumed independent on flow rate, pressure difference and outside temperature (constant discharge coefficient C_d are used for all openings).

By applying the conceptual multi-zone method, the building is compartmentalized into several macroscopic homogeneous conceptual zones horizontally so that the non-linear differential equation relating the zonal temperature and zonal concentration can be derived based on the energy and mass balance equation for each zone as (2.1). The subscript i denotes the zone number. The following energy transfer terms appear in the temperature zonal model (2.1): the inter-zonal heat exchange $\dot{Q}_{i+1,i}$ and $\dot{Q}_{i,i+1}$; the heat transfer by mass flow through inlet and outlet $\dot{Q}_{in,i}$ (2.2) and $\dot{Q}_{out,i}$ (2.3); the transmission of heat loss through building envelope by convection and radiation $\dot{Q}_{transmission,i}$ (2.4); the heat source in the zone $\dot{Q}_{source,i}$ mainly from the dissipation of heating system and animal heat production, which approximated by the rate of heat loss through the pipe and radiator (see 2.5). The calculation of animal heat production has been researched in [Pedersen and Sallvik, 2002].

$$M_i c_{p,i} \frac{dT_i}{dt} = \dot{Q}_{i+1,i} + \dot{Q}_{i,i+1} + \dot{Q}_{in,i} + \dot{Q}_{out,i} + \dot{Q}_{transmission,i} + \dot{Q}_{source,i}, \tag{2.1}$$

$$\dot{Q}_{in,i} = c_{p,o} \cdot \dot{m}_{in,i} \cdot T_o, \tag{2.2}$$

$$\dot{Q}_{out,i} = c_{p,i} \cdot \dot{m}_{out,i} \cdot T_i, \tag{2.3}$$

$$\dot{Q}_{transmission,i} = U \cdot A_{wall,i} \cdot (T_i - T_o), \tag{2.4}$$

$$\dot{Q}_{source,i} = \dot{m}_{water} \cdot c_{p,water} \cdot (T_{water,in} - T_{water,out}), \tag{2.5}$$

$$\dot{Q}_{i,i+1} = c_{p,i} \cdot \dot{m}_{i,i+1} \cdot T_i. \tag{2.6}$$

where the inter-zonal mass flow rate $\dot{m}_{i,i+1}$ is the sum of several different flow elements, such as the airflow interaction $\dot{m}_{i,i+1,\cdot V}$ caused by the extracted fans, the airflow zonal crossing $\dot{m}_{i,i+1,\cdot IN}$ resulted from the inlet jet trajectory, and the airflow mixing $\dot{m}_{i,i+1,T}$ due to the inter-zonal convective phenomena e.g. the convective flows at surface, thermal plume and so on. We propose $k_{i,i+1} \cdot \Delta T_{i,i+1}$ to compute $\dot{m}_{i,i+1,T}$, where $k_{i,i+1}$ is the inter-zonal airflow mixing parameter and could be determined through experiment calibration with e.g. the gas tracer method. Obeying the principle of conservation of mass, there are 4 patterns (*I*,*II*,*III* and *IV*) of airflow interaction (see Fig. 2.7(a)) computed through the differentiate of ventilation rate, where part of the amount accounts for the well-mixed zone air interaction by fans, and the other part of the amount accounts for the external air interaction by the inlet jet. The major elements of the zonal heat transfer is shown in Fig. 2.7 (b). The different airflow patterns play important effects on the system nonlinearities and determine the different operating conditions. The computational approach to quantify the inter-zonal mass flow rate according to the local(zonal) and global (entire building) mass balance equation is shown as follows:

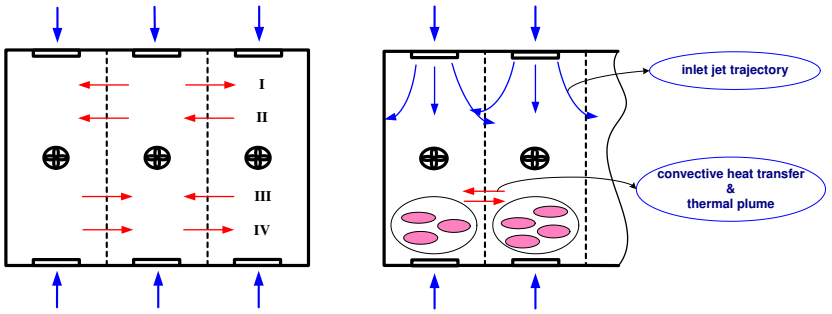

Figure 2.7: The two modes of intern zonal-flow patterns

Pattern I :

$$\dot{m}_{in,1}+\dot{m}_{in,4}-\dot{m}_{out,1}\leq 0,$$
$$\dot{m}_{21}=\dot{m}_{T,21}-\mu\cdot(\dot{m}_{in,1}+\dot{m}_{in,4}-\dot{m}_{out,1}),\dot{m}_{12}=\dot{m}_{T,12},$$
$$\dot{m}_{in,1}+\dot{m}_{in,4}-\dot{m}_{out,1}+\dot{m}_{in,2}+\dot{m}_{in,5}-\dot{m}_{out,2}\geq 0,$$
$$\dot{m}_{23}=\dot{m}_{T,23}+\mu\cdot(\dot{m}_{in,1}+\dot{m}_{in,4}-\dot{m}_{out,1}+\dot{m}_{in,2}+\dot{m}_{in,5}-\dot{m}_{out,2}),\dot{m}_{32}=\dot{m}_{T,32};$$

Pattern II :

$$\dot{m}_{in,1}+\dot{m}_{in,4}-\dot{m}_{out,1}\leq 0,$$
$$\dot{m}_{21}=\dot{m}_{T,21}-\mu\cdot(\dot{m}_{in,1}+\dot{m}_{in,4}-\dot{m}_{out,1}),\dot{m}_{12}=\dot{m}_{T,12},$$
$$\dot{m}_{in,1}+\dot{m}_{in,4}-\dot{m}_{out,1}+\dot{m}_{in,2}+\dot{m}_{in,5}-\dot{m}_{out,2}\leq 0,$$
$$\dot{m}_{32}=\dot{m}_{T,32}-\mu\cdot(\dot{m}_{in,1}+\dot{m}_{in,4}-\dot{m}_{out,1}+\dot{m}_{in,2}+\dot{m}_{in,5}-\dot{m}_{out,2}),\dot{m}_{23}=\dot{m}_{T,23};$$

Pattern III :

$$\dot{m}_{in,1}+\dot{m}_{in,4}-\dot{m}_{out,1}\geq 0,$$
$$\dot{m}_{12}=\dot{m}_{T,12}+\mu\cdot(\dot{m}_{in,1}+\dot{m}_{in,4}-\dot{m}_{out,1}),\dot{m}_{21}=\dot{m}_{T,21},$$
$$\dot{m}_{in,1}+\dot{m}_{in,4}-\dot{m}_{out,1}+\dot{m}_{in,2}+\dot{m}_{in,5}-\dot{m}_{out,2}\leq 0,$$
$$\dot{m}_{32}=\dot{m}_{T,32}-\mu\cdot(\dot{m}_{in,1}+\dot{m}_{in,4}-\dot{m}_{out,1}+\dot{m}_{in,2}+\dot{m}_{in,5}-\dot{m}_{out,2}),\dot{m}_{23}=\dot{m}_{T,23};$$

Pattern IV :

$$\dot{m}_{in,1}+\dot{m}_{in,4}-\dot{m}_{out,1}\geq 0,$$
$$\dot{m}_{12}=\dot{m}_{T,12}+\mu\cdot(\dot{m}_{in,1}+\dot{m}_{in,4}-\dot{m}_{out,1}),\dot{m}_{21}=\dot{m}_{T,21},$$
$$\dot{m}_{in,1}+\dot{m}_{in,4}-\dot{m}_{out,1}+\dot{m}_{in,2}+\dot{m}_{in,5}-\dot{m}_{out,2}\geq 0,$$
$$\dot{m}_{23}=\dot{m}_{T,23}+\mu\cdot(\dot{m}_{in,1}+\dot{m}_{in,4}-\dot{m}_{out,1}+\dot{m}_{in,2}+\dot{m}_{in,5}-\dot{m}_{out,2}),\dot{m}_{32}=\dot{m}_{T,32}.$$

where, the parameter μ represents the percentage of the interacting mass flow transferred from the neighbor zones and $1-\mu$ is the percentage of the interacting mass flow influenced directly by the inlet jet trajectory. Thus $0 \leq \mu \leq 1$. When $\mu = 1$, the incoming outdoor air is assumed to be well mixed with the indoor air of the corresponding zone before interacting with neighbor zones; when $\mu = 0$, the outdoor air goes directly through the inlet into the building and cross the zone boundaries. As the matter of fact, the determination of μ depends on the inlets and fans' installation and distribution properties. For simplicity, μ is assumed to equal to 1 in further modeling and controller design.

The dynamic model for zonal contaminant gas concentration is developed as (2.7)

$$\frac{dC_{r,i}}{dt} = C_{r,i+1} \cdot \dot{n}_{i+1,i} + C_{r,i} \cdot \dot{n}_{i,i+1} + C_{r,i} \cdot \dot{n}_{out} + C_{r,o} \cdot \dot{n}_{in} + \frac{G_i}{V_i}. \tag{2.7}$$

where, the rate of concentration is indicated as $C_{r,i} \cdot \dot{n}_i$, in which $C_{r,i}$ (m^3/m^3) represents the zonal concentration and $\dot{n}_i$ (h^{-1}) is the air exchange rate. The rate of the animal carbon dioxide generation denoted by G_i $(10^{-3}m^3/h)$ is approximately 12 times the actual activity level denoted by M_a (l/h), which is measured in *met* (see 2.8). The zonal volume is V_i (m^3),

$$G_i = 12 \cdot M_{a,i}. \tag{2.8}$$

2.3.2 Inlet and Exhaust System Model

The volume flow rate through the inlet is calculated by (2.9). The pressure difference ΔP across the opening can be computed by a set of routines solving thermal buoyancy and wind effect as (2.10), where, P_i is the internal pressure at the height of Neutral Pressure Level (NPL). The value of wind induced pressure coefficient C_P changes according to the wind direction, the building surface orientation and the topography and roughness of the terrain in the wind direction.

$$\dot{q}_{in} = C_d \cdot A_{inlet} \cdot \sqrt{\frac{2 \cdot \Delta P_{inlet}}{\rho_o}}, \tag{2.9}$$

$$\Delta P_{in} = \frac{1}{2} C_P \rho_o V_{ref}^2 - P_i + \rho_o g \frac{T_i - T_o}{T_i} (H_{NPL} - H_{inlet}). \tag{2.10}$$

Fig. 2.8 (a) demonstrates the characteristic curve of the air volume flow rate through the inlet opening corresponding to the pressure differences. The colorful curves represent different opening percentages.

Introducing a fan law to the exhaust unit, the relationship between the total pressure difference ΔP_{fan}, volume flow rate q_{out}, supplied voltage V_{volt} and the shutter opening angle θ can be approximated in a nonlinear static equation (2.11), where the parameters a_0, a_1, a_1, b_0, b_1, b_1 are empirically determined from experiments made by SKOV A/S in Denmark. As shown in (2.12), the total pressure difference across the fan is the difference

between the wind pressure on the roof and the internal pressure at the entrance of the fan which considers the pressure distribution calculated upon the internal pressure P_i.

$$\Delta P_{fan} = (b_0 + b_1 \cdot \theta + b_2 \cdot \theta^2) \cdot \dot{q}_{out}^2 + a_0 \cdot {V_{volt}}^2 + a_1 \cdot \dot{q}_{out} \cdot V_{volt} + a_2 \cdot \dot{q}_{out}^2 \tag{2.11}$$

$$\Delta P_{fan} = \frac{1}{2}\rho_o C_{P,r} V_{ref}^2 - P_i - \rho_i g \frac{T_i - T_o}{T_o}(H_{NPL} - H_{fan}). \tag{2.12}$$

Fig. 2.8 (b) demonstrates the characteristic curve of the exhaust fan system with the shutter opening angle varying from 0 to 90 degrees.

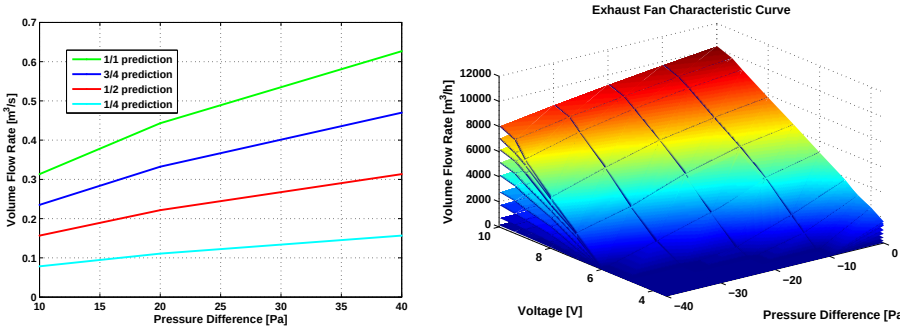

(a) (b)

Figure 2.8: (a) Inlet Characteristic Curve (b) Exhaust Fan Characteristic Curve with Swivel Shutter Opening Angle Varying From 0 to 90 Degree

The inlet and outlet air flow is connected with internal pressure at Neutral Pressure Level (NPL), where the difference between indoor and outdoor pressure is zero. The relationship between the pressure difference across the inlet and the outlet is explained as Fig. 2.9 (a), the pressure loop for the dominant airflow path. The principle of determining the NPL is shown in Fig. 2.9 (b), where P_1 represents the pressure cross at the inlet level, P_2 represents the pressure cross at the outlet level, and the pressure is assumed to be hydrostatically distributed based on the reference pressure. According to the mass balance equation (2.13), the internal pressure at NPL is derived from iterative searching through optimization computation, so that the airflow is calculated and acts as an intermediate signal to combine the manipulated variable such as the rotating speed of the fan and opening angle of the shutter, with the controlled variable such as the temperature and the concentration level.

$$\sum_{j=1}^{6} \dot{q}_{in}(k) \cdot \rho_o - \sum_{i=1}^{3} \dot{q}_{out}(k) \cdot \rho_i = 0. \tag{2.13}$$

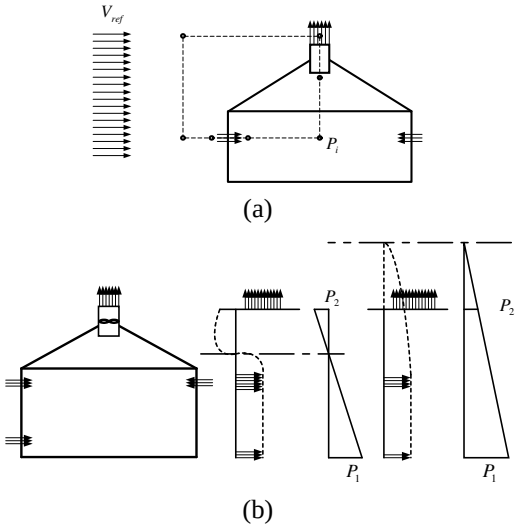

Figure 2.9: The Pressure Loop of Dominant Airflow Path and Determination of Neutral Pressure Level

2.3.3 Process Analysis

The mathematical models for the entire process have been well researched and developed from its physical principles. Before going further for controller study, it is important to investigate the open loop (without controller) process dynamics and the system degree of freedom, in order to get thorough understanding of the system transient behavior and prepare for the control variables definition and control performance analysis in the future.

Analysis of the Degrees of Freedom

Aiming at knowing the number of degrees of freedom, the following equation is applied,

$$N_m = N_x + N_u - N_e, \tag{2.14}$$

where, N_x is the number of dependent variables, N_u is the number of inputs and disturbances variables, N_e is the number of equations as identified in Table 2.3. Noting that, the number of the zone is denoted by the subscript i and $i = 1...3$, the subscript j denotes the number of the inlets on windward and leeward side of the building, and $j = 1...6$.

Through above analysis of both the actuator system and the indoor climate system, the number of degrees of freedom of the entire system for thermal comfort is 20, where, $A_{in,j}$, $V_{volt,i}$, $\theta_{shutter,i}$ (inlet vents openings, supplied voltage to the fans and swivel shutter openings) are taken as manipulated variables. While, $\dot{Q}_i$, V_{ref}, $c_{P,w}$, $c_{P,l}$, $c_{P,r}$, T_o (zonal

N_x	N_u	N_e
T_i		Equation 2.1
$\dot{q}_{in,j}$		Equation 2.9
$\dot{q}_{out,i}$		Equation 2.11
P_i		Equation 2.10, 2.12, 2.13
	$A_{in,j}$	
	$V_{volt,i}$	
	θ_i	
	Q_i	
	V_{ref}	
	$C_{p,w}$	
	$C_{p,l}$	
	$C_{p,r}$	
	T_o	
13	20	13

Table 2.3: Degrees of Freedom Analysis for the Thermal Comfort System

heat sources, wind speed, wind pressure coefficient on the windward, leeward and roof, external temperature) are taken as disturbances to the process. Therefore, 12 degrees of freedom remains to be used to control the process, for example to reject the 8 disturbance variables. Through the same analysis procedure, the number of degrees of freedom of the entire system for indoor air quality is 21, with the same manipulated variables as the thermal comfort system, and the external contaminant concentration level C_o is included into the disturbance variables, thus 12 degrees of freedom are used to reject 9 disturbance variables.

Analysis of the Process Dynamics

The goal of this section is to obtain an understanding of the process dynamics in an open-loop operation. The step responses are analyzed when the changes are made in the input variables of the process. In our system, four input variables deserve our attention to investigate, they are the zonal extracted flow rate (manipulated by the fans speed and swivel shutters), the zonal inlet flow rate (manipulated by the opening angles of inlet flaps), the external weather condition (temperature, wind speed etc.), and the zonal heat sources. The following description show the step responses analysis for understanding the influence of each input variables on the system performances.

Case No. 1 : The step response is analyzed when a change is made in one of the manipulated variable: the supplied fan voltage. The other input variables maintain at constant operation values. Fig. 2.10 shows the zonal temperature affected by one of this extracted flow rate change.

Observed from Fig. 2.10, that an outlet flow rate change in one of the zone, has influence on temperature variation in each of the zone, but the degree of influence

depends on the setting of μ. When $\mu = 1$, the degree of influence on each one of the zonal temperature is simultaneous, while with the decrease of μ, e.g. when $\mu = 0.7$, the corresponding zone's temperature is affected more severely than the others. The relation is proportional, because when fan speed increases, the amount of flow rate extracted out of the corresponding zone also increases, thus the indoor temperature decreases;

In the same way, the step in the fan speed change of the other zones are analyzed. The obtained results are similar to above case.

Case No. 2 : The step response is analyzed when a change is made in the inlet valve opening of one zone while the others are maintained to be constant. Fig. 2.11 shows the zonal temperature changes. When $\mu = 0$, the degree of influence on zonal temperature is simultaneous, while with the increase of the fraction of μ, such as $\mu = 0.3$, the other zones temperature do not behave as aggressive as the corresponding zone, because 0.3 of the incoming air is mixed with the zonal warm air before interacting with the neighbor zones. Analogously, this analysis might be obtained when the other zones' inlets are changed with the steps.

In conclusion, with the sliding of μ from 1 to 0, the cause of the zonal flow mixing effect changes from the exhaust fans driving force $\dot{m}_{i,i+1,\cdot V}$ to the inlet jet driving force $\dot{m}_{i,i+1,\cdot IN}$.

Case No. 3 : A step change is made in the external temperature, and the system response is shown in Fig. 2.12. The increase of outside temperature results in the increase of indoor temperature. The response performance is also analyzed with step change on the external wind speed. The system behavior to the wind speed is in the same relation with that to the external temperature. Concluded from Fig. 2.12, the weather condition is the disturbance which have the leading effect on the indoor climate.

Case No. 4 : Fig. 2.13 shows how the corresponding zone's temperature is affected by the step change in the local zonal heat source, while other inputs remain the same. In this case, the airflow interaction $\dot{m}_{i,i+1,T}$ due to the heat transfer through surface convection and heat plume play important role in indoor zonal performance. The variation of μ in case No. 3 and 4 does not illustrate obvious difference in system behavior.

Based on the above analysis, the assumption of $\mu = 1$ is used in the control system design, and this assumption might lead to the underestimate of the immediate influenced zone's temperature, and overestimation of its neighbor zones' temperature or vice versa. The change of μ does not have direct effect on the system dynamics.

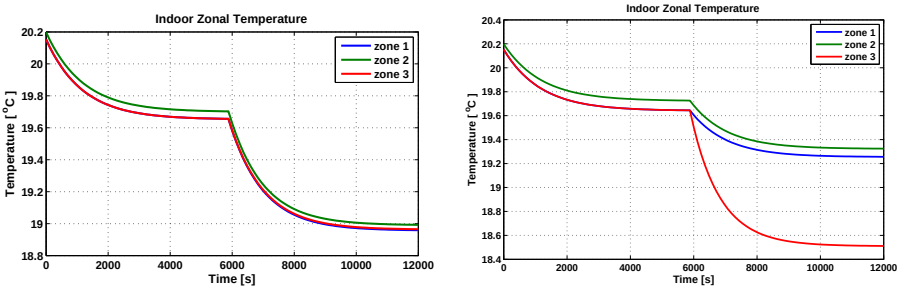

Figure 2.10: System behavior when a step is introduced in supplied fan voltage of zone 3 from $7V$ to $9V$ at time $t = 6000s$. The other inputs are constant at the operating conditions. (a) $\mu = 1$; (b) $\mu = 0.7$

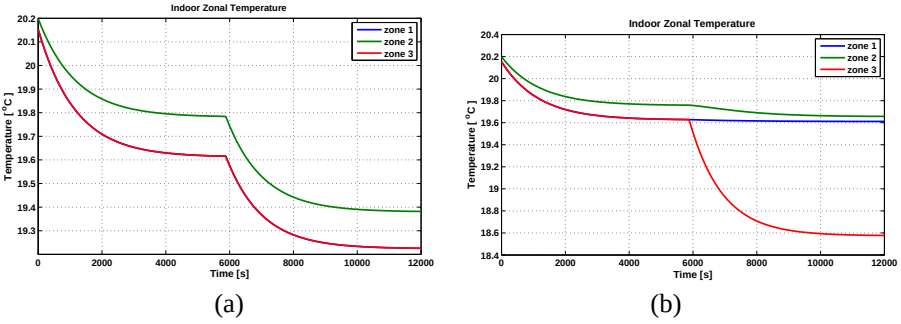

Figure 2.11: System behavior when a step is introduced in inlet vent opening of zone 3 from $0.15m^2$ to $0.35m^2$ at time $t = 6000s$. The other inputs are constant at the operating conditions. (a) $\mu = 0$; (b) $\mu = 0.3$

2.4 System Verification

The dynamic models of the actuator and the multi-zone indoor climate system are expressed nonlinearly with respect to some dynamic parameters, which then can be estimated by using constrained nonlinear least square techniques based on the data-set collected from experiments. This parameter estimation method can not only yields consistent positive estimates of the parameter values, but also exhibits close to optimum performance in the analyzed models. The constraints to the optimization routines are the non-negativity for all of the parameters.

The coefficient C_d for the inlet system, varies considerably with the inlet type, opening area, as well as incoming air temperature and flow rate. However, for simplifying

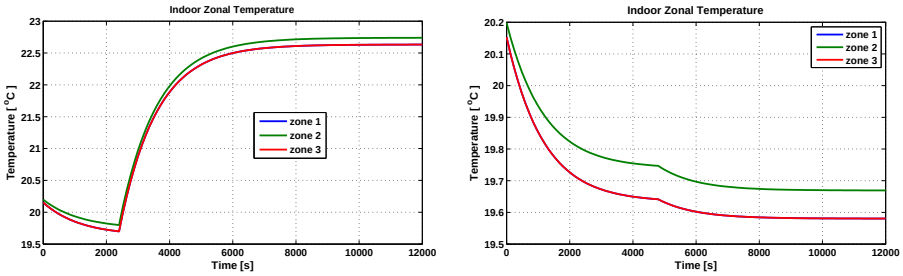

Figure 2.12: System behavior when a step is introduced in (a) external temperature from 10^oC to 13^oC at time $t = 2400s$; (b) external wind speed from $10m/s$ to $12m/s$ at time $t = 4800s$. The other inputs are constant at the operating conditions.

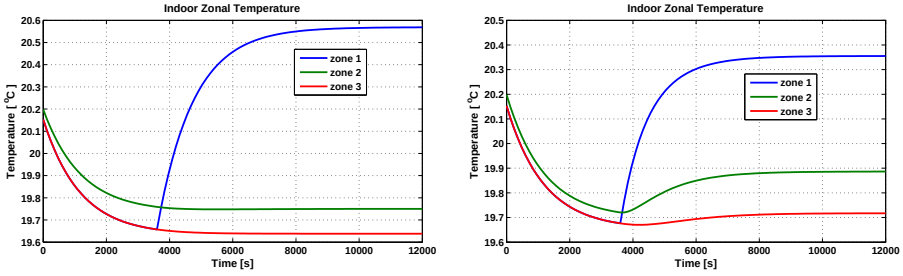

Figure 2.13: System behavior when a step is introduced in local heat source of zone 1 from $6000J/s$ to $7000J/s$ at time $t = 3600s$. The other inputs are constant at the operating conditions. (a) $\dot{m}_{i,i+1,T} = 0.01kg/s$; (b) $\dot{m}_{i,i+1,T} = 0.5kg/s$

the computation, we use a constant value which is determined through experiment for all openings, even though it might lead to over/under-prediction of airflow capacity and thereby larger openings than necessary. Fig. 2.14 demonstrates the comparison of the characteristic curve of the air volume flow rate through the inlet opening obtained from the measurement and the simulation model.

Fig. 2.15 (b) illustrates the performances of the exhaust fan at a specific swivel shutter opening with the measurement and the validation data. The surface represents the character of the fan with pressure-voltage-flow data which is approximated by the quadratic equation (2.11).

The parameters employed in the multi-zone climate model, are identified from the experiments conducted in the real scale livestock stable. Two scenarios, one in summer and one in winter, with various external temperatures and mild wind level have been used

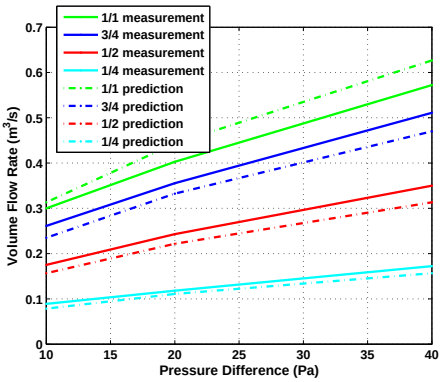

Figure 2.14: Comparison of Inlet Characteristic Curves

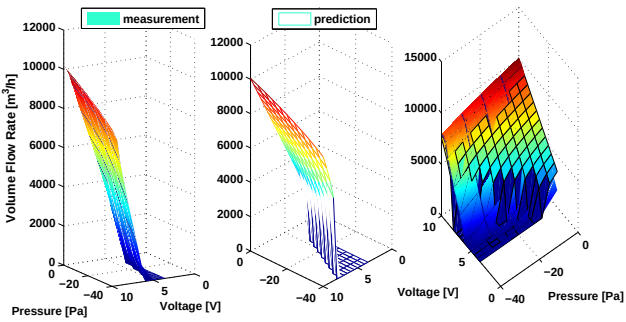

Figure 2.15: Comparison of Exhaust Fan Characteristic Curve at Specific Swivel Shutter Opening Angle

for comparison (see Chapter 10). Those two scenarios are thought to represent the typical but not the only two cases encountered in the steady state and dynamic behavior of the indoor climate model for parameter estimation.

Due to the existence of unpredictable airflow path like the shot-circuiting and stagnant zones in ventilated spaces, and the neglect of some influencing factors and uncertainties, for example the zonal air interaction, the slow dynamics of the heat convection of the surfaces, the insulation of the construction material, the latent heat loss through evaporation, the building leakage and the wind effect and so on, the steady state fluctuation and the discrepancy between the identified and the realistic parameter values deserve our further investigation. Especially, the simplified assumption on the inlet jet trajectory, and the degree of the zonal air mixing leads to a considerable large value of the effective volume compared with the physical size of the zone volume. The horizontal temperature gradients and the inter-zonal flow are qualified but not quantified, because of the undetermined mixing parameter $k_{i,i+1}$ and the parameter μ.

The validation are carried out with the input signals which were not used in the estimation processes and then the predicted output was compared with the measurements. Even though, it is hard of being able to perform tightly planned experiment under laboratory conditions, and the validation results seem to be lacking of further accuracy discussion, the most important phenomena represented in the proposed model are analyzed and manifested. We could conclude that the overall indoor climate model is appropriate and sufficient for capturing the salient dynamics of indoor climate in large, heterogeneous, partition-less buildings, for the purpose of measurement and control.

2.5 Conclusion

The coincidence between the measured data and the predicted output supports the developed models with the proposed method. The most of output performance discrepancies are acceptable, and proves that the simplified model, especially, the concept of zone compartmentalization in the large partition-less building is appropriate for depicting the horizontal heterogeneity. However, the assumption of the inter-zonal mixing flow rate need to be further manifested and the simplification of the system dynamics need to be further investigated. All in all, the ventilation system and indoor climate models, provide a essential and usable testing tools for model-based control studies, clarify the zonal climate control objective, and refine the multi-variable control strategy.

Chapter 3

Estimation, Control and Optimization

Livestock environmental control plays vital role in preserving animal well-being and improving the efficiency of animal production. The model used for forecasting the future behavior of the system, is the essence of model-based predictive control strategy. Firstly, the nonlinear system is linearized, coupled and transformed into a state space representation. Secondly, the moving horizon estimation and control, accompanied with target calculation and disturbance modeling are implemented. An autocovariance least square method plays a part for performance improvement by adaptively recovering the system noise covariances. A novel approach for improving system utilization and optimizing the energy consumption by exploiting the redundant actuator nonlinearities is applied by solving a constrained convex optimization and integrated with the Model Predictive Control scheme. The goal is to compromise between passively rejecting the disturbance beyond the system bandwidth and saving the energy use. A literature review for the control and estimation techniques is provided. The chapter is closed with a summary describing the superiority of the proposed control technique.

3.1 Control and Optimization Methodology

3.1.1 Methods Introduction

Traditionally, the livestock ventilation system has been controlled using classical Single Input and Single Output (SISO) controllers through single zone analysis. The challenge of this work is to introduce a more efficient and comprehensive multi-variable control

scheme, to allow a better trade off between the optimum performances of indoor climate and energy consumption saving. The controller mainly focuses on minimizing the variation of the indoor temperature and contaminant gas concentration level, keeping both variables within the comfort and acceptable zones with an optimum energy consumption approach, in the presence of actuator saturation, random noise, and disturbances at different frequencies.

The proposed control method is called moving horizon estimation and control which is also referred as Model Predictive Control (MPC) as well as receding horizon estimation and control. The advantages and superior of this technique over the conventional control schemes are as follows: realizes simultaneous control based on coupled state space models; incorporates certain goals for multiple objectives optimization particularly associated with the cost (fuel/energy consumption); takes into account of hard actuator saturation and soft output limitation, allows operation closer to the constraints which leads to more profitable operation; needs minimum design and tuning effort but optimum solution; copes with measured/unmeasured disturbances in a feed-forward way; tracks time varying reference with zero steady state offset.

Moving Horizon Estimation (MHE), being as a integral part of MPC, is a moving horizon-based approach for Least-Squares estimation, which is mainly concerned with time-varying parameters and states. This on-line method helps to achieve a compromise between the recursive approximation and the least-squares solution at the cost of increased computational requirement. By solving a quadratic programming or nonlinear programming, the inequality constraints for the unknown variables (e.g. variables such as temperature, pressure, flow rates and concentrations, must be nonnegative and can not go above some upper bound; the rate of change of these variables is also bounded by mass and energy balance considerations) are incorporated. In this framework, the unknown variables such as the initial errors, disturbances and noise are modeled as truncated normal variables, and this concept offers a significant advantage in terms of the robustness of the estimates and modeling the random variables.

A new Auto-covariance Least-Squares (ALS) method is a data based technique to improve the state estimation in MPC. It estimates the noise covariances using routine operating data and adaptively determines an optimal filter gain or the weighting matrix in moving horizon estimation computation. Because of its probabilistic and statistic advantages, it could further reduce output variances and compensate un-modeled disturbances or model/plant mismatch.

Energy consumption, actuator saturation and disturbances in wide range of frequencies, e.g. wind speed variation are crucial issues in designing an applicable and utilizable indoor climate control system for modern livestock stable. The manipulators which possess actuator redundancy is exploited to accommodate the limitation of the bandwidth of the closed-loop system as well as pursuit of an optimum energy solution through on-line optimization taking into account of actuator constraints. By assigning different weights in the objective function which is based on energy consumption considerations, according to the covariance of the high frequency disturbances, the modified optimal control command

are reallocated to the end effectors.

For the purposes outlined above, the proposed methods consists of five major parts of formulation and computation and is summarized as: (a) a Linear Time Invariant (LTI) model which represents the entire system knowledge which reflects the influence from the manipulated inputs, disturbances and system noise on the controlled outputs; (b) system model is augmented with integrated white noise accommodating the unmeasured disturbances entering through the process input, state or output; (c) moving horizon estimation and control incorporating combined quadratic and linear term soft constraints, implemented through dynamic optimization for obtaining better estimation of the unmeasurable states, rejecting disturbances and uncertainties, guaranteeing offset-free tracking (step change or time varying references) and improving output performances within hard actuator saturations; (d) auto-covariance least square method for recovering the covariances of unknown noises, and adaptively determine the penalty in the moving horizon estimation objective function; (e) actuator redundancy is applied through exploiting the nonlinearities of the actuators to passively attenuate the high frequency disturbances (wind gust), therefore enhances the resilience of the control system to disturbances beyond its bandwidth, and reduces energy consumption through on-line optimization. In the designed control system, researches are mainly focus on an outer feedback closed-loop dynamic controller which generates the demand airflow rate required for tracking the comfort indoor climate criterion, and an inner feed-forward redundancy optimization that taking advantage of the actuator redundancy for the purpose of rejecting wind gust, increasing the efficiency of actuator utilization and saving energy. The proposed overall control technique is proved to be advanced and advantageous through comparative simulations and is expected to be feasible in the real livestock buildings.

3.1.2 Literature Review

Model predictive control is the predominant paradigm of advanced control in the process industry. The predictive control method proposed by [Richalet *et al.*, 1978] with the name *Model Predictive Heuristic Control* and another scheme called *Dynamic Matrix Control* proposed by [Cutler and Ramaker, 1980] have been regarded as the origins of model predictive control.

The applications of MPC are mainly for the economically important, large-scale, multi-variable processes, and the rationale for its success is because of its feature for dealing with Multiple Input and Multiple Output (MIMO) system with strong nonlinearities naturally and handling actuator constraints flexibly. [Morari and Lee, 1999] presents the development of MPC and future perspective from a theoretical point of view. [Rao and Rawlings, 2000] provides a good introductory tutorial on the essential principles of linear/nonlinear model predictive control aimed at control practitioners. [Qin and Badgwell, 2003] presents a comprehensive survey on the industrial model predictive control technology and implementation. [Pannocchia *et al.*, 2005] makes a systematical comparison between the conventional PID controller and the off-set free constrained Linear Quadratic

(LQ) controller for SISO system, and concludes that the constrained LQ outperforms PID both in set-point changes and disturbance rejection. MPC technique is robust to model errors, insensitive to measurement noise, simple to tune and implement in software and hardware with competitive computational efficiency, and it handles constraints better than common anti-windup PID.

[Rao, 2000], [Tenny and Rawlings, 2002] and [Jorgensen, 2005] present excellent work on nonlinear moving horizon estimation and control, including the computational methods and numerical solution technique and a comprehensive survey of recent theoretical developments. [Muske and Badgwell, 2002] and [Pannocchia and Rawlings, 2003] present a general disturbance model for guaranteeing offset-free control in presence of system errors, and provide the sufficient and necessary condition for checking detectability. [Muske and Rawlings, 1993b] and [Muske and Rawlings, 1993a] present the linear model predictive control for stable and unstable system, and proposes a parametrization method for the predictive control problem with infinite horizons in terms of a finite number of parameters. Other research work on stability issue include [Scokaert, 1997], [Scokaert and Rawlings, 1998], [Rawlings and Muske, 1993] and [Mayne *et al.*, 2000]. Several notable research books such as [Maciejowski, 2002] and [Rossiter, 2003] provide good description on both theoretical and practical issues associated with MPC technology.

[Odelson, 2003],[Odelson *et al.*, 2007] and [Odelson *et al.*, 2006] proposed a new Auto-covariance Least-Square (ALS) method for estimating noise covariances and proved the superior advantages of ALS method convincingly through comparing with previous work. [Rajamani and Rawlings, 2007] presented the necessary and sufficient conditions for the uniqueness of the covariance estimates, and formulated the optimal weighting.

The most common researches on developing manipulators which possess actuator redundancy are on the application of robotics. The major contributions include the computation approach for inverse dynamics of closed-link mechanisms that contain redundant actuators and their redundancy optimization ([Colbaugh and Glass, 1992], [Nakamura and Ghodoussi, 1989] and [Ohta *et al.*, 2004]). In this thesis, the actuator redundancy is developed by exploring the nonlinearities of the exhaust and inlet system. An optimization system which could not only efficiently utilize the actuators within constraints, but also optimize the energy consumptions is formulated and integrated with the Model Predictive Control scheme. This strategy demonstrates the novel achievement of this thesis and its advantageous potential has been manifested through comparison in presence of wild frequency disturbances.

3.2 State Space Model Formulation

We regard the livestock ventilation system as consisting of two parts by noting that the overall system consists of a static air distribution system (inlet-exhaust air flow system) and a dynamic environmental system (thermal comfort and indoor air quality). The two parts are interconnected through air flow rate. The heating power is switched on when it is necessary but will not be regarded as a manipulated variable in this thesis. The block

diagram of the process models are shown in Fig. 3.1. This strongly coupled Multiple

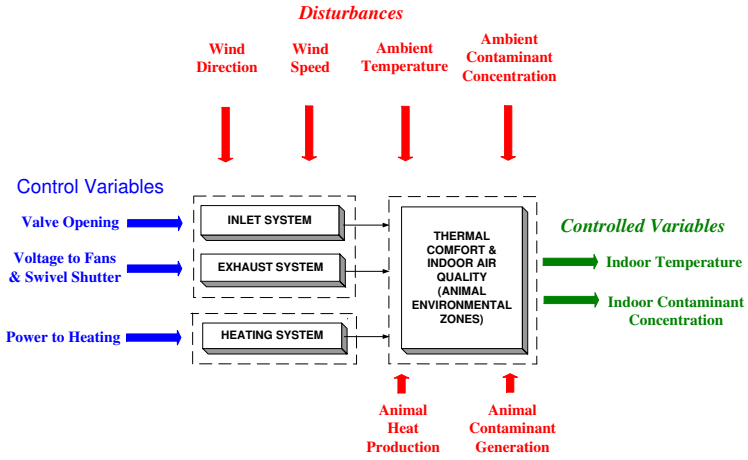

Figure 3.1: Block Diagram of Process Models

Input and Multiple Output (MIMO) dynamic nonlinear system could be expressed as a Linear Time Invariant (LTI) state space representation around the equilibrium points by linearization through Taylor expansion theory. The selection of system operating point is mainly based upon the analysis of dominant inter-zonal airflow patterns.

Let the nonlinear continuous time model represented with three coupled equations for thermal comfort (2.1) be approximated in the discrete time linearized dynamics state space form as (3.1):

$$x_T(k+1) = A_T \cdot x_T(k) + B_T \cdot q(k) + B_{Td} \cdot d_T(k), \tag{3.1a}$$

$$y_T(k) = C_T \cdot x_T(k) + D_T \cdot q(k) + D_{Td} \cdot d_T(k), \tag{3.1b}$$

where, $A_T \in \mathbb{R}^{3\times3}$, $B_T \in \mathbb{R}^{3\times12}$, $B_{Td} \in \mathbb{R}^{3\times8}$, $C_T \in \mathbb{R}^{3\times3}$, $D_T \in \mathbb{R}^{3\times12}$, $D_{Td} \in \mathbb{R}^{3\times8}$ are the coefficient matrices with subscript T denoting the model for the thermal comfort system. k is the current sample number. In the similar procedure, we could derive the state space form for the indoor air quality system as (3.2) according to (2.7):

$$x_C(k+1) = A_C \cdot x_C(k) + B_C \cdot q(k) + B_{Cd} \cdot d_C(k), \tag{3.2a}$$

$$y_C(k) = C_C \cdot x_C(k) + D_C \cdot q(k) + D_{Cd} \cdot d_C(k), \tag{3.2b}$$

where, $A_C \in \mathbb{R}^{3\times3}$, $B_C \in \mathbb{R}^{3\times12}$, $B_{Cd} \in \mathbb{R}^{3\times12}$, $C_T \in \mathbb{R}^{3\times3}$, $D_T \in \mathbb{R}^{3\times12}$, $D_{Td} \in \mathbb{R}^{3\times12}$ are the coefficient matrices with subscript C denoting the model for the concentration system.

By applying the conservation of mass for the livestock building with one single zone concept (2.13), and through linearization of air flow model deducted through (2.9) to

(2.12), we can derive the static equation (3.3).

$$E \cdot \bar{q}(k) + F \cdot u(k) + G \cdot w(k) + K \cdot x_T(k) = 0, \tag{3.3}$$

where, E,F,G,K are coefficients matrices. The definition of $\bar{q} \in \mathbb{R}^{9+1}$ is: $[q_{in,m}, q_{out,n}, P_i]^T$, $m = 1 \cdots 6$, $n = 1 \cdots 3$, where, $[q]^T_{1\times 9} = [q_{in,m}, q_{out,n}]^T$ is a airflow input vector which combines the actuators' signals u and the thermal process controlled variables x_T and x_C.

Connecting and coupling of the airflow model (3.3) with the environmental models (3.1) and (3.2), evolve a finalized LTI state space model representing the entire knowledge of the performances for thermal comfort and indoor air quality around the equilibrium point. The augmented process model is shown in (3.4)

$$x(k+1) = A \cdot x(k) + B \cdot u(k) + B_d \cdot \begin{bmatrix} d_{umd}(k) \\ d_{md}(k) \end{bmatrix}, \tag{3.4a}$$

$$y(k) = C \cdot x(k) + D \cdot u(k) + D_d \cdot \begin{bmatrix} d_{umd}(k) \\ d_{md}(k) \end{bmatrix}, \tag{3.4b}$$

$$z(k) \equiv y(k), \tag{3.4c}$$

where, $A \in \mathbb{R}^{6\times 6}$, $B \in \mathbb{R}^{6\times 9}$, $C \in \mathbb{R}^{6\times 6}$, $D \in \mathbb{R}^{6\times 9}$, $B_d \in \mathbb{R}^{6\times 12}$, $D_d \in \mathbb{R}^{6\times 12}$ are the coefficient matrices. The disturbance transient matrices B_d and D_d are formulated as (3.5) corresponding to the unmeasured and measured disturbances.

$$B_d = \begin{bmatrix} B_{dumd} & B_{dmd} \end{bmatrix}, D_d = \begin{bmatrix} D_{dumd} & D_{dmd} \end{bmatrix}. \tag{3.5}$$

x, z, u, d_{umd}, d_{md} denote the sequences of vectors representing the deviation variable values, where, x is for the process state of zonal temperature x_T and concentration x_C, z is for the controlled output, u is for the manipulated input which consists of the inlet valves opening areas, voltages supplied to the fans and the swivel shutter opening angles, d_{umd} is for the unmeasurable disturbances of animal heat and carbon dioxide generation, d_{md} is for the measurable disturbances as the wind speed, wind direction, ambient temperature and concentration level. y denotes the measured output, and is usually assumed to be same with the controlled output z. The representation of these vectors is shown in (3.6)

$$x = \begin{bmatrix} \bar{T}_1 & \bar{T}_2 & \bar{T}_3 & \bar{C}_{r,1} & \bar{C}_{r,2} & \bar{C}_{r,3} \end{bmatrix}^T_{6\times 1}, \tag{3.6a}$$

$$u = \begin{bmatrix} \bar{A}_{in,i=1\ldots 6} & \bar{V}_{volt,j=1\ldots 3} & \bar{\theta}_{shutter,j=1\ldots 3} \end{bmatrix}^T_{12\times 1}, \tag{3.6b}$$

$$d_{umd} = \begin{bmatrix} \bar{\dot{Q}}_1 & \bar{\dot{Q}}_2 & \bar{\dot{Q}}_3 & \bar{G}_1 & \bar{G}_2 & \bar{G}_3 \end{bmatrix}^T_{6\times 1}, \tag{3.6c}$$

$$d_{md} = \begin{bmatrix} \bar{V}_{ref} & \bar{c}_{P,w} & \bar{c}_{P,l} & \bar{c}_{P,r} & \bar{T}_o & \bar{C}_{r,o} \end{bmatrix}^T_{6\times 1}. \tag{3.6d}$$

The linearized model matrices and the detailed procedure of coupling are described in Appendix A. Through step response analysis and bode plot comparison, we realize

that, the plant nonlinearities are not highly significant. By varying the disturbances such as the zonal heat sources which cause the direction change of the inter zonal airflow, and varying the external temperature which are the leading factors of the variation of the indoor thermal comfort, we obtain similar system behaviors based on a series of LTI models.

Concluded through systematical analysis, the pair (A,B) is controllable, the pair (C,A) is observable, and the plant is stable. Further more, the controlled and manipulated variables are scaled in order to avoid numerical errors in the optimization computation for estimation and control. To do this, decisions are made on the expected magnitude of disturbances and reference changes, on the allowed magnitude of each input signal, and on the allowed deviation of each input ([Skogestad and Postlethwaite, 1996]). The detail on scaling procedure is stated in Appendix B. Thus, the model transformation is accomplished and well prepared for solving of the optimization problem in the following described control strategies.

3.3 Moving Horizon Estimation and Control

Moving horizon estimation and control is implemented through dynamic optimization calculations. These calculations are conducted on-line and repeated each time when new information such as process measurements become available, the horizon of the estimator and the regulator are shifted one sample forward. At each time, the dynamic optimization considers a fixed window backward of the past measurements to estimate the current state of the system, then the estimated state is used in the process model to forecast the process future behavior within a fixed window forward. The dynamic optimization computes the optimal sequence of manipulable variables (control inputs) so that the predicted process behavior is as close to the desired setting reference as possible subject to the physical and operational constraints of the system. Only the first element in the sequence of optimal manipulable variables is implemented on the process. The following Fig. 3.2 (originated from [Jorgensen, 2005]) demonstrates the principle of moving horizon estimation and control expressed as the finite horizon optimization. As the matter of fact, the past and future data outside the window are approximated by a cost-to-arrive and cost-to-go functions which are used to approximately account for the past and future estimation and control respectively. More detailed description and proofs haven been presented by [Rao, 2000] and [Jorgensen, 2005].

3.3.1 Target Calculation

As discussed in [Rao and Rawlings, 1999] and [Rawlings, 2000], the target tracking optimization could be formulated as a least-square objective function subjected to the constraints (see 3.7), in which the steady state target of input u_s and state vector x_s can be determined from the solution of the following computation when tracking a nonzero target vector z_t. The objective of the target calculation is to find the feasible steady states

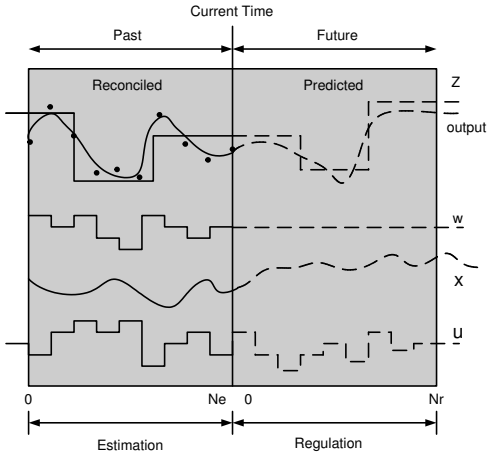

Figure 3.2: Moving Horizon Estimation and Control

(z_s, x_s, u_s) such that z_s and u_s are as close as possible to z_t and u_t, where u_t is the desired value of the input vector at steady state, and, $z_s = Cx_s$.

$$\min_{[x_s,u_s]^T} \Psi = (u_s - u_t)^T R_s (u_s - u_t) \tag{3.7a}$$

$$s.t. \begin{cases} \begin{bmatrix} I-A & -B \\ C & 0 \end{bmatrix} \begin{bmatrix} x_s \\ u_s \end{bmatrix} = \begin{bmatrix} 0 \\ z_t \end{bmatrix} \\ u_{\min} \le u_s \le u_{\max} \end{cases} \tag{3.7b}$$

In this quadratic program, R_s is a positive definite weighting matrix for the deviation of the input vector from u_t. The equality constraints in (3.7) guarantees a steady-state solution and offset free tracking of the target vector. In order to guarantee the uniqueness of the solution through the target calculation, assuming the feasible region is nonempty, the system must be detectable which is also a necessary condition for the nominal stability of the regulator as discussed in the following section [Rao and Rawlings, 1999].

3.3.2 Moving Horizon Control

In [Muske and Rawlings, 1993b], the moving horizon control is formulated as (3.8) by a quadratic cost function on finite horizon subjected to the following linear equality and inequalities formed by the system dynamics (3.4) and constraints on the controlled and

manipulated variables.

$$\min_{u^N} \Phi_k^N = \sum_{j=1}^{N} \frac{1}{2} \left\| z_{k+j} - r_{k+j} \right\|_{Q_z}^2 + \frac{1}{2} \sum_{j=0}^{N-1} \left\| \Delta u_{k+j} \right\|_S^2 + \left\| u_{k+j} - u_s \right\|_R^2, \tag{3.8a}$$

$$s.t. \begin{cases} x_{k+j+1} = Ax_{k+j} + Bu_{k+j} + B_d d_{k+j} \\ z_{k+j} = Cx_{k+j} \\ z_{\min} \leq z_{k+j} \leq z_{\max}, j = 1, 2, \cdots N \\ u_{\min} \leq u_{k+j} \leq u_{\max}, j = 0, 1, \cdots N-1 \\ \Delta u_{\min} \leq \Delta u_{k+j} \leq \Delta u_{\max}, j = 0, 1, \cdots N-1 \end{cases} \tag{3.8b}$$

where, Φ is the performance index to be minimized by penalizing the deviations of the output z_{k+j} from the reference r_{k+j}, the slew rate of actuator Δu_{k+j} and the control input u_{k+j} from the desired steady states u_s at time j. The achievable steady state input vector u_s can be determined from the solution of target calculation. $Q_z \in \mathbb{R}^{6\times6}$ and $S \in \mathbb{R}^{9\times9}$ are symmetric positive semi-definite penalty matrices for process states and rate of input change, $R \in \mathbb{R}^{9\times9}$ is a symmetric positive definite penalty matrix. The vector u^N contains the N future open-loop control moves as shown below

$$u^N = \begin{bmatrix} u_k \\ u_{k+1} \\ \vdots \\ u_{k+N-1} \end{bmatrix}. \tag{3.9}$$

At time $k+N$, the input vector u_{k+j} is set to zero and kept at this value for all $j \geq N$ in the optimization calculation. Since the plant is stable, according to the parametrization method proposed in [Muske and Rawlings, 1993b], the end prediction $z_{k+1} = CAx_k$, implies $z_k = CA^{k-N}x_N$ for $k \geq N$ such that

$$\sum_{k=N}^{\infty} z_k^T Q_z z_k = x_N^T \left(\sum_{k=N}^{\infty} \left(CA^{k-N} \right)^T Q_z CA^{k-N} \right) x_N = x_N^T Q_N x_N, \tag{3.10}$$

in which, (A, B) is stabilizable, and $(A, Q^{1/2}C)$ is detectable, Q_N may be computed from the Lyapunov equation

$$Q_N = \sum_{k=N}^{\infty} \left(CA^{k-N} \right)^T Q_z CA^{k-N} = \sum_{j=0}^{\infty} \left(CA^j \right)^T Q_z CA^j = C^T Q_z C + A^T Q_N A. \tag{3.11}$$

It proved to be clear that the solution generated from the finite horizon optimization formulation with a terminal equality constraint is the approximate solution to the infinite horizon linear quadratic optimal control problem for stable systems. The selection of horizon N has been subject of extensive research ([Muske and Rawlings, 1993a], [Rawlings and Muske, 1993], [Scokaert and Rawlings, 1998], and [Mayne *et al.*, 2000]) and

the topic on the dual-mode receding horizon controller for the nonlinear system is discussed in [Mayne and Michalska, 1990]. Consequently, this regulator formulation could guarantee nominal stability for all choices of tuning parameters satisfying the conditions outlined above.

3.3.3 Moving Horizon Estimation

The linear Moving Horizon Estimation (MHE) solves the constrained linear least square problem expressed as the constrained linear quadratic optimization (3.12). This formulation of MHE was first proposed by [Muske *et al.*, 1993] and [Robertson *et al.*, 1996]. The choice of the moving estimation horizon N allows a trade-off between the accuracy of the estimation and computational requirements.

$$\min_{\left[\hat{x}_{k-N/k},\hat{w}^N\right]} \Psi_k^N = \frac{1}{2}\left\|\hat{x}_{k-N/k} - \bar{x}_{k-N/k-N-1}\right\|^2_{P^{-1}_{k-N/k-N-1}} + \frac{1}{2}\sum_{j=k-N}^{k-1}\left\|w_{j/k}\right\|^2_{Q_w^{-1}} + \left\|v_{j/k}\right\|^2_{R_v^{-1}} \tag{3.12a}$$

$$s.t. \begin{cases} x_{k+j+1} = Ax_{k+j} + Bu_{k+j} + B_d d_{k+j} + Gw_{k+j} \\ z_{k+j} = Cx_{k+j} + v_{k+j} \\ x_{\min} \leq \hat{x}_{k-N/k} \leq x_{\max} \\ w_{\min} \leq \hat{w}_k \leq w_{\max} \\ z_{\min} \leq z_k \leq z_{\max} \end{cases} \tag{3.12b}$$

The estimator selects the state $x_{(k-N/k)}$, a sequence of process noise $\left\{w_{j/k}\right\}_{j=k-N}^{k}$ and a sequence of measurement noise $\left\{v_{j/k}\right\}_{j=k-N}^{k}$ such that the agreement with the measurement $\left\{y_{j/k}\right\}_{j=k-N}^{k}$ is as good as possible while still respecting the process dynamics, the output relation, and the constraints. The process noise w and measurement noise v are assumed to be uncorrelated zero-mean Gaussian processes with the covariances of Q_w and R_v as 3.13 (a), and the initial condition is as 3.13 (b), with the initial estimation error covariance $P_{k-N/k-N-1}$.

$$\begin{bmatrix} w \\ v \end{bmatrix} \sim \mathrm{N}\left(\begin{bmatrix} 0 \\ 0 \end{bmatrix}, \begin{bmatrix} Q_w & 0 \\ 0 & R_v \end{bmatrix} \right), \tag{3.13a}$$

$$x_{k-N/k-N-1} \sim \mathrm{N}\left(\bar{x}_{k-N/k-N-1}, \quad P_{k-N/k-N-1} \right). \tag{3.13b}$$

The symmetric positive definite weighting matrices R_v^{-1}, Q_w^{-1} and $P^{-1}_{k-N/k-N-1}$ are quantitative measures of our confidence in the output model, the dynamic system model and the initial estimate, respectively. As described in [Rao and Rawlings, 2000], [Rao, 2000], [Tenny, 2002], and [Rao and Rawlings, 2002], the covariance $P_{k-N/k-N-1}$ is derived by

the solution of the Lyapunov Equation $P_{k-N/k-N-1} = \bar{A}^T P_{k-N/k-N-1}\bar{A} + \bar{G}^T \bar{Q}\bar{G}$, in which,

$$\bar{A} = \begin{bmatrix} A - ALC \end{bmatrix}, \bar{G} = \begin{bmatrix} G & -AL \end{bmatrix}, \bar{Q} = \begin{bmatrix} Q_w & 0 \\ 0 & R_v \end{bmatrix}. \tag{3.14}$$

$(\bar{A}, \bar{Q}^{1/2})$ is stabilizable.

To achieve offset-free control of the output to their desired targets at steady state, in the presence of plant/model mismatch and/or unmeasured disturbances, the system model expressed in (3.4) is augmented with an integrated disturbance model as proposed in [Muske and Badgwell, 2002] and [Pannocchia and Rawlings, 2003] to form an augmented moving horizon estimator. The dynamics of the disturbance model will be the stochastic generation process of animal heat and contaminant gas. The resulting augmented system with process noise n_w and measurement noise n_v is

$$\tilde{x}(k+1) = \tilde{A}\tilde{x}(k) + \tilde{B}u(k) + \tilde{G}n_w(k), \tag{3.15a}$$
$$y(k) = \tilde{C}\tilde{x}(k) + n_v(k), \tag{3.15b}$$
$$n_w(k) \sim \mathrm{N}(0, Q_w(k)), \tag{3.15c}$$
$$n_v(k) \sim \mathrm{N}(0, R_v(k)), \tag{3.15d}$$

in which the augmented state and system matrices are defined as follows,

$$\begin{aligned} \tilde{x}(k) &= \begin{bmatrix} x(k) \\ x_{umd}(k) \end{bmatrix}_{12\times 1}, \tilde{A} = \begin{bmatrix} A & B_{dumd}C_{dumd} \\ 0 & A_{dumd} \end{bmatrix}_{12\times 12}, \\ \tilde{B} &= \begin{bmatrix} B \\ 0 \end{bmatrix}_{12\times 12}, \tilde{C} = \begin{bmatrix} C & 0 \end{bmatrix}_{6\times 12}, \tilde{G} = \begin{bmatrix} B_{dmd} & 0 \\ 0 & B_{dumd} \end{bmatrix}_{12\times 12}. \end{aligned} \tag{3.16}$$

In this model, the original process state $x \in \mathbb{R}^6$ is augmented with the integrated unmeasurable disturbance state $x_{umd} \in \mathbb{R}^6$. A new Auto-covariance Least Square (ALS) method is applied to recover the covariances of unknown noises, and adaptively determine the penalty in the moving horizon estimation objective function. [Rajamani and Rawlings, 2007] presented the necessary and sufficient conditions for the uniqueness of the covariance estimates, and formulated the optimal weighting. The detectability of the augmented system in (3.15) is guaranteed when the condition holds ([Pannocchia and Rawlings, 2003]):

$$Rank \begin{bmatrix} (I - \tilde{A}) & -\tilde{G} \\ \tilde{C} & 0 \end{bmatrix} = n + s_d, \tag{3.17}$$

in which, n is the number of the process states, s_d is the number of the augmented disturbance states. This condition ensures a well-posed target tracking problem. This methods for checking detectability and proofs are provided in [Muske and Badgwell, 2002] and [Pannocchia and Rawlings, 2003].

For time varying reference tracking, a reference model with the reference state x_r could be augmented into the system 3.16 as shown in 3.18.

$$\tilde{x}(k) = \begin{bmatrix} x(k) \\ x_{umd}(k) \\ x_r(k) \end{bmatrix}_{18\times 1}, \tilde{A} = \begin{bmatrix} A & B_{dumd}C_{dumd} & 0 \\ 0 & A_{dumd} & 0 \\ 0 & 0 & I \end{bmatrix}_{18\times 18}, \\ \tilde{B} = \begin{bmatrix} B \\ 0 \\ 0 \end{bmatrix}_{18\times 12}, \tilde{C} = \begin{bmatrix} C & 0 & 0 \end{bmatrix}_{6\times 18}, \tilde{G} = \begin{bmatrix} B_{dmd} & 0 \\ 0 & B_{dumd} \\ 0 & 0 \end{bmatrix}_{18\times 12}. \tag{3.18}$$

An alternative way of tracking time varying reference through dynamic optimization is to combine the reference model with the reformulated system with Δu-form as 3.19, as has been stated in [Kvasnica *et al.*, 2004].

$$\begin{bmatrix} \tilde{x}(k+1) \\ x_{md}(k+1) \\ u(k) \\ x_r(k+1) \end{bmatrix} = \begin{bmatrix} \tilde{A} & B_d C_{md} & \tilde{B} & 0 \\ 0 & A_{md} & 0 & 0 \\ 0 & 0 & I & 0 \\ 0 & 0 & 0 & I \end{bmatrix} \cdot \begin{bmatrix} \tilde{x}(k) \\ x_{md}(k) \\ u(k-1) \\ x_r(k) \end{bmatrix} + \begin{bmatrix} \tilde{B} \\ 0 \\ I \\ 0 \end{bmatrix} \cdot \Delta u(k) \tag{3.19}$$

For moving horizon estimation and control, the quadratic programming formulations are summarized as in Appendix B.

The block diagram of the moving horizon estimation and control is illustrated in Fig. 3.3, where the regulator and estimator are implemented through the moving horizon approach, the covariances of the state and output noise are determined by a adaptive estimator with the Auto-covariance Least-Square (ALS) method. The evolving procedure of this method is discussed in section 3.4.

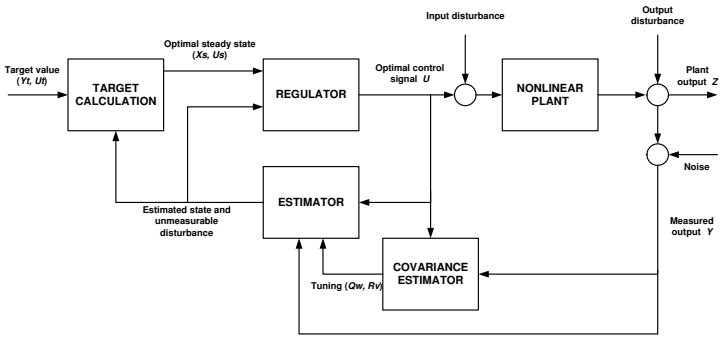

Figure 3.3: Block Diagram of the Entire Dynamic Control System

3.3.4 Unconstrained Infinite Horizon Optimization

The feedback gain of moving horizon control derived from the unconstrained linear quadratic optimization with terminal cost penalty, together with the estimator gain derived from Kalman Filter provide the framework for analyzing properties such as the stability and bandwidth of the system in frequency domain. The formulation of finite horizon quadratic programming without constraint has been discussed in [Rawlings and Muske, 1993] for stability analysis and briefly described as follows:

$$\min_{u^N} \Phi_k^N = \frac{1}{2} {u^N}^T H u^N + g^T u^N \tag{3.20}$$

in which, $H = \Gamma^T Q_z \Gamma + H_S$ is the hessian matrix, $g = M_{x_0} x_0 + M_R R + M_{u_{-1}} u_{-1} + M_D D$, $M_{x_0} = \Gamma^T Q_z \Phi$, $M_R = -\Gamma^T Q_Z$, $M_D = \Gamma^T Q_z \Gamma_D$

$$\begin{aligned}
\Phi &= \begin{bmatrix} C_z A \\ C_z A^2 \\ \vdots \\ C_z A^N \end{bmatrix}, \Gamma = \begin{bmatrix} H_1 & 0 & 0 & \cdots & 0 \\ H_2 & H_1 & 0 & \cdots & 0 \\ H_3 & H_2 & H_1 & & 0 \\ \vdots & \vdots & \vdots & \ddots & \vdots \\ H_N & H_{N-1} & H_{N-2} & \cdots & H_1 \end{bmatrix} \\
\Gamma_D &= \begin{bmatrix} H_{1,d} & 0 & 0 & \cdots & 0 \\ H_{2,d} & H_{1,d} & 0 & \cdots & 0 \\ H_{3,d} & H_{2,d} & H_{1,d} & & 0 \\ \vdots & \vdots & \vdots & \ddots & \vdots \\ H_{N,d} & H_{N-1,d} & H_{N-2,d} & \cdots & H_{1,d} \end{bmatrix}, \\
H_S &= \begin{bmatrix} 2S & -S & & \cdots & 0 \\ -S & 2S & -S & \cdots & \vdots \\ & & \ddots & & \\ \vdots & \cdots & -S & 2S & -S \\ 0 & \cdots & & -S & S \end{bmatrix}, M_{u_{-1}} = - \begin{bmatrix} S \\ 0 \\ 0 \\ 0 \\ 0 \end{bmatrix}.
\end{aligned} \tag{3.21}$$

where,$H_i = CA^{i-1}B, H_{i,d} = CA^{i-1}B_d$, for $1 \le i \le N$. The optimal u^N could be found by taking gradient of Φ_k and set it to zero. The first control move u_k at current time k will be applied to the plant.

$$u_k = K_{MPC} \cdot \begin{bmatrix} x_0 \\ R \\ u_{-1} \\ D_d \end{bmatrix}, \tag{3.22}$$

where, S_H is the square root of the hessian matrix $H = {S_H}^T S_H$

$$ {S_H}^T S_H K_{x0} = -M_{x0}, \tag{3.23a} $$

$$ {S_H}^T S_H K_R = -M_R, \tag{3.23b} $$

$$ {S_H}^T S_H K_{u-1} = -M_{u-1}, \tag{3.23c} $$

$$ {S_H}^T S_H K_D = -M_D. \tag{3.23d} $$

Therefore,

$$ K_{full} = \begin{bmatrix} K_{x0} & K_R & K_{u-1} & K_D \end{bmatrix}, \tag{3.24} $$

and,

$$ K_{MPC} = K_{full}(1:\ell,:). \tag{3.25} $$

Figure 3.4 demonstrates the structure of the entire feedback control system with estimator and the control law described in 3.22 with derived feedback gain 3.24.

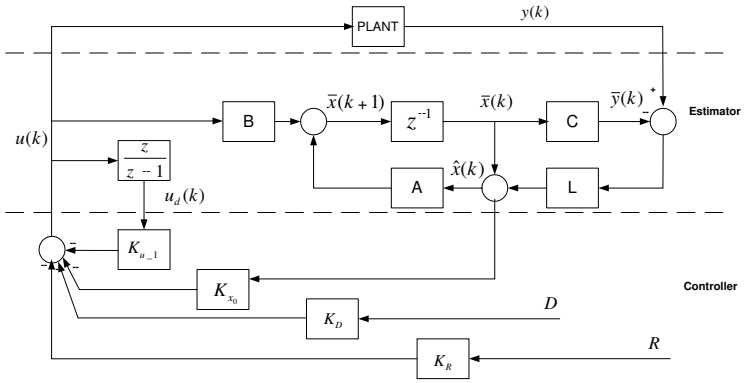

Figure 3.4: Structure of the Feedback Control System

As has been discussed in [Rawlings and Muske, 1993] and [Scokaert, 1997], the feedback gain F_N derived from the infinite-horizon Linear Quadratic (LQ) optimal control by solving the discrete recursive Algebraic *Riccati* Equation (ARE) (3.26) can also be an alternative way of ensuring a stable (unconstrained) predictive control law, as long as the ARE or the so-called Fake Algebraic Riccati Equation (FACE) as proposed in [Maciejowski, 2002], has a solution Π_N which is positive semi-definite.

$$ F_N = -\left[B^T \Pi_N B + R\right]^{-1} B^T \Pi_N A, \tag{3.26a} $$

$$ \Pi_N = A^T \Pi_N A + Q - A^T \Pi_N B \left[B^T \Pi_N B + R\right]^{-1} B^T \Pi_N A. \tag{3.26b} $$

[Wu *et al.*, 2005] presents the description and comparative simulation results of the application of LQ optimal control for indoor climate in livestock building.

3.4 Auto-covariance Least-Square Method

The ALS technique is not only expected to adaptively give an optimal estimator gain, but also to improve the closed loop performance in the presence of disturbances and model/plant mismatch. The technique described in this section is originated in [Odelson *et al.*, 2007] and [Odelson *et al.*, 2006], and the corresponding software tool-box is developed by J.B.Rawlings and M.R.Rajamani. Consider the LTI discrete-time model of the augmented system as (3.16), estimates of the states of the system are constructed using the standard Kalman filter as (3.27)

$$\hat{x}_{k+1/k} = A\hat{x}_{k/k-1} + Bu_k + AL_k(y_k - C\hat{x}_{k/k-1}). \tag{3.27}$$

The estimate error is defined as $\varepsilon_k = x_k - \hat{x}_{k/k-1}$, with covariance $P_{k/k-1}$. This covariance $P_{k/k-1} = E\left[\varepsilon_k \varepsilon_k^T\right]$ is the solution to the Riccati equation (3.28)

$$\begin{aligned} P_{k+1/k} = {} & AP_{k/k-1}A^T + GQ_wG^T \\ & - AP_{k/k-1}C^T\left[CP_{k/k-1}C^T + R_v\right]^{-1}CP_{k/k-1}A^T, \end{aligned}$$

and the Kalman gain L_k is defined as (3.28)

$$L_k = P_{k/k-1}C^T\left[CP_{k/k-1}C^T + R_v\right]^{-1}. \tag{3.28}$$

Assume we process the y_k to obtain state estimates using a linear filter with gain L, which is not necessarily the optimal L for the system. The state estimation error ε_k evolves according to (3.29)

$$\varepsilon_{k+1} = (A - ALC)\varepsilon_k + \begin{bmatrix} G & -AL \end{bmatrix}\begin{bmatrix} w_k \\ v_k \end{bmatrix}. \tag{3.29}$$

The state space model of the innovations $\mathscr{Y} = y_k - C\hat{x}_{k/k-1}$ is defined as (3.30)

$$\varepsilon_{k+1} = \bar{A}\varepsilon_k + \bar{G}\bar{w}_k, \tag{3.30a}$$

$$\mathscr{Y}_k = C\varepsilon_k + v_k, \tag{3.30b}$$

in which,

$$\bar{A} = \left[A - ALC\right]_{n\times n}, \bar{G} = \begin{bmatrix} G & -AL \end{bmatrix}_{n\times(g+p)}, \bar{w} = \begin{bmatrix} w_k \\ v_k \end{bmatrix}_{(g+p)\times 1}. \tag{3.31}$$

n is the number of states in (3.16), p is the number of outputs, g is the number of independent noises. (A,C) is detectable, $\bar{A} = A - ALC$ is stable, the initial estimate error is distributed with mean m_0 and covariance P_0^-. We choose k sufficiently large so that the effects of the initial condition can be neglected, or equivalently, we choose the steady-state distribution as the initial condition:

$$E(\varepsilon_0) = m_0 = 0, \mathrm{cov}(\varepsilon_0) = P_0^- = P^-. \tag{3.32}$$

Now we consider the auto-covariance which is defined as the expectation of the data with some lagged version of itself [Jenkins and Watts, 1968]

$$\mathscr{C}_j = E\left[\mathscr{Y}_k \mathscr{Y}_{k+j}^T\right], \tag{3.33}$$

and the symmetric auto-covariance matrix (ACM) is then defined as (3.34)

$$\mathscr{R}(N_a) = \begin{bmatrix} \mathscr{C}_0 & \cdots & \mathscr{C}_{N-1} \\ \vdots & \ddots & \vdots \\ \mathscr{C}_{N_a-1}^T & \cdots & \mathscr{C}_0 \end{bmatrix}, \tag{3.34}$$

where, N_a is the user-defined number of lags used in ACM. Accordingly, an ACM of the innovations can be written as follows:

$$\begin{aligned} [\mathscr{R}(N_a)]_s = &\left[(\mathscr{O}\otimes\mathscr{O})(I_{n^2} - \bar{A}\otimes\bar{A})^{-1} + (\Gamma\otimes\Gamma)\mathscr{I}_{n,N_a}\right](G\otimes G)(Q_w)_s \\ &+ \left\{\left[(\mathscr{O}\otimes\mathscr{O})\left(I_{n^2} - \bar{A}\otimes\bar{A}\right)^{-1} + (\Gamma\otimes\Gamma)\mathscr{I}_{n,N_a}\right](AL\otimes AL)\right. \\ &\left. + \left[\Psi\oplus\Psi + I_{p^2N^2}\right]\mathscr{I}_{p,N_a}\right\}(R_v)_s, \end{aligned} \tag{3.35}$$

in which

$$\mathscr{O} = \begin{bmatrix} C \\ C\bar{A} \\ \vdots \\ C\bar{A}^{N_a-1} \end{bmatrix}, \Psi = \Gamma\left[\bigoplus_{j=1}^{N_a}(-AL)\right], \Gamma = \begin{bmatrix} 0 & 0 & 0 & 0 \\ C & 0 & 0 & 0 \\ \vdots & \ddots & \vdots & \vdots \\ C\bar{A}^{N_a-2} & \cdots & C & 0 \end{bmatrix}. \tag{3.36}$$

$\mathscr{I}_{n,N_a}$ is a permutation matrix that converts the direct sum to a vector, i.e. $\mathscr{I}_{n,N_a}$ is the $(pN_a)^2 \times p^2$ matrix of zeros and ones satisfying

$$\left(\bigoplus_{i=1}^{N_a} R_v\right)_s = \mathscr{I}_{p,N_a}(R_v)_s, \tag{3.37}$$

where, the subscript s denotes the outcome of applying the *vec* operator. Practically, the estimate of the auto-covariance from real data is computed as

$$\hat{\mathscr{C}}_j = \frac{1}{N_d - j}\sum_{i=1}^{N_d-j}\mathscr{Y}_i\mathscr{Y}_{i+j}^T, \tag{3.38}$$

where, N_d is the sample size. Therefore, the estimated ACM $\hat{\mathscr{R}}(N)$ is analogously defined using the computed $\hat{\mathscr{C}}_j$.

We define the ALS estimate as

$$\hat{x} = \left[(\hat{Q}_w)_s^T(\hat{R}_v)_s^T\right]^T = \arg\min_x \left\|\mathscr{A}\cdot\hat{x} - \hat{\mathscr{R}}(N_a)_s\right\|_2^2, \tag{3.39}$$

and the solution for estimating Q_w, R_v is the well-known

$$\hat{x} = (\mathscr{A}^T \mathscr{A})^{-1} \mathscr{A}^T \cdot \hat{b}, \tag{3.40}$$

where, $\mathscr{A}$ indicates the left hand side matrix to the least square problem, and

$$\mathscr{A} = \left[D(G \otimes G) \quad D(AL \otimes AL) + \left[\Psi \oplus \Psi + I_{p^2 {N_a}^2} \right] \mathscr{I}_{p,N_a}, \right] \tag{3.41}$$

$$D = \left[(\mathscr{O} \otimes \mathscr{O})(I_{n^2} - \bar{A} \otimes \bar{A})^{-1} + (\Gamma \otimes \Gamma) \mathscr{I}_{n \times N_a} \right], \tag{3.42}$$

$$x = \left[\begin{array}{cc} (Q_w)_s^T & (R_v)_s^T \end{array} \right]^T, b = \mathscr{R} N_{as}. \tag{3.43}$$

The uniqueness of the estimate is a standard result of least-squares estimation [Lawson and Hanson, 1995]. The covariance can be found uniquely when the matrix $\mathscr{A}$ has full column rank. However, in the augmented system as (3.16), the dimension of the driving noise is $w \in \Re^{11}$, according to [Odelson *et al.*, 2007] and [Odelson *et al.*, 2006], it is unlikely to find unique estimates of the covariance (Q_w, R_v), and the solution may not be positive semi-definite. In order to avoid leading to any meaningless solution, adding the semi-definite constraint directly to the estimation problem to maintain a convex program as (3.44) will ensure uniqueness of the covariance estimation.

$$V = \min_{Q_w, R_v} \left\| \mathscr{A} \left[\begin{array}{c} (Q_w)_s \\ (R_v)_s \end{array} \right] - \hat{b} \right\|_2^2 \tag{3.44a}$$

$$s.t. \left\{ \begin{array}{l} Q_w \geq 0 \\ R_v \geq 0 \end{array} \right. \tag{3.44b}$$

The constraints in (3.44) are convex, and the optimization is in the form of a semi-definite programming (SDP) problem, which can be solved efficiently with Newton's method [Nocedal and Wright, 1999].

3.5 Actuator Redundancy

Concerning the major source of energy consumption which is from the exhaust fan system, and the presence of high frequency component of wind speed variation, an actuator redundancy is exploited to accommodate the limitation of the bandwidth of the closed-loop system as well as pursuit of an optimum energy solution through on-line optimization computation. From the overview of the entire control structure for the livestock indoor climate system as shown in Fig. 3.5, the introduced actuator redundancy is integrated with the feedback dynamic control loop as shown in Fig. 3.3, and implemented in a feed-forward approach. The addition of actuator redundancy improves the system output response to input disturbance - wind speed variation by adjusting the system bandwidth, without influencing the stability of the entire control system. The redundancy optimization takes the optimal control command generated from the dynamic controller as the

reference, and the actuators' limitation as the hard constraints. The objective is to optimize the rotating speed of the impeller and the opening angle of the shutter, so that the energy consumption is minimized and the wind gust is attenuated.

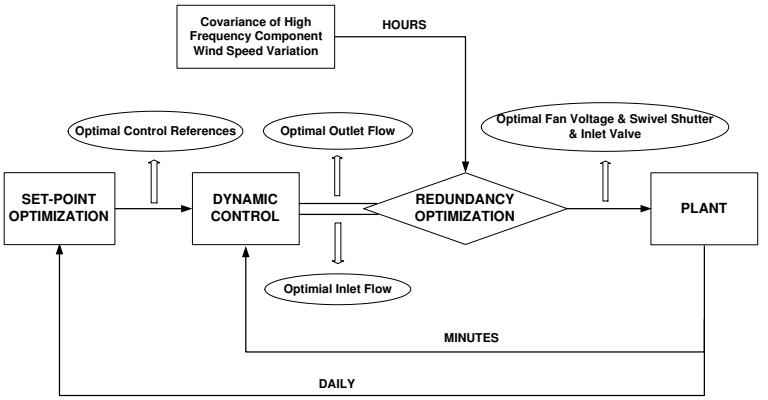

Figure 3.5: Structure of the Entire Control System with Moving Horizon Control and Actuator Redundancy

Based on the energy consumption consideration, and the analysis of the exhaust unit characteristics which possesses the actuator redundancy, a constrained nonlinear optimization is formulated as (3.45), to solve the exhaust system redundancy problem, in which the stage cost is the quadratic function with quadratic terms and the equality constraint is the nonlinear algebraic equation of the exhaust system. By assigning different weights in the objective function which is based on energy consumption considerations, according to the covariance of the high frequency disturbances, the modified optimal control command are reassigned to the actuators.

$$\min_{[V,\theta]^T} \mathrm{E}_k = \|V_k\|^2_{Q_V} + \|\theta_k\|^2_{\sigma \cdot R_\theta} \tag{3.45a}$$

$$s.t. \begin{cases} \Delta P = (b_0 + b_1\theta + b_2\theta^2)q^2 + a_0V^2 + a_1qV + a_2q^2 \\ V_{\min} \le V \le V_{\max} \\ \theta_{\min} \le \theta \le \theta_{\max} \end{cases} \tag{3.45b}$$

Q_V and R_θ are symmetric positive definite matrices. σ represents the covariance of the high frequency component of wind speed variation. The wind speed signal is processed with digital filters. σ is the adjusting factor for assigning different penalties on the energy associated decision variable supplied voltage V_k and the wind gust attenuation variable shutter opening angle R_θ. The cost function and the nonlinear characteristic curve of the constraints for the exhaust fan unit are demonstrated in Fig. 3.6. This redundancy affords flexible and adaptable operating behavior of the exhaust system, so that the goal

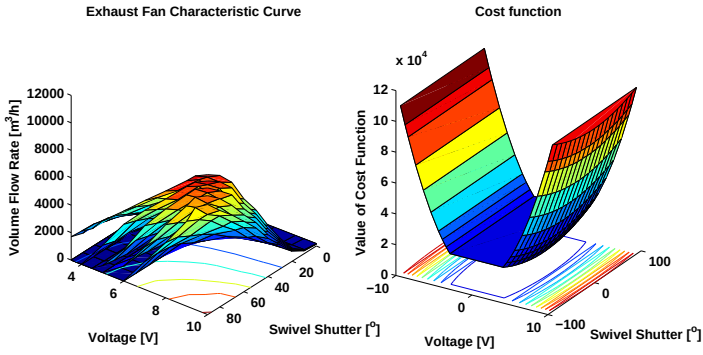

Figure 3.6: (a) Nonlinear Equality Constraints (b) Cost Function

of optimizing energy use, increasing the efficiency of actuator utilization and rejecting the disturbances, are achieved.

Fig. 3.7 depicts the base for optimum point searching trajectory. The surface is derived with a constant pressure difference across the exhaust fan unit, and the contour lines represent the different air volume flow rate through the unit. In order to guarantee a comfort indoor climate, the demand certain ventilation rate is calculated through the dynamic controller, then, the redundancy optimization is to attain the optimal point through moving along a specific line at a specific surface.

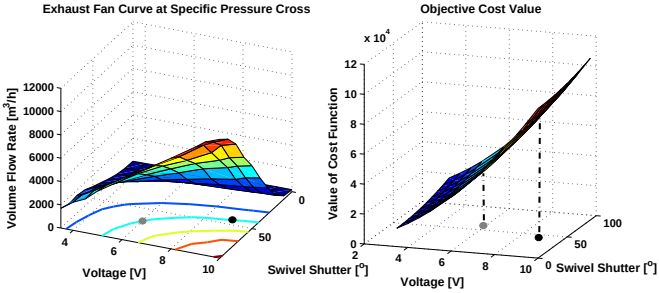

Figure 3.7: Redundancy Optimization for Optimal Actuator Operating Behavior

This strategy enhances the resilience of the control system to disturbances beyond its bandwidth, strengthens the system with the passive disturbance attenuation, and reduces energy consumption through on-line optimization. The same strategy can be applied for the redundancy optimization of the inlet system as well. The objective is to compromise between rejecting the wind gust on the windward side, reducing draft and guaranteeing a

comfort air velocity around the animals. The cost function and constraints are formulated as

$$\min_{[A_w,A_l]^T} \mathrm{A}_k = \|A_w\|^2_{Q_{A_w}} + \|A_l\|^2_{\gamma \cdot R_{A_l}} \tag{3.46a}$$

$$s.t. \begin{cases} \sum_{i=1}^{6} q_{in}(k) \cdot \rho_o - \sum_{j=1}^{3} q_{out}(k) \cdot \rho_i = 0 \\ q_{in} = C_d \cdot A \cdot \sqrt{\frac{2 \cdot \Delta P_{in}}{\rho}} \\ A_{w,\min} \leq A_w \leq A_{w,\max} \\ A_{l,\min} \leq A_l \leq A_{l,\max} \end{cases} \tag{3.46b}$$

where, the adjusting factor γ represents the covariance of the high frequency wind gust. This factor allows for determining the penalty on the inlet valve opening area on different side walls. The system is subjected to the mass balance equation, the inlet system dynamic model and the hard limitation of the actuators. It would be necessary to consider the air inlet jet trajectory involving the calculation of air velocity decay and trajectory/penetration length which has been investigated by [Heiselberg and Nielsen, 1996], into the constraints.

The expected results will be the optimum inlet flaps opening angles, such that the windward inlets will be able to protect against wind gust, and the leeward inlets will be adjusted to satisfy the required ventilation rate. The control behavior of inlet system is optimized with respect to the constraints, and the animal comfort is assured without causing too much draft.

3.6 Application and Results

To demonstrate the advanced potential of the proposed estimation, control and optimization methodologies, the application for the livestock indoor climate and derived simulation results are analyzed. The sampling time step is $T_s = 120(s)$, the prediction horizon is $N = 20$.

3.6.1 Off-set Free Tracking and Disturbance Rejection for MIMO System

Fig. 3.8 depicts the dynamic performance of indoor zonal temperature and concentration level, in presence of step and pulse changes of the external temperature and variation of contaminant gas concentration, large covariances of wind speed variation and different zonal heat sources. Fig. 3.9 shows the corresponding actuator behaviors with the emphasizes on the comparison of the exhaust unit with and without implementing redundancy optimization.

Analyzed from the results, with a step change of the reference value, the indoor zonal temperatures keep tracking the reference with slight variations, the zonal concentration

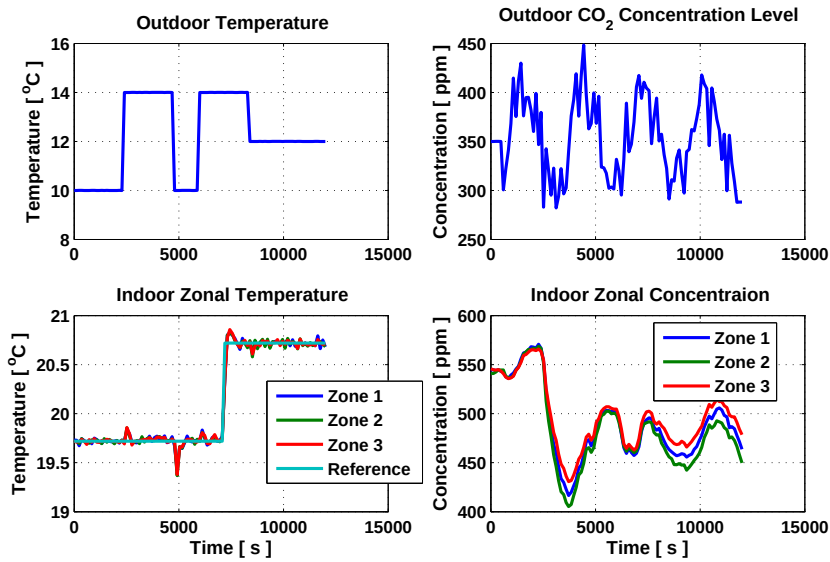

Figure 3.8: Reference Tracking and Rejection of Deterministic Disturbance. Dynamic Performances of Zonal Temperature and Concentration

level vary with the change of the actuators and stay below the limitation. The voltage and swivel shutter rise and fall in response to the onset and cease with the variation of external weather condition. The inlet valve openings on the windward and leeward side are adjusted differently according to the horizontal heating load difference. The functionality of fans is same in each one of the zone, thus one of them is picked up for demonstration. These results clarify the advantages of the actuator redundancy together with the moving horizon estimation and control scheme in handling constraints, improving output performances, attenuating disturbances with wide frequency range, and fulfilling off-set free tracking for multi-variable system.

3.6.2 Comparison of Closed-loop System with and without Actuator Redundancy

Fig. 3.10 (a) shows the wind speed disturbances and its low and high frequency components. Fig. 3.10 (b) compares the effect of the operating behavior for exhaust unit with and without the actuator redundancy.

The comparison of the control signals for exhaust unit manifests the substantial improvement of the actuators behavior and the increase of the efficiency of actuators utilization by applying redundancy optimization on pursuing optimum energy consumption

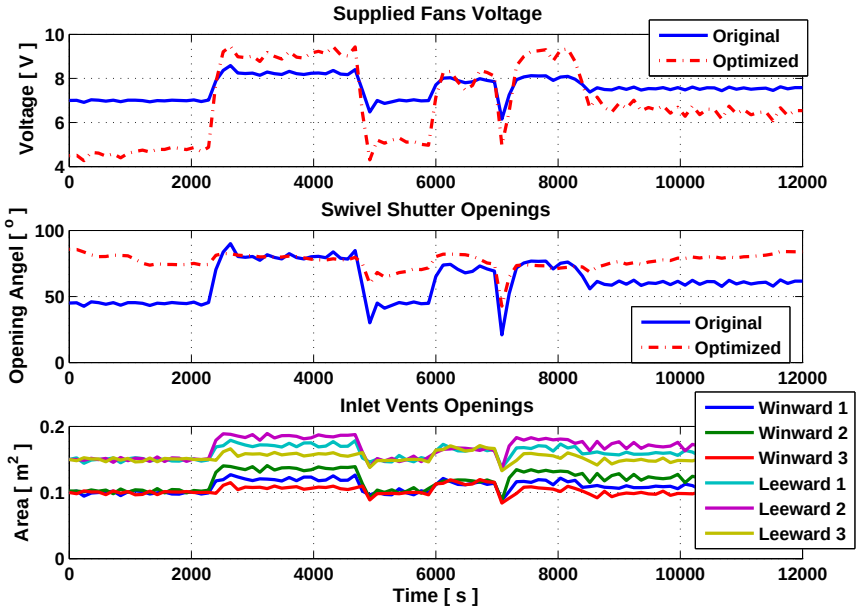

Figure 3.9: Optimal Control Signals. Solid line (without Actuator Redundancy); Dashed dot line (with Actuator Redundancy)

and attenuation of high frequency wind variation. From the economic point of view, this improvement means saving of energy - lowering cost.

3.6.3 Comparison of Moving Horizon Estimation and Kalman Filter in Output Performance

Seen from Fig. 3.11, the output performance have been modified with moving horizon approximations in presence of unmeasured disturbances and noises from both system and measurement. The simulation results convincingly confirm the value of applying moving horizon estimation and the advantages over the nominal Kalman Filter.

3.6.4 Comparison of Closed-loop System with and without ALS method

The advantages of using ALS method in process of estimation over the nominal way, is illustrated in Fig. 3.12 accompanied with the comparison of actuator's actions (see

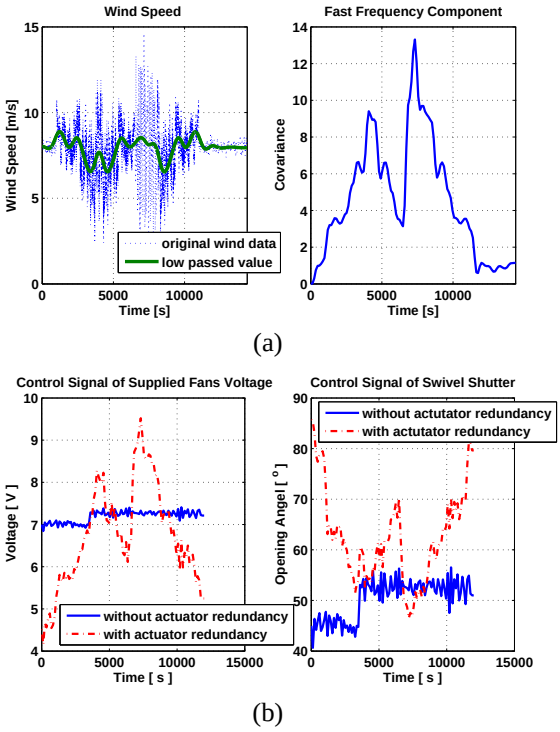

Figure 3.10: (a) Wind Speed Disturbance and the Amplitude of its High Frequency Components (covariance) (b) Comparison of the Control Signal of Exhaust Fan System

Fig. 3.13), assuming that the real covariances are difficult to know and cost a lot of trial and error tuning effort. The result is derived with a step change of un-modeled output disturbance which could account for the model/plant mismatch. The initial assumption for the state noise covariance $Q_w = 0.01$ and the measurement noise $R_v = 0.001$. The data set used for computation is collected from open loop nonlinear plant simulation. Let $N_a = 12$ and $N_d = 200$.

The comparison of output performance in Fig. 3.12, prove that with ALS estimator, the regulator is able to reject the un-modeled disturbances and tracking the reference faster and further reduce the steady state variances. The histogram in Fig. 3.13, show that the improved closed loop performance does not require more aggressive manipulated inputs through using ALS estimator.

The covariance estimation techniques are based on the properties of the process innovations. Implementing ALS has high potential for improving the quality of estimation. This may be illustrated as Fig. 3.14 by comparing the innovations $\mathscr{Y} = y_k - C\hat{x}_{k/k-1}$ for ALS with that of an nominal estimator.

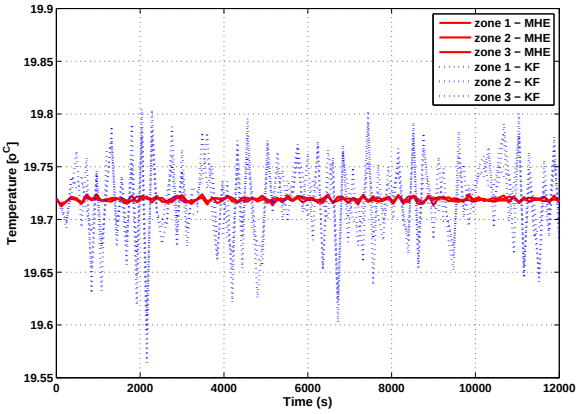

Figure 3.11: Comparison of the System Performances with MHE technique vs. Nominal Kalman Filter Method

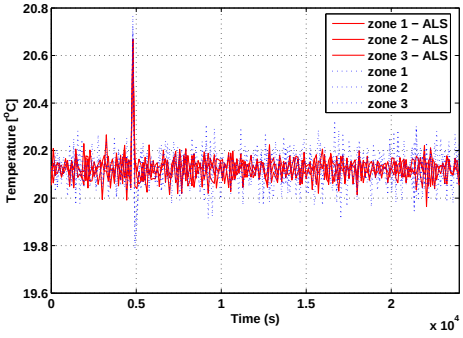

Figure 3.12: Comparison of Closed loop Performances for Set-point Tracking with ALS and Nominal Estimator

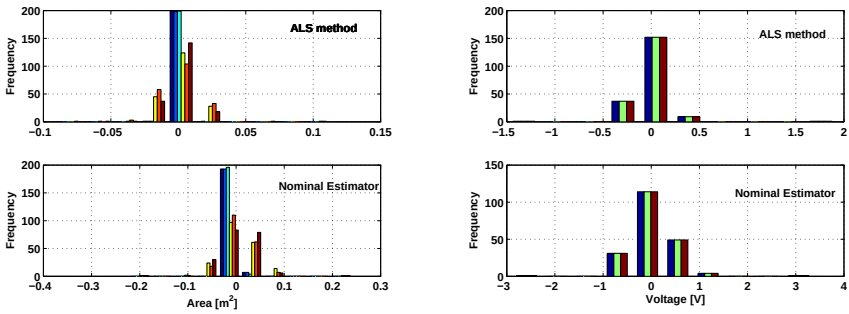

Figure 3.13: Histogram of the Changes in Manipulated Inputs - (a) Inlet Vent Openings (b) Supplied Fan Voltages

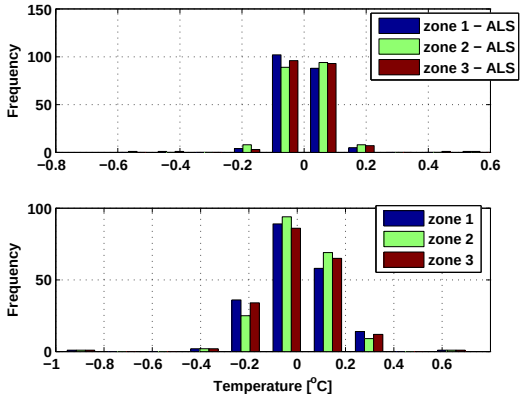

Figure 3.14: Histogram of the Innovations with ALS method and Nominal Estimator

3.7 Conclusion

Through demonstration and comparison both for output performances and actuators behaviors, we could recognize that with the moving horizon estimation and control implemented through on-line dynamic optimization for the Multiple Input and Multiple Output (MIMO) system, the output behavior has been profoundly modified, and the variance of the output has been reduced considerably. The utilization of actuators is optimized and increased with a actuator redundancy optimization, thus the optimal system performance is guaranteed with a low energy consumption approach. The estimation with ALS method plays an important role in rejecting the model/plant mismatch or the un-modeled disturbances, lowering output variances through a least-square approximating formulation.

Consequently, the optimization based estimation and control algorithm together with the actuator redundancy scheme are very effective in improving the system performance, increasing asset utilization, handling constraints, and allowing trade off between the energy consumption and indoor environment, and leads to the ultimate goal - the balance between the cost (energy/fuel) and quality (productivity).

Chapter 4

Conclusions

This part contains a discussion of the major contributions, the conclusion of the thesis and the perspectives.

4.1 Contributions of this Thesis

The following summarizes the main contributions of this thesis.

A Multi-zone Climate Model A multi-zone climate model concept is proposed based on the mass and energy balance equation to capture a better prediction of the horizontal variation of the temperature and contaminant concentration, according to the localization of sensors and dominant airflow distribution. This zone-based model takes into account the inter-zonal airflow which is usually neglected by applying the traditionally single zone model method, and most importantly, it units the simplicity and sufficiency for control oriented purpose of MIMO system instead of using e.g. the complex and time consuming Computer Fluid Dynamic (CFD) analysis approach. The model was first proposed in [Wu *et al.*, 2005] of Chapter 5.

State Space Representation and Linear Quadratic Optimal Control Through linearization and coupling, a Linear Time Invariant (LTI) state space representation describing the entire knowledge of the thermal comfort, air quality and hybrid ventilation system is derived to be adaptive to the multi-variable optimal control, such as the Linear Quadratic Regulation (LQR) as has been published in [Wu *et al.*, 2005] of Chapter 5 and the Model Predictive Control (MPC) as has been published in [Wu *et al.*, 2006] of Chapter 6. In the algorithm of constrained optimization, the actuator saturation, objective criterion and process noise are considered.

Model Predictive Control for Multiple Objectives Off-set free tracking, disturbance rejection and model/plant mismatch compensation for multiple objective optimization are achieved through target calculation, receding horizon regulation and integrating disturbance model with Kalman Filter. The work is published in [Wu *et al.*, 2007b] of Chapter 7.

Adaptive Estimation with ALS method A new auto-covariance least square (ALS) method is applied to adaptively determine the filter gain and recover the unknown noise covariance, and consequently, improve output performances, reduce variances and reject the unmeasured disturbances. The detail could be found in the published paper [Wu *et al.*, 2007a] of Chapter 8.

Moving Horizon Estimation Moving horizon estimation technique together with moving horizon control is implemented to the process through dynamic optimization computation. Stability of the control and estimation strategy is ensured by adding terminal cost penalty. The theory description and application are stated in published paper [Wu *et al.*, 2008b] of Chapter 9.

Energy Optimization through Actuator Redundancy A new control strategy involves exploiting actuator redundancy in a multi-variable system is developed for passively attenuating the covariance of the high frequency disturbances and pursuing optimum energy solution. This strategy enhances the resilience of the control system to disturbances beyond its bandwidth and reduces energy consumption by solving convex optimization. The work could also be found in the published paper [Wu *et al.*, 2008b] of Chapter 9.

Model Parameter Identification For a full scale livestock building located in Syvsten, Denmark, the significant parameters explored in the models are identified and validated through some experimental time series data collected during summer and winter. The comparative results confirm the value of the conceptual multi-zone climate model approach. This work will be published in [Wu *et al.*, 2008a] as in Chapter 10.

4.2 Conclusion and Perspectives

4.2.1 Conclusion

From proposing the Conceptual Multi-Zone Modeling method to finally building up a nonlinear coupled model expressed as algebraic dynamic differential equation, the primary experience has been gathered from the analysis of the intern-zonal airflow interaction and the zonal climate. The horizontal variation of indoor temperature and contaminant gas concentration is usually regarded as the indication variables to quantify and qualify the indoor climate. The conventional way of predicting indoor climate, is based

on the assumption of uniform distributions. However, neglecting the existence of stratification or the horizontal variation will obviously result in the significant deviation from the real environment condition. Through the systematic investigation and system identification, the Conceptual Multi-Zone Climate Modeling (CMZCM) method is proved to be appropriate to account more accurately for the indoor climate conditions and capture the major heterogeneity inside the large, partition-less livestock building, and the related assumptions are pinpointed. The phenomenon of the horizontal variation could be explained by the fact of different localization of the heating source and the dominant airflow pathes. As has been illustrated in the figures of pervious Chapters, if the heating load suddenly increases in one zone and sequently lead to the substantial rise of zonal temperature, the most effective way to remedy this situation is to enlarge the opening area of the inlets in this zone to allow more fresh air to come in and reach the heating source of this zone. Therefore, the zonal thermal stress can be alleviated without intervening other zones, and causing excessive ventilation rate and energy consumption. The functionality of the exhaust units are primarily on generating the average pressure changes. Consequently, the developed conceptual multi-zone climate model is of particular importance in predicting the indoor climate of large scale partition-less livestock building and designing an intelligent ventilation control system.

The fascinating properties of Model Predictive Control (MPC) are its capabilities of dealing with nonlinearities of Multiple Input and Multiple Output (MIMO) system naturally, handling constraints flexibly, and allowing system operate close to the constraints. MPC is implemented through dynamic optimization in a moving horizon approximation approach. The essence of MPC is to optimize forecasts of process behavior. The forecasting is accomplished with a process model, and therefore, the model is the essential element of an MPC controller [Rawlings, 2000]. Based on the mass balance equation and through the linearization, an Linear Time Invariant (LTI) model in terms of state space representation which combines the thermal comfort system and indoor air quality system in connection with the air distribution system is derived. The finalized linear system is stable, controllable and observable, which provides the basis of model-based predictive control.

The major strength of MPC is reflected in the cost function and the ability of incorporating constraints. It allows the tradeoff between tracking set-point and saving energy. It could also compromise multiple objectives by adjusting the weighting matrix in order to satisfy special requirements and reach certain goals. The off-set free tracking is achieved through target calculation (shifting the origin to the optimal steady state to follow ideal trajectory and target control behavior), receding horizon regulation (generating the optimal control signal within prediction horizon to track reference and reject disturbances) and including input/output disturbance models (introducing the integral control action to compensate model/plant mismatch). The stability is guaranteed with terminal equality constraints parametrization, and the control strategy could be regarded as a constrained Linear Quadratic (LQ) optimal control problem with infinite horizon. As the matter of fact, without considering constraints, the open loop predictive control is converted into

feedback control with the optimal and stabilized control law derived from discrete algebraic *Riccati* equation.

In this thesis, the moving horizon approximation is applied both for estimation and control with full infinite horizon. The Moving Horizon Estimation (MHE) formulation incorporates the inequality constraints and allows the tradeoff between the following of the model forecast, and tracking the measurement, thus improving the estimation quality and output performances through a series of reconciliations. Without considering constraints, moving horizon estimator is the Kalman Filter (Extended Kalman Filter for nonlinear system), where the separation principle applied [Andersen, 2007]. Therefore, as stated in [Jorgensen, 2005], the constrained linear-quadratic optimal control problem plays the central enabling role in numerical realization of MPC for large-scale nonlinear system.

Auto-covariance Least Square (ALS) method is a data-based techniques aiming at improving the state estimation in MPC, which uses the correlations between routine operating data to form a least-squares problem to estimate the covariances for the disturbances. The ALS technique guarantees positive semi-definite covariance estimates by solving a semi-definite programming (SDP) problem [Rajamani, 2007]. For livestock indoor climate system which is exposed to both internal and external disturbances with random noises and uncertainties, the proposed estimation techniques play large role in lowering closed-loop output variances and compensating the model/plant mismatch through improving the quality of estimation and recovering the unknown noise covariances.

The application of actuator redundancy expands the frequency bandwidth of the system by exploring the nonlinearities of the actuators and generating the optimum solution by solving a convex optimization subject to the nonlinear equalities. This novel part is integrated inside the MPC loop and optimizes the operating behavior of the actuators naturally, and reallocates the signals in a feed-forward approach. This strategy increases the control system's flexibility and utility substantially.

The online implementation of estimation and control is through the quadratic programming, which have lead to the issue of computer power and the cost time. However, for moderate models like the indoor climate system, and with the increasingly fast development of modern computing hardware, together with the improvements in optimization algorithms, it is no longer a problem and confined to 'slow' process, needless to say that our climate system is truly slow.

Concluded from above, the main achievement of this project is the proposal and development of Conceptual Multi-Zone Climate Model (CMZCM), and efficient application of optimization techniques in estimation and control for MIMO system. The combination and implementation of the proposed methods, which to the best of authors' knowledge, have been far less investigated by previous researches in the field of livestock ventilation system. The significant advantages of the designed control strategy lie in the optimization nature which not only enable to improve indoor climate performances, but also to save energy and increase the actuator's utilization. In other words, the goal of lowering cost, increasing quality and enriching productivity is reasonably realized.

4.2.2 Perspectives

Based on above discussion, the proposed methodologies are proved to have high potential. The simplicity concerning the parametering for modeling and the advancement for control makes the work interesting for not only the laboratory research, as well as for the manufacturers of controllers. Obviously, the proposed control strategies for animal house could also be applied to other similar structured buildings such as the green house, however before that, a few issues deserve our further attention.

First of all, the feasibility and reliability of the designed entire control system should be verified through the experiments in the real scale poultry house, and the results will be compared with the currently used decentralized PID controller. [Skogestad and Postlethwaite, 1996], among other research, provides the solid theoretical framework and approaches for analysis and design of multi-variable system, which we could use to investigate and compare the properties with the decentralized PID control.

Due to the large amount of uncertainties and disturbances, the developed model could be enhanced with some other dynamics, including the animal/plant heat production, the surface heat convection and the heat transmission of conduction materials, building leakages and wind direction variations or some uncertainty approximations.

The nonlinearity analysis of the system model remains an incomplete issue, the related works on deriving linearized models around different operating points with major focus on the one closed to the constraints need more attention. The gain-scheduled predictive control strategy corresponding different linearized models or Moving Horizon Estimation and Control based on the nonlinear dynamics could be taken into future considerations, and we could consult [Rao, 2000], [Tenny, 2002] and [Jorgensen, 2005] for theoretical studies.

The structure of MPC allows for multiple objectives selected from the requirement and certain goals, therefore, several other considerations could be injected into the optimization formula, such as the minimum ventilation rate and comfort air movement around the animals/plant. The research on comfort airflow model could refer to [Heiselberg and Nielsen, 1996]. The actuator redundancy should be also applied for the inlet system, in order to protect animals/plant from wind gust and improve comfort without causing draft.

Part II

Contributed Papers

This part presents the major achievements in terms of peer reveiwed papers. Six published and accepted conference papers from 2005 to 2008 are included. The order of the arrangement of papers could be interpreted as the progress of the research works during the past three and a half years. The papers have been reformatted from the original layout to comply with the layout in this thesis.

Chapter 5

Modeling and Control of Livestock Ventilation Systems and Indoor Environments

Zhuang Wu [1*], Per Heiselberg [2], Jakob Stoustrup [1]

[1] *Department of Electronic Systems, Aalborg University, Fredrik Bajersvej 7C, 9220 Aalborg East, Denmark*
[2] *Department of Building Technology and Structural Engineering, Aalborg University, Sohngaardsholmsvej 57, 9000 Aalborg, Denmark*

This conference paper was presented at the 26th Air Infiltration and Ventilation Center (AIVC) Conference on Relation to the Energy Performance of Buildings, September, 2005. This paper is reproduced under the conditions of the copyright agreement with the International Network for Information on Ventilation and Energy Performance (INIVE) of European Economic Interest Grouping (EEIG). *The Conceptual Multi-Zone Climate Model method is proposed under necessary assumption and simplifications. An infinite horizon Linear Quadratic optimal control strategy is designed for this nonlinear Multiple Input and Multiple Output system.*

Abstract

The hybrid ventilation systems have been widely used for livestock barns to provide optimum indoor climate by controlling the ventilation rate and air flow distribution within the ventilated building structure. The purpose of this paper is to develop models for livestock ventilation systems and the associated indoor environments with a major emphasis on the prediction of indoor horizontal variation of temperature and contaminant gas concentration that adapted to the design of appropriate controlling strategy and control systems. The Linear Quadratic (LQ) optimal control method taking into account of the effect of disturbances and random noises is designed based on the linearized process model with Multiple Input and Multiple Output (MIMO). The well designed control systems are able to determine the demand ventilation rate and the ralated airflow pattern, improve and optimize the indoor Thermal Comfort (TC), the Indoor Air Quality (IAQ) and the energy use.

Nomenclature

T	Temperature
C_r	Air Contaminant gas concentration
$\dot{Q}$	Heat transfer rate
g	Gravitational acceleration
M	Air mass
V	Volume
A	Area
H	Height
ρ	Density
U	Heat transfer coefficient of building construction material
c_p	Heat capacity at constant pressure
$\dot{m}$	Mass flow rate
$\dot{q}$	Air volume flow rate
$\dot{n}$	Air exchange rate
$\dot{G}$	Contaminant gas generation rate from animals
P	Pressure
ΔP	Pressure difference
C_d	Discharge coefficient of inlet valve system
P_i	Internal Pressure at reference height
C_p	Surface pressure coefficient
V_{ref}	Wind speed at reference level

Subscript

i	Indoor zonal numbers
o	Outdoor
in	Input to the building
out	Output from the building
$wall$	Building envelope
$transmission$	Heat transfer through convection, conduction and radiation
$source$	Production or generation source
$inlet$	Inlet valve system
fan	The exhaust unit
NPL	Neutral Pressure Level

5.1 Introduction

Hybrid ventilation systems have been widely used for livestock buildings. Livestock ventilation is concerned with comfort interpreted through animal welfare, behavior and health, and most importantly, it is concerned with factors such as conversion ratio, growth rate and mortality ([Carpenter, 1981]). Most existing analysis for the livestock ventilation system assume that the indoor air temperature and concentration is uniformly distributed as discussed in [Cunha *et al.*, 1997],[Moor and Berckmans, 1996b], [Taylor *et al.*, 2004]. However, as analyzed by [Clark, 1981], the actual indoor environment at any controlling sensor (especially when the sensors are located horizontally) will depend on the air flow distribution that is usually depicted as a map of the dominant air paths. Therefore, the control system for large scale partition-less livestock barns neglecting the horizontal variations could obviously result in the significant deviations from the optimal environment for the sensitive pigs or chickens.

In this paper, the livestock indoor environment and its ventilation control system will be regarded as a feedback loop in which the controller provides the optimal actions to the actuators taking into account of the necessary disturbances and random noises. The purpose of this paper is to design an appropriate control strategy to improve the indoor animal Thermal Comfort (TC) and Indoor Air Quality (IAQ) through an optimal energy using approach.

5.2 System Modeling

The fan assisted natural ventilation principle will be investigated in this work. As seen in Figure 5.1(a), 5.1(b) and 5.1(c), the livestock ventilation system consists of evenly distributed exhaust units and fresh air inlet openings on the walls. From the view of direction A and B, Figure 5.1(A) and 5.1(B) provide a description of the dominant air flow map of the building includes the airflow interaction between each conceptual zones by applying the Conceptual Multi-Zone Climate Model (CMZCM) method. In each zone, it is possible to monitor the zonal climate and the effect of the control signals through the actuators movements: inlet valves, exhaust axial type fans and swivel shutters.

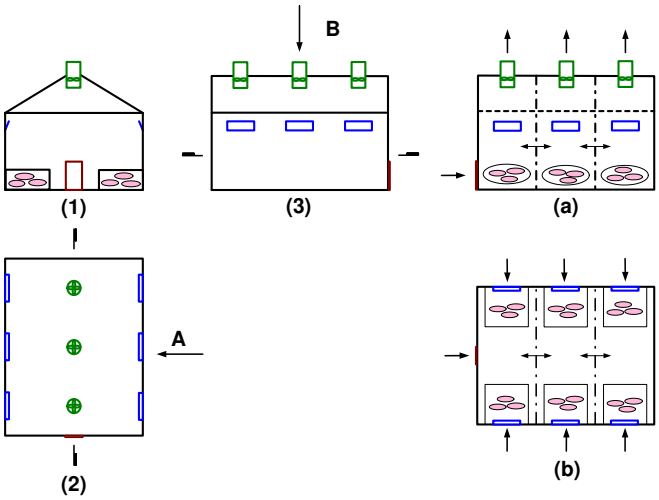

Figure 5.1: Synoptic of Large Scale Livestock Barn and the Dominant Airflow Map of the Barn

The necessary simplifying assumptions for developing models are as follows:

- An ideal uniform flow process is assumed, which means that the fluid flow at any inlet or outlet is uniform and steady, and thus the fluid properties do not change with time or position over the cross section of an inlet or outlet.
- The interactive airflow between internal zones, which is influenced by the inlet air jet trajectory, thermal buoyancy forces and convective heat plume are assumed to be constant.
- Heat gain from animals and solar radiation are assumed to be constant.
- The rate of the heat loss by evaporation is neglected.
- The thermal properties of the airflow are assumed to have bulk average values.
- Airflow involves no mass accumulation inside the building.
- The heat transfer coefficient of building envelope is assumed to be constant.
- The pressure is assumed to be constant on each building surface (same value of pressure coefficient C_p is used for all openings on the same side of the building).
- A hydrostatic pressure distribution is assumed in the space.

- Opening characteristics are assumed independent on flow rate, pressure difference and outside temperature (constant discharge coefficient C_d are used for all openings).

5.2.1 Models of Indoor Climate

A conceptual multi-zone modeling method is employed to analyze and develop the indoor climate model. The livestock building is compartmentalized into several macroscopic homogeneous conceptual zones horizontally so that the nonlinear differential-algebraic equation (5.1) and (5.3) relating the zonal temperature and zonal concentration can be derived by applying the theory of conservation of energy and mass. By substituting *i* with the zone number into (5.1) and (5.3), we could derive three coupled differential equations for indoor thermal comfort in terms of zonal temperature and for indoor air quality in terms of zonal air contaminant gas for example the carbon dioxide concentration level, respectively.

For (5.1), the rate of energy $\dot{Q}$ transferred by mass flow can be calculated by (5.2). $\dot{Q}_{i+1,i}$ and $\dot{Q}_{i,i+1}$ indicate the heat exchange due to the air flow across the conceptual boundary of zone i and zone $i+1$, while for the middle zones which have heat exchange with neighbor zones on each side, two more parts $\dot{Q}_{i-1,i}$ and $\dot{Q}_{i,i-1}$ will be added to (5.1). The value of interactive mass flow between internal zones is the sum of influence from air jets, heat plume, thermal buoyancy and air exchange rate. $\dot{Q}_{in,i}$, $\dot{Q}_{out,i}$ and $\dot{Q}_{leakage,i}$ represent the heat transfer by mass flow through inlet, outlet and leakage of the zone respectively. The convective heat loss through the building envelope is denoted by $\dot{Q}_{tranmission,i}$ and described as $\dot{Q}_{transmission,i} = U \cdot A_{wall,i} \cdot (T_i - T_o)$. The heat source of the zone $Q_{source,i}$ includes the heat gain from animal heat production, solar radiation and heating system. For (5.3), the rate of concentration is indicated as $C_r \cdot n$, where C_r represents the concentration level and the air exchange rate n is calculated by (5.4). For the middle zones which have mass flow interaction with neighbor zones on both sides, two more parts $\dot{C}_{r,i} \cdot n_{i,i-1}$ and $C_{r,i-1} \cdot n_{i-1,i}$ should be added to (5.3). The rate of contaminant generation is denoted by G_i and the zonal volume is denoted by V_i .

$$M_i c_{p,i} \frac{dT_i}{dt} = \dot{Q}_{i+1,i} + \dot{Q}_{i,i+1} + \dot{Q}_{in,i} + \dot{Q}_{out,i} + \dot{Q}_{tranmission,i} + \dot{Q}_{source,i}, \tag{5.1}$$

$$\dot{Q}_{i,i+1} = c_p \cdot \dot{m} \cdot T_i, \tag{5.2}$$

$$\frac{dC_{r,i}}{dt} = C_{r,i+1} \cdot \dot{n}_{i+1,i} + C_{r,i} \cdot \dot{n}_{i,i+1} + C_{r,i} \cdot \dot{n}_{out} + C_{r,o} \cdot \dot{n}_{in} + \frac{G_i}{V_i}, \tag{5.3}$$

$$\dot{n} = \frac{\dot{m} \cdot 3600}{\rho \cdot V}. \tag{5.4}$$

5.2.2 Models of Inlet and Exhaust Units

Equation (5.5) gives the relationship between the volume flow rate and pressure difference across the inlet openings based on the mass balance equation. The ventilation flow rate can be determined from (5.6) and the pressure difference is the combing driving forces of thermal buoyancy and wind as (5.7). Therefore, (5.5) will then result in a linear equation from which we can solve for the internal pressure Pi. The computation of the outlet volume flow rate could be derived by clarifying the straightforward relationship between the total pressure difference, rotating speed of the axial type fan and the opening angle of the swivel shutter. The nonlinear static equation is referred to [Heiselberg, 2004a]. For simplicity, in this paper, the volume flow rate is regarded as the manipulated variables.

$$\sum q_{in} \cdot \rho_o \cdot \frac{\Delta P_{inlet}}{|\Delta P_{inlet}|} + \sum q_{out} \cdot \rho_i = 0, \tag{5.5}$$

$$q_{in} = C_d A \cdot \sqrt{\frac{2\,|\Delta P_{inlet}|}{\rho}} \operatorname{sgn}(\Delta P_{inlet}), \tag{5.6}$$

$$\Delta P_{inlet} = \frac{1}{2}\rho_o C_{P,r} V_{ref}^2 - P_i - \rho_i g \frac{T_i - T_o}{T_o}(H_{NPL} - H_{inlet}). \tag{5.7}$$

5.2.3 Performance Simulation

The open loop dynamic performances of zonal variation for indoor temperature and CO_2 concentration within a day based on the developed TC model and IAQ models are demonstrated in Fig. 5.2 (a) and (b). The system started from operating points which maintain the system behavior (indoor climate and indoor air quality) at the required condition with exceptionally low horizontal variation. The system is stimulated by a serious of step changes of the indoor zonal heat source and zonal contaminant load during the entire time horizon. The simulation is implemented with the disturbances from the stochastic external temperature as shown in Fig. 5.2 (c), wind speed as in Fig. 5.2 (d) and ambient concentration as in Fig. 5.2 (e), which are generated from random sources through low-pass filters.

The simulation results proved to be evident, that the conceptual multi-zone models for TC and IAQ contain significant information on horizontal variation which is not able to be captured by the single zone model with mean temperature and concentration, under the circumstances that the zonal disturbances changes.

5.3 Design of Control System

The entire livestock ventilation system and indoor environment is a Multiple Input and Multiple Output (MIMO) dynamic nonlinear process and strongly coupled intrinsic system. It is exposed to external disturbances and noises and has actuators with saturation.

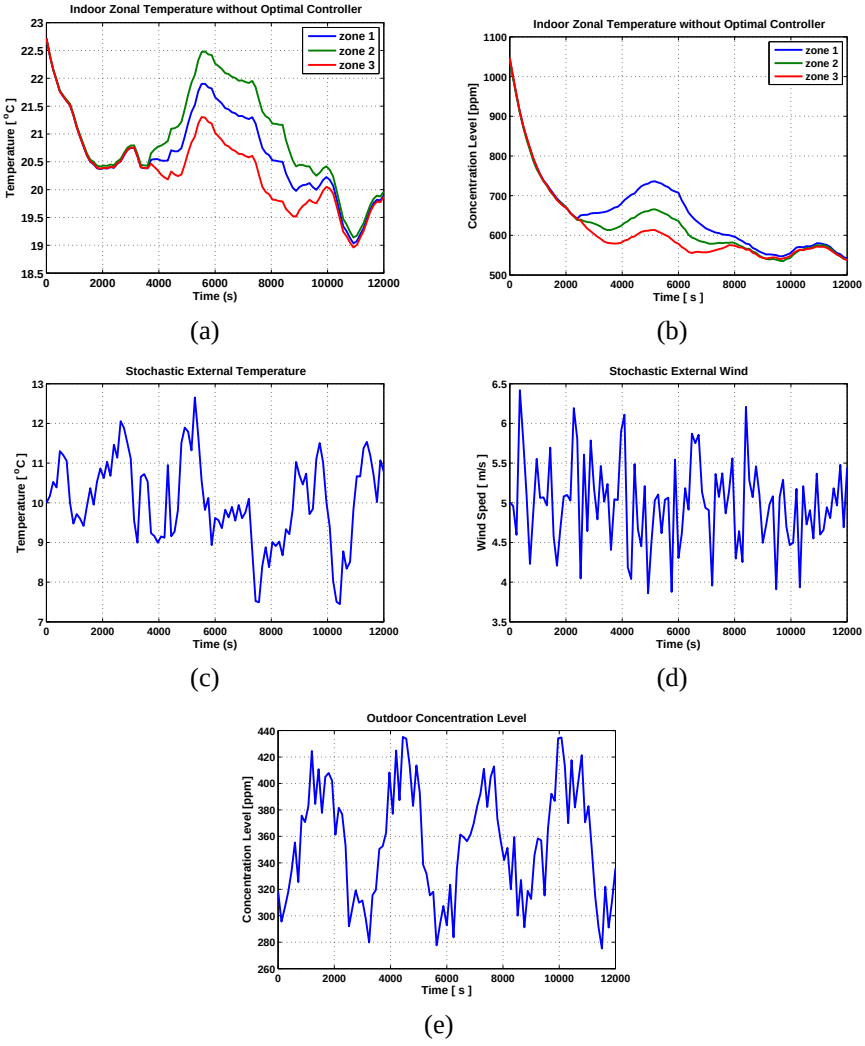

Figure 5.2: Dynamic Performance of Plant without Optimal Control (a) Indoor Zonal Temperature (b)Indoor Zonal Concentration Level; Outdoor Weather Disturbances Variation (c) Outdoor Temperature (d) Outdoor Wind Speed (e) Outdoor CO_2 concentration level

Consequently, it is necessary to explore the application of advanced control algorithms, such as the optimal control, predictive control etc. to satisfy the equilibrium between the indoor air quality, thermal comfort and energy consumption. Linear Quadratic (LQ) optimal control is a good method for ventilation control system analysis and design, before applying other more complex control schemes. The LQ control deals with a linear state space model as described in (5.8) which is derived from the system linearization around the equilibrium point, where the Thermal Neutral Zone (TNZ) and animal demand indoor air quality are selected to be the reference values. Equations (5.9 (a), (b), (c)) show the vectors of deviation variables: the measurable states or controlled variables vector x (zonal temperature and zonal concentration), the control signal or manipulated variables vector u (inlet and outlet volume flow rate), and the disturbance vector d (external weather condition and animal heat and contaminant gas generation).

$$x(k+1) = A \cdot x(k) + B \cdot q(k) + B_d \cdot d(k) \tag{5.8a}$$

$$y(k) = C \cdot x(k) + D \cdot q(k) + D_d \cdot d(k), \tag{5.8b}$$

where,

$$x = \left[\bar{T}_1 \quad \bar{T}_2 \quad \bar{T}_3\right]^T_{3\times 1}, \tag{5.9a}$$

$$u = \left[\bar{q}_{in,i=1\ldots6} \quad \bar{q}_{out,j=1\ldots3}\right]^T_{9\times 1}, \tag{5.9b}$$

$$d = \left[\bar{\dot{Q}}_1 \quad \bar{\dot{Q}}_2 \quad \bar{\dot{Q}}_3 \quad \bar{V}_{ref} \quad \bar{c}_{P,w} \quad \bar{c}_{P,l} \quad \bar{c}_{P,r} \quad \bar{T}_o\right]^T_{8\times 1}. \tag{5.9c}$$

The performance function for LQ control is:

$$\min \sum_{k=0}^{N-1} \left[x_k^T Q_1 x_k + u_k^T Q_2 u_k\right] + x_N^T Q_N x_N \tag{5.10}$$

where k denotes the sample time, N denotes the time horizon, the weighting matrices Q_1 and Q_N are positive definite and Q_2 is positive semi-definite, and they are defined as diagonal matrices. The diagonal elements are the inverse value of the square of the maximum allowed deviations in the states and the control signals. By using Dynamic Programming, we could obtain a linear time varying controller, where the dynamic gain is determined by the discrete recursive *Riccati* equations as (5.11) (see [Andersen, 2007]). The optimal control signals are generated from this linear feedback MIMO controller taking into account of the disturbances. The generated optimal control signals are input to the process to predict the zonal temperature and concentration. The applied sensor and motor dynamics is relatively fast compared with the entire system response and could be neglected.

$$F_N = -\left[B^T \Pi_N B + R\right]^{-1} B^T \Pi_N A, \tag{5.11a}$$

$$\Pi_N = A^T \Pi_N A + Q - A^T \Pi_N B \left[B^T \Pi_N B + R\right]^{-1} B^T \Pi_N A. \tag{5.11b}$$

To guarantee offset-free control, the system model expressed in (5.8) is reformulated into a Δu-form to introduce an integral controller [Maciejowski, 2002]. The augmented state and system matrices are defined as follows:

$$\begin{bmatrix} x(k+1) \\ x_{md}(k+1) \\ u(k) \end{bmatrix} = \begin{bmatrix} A & B_d C_{md} & B \\ 0 & A_{md} & 0 \\ 0 & 0 & I \end{bmatrix} \cdot \begin{bmatrix} x(k) \\ x_{md}(k) \\ u(k-1) \end{bmatrix} + \begin{bmatrix} B \\ 0 \\ I \end{bmatrix} \cdot \Delta u(k), \tag{5.12}$$

The full process state are assumed to be measurable. The feedback information is directly taken from plant output y. The measurable disturbance state is $x_{md} \in \Re^8$. Substitute the augmented system into the *Riccati* Equations to derive the optimal feedback gain F_N and the control law is:

$$\Delta u(k) = -F_N \begin{bmatrix} x(k) \\ x_{md}(k) \\ \Delta u(k-1) \end{bmatrix}. \tag{5.13}$$

5.4 Simulation Results

Fig. 5.3 illustrates the closed-loop dynamic performances of the indoor temperature and air concentration with a linear feedback gain for animal thermal comfort and indoor air quality. The applied variable values and the disturbances are same with those applied for the process behavior simulation as shown in Fig. 5.2. A certain amount of trial and error is required with an interactive computer simulation before a satisfactory design is obtained, for example, one of possibilities is to adjust the weighting matrix. Through comparing the simulation results of the process with and without controller, we could recognize that the system with optimal control adjustment has much shorter response time to reach the steady state, has the capability to reject the indoor and outdoor disturbances, and reduce the output variation and noise level by adjusting the air flow rate through six inlet and three outlet flow rate.

5.5 Conclusion and Future Work

5.5.1 Conclusion

Aiming at improvement of performances and optimization of energy, the main achievement of this work is the successful application of the LQ optimal controller for livestock ventilation systems analyzed by a conceptual multi-zone modeling method. The results proved to be fruitful that the designed control scheme is feasible and flexible to reach the purpose.

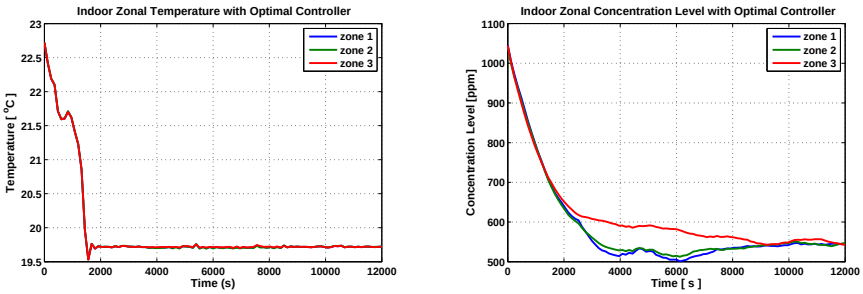

(a) (b)

Figure 5.3: Dynamic Performance of Plant with Optimal Control (a) Indoor Zonal Temperature (b)Indoor Zonal Concentration Level

5.5.2 Future Work

Some parameters of the mathematical models will be identified through experiment in a real scale livestock barn equipped with hybrid ventilation systems. The interfacial mixing parameters which describe the airflow interaction of internal zones will be calibrated with experimental measurement for example, by using gas tracer. Advanced control methods, dynamic disturbances models, estimator for weather condition and unmeasurable states will be further investigated. More actuators such as the heating system, air-conditioning systems and shade screen for solar radiation could be taken into account.

5.6 Acknowledgement

The authors would like to acknowledge financial support from the Danish Ministry of Science and Technology (DMST) and Center for Model Based Control (CMBC) with Grant number: 2002-603/4001-93.

Chapter 6

Model Predictive Control of the Hybrid Ventilation for Livestock

Zhuang Wu [1*], Jakob Stoustrup [1], Klaus Trangbaek [1], Per Heiselberg [2], Martin Riisgaard Jensen [3]

[1] *Department of Electronic Systems, Aalborg University, Fredrik Bajersvej 7C, 9220 Aalborg East, Denmark*
[2] *Department of Building Technology and Structural Engineering, Aalborg University, Sohngaardsholmsvej 57, 9000 Aalborg, Denmark*
[3] *Skov A/S, Glyngoere, 7870, Denmark*

This conference paper was presented at the 45th IEEE Conference on Decision and Control (CDC), December, 2006. This paper is reproduced under the conditions of the copyright agreement with the Institute of Electrical and Electronics Engineers (IEEE). *The Model Predictive Control algorithm is introduced and implemented for the nonlinear process based upon the coupled linearized time invariant state space model. The control decision is made with the estimation from an infinite horizon Kalman Filter. The offset free tracking is achieved.*

6.1 Abstract

In this paper, design and simulation results of model predictive control (MPC) strategy for livestock hybrid ventilation systems and associated indoor climate through variable operation of inlet and exhaust units, are presented. The design is based on thermal comfort parameters for poultry in barns. The dynamic model describing the nonlinear behavior of ventilation and associated climate, by applying a so-called conceptual multi-zone modeling method and the conservation of energy and mass is developed. The simulation results illustrate the high potential of MPC in dealing with nonlinearities, handling constraints and performing off-set free tracking. The purpose of this paper is to apply MPC for multivariable system taking into account of the random disturbances and necessary constraints in order to calculate the optimal ventilation rate, predict the horizontal variation of indoor climate and pursue an optimum energy consumption.

6.2 Introduction

Livestock ventilation is concerned with comfort interpreted through animal welfare, behavior and health, and most importantly, it is concerned with factors such as conversion ratio, growth rate and mortality ([Carpenter, 1981]). The alleviation of thermal strain and the maintenance of comfort environment significantly depend on the measurement and control of the air temperature and the humidity which have pretty well defined the thermal comfort in the presence of air movement and radiation through ventilation systems. Assuming that in the researched laboratory livestock building, an advanced waste-handling system equipped and the manure storage units are frequently cleaned, then if the ventilation rate are adequate to remove heat and contaminant organisms or gas, the moisture is usually well diluted and present no problem. Further more, humidity has little effect on thermal comfort sensation at or near comfortable temperatures unless it is extremely low or high. Therefore the humidity is not considered in this work.

Hybrid ventilation system combines the natural ventilation and the mechanical ventilation, and have been widely used for livestock in Denmark. Most existing control systems used for livestock barns are based on the analysis with single zone method, which assumes that the indoor air temperature and contaminants concentration are uniform as discussed in [Cunha *et al.*, 1997],[Moor and Berckmans, 1996b], [Taylor *et al.*, 2004]. However, as analyzed in [Clark, 1981], the actual indoor environment at any controlling sensors (especially when the sensors are located horizontally) will depend on the air flow distribution that is usually depicted as a map of the dominant air paths. Therefore, the control system for large scale partition-less livestock barns neglecting the horizontal variations could obviously result in the significant deviations from the optimal environment for the sensitive pigs or poultry. Furthermore, the performance of currently used control scheme for livestock building appears limited when large disturbance occur in the presence of inputs saturation.

As stated in books [Maciejowski, 2002] and [Rossiter, 2003], papers [Rawlings, 2000],

[Qin and Badgwell, 2003] and [Pannocchia *et al.*, 2005], Model Predictive Control (MPC) has become the advanced control strategy of choice by industry mainly for the economically important, large-scale, multi-variable processes in the plant. The rationale for MPC in these applications is that it can deal with high non-linearities, handle constraints and modeling error, fulfill offset-free tracking, and it is easy to tune and implement.

In this paper, the livestock indoor environment and its ventilation control system will be regarded as a feedback loop in which the predictive controller provide the optimal actions to the actuators taking into account of the significant disturbances and constraints. This strategy is not only expected to give good regulation of zonal temperatures, but also to minimize the energy consumption involved with operating the inlet valves, the exhaust fans and the swivel shutters.

6.3 Livestock Indoor Climate and Ventilation System Modeling

6.3.1 System Description and Dynamic Models

The schematic diagram of a large scale livestock barn equipped with hybrid ventilation system analyzed with conceptual multi-zone method is shown in Fig. 6.1(1), Fig. 6.1(2) and Fig. 6.1(3). The livestock ventilation system consists of evenly distributed exhaust units mounted in the ridge of the roof and fresh air inlet openings installed on the walls. From the view of direction A and B, Fig. 6.1(a) and Fig. 6.1(b) provide a description of the dominant air flow map of the building including the airflow interaction between each conceptual zones. Through the inlet system, the incoming fresh cold air mixes with indoor warm air and then drops down to the animal environmental zones slowly in order to satisfy the zonal comfort requirement. Therefore, the exhaust system is the most important link in this circulation chain, because it controls the indoor relative pressure.

By applying a conceptual multi-zone method, the building will be compartmentalized into several macroscopic homogeneous conceptual zones horizontally so that the nonlinear differential equation relating the zonal temperature can be derived based on the energy balance equation for each zone as (6.1). By substituting the subscript i with the zone number, we could obtain three coupled differential algebraic equations governing a sensible heat model for indoor thermal comfort.

$$M_i c_{p,i} \frac{dT_i}{dt} = \dot{Q}_{i+1,i} + \dot{Q}_{i,i+1} + \dot{Q}_{in,i} + \dot{Q}_{out,i} + \dot{Q}_{transmission,i} + \dot{Q}_{source,i}, \qquad (6.1)$$

where T_i is the indoor zonal air temperature (^oC), $c_{p,i}$ is the specific heat of the air ($J \cdot kg^{-1} \cdot K^{-1}$), M_i is the mass of the air (kg), $\dot{Q}_{i+1,i}$, $\dot{Q}_{i,i+1}$, indicate the heat exchange (J/s) due to the air flow across the conceptual boundary of zone i and zone $i+1$, while for the middle zones which have heat exchange with neighbor zones on each side, two more parts $\dot{Q}_{i-1,i}$, $\dot{Q}_{i,i-1}$ will be added. $\dot{Q}_{in,i}$, $\dot{Q}_{out,i}$ represent the heat transfer (J/s) by mass flow through inlet and outlet of the zone respectively. The convective heat loss through the

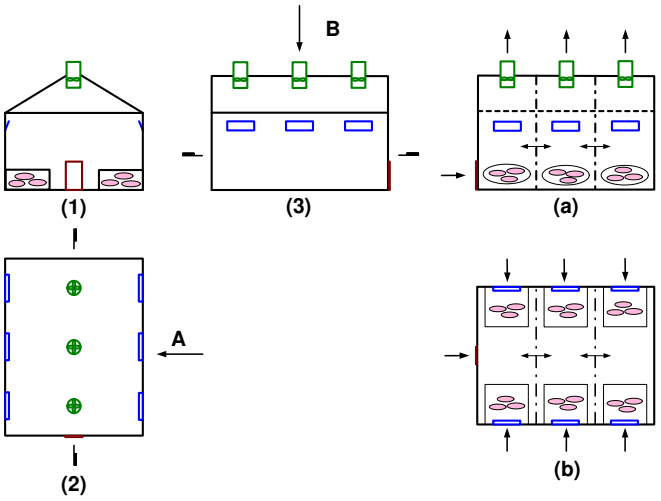

Figure 6.1: Synoptic of Large Scale Livestock Barn and the Dominant Airflow Map of the Barn

building envelope is denoted by $\dot{Q}_{transmission,i}$ (J/s). The heat source of the zone $\dot{Q}_{source,i}$ includes the heat gain from animal heat production and heating system.

The inlet systems provide variable airflow directions and the amount of incoming fresh air by adjusting the bottom hanged flaps. Proper design and applications of the performance of inlet openings in the facade can expand the period of use of hybrid ventilation and increase both air and cooling capacity. The volume flow rate through the inlet is calculated by (6.2), where C_d is the discharge coefficient, A is the geometrical opening area (m^2), ΔP (Pa) is the pressure difference across the opening and can be computed by a set of routines solving thermal buoyancy and wind effect as (6.3). The subscript ref stands for the value at reference height, NPL stands for the Neutral Pressure Level.

$$q_{in} = C_d \cdot A_{inlet} \cdot \sqrt{\frac{2 \cdot \Delta P_{inlet}}{\rho}}, \tag{6.2}$$

$$\Delta P_{inlet} = \frac{1}{2} C_P \rho_o V_{ref}^2 - P_i + \rho_o g \frac{T_i - T_o}{T_i} (H_{NPL} - H_{inlet}). \tag{6.3}$$

The exhaust unit consists of an axial-type fan and a swivel shutter. The airflow capacity is controlled by adjusting the r.p.m. of the fan impeller and the swivel shutter opening angle. We introduce a fan law, as the straightforward relationship between the total pressure difference ΔP_{fan}, volume flow rate q_{out}, supplied voltage V_{volt} and the shutter opening angle θ can be clarified in a nonlinear static equation (6.4), where the parameters a_0, a_1, a_1, b_0, b_1, b_2 are empirically determined from experiments. As shown in (6.5), the total

pressure difference across the exhaust unit is the difference between the wind pressure on the roof and the internal pressure at the entrance of the fan which considers the pressure distribution calculated upon the internal pressure at reference height denoted by P_i.

$$\Delta P_{fan} = (b_0 + b_1 \cdot \theta + b_2 \cdot \theta^2) \cdot q_{out}^2 + a_0 \cdot {V_{volt}}^2 + a_1 \cdot q_{out} \cdot V_{volt} + a_2 \cdot q_{out}^2 \tag{6.4}$$

$$\Delta P_{fan} = \frac{1}{2}\rho_o C_{P,r} V_{ref}^2 - P_i - \rho_i g \frac{T_i - T_o}{T_o}(H_{NPL} - H_{fan}). \tag{6.5}$$

For detailed description and necessary simplifying assumptions for developing the models, please refer to [Heiselberg, 2004a] and [Wu *et al.*, 2005].

6.3.2 Dynamic Parameter Estimation

The dynamic model can be linearly expressed with respect to the dynamic parameters, which then can be estimated by using least-square techniques based on the measurement data collected from the experiments made by SKOV A/S in Denmark.

The discharge coefficient C_d for inlet system, varies considerably with the inlet type, opening area, as well as incoming air temperature and flow rate. However, for simplicity, we use a constant value of this coefficient for all openings, even though it might lead to over-prediction of airflow capacity and thereby larger openings than necessary. Fig. 6.2 demonstrates the characteristic curve of the air volume flow rate through the inlet opening corresponding to pressure differences. The colored curves represent different opening percentages.

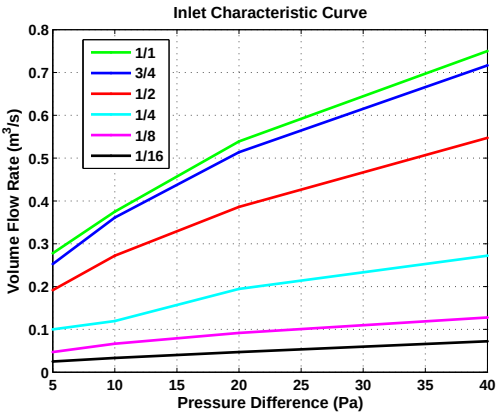

Figure 6.2: Inlet Opening Characteristic Curve with Flap Adjustment

Fig. 6.3 illustrates the performance of the exhaust units by controlling the swivel shutter at every 10^o from 0^o to 90^o. Each surface represents the character of the fan at

specific shutter opening angle with pressure-voltage-flow data, and is approximated by the quadratic equation (6.4), in which the parameters are determined empirically from the experiments.

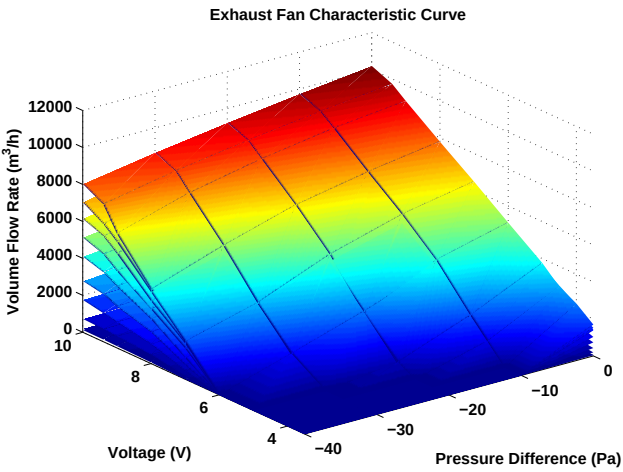

Figure 6.3: Exhaust Fan Performance with Shutter Change from 0^o to 90^o

6.4 Model Predictive Control

The entire livestock ventilation system and the associated indoor environment is a Multiple Input and Multiple Output (MIMO) dynamic nonlinear process and strongly coupled intrinsic system. It is exposed to external disturbances and noise and have actuators with saturation. Consequently, it is necessary to explore the advanced control algorithms such as the Model Predictive Control (MPC) to provide the trade-off between the thermal comfort and energy consumption. The predictive controller has an internal model which is used to predict the behavior of the plant, starting at the current time, over a future prediction horizon [Maciejowski, 2002]. Therefore, for the entire nonlinear process, a series of Linear Time Invariant (LTI) state space models which are derived from the system linearization around the equilibrium points need to be defined, and the Thermal Neutral Zone [Ingram, 1974] is selected to be the criterion that represents the control objective. Based on the analysis, there are at least four operating points corresponding to the different inter-zonal airflow direction, and one of these is picked up for analysis as follows.

6.4.1 Internal Modeling

We regard the livestock ventilation system as two parts by noting that the overall system consists of a static air distribution system (inlet-exhaust air flow system) and a dynamic thermal system (animal environmental zones). Fig. 6.4 shows the synoptic of the entire process model and the climate control variables.

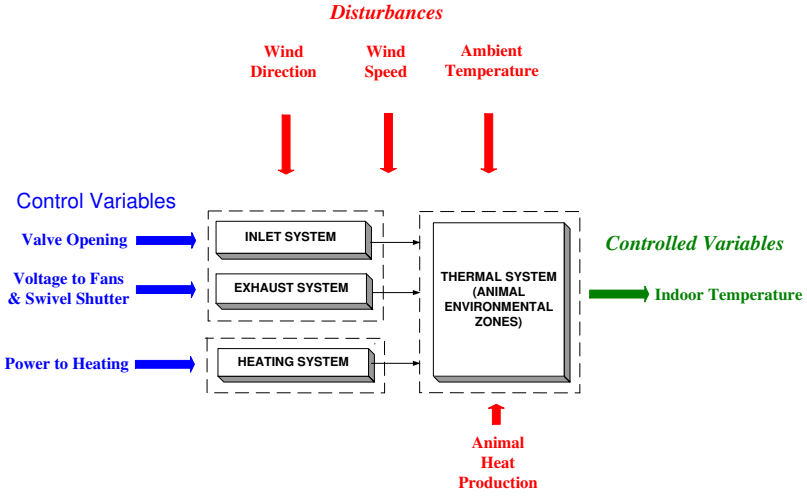

Figure 6.4: Synoptic of Entire System Model and Climate Control Variables

Let the discrete time linearized dynamics of a general thermal model (6.1) which is represented with three coupled equations be described in the state space form as (6.6):

$$x(k+1) = A_T \cdot x_T(k) + B_T \cdot q(k) + B_{Td} \cdot d_T(k), \tag{6.6a}$$

$$y(k) = C_T \cdot x_T(k) + D_T \cdot q(k) + D_{Td} \cdot d_T(k), \tag{6.6b}$$

where, A_T, B_T, B_{Td}, C_T, D_T, D_{Td} are the coefficient matrices with subscript T denoting the model for the thermal system. k is the current sample number.

By applying the conservation of mass for the livestock building with one single zone concept (6.7), and through linearization of air flow model deducted through (6.2) to (6.5), we can derive the static equation (6.8).

$$\sum_{i=1}^{6} q_{in}(k) \cdot \rho_o - \sum_{j=1}^{3} q_{out}(k) \cdot \rho_i = 0, \tag{6.7}$$

$$E \cdot \bar{q}(k) + F \cdot u(k) + G \cdot w(k) + K \cdot x(k) = 0, \tag{6.8}$$

where, E,F,G,K are coefficients matrices. The definition of $\bar{q} \in \Re^{9+1}$ is: $[q_{in,m}, q_{out,n}, P_i]^T$, $m = 1 \cdots 6$, $n = 1 \cdots 3$, where, $[q]^T_{1\times 9} = [q_{in,m}, q_{out,n}]^T$ is a airflow input vector which

combines the actuators' signals u in (6.8) and the process controlled variables x in (6.6). q can be expressed explicitly as (6.9). P_i is the internal pressure which will be neglected in procedure of multiplication and substitution. The general form of a finalized LTI state space model (6.10) connecting the airflow model with thermal model, and representing the entire system dynamics around the equilibrium point is obtained.

$$q(k) = \begin{bmatrix} I_{9\times 9} & 0_{9\times 1} \end{bmatrix}_{9\times 10} \cdot -E^{-1} \cdot [F \cdot u(k) + G \cdot w(k) + K \cdot x(k)], \tag{6.9}$$

$$x(k+1) = A \cdot x(k) + B \cdot u(k) + B_d \cdot \begin{bmatrix} d_{umd}(k) \\ d_{md}(k) \end{bmatrix}, \tag{6.10a}$$

$$y(k) = C \cdot x(k) + D \cdot u(k) + D_d \cdot \begin{bmatrix} d_{umd}(k) \\ d_{md}(k) \end{bmatrix}, \tag{6.10b}$$

where,

$$B_d = \begin{bmatrix} B_{dumd} & B_{dmd} \end{bmatrix}, D_d = \begin{bmatrix} D_{dumd} & D_{dmd} \end{bmatrix}. \tag{6.11}$$

and $A \in \Re^{3\times 3}$, $B \in \Re^{3\times 12}$, $C \in \Re^{3\times}$, $D \in \Re^{3\times 12}$, $B_d \in \Re^{3\times 8}$, $D_d \in \Re^{3\times 8}$ are the coefficient matrices at the equilibrium point. x, y, u, d, w denote the sequences of vectors representing small signal values of the process state for the indoor temperature of each conceptual zone, the measured output which is equal to the state, the manipulated input which consists of the inlet valve openings, voltage supplied to the fans and the shutter opening angles, the disturbances of the heat generated from animals and heating system, and the disturbances of external wind speed, wind direction and ambient temperature. Assuming that $z(k) \equiv y(k)$, which means that the controlled output z is always same with the measured output y.

$$x = \begin{bmatrix} \bar{T}_1 & \bar{T}_2 & \bar{T}_3 & \bar{C}_{r,1} & \bar{C}_{r,2} & \bar{C}_{r,3} \end{bmatrix}^T_{6\times 1}, \tag{6.12a}$$

$$u = \begin{bmatrix} \bar{A}_{in,i=1\ldots 6} & \bar{V}_{volt,j=1\ldots 3} & \bar{\theta}_{shutter,j=1\ldots 3} \end{bmatrix}^T_{12\times 1}, \tag{6.12b}$$

$$d_{umd} = \begin{bmatrix} \bar{\dot{Q}}_1 & \bar{\dot{Q}}_2 & \bar{\dot{Q}}_3 \end{bmatrix}^T_{3\times 1}, \tag{6.12c}$$

$$d_{md} = \begin{bmatrix} \bar{V}_{ref} & \bar{c}_{P,w} & \bar{c}_{P,l} & \bar{c}_{P,r} & \bar{T}_o \end{bmatrix}^T_{5\times 1}. \tag{6.12d}$$

Concluded from systematical analysis, the pair (A,B) is controllable, the pair (C,A) is observable, and the plant is stable. Thus, the internal modeling is accomplished and it is well prepared for solving of the optimization problem in predictive control and estimation scheme.

6.4.2 MPC Formulation

The constrained optimization problem is formulated as (6.13) by a quadratic cost function on finite horizon, subjected to the system dynamics (6.10) and the linear inequalities

imposed by the equipment limitation on the operation and slew rate, and the constraints on the controlled variables.

$$V(k) = \sum_{i=0}^{H_p} \|\hat{z}(k+i/k) - r(k+i)\|^2_{Q(i)} + \sum_{i=0}^{H_u-1} \|\Delta u(k+i/k)\|^2_{R(i)} + \sum_{i=0}^{H_u-1} \|u(k+i/k) - u_s\|^2_{S(i)}, \tag{6.13a}$$

$$s.t. \begin{cases} u_{\min} \le u \le u_{\max} \\ \Delta u_{\min} \le \Delta u \le \Delta u_{\max} \\ z_{\min} \le z \le z_{\max} \end{cases} \tag{6.13b}$$

where, V is the performance index to be minimized by penalizing the deviation of the predicted controlled (estimated) output $\hat{z}$ from the reference trajectory r over the prediction horizon H_p , and the change of the control input $\Delta\hat{u}$ which is adjusted according to the estimation over the control horizon H_u. H_w is the window horizon and $H_w \le 1 \le H_p$. The weighting matrices $Q \in \Re^{3\times3}$ and $R \in \Re^{12\times12}$ are positive semi-definite and act as tuning parameters which are adjusted to give satisfactory dynamic performance. An additional form of the term $\sum_{i=0}^{H_u-1} \|\hat{u}(k+i/k) - u_s\|^2_{S(i)}$, $S \in \Re^{12\times12}$ will be added to the cost function, which penalizes deviation of the input vector from *ideal resting value* u_s , for there are more inputs than the controlled variables as described in [Maciejowski, 2002].

To guarantee offset-free control of the output in the presence of plant/model mismatch and/or unmeasured integrating disturbances, the system model expressed in (6.10) is augmented with an integrating disturbance and verified to be detectable according to the general methodology proposed in [Pannocchia and Rawlings, 2003] and [Muske and Badgwell, 2002]. The process states are influenced by the input disturbances from animal heat production, heating system and external weather condition. In this work, the external weather for the wind and temperature is measured through a weather monitor. The resulting augmented system with state noise w and measurement noise v is:

$$\tilde{x}(k+1) = \tilde{A}\tilde{x}(k) + \tilde{B}u(k) + \tilde{G}w(k) \tag{6.14a}$$

$$y(k) = \tilde{C}\tilde{x}(k) + v(k) \tag{6.14b}$$

$$w(k) \sim \mathrm{N}(0, Q_w(k)) \tag{6.14c}$$

$$v(k) \sim \mathrm{N}(0, R_v(k)) \tag{6.14d}$$

in which the augmented state and system matrices are defined as follows,

$$\tilde{x}(k+1) = \begin{bmatrix} x(k+1) \\ x_{umd}(k+1) \end{bmatrix}_{6\times1}, \tilde{G} = \begin{bmatrix} B_{dmd} & 0 \\ 0 & B_{dumd} \end{bmatrix}_{8\times8}$$
$$\tilde{A} = \begin{bmatrix} A & B_{dumd}C_{umd} \\ 0 & A_{umd} \end{bmatrix}_{6\times6}, \tilde{B} = \begin{bmatrix} B \\ 0 \end{bmatrix}_{6\times12}, \tilde{C} = \begin{bmatrix} C & 0 \end{bmatrix}_{1\times6}. \tag{6.15}$$

The full process state $x \in \Re^3$ and unmeasurable disturbance state $x_{umd} \in \Re^3$ are estimated from the plant measurement y by means of an infinite horizon Kalman Filter. Q_w is the process noise covariance matrix and R_v is the measurement error covariance matrix. The process and measurement noise w and v are assumed to be uncorrelated zero-mean Gaussian processes. The measurable disturbance state $x_{md} \in \Re^5$ is assumed to remain unchanged within the prediction horizon and equal to the constant at the last measured value, namely $x_{umd}(k) = \hat{x}_{umd}(k+1/k) = \cdots = \hat{x}_{umd}(k+H_p-1/k)$. For time varying reference tracking, it is necessary to reformulate the system dynamics in Δu-form to introduce an integral controller [Kvasnica *et al.*, 2004] as stated in (6.16):

$$\begin{bmatrix} \tilde{x}(k+1) \\ x_{md}(k+1) \\ u(k) \\ x_{ref}(k+1) \end{bmatrix} = \begin{bmatrix} \tilde{A} & B_d C_{md} & \tilde{B} & 0 \\ 0 & A_{md} & 0 & 0 \\ 0 & 0 & I & 0 \\ 0 & 0 & 0 & I \end{bmatrix} \cdot \begin{bmatrix} \tilde{x}(k) \\ x_{md}(k) \\ u(k-1) \\ x_{ref}(k) \end{bmatrix} + \begin{bmatrix} \tilde{B} \\ 0 \\ I \\ 0 \end{bmatrix} \cdot \Delta u(k). \tag{6.16}$$

6.5 Simulation Results

In order to demonstrate the high potential of MPC for multi-variable control of the ventilation systems and the associated indoor climate in livestock stable, the simulation comparison between the system behaviors performed with and without controller, are presented.

Fig. 6.5 is derived in the presence of stochastic disturbances from external temperature with mean value 10 ^oC and wind speed with mean value 5 m/s, which are both generated from random sources through low-pass filters. The heat dissipated from animals of each zone is set by pulse change, for instance, adding 2000 J/s in the middle zone, and adding 1000 J/s in one of the other two zones. The system initially started from operating point which is defined by heating status and the outside disturbances aiming at maintaining the system behavior at the required condition with low horizontal variation. The output reference value is 19.7 ^oC and the reference control signal for air inlet opening on the windward side are 0.05, 0.053, 0.05, on the leeward side are 0.15, 0.15, 0.15, and supply 7 Voltage for each of the exhaust fan, 45 ^{o} for each of the swivel shutter.

The nonlinear process performing curves (dashed lines) in Fig. 6.5 demonstrates the system dynamic performances with fixed reference control inputs to the nonlinear system, and clarifies how the indoor climate influenced by the external weather and indoor heat sources. The close-loop performing curves (solid lines) in Fig. 6.5 illustrates the results with updated optimum control inputs to the nonlinear system computed from optimization computations at each sample time. The control algorithm is implemented within the MATLAB programming environment applying the Multi-Parametric Toolbox [Kvasnica *et al.*, 2004]. Because of the slow response of the nonlinear system behavior (the time constant is around 30 min), the sampling time step is defined to be 2 min, the prediction horizon is $H_p = 20(24\,\text{min})$, and the control horizon is $H_u = 3(6\,\text{min})$. The inlet valve opening area is limited within $0m^2$-$0.3m^2$, the supplied voltage to the fan is limited within

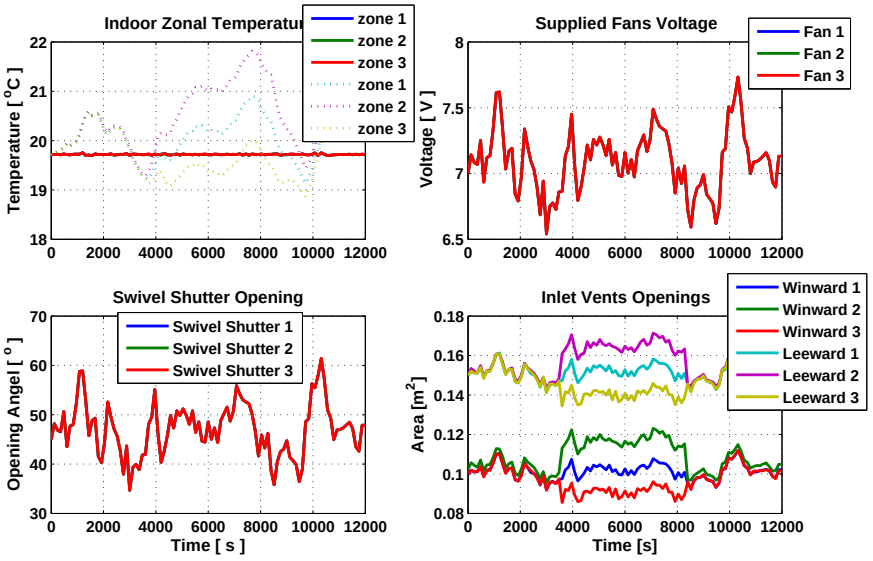

Figure 6.5: Comparison of Dynamic Performances of Zonal Temperature with and without MPC; The Response of Control Signals

$0V$-$10V$, the swivel shutter opening angle is limited within 0^o-90^o, the slew rate of the actuators are very fast compared with the sample rate and could be ignored. For animal thermal comfort, the indoor temperature is limited to $\pm 1.5^oC$ around the reference value. Tracking errors are penalized over the whole prediction horizon. The weights on tracking errors Q is same at each point in the prediction horizon, the weights on control moves R is same at each point in the control horizon.

Through comparing the simulation results, we could recognize that with the application of MPC, the system behavior has been profoundly modified, the variance of the output has been reduced considerably by adjusting the inlet valve openings and exhaust units individually as shown in Fig. 6.5, and therefore, the majority of the outdoor disturbances to the inside temperature have been effectively rejected without causing excessive energy consumptions.

To some extent, for the above introduced magnitude of the disturbance change, none of the constraints are active at any point of the transient. Suppose now, the system is operated with some pulse changes appeared in the external temperature which will lead to the large offset from the reference value and operation close to the active constraints. The reference has a step change of around 1^oC. As described in Fig. 6.6, the indoor temperature tendency spreads smoothly around the set-point value without large variations and track the reference without off-set; the voltages of the fans and the swivel shutter openings

are immediately raised in response to the onset of the disturbance, and be ranged against the constraint, hold the value below the constraint while the disturbance is present, and finally fall down when the disturbance ceases; the inlet valve openings are controlled within constraints and depict the clear response to the zonal local heating source disturbances. Therefore, the nonlinearities of MPC in handling constraints in a natural and flexible way, is manifested through this example.

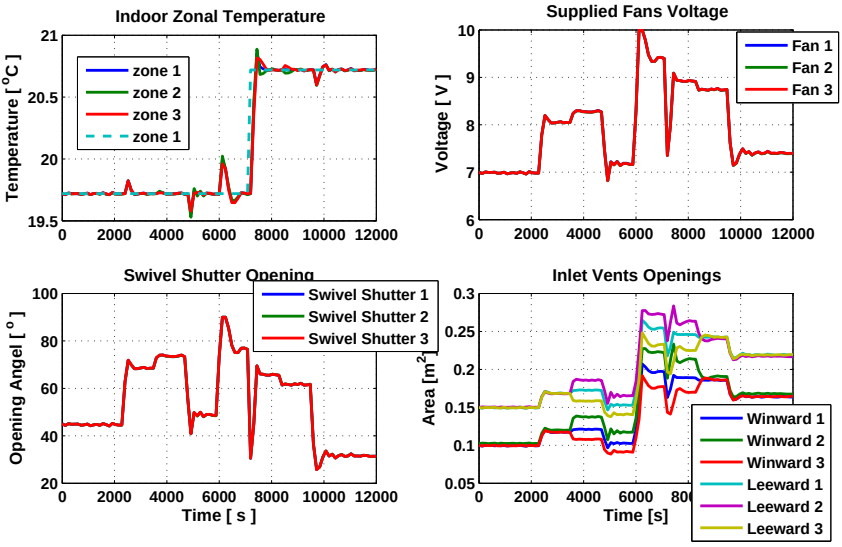

Figure 6.6: Reference Tracking and Disturbance Rejection; The Response of Control Signals

The above simulations are carried out based on one controller for nonlinear plant, by assuming that the heating system is controlled to remain at a constant value. Through step response analysis and behavior observation, we realize that, the plant nonlinearities is not very obvious. By varying the disturbances such as the zonal heat sources which cause the direction change of the inter zonal airflow, and external temperature which is the most direct influence in leading to the variation of the indoor thermal comfort, we obtain similar system performance with a serious of LTI models.

6.6 Conclusion and Future Work

6.6.1 Conclusion

For the purpose of improvement of performances and optimization of energy consumption, the main achievement of this work is the efficient application of MPC for livestock ventilation systems.

In this paper, through linearization of the nonlinear system, an LTI model in terms of state space representation which connected the thermal system and air distribution system is derived. The process model is augmented by the disturbance model to achieve offset-free control. The presented simulation results show the significant advantages of using MPC over linear models for control and estimation by choosing appropriate horizon length, weighting matrix and noise covariance matrix. Further more, it proves to be fruitful that the conceptual multi-zone modeling method for indoor thermal comfort contain significant information on horizontal variation which is not able to be captured by the single zone model with mean temperature and concentration, under the circumstances that the zonal disturbances changes.

6.6.2 Future Work

A weather filter will be designed according to the high and slow frequency change of the wind and temperature, so that the swivel shutter of the fan and heating system will be controlled automatically to attenuate the wind gust and adjust the indoor thermal environment. The entire control system will be identified through experiments in a real scale livestock barn equipped with hybrid ventilation systems in Syvsten, Denmark, and the result will be compared with those obtained with currently used classical PID controller.

6.7 Acknowledgment

The authors gratefully acknowledge the contribution and financial support from the Danish Ministry of Science and Technology (DMST), and Center for Model Based Control (CMBC) under Grant: 2002-603/4001-93.

Chapter 7

Model Predictive Control of Thermal Comfort and Indoor Air Quality in Livestock Stable

Zhuang Wu [1*], Murali R. Rajamani [2], James B. Rawlings [2], Jakob Stoustrup [1]

[1] *Department of Electronic Systems, Aalborg University, Fredrik Bajersvej 7C, 9220 Aalborg East, Denmark*
[2] *Department of Chemical and Biological Engineering, University of Wisconsin, Madison, WI 53706, U.S.A.*

This conference paper was presented at the IEEE European Control Conference (ECC), July, 2007. This paper is reproduced under the conditions of the copyright agreement with European Union Control Association (EUCA). The offset free tracking is achieved through using Target Calculation, Receding Horizon Regulation and Integration of Disturbance Model. The significant potential of applying Model Predictive Control for multiple objectives is illustrated.

Abstract

In this paper, the implementation of a Model Predictive Control (MPC) strategy for livestock ventilation systems and the associated indoor climate through variable operation of inlet and exhaust units, is presented. The design is based on Thermal Comfort (TC) and Indoor Air Quality (IAQ) parameters for poultry in barns. The dynamic models describing the nonlinear behavior of ventilation and associated indoor climate system, by applying a so-called conceptual multi-zone modeling method are used for prediction of indoor horizontal variation of temperature and carbon dioxide concentration. The simulation results illustrate the significant potential of MPC in dealing with nonlinearities, handling constraints and performing off-set free tracking for multiple control objectives. The entire control systems are able to determine the demand ventilation rate and airflow pattern, optimize the Thermal Comfort, Indoor Air Quality and energy use.

7.1 Introduction

An optimum livestock indoor climate should enhance voluntary feed intake and minimize thermal stresses that affect animals. The alleviation of thermal strain and the maintenance of comfort environment significantly depend on the measurement and control of the air temperature and the humidity. On the other hand, proper indoor air quality is imperative to maintain the health and productivity of farm workers and animals. Hence, the concentration level of contaminant gases, such as the carbon dioxide, has to be controlled through the ventilation system. Assuming that in the researched laboratory livestock building, an advanced waste-handling system equipped and the manure storage units are frequently cleaned, then if the ventilation rate are adequate to remove heat and contaminant organisms or gas, the moisture is usually well diluted and present no problem. Further more, humidity has little effect on thermal comfort sensation at or near comfortable temperatures unless it is extremely low or high. Therefore the humidity is not considered in this work.

Hybrid ventilation system combines the natural ventilation and mechanical ventilation, and have been widely used for livestock. Most existing control systems used for livestock barns are based on analysis with the single zone method, which assumes the indoor air temperature and contaminant concentration level are uniform and use the mean value for calculation, as has been discussed in [Cunha *et al.*, 1997],[Moor and Berckmans, 1996b] and [Taylor *et al.*, 2004]. However, as analyzed by [Clark, 1981], the actual indoor environment at any controlling sensors (especially when the sensors are located horizontally) will depend on the air flow distribution that is usually depicted as a map of the dominant air paths. Therefore, the control system for large scale livestock barns neglecting the horizontal variations could obviously result in significant deviations from the optimal environment for the sensitive pigs or poultry. Furthermore, the performance of currently used control schemes for livestock appear limited when large disturbances occur in the presence of input saturation.

As stated in books [Maciejowski, 2002], [Rossiter, 2003] and papers [Rawlings, 2000], [Mayne *et al.*, 2000], [Qin and Badgwell, 2003] and [Pannocchia *et al.*, 2005], Model Predictive Control (MPC) has become the advanced control strategy of choice by industry mainly for the economically important, large-scale, multi-variable processes in the plant. The rationale for MPC in these applications is that it can deal with strong non-linearities, handle constraints and modeling errors, fulfill offset-free tracking, and it is easy to tune and implement.

In this paper, the livestock indoor environment and its ventilation control system will be regarded as a feedback loop in which the predictive controller provides the optimal actions to the actuators taking into account the significant disturbances and random noises. The MPC strategy is not only expected to give good regulation of the horizontal variation of temperature and concentration, but also to minimize the energy consumption involved with operating the inlet valves, the exhaust fans and the swivel shutters.

7.2 Process Dynamic Modeling

7.2.1 Modeling of Thermal Comfort and Indoor Air Quality

The schematic diagram of a large scale livestock barn equipped with hybrid ventilation system analyzed with the conceptual multi-zone method is shown in Fig. 7.1(1), Fig. 7.1(2) and Fig. 7.1(3). The livestock ventilation system consists of evenly distributed exhaust units mounted in the ridge of the roof and fresh air inlet openings installed on the walls. From the view of direction A and B, Fig. 7.1(a) and Fig. 7.1(b) provide a description of the dominant air flow map of the building including the airflow interaction between each conceptual zones. Through the inlet system, the incoming fresh cold air mixes with indoor warm air and then drops down to the animal environmental zones slowly in order to satisfy the zonal comfort requirement.

By applying a conceptual multi-zone method, the building will be compartmentalized into several macroscopic homogeneous conceptual zones horizontally so that the nonlinear differential equation relating the zonal temperature and zonal concentration can be derived based on the energy and mass balance equation for each zone as (7.1) and (7.2). The subscript i denotes the zone number.

$$M_i c_{p,i} \frac{dT_i}{dt} = \dot{Q}_{i+1,i} + \dot{Q}_{i,i+1} + \dot{Q}_{in,i} + \dot{Q}_{out,i} + \dot{Q}_{transmission,i} + \dot{Q}_{source,i}, \tag{7.1}$$

$$\frac{dC_{r,i}}{dt} = C_{r,i+1} \cdot \dot{n}_{i+1,i} + C_{r,i} \cdot \dot{n}_{i,i+1} + C_{r,i} \cdot \dot{n}_{out} + C_{r,o} \cdot \dot{n}_{in} + \frac{G_i}{V_i}. \tag{7.2}$$

For (7.1), T_i is the indoor zonal air temperature (^oC), $c_{p,i}$ is the specific heat of the air ($J \cdot kg^{-1} \cdot K^{-1}$), M_i is the mass of the air (kg), $\dot{Q}_{i+1,i}$ and $\dot{Q}_{i,i+1}$ indicate the heat exchange (J/s) due to the air flow across the conceptual boundary of zone i and zone $i+1$, while for the middle zones which have heat exchange with neighbor zones on each side, two more parts $\dot{Q}_{i-1,i}$, $\dot{Q}_{i,i-1}$ will be added. $\dot{Q}_{in,i}$, $\dot{Q}_{out,i}$ represent the heat transfer (J/s) by

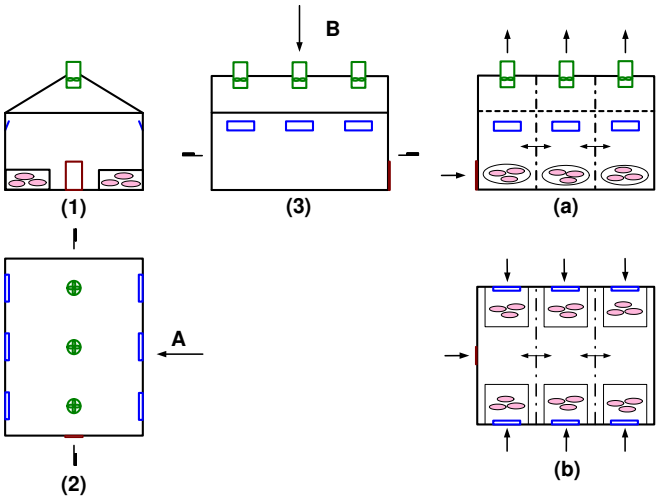

Figure 7.1: Synoptic of Large Scale Livestock Barn and the Dominant Airflow Map of the Barn

mass flow through the inlet and outlet respectively. The convective heat loss through the building envelope is denoted by $\dot{Q}_{transmission,i}$ (J/s) and described as $U \cdot A_{wall,i} \cdot (T_i - T_o)$, where U is the heat transfer coefficient, and A_{wall} is the area of the wall. The heat source of the zone $\dot{Q}_{source,i}$ includes the animal heat productivity and heat dissipated from heating system.

For (7.2), the rate of concentration is indicated as $C_{r,i} \cdot \dot{n}_i$, in which $C_{r,i}$ (m^3/m^3) represents the zonal concentration and $\dot{n}_i$ (h^{-1}) is the air exchange rate. The rate of the animal carbon dioxide generation denoted by G_i $(10^{-3}m^3/h)$ is approximately 12 times the actual activity level denoted by M_a (l/h), which is measured in *met* as stated in (7.3). The zonal volume is V_i (m^3).

$$G = 12 \cdot M_a. \tag{7.3}$$

7.2.2 Modeling of Inlet and Exhaust Fan System

The inlet system provides variable airflow directions and controls the amount of incoming fresh air by adjusting the bottom hanged flaps. The volume flow rate through the inlet is calculated by (7.4), where C_d is the discharge coefficient, A is the geometrical opening area (m^2), ΔP (Pa) is the pressure difference across the opening and can be computed by a set of routines solving thermal buoyancy and wind effect as (7.5). V_{ref} stands for the wind speed at reference height. C_P is the wind induced pressure coefficient and its value changes according to the wind direction, the building surface orientation and the topography and roughness of the terrain in the wind direction. The subscript NPL stands for the

Neutral Pressure Level. The coefficient C_d for the inlet system, varies considerably with the inlet type, opening area, as well as incoming air temperature and flow rate. However, for simplicity, we use a constant value of this coefficient for all openings, even though it might lead to over/under-prediction of airflow capacity and thereby larger openings than necessary.

$$q_{in} = C_d \cdot A_{inlet} \cdot \sqrt{\frac{2 \cdot \Delta P_{inlet}}{\rho}}, \tag{7.4}$$

$$\Delta P_{inlet} = \frac{1}{2} C_P \rho_o V_{ref}^2 - P_i + \rho_o g \frac{T_i - T_o}{T_i} (H_{NPL} - H_{inlet}). \tag{7.5}$$

In the exhaust unit, the airflow capacity is controlled by adjusting the r.p.m. of the fan impeller and the swivel shutter opening angle. We introduce a fan law, as a relationship between the total pressure difference ΔP_{fan}, volume flow rate q_{out}, supplied voltage V_{volt} and the opening angle of swivel shutter θ which can be approximated in a nonlinear static equation (7.6), where the parameters a_0, a_1, a_1, b_0, b_1, b_2 are empirically determined from experiments made by SKOV A/S in Denmark. As shown in (7.7), the total pressure difference across the fan is the difference between the wind pressure on the roof and the internal pressure at the entrance of the fan which considers the pressure distribution calculated upon the internal pressure at Neutral Pressure Level denoted by P_i.

$$\Delta P_{fan} = (b_0 + b_1 \cdot \theta + b_2 \cdot \theta^2) \cdot q_{out}^2 + a_0 \cdot {V_{volt}}^2 + a_1 \cdot q_{out} \cdot V_{volt} + a_2 \cdot q_{out}^2 \tag{7.6}$$

$$\Delta P_{fan} = \frac{1}{2} \rho_o C_{P,r} V_{ref}^2 - P_i - \rho_i g \frac{T_i - T_o}{T_o} (H_{NPL} - H_{fan}). \tag{7.7}$$

For a detailed description for developing the models and significant dynamic parameters estimation, we refer to [Wu *et al.*, 2005] and [Wu *et al.*, 2006].

7.3 Model Predictive Control

Model Predictive Control (MPC) refers to a class of control algorithms that compute a sequence of manipulated variable adjustments by utilizing a process model to optimize forecasts of process behavior based on a linear or quadratic open-loop performance objective, subject to equality or inequality constraints over a future time horizon.

7.3.1 Model Transformation

We regard the livestock ventilation system as two parts by noting that the overall system consists of a static air distribution system (inlet-exhaust air flow system) and a dynamic environmental system (thermal comfort and indoor air quality). Both of these two systems are mildly nonlinear Multiple Input and Multiple Output (MIMO) systems. However, representing or approximating a nonlinear model's dynamic response with some form of linear dynamics is an easy and illuminating way to analyze and solve on-line optimization,

and especially, for processes maintained at nominal operating conditions and subject to small disturbances, the potential improvement of using a nonlinear model in MPC would appear small. Therefore, the developed nonlinear process models are transformed into a series of Linear Time Invariant (LTI) state space models through linearization around the equilibrium points corresponding to different inter-zonal airflow direction. The Thermal Neutral Zone (TNZ) [der Hel *et al.*, 1986], [Geers *et al.*, 1991], and the demand concentration level are selected to be the criterion that represent the control objective. Fig. 7.2 shows the synoptic of the entire system model and the climate control variables.

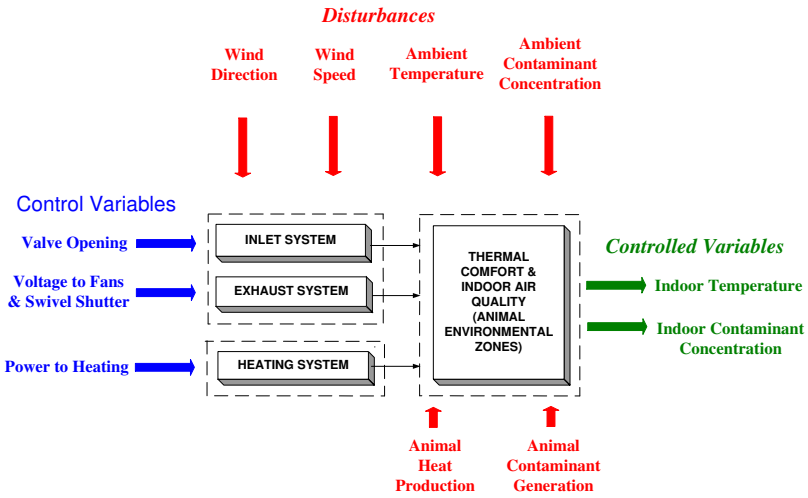

Figure 7.2: Synoptic of Entire System Model and Climate Control Variables

Let the nonlinear continuous time model (7.1) which is represented with three coupled equations for thermal comfort be described in the discrete time linearized dynamics state space form as (7.8):

$$x_T(k+1) = A_T \cdot x_T(k) + B_T \cdot q(k) + B_{Td} \cdot d_T(k), \tag{7.8a}$$

$$y_T(k) = C_T \cdot x_T(k) + D_T \cdot q(k) + D_{Td} \cdot d_T(k), \tag{7.8b}$$

where, $A_T \in \mathbb{R}^{3\times3}$, $B_T \in \mathbb{R}^{3\times12}$, $B_{Td} \in \mathbb{R}^{3\times8}$, $C_T \in \mathbb{R}^{3\times3}$, $D_T \in \mathbb{R}^{3\times12}$, $D_{Td} \in \mathbb{R}^{3\times8}$ are the coefficient matrices with subscript T denoting the model for the thermal comfort system. k is the current sample number. In the similar procedure, we could derive the state space form for the indoor air quality system as (7.9) according to (7.2):

$$x_C(k+1) = A_C \cdot x_C(k) + B_C \cdot q(k) + B_{Cd} \cdot d_C(k), \tag{7.9a}$$

$$y_C(k) = C_C \cdot x_C(k) + D_C \cdot q(k) + D_{Cd} \cdot d_C(k), \tag{7.9b}$$

where, $A_C \in \mathbb{R}^{3\times3}$, $B_C \in \mathbb{R}^{3\times12}$, $B_{Cd} \in \mathbb{R}^{3\times12}$, $C_T \in \mathbb{R}^{3\times3}$, $D_T \in \mathbb{R}^{3\times12}$, $D_{Td} \in \mathbb{R}^{3\times12}$ are the coefficient matrices with subscript C denoting the model for the concentration system.

By applying the conservation of mass for the livestock building with one single zone concept (7.10), and through linearization of air flow model deducted through (7.4) to (7.7), we can derive the static equation (7.11).

$$\sum_{i=1}^{6} q_{in}(k)\cdot\rho_o - \sum_{j=1}^{3} q_{out}(k)\cdot\rho_i = 0, \tag{7.10}$$

$$E\cdot\bar{q}(k) + F\cdot u(k) + G\cdot w(k) + K\cdot x_T(k) = 0, \tag{7.11}$$

where, E,F,G,K are coefficients matrices. The definition of $\bar{q}\in\mathbb{R}^{9+1}$ is: $[q_{in,m}, q_{out,n}, P_i]^T$, $m = 1\cdots6$, $n = 1\cdots3$, where, $[q]^T_{1\times9}$ is a airflow input vector which combines the actuators' signals u and the thermal process controlled variables x_T and x_C.

Connecting and coupling of the airflow model (7.11) with the environmental models (7.8) and (7.9), evolve a finalized LTI state space model representing the entire knowledge of the performances for thermal comfort and indoor air quality around the equilibrium point. The combined process model is shown in (7.12)

$$x(k+1) = A\cdot x(k) + B\cdot u(k) + B_d\cdot d(k), \tag{7.12a}$$

$$y(k) = C\cdot x(k) + D\cdot u(k) + D_d\cdot d(k), \tag{7.12b}$$

where, $A\in\mathbb{R}^{6\times6}$, $B\in\mathbb{R}^{6\times12}$, $C\in\mathbb{R}^{6\times6}$, $D\in\mathbb{R}^{6\times12}$, $B_d\in\mathbb{R}^{6\times12}$, $D_d\in\mathbb{R}^{6\times12}$ are the coefficient matrices. The disturbance transient matrices B_d and D_d are formulated as (7.13) corresponding to the unmeasured d_{md} and measured d_{umd} disturbances.

$$B_d = \begin{bmatrix} B_{dumd} & B_{dmd} \end{bmatrix}, D_d = \begin{bmatrix} D_{dumd} & D_{dmd} \end{bmatrix}. \tag{7.13}$$

x, y, u, d_{umd}, d_{md} denote the sequences of vectors representing the deviation variable values of the process state of zonal temperature x_T and concentration x_C, the measured output, the manipulated input which consists of the inlet valve openings, voltage supplied to the fans and shutter opening angle, the unmeasurable disturbances of animal heat and carbon dioxide generation, the measurable disturbances as the wind speed, wind direction, ambient temperature and concentration level. Assuming that $z(k)\equiv y(k)$, which means that the controlled output z is always same with the measured output y. The representation of these vectors is shown in (7.14)

$$x = \begin{bmatrix} \bar{T}_1 & \bar{T}_2 & \bar{T}_3 & \bar{C}_{r,1} & \bar{C}_{r,2} & \bar{C}_{r,3} \end{bmatrix}^T_{6\times1}, \tag{7.14a}$$

$$u = \begin{bmatrix} \bar{A}_{in,i=1\ldots6} & \bar{V}_{volt,j=1\ldots3} & \bar{\theta}_{shutter,j=1\ldots3} \end{bmatrix}^T_{12\times1}, \tag{7.14b}$$

$$d_{umd} = \begin{bmatrix} \bar{\dot{Q}}_1 & \bar{\dot{Q}}_2 & \bar{\dot{Q}}_3 & \bar{G}_1 & \bar{G}_2 & \bar{G}_3 \end{bmatrix}^T_{6\times1}, \tag{7.14c}$$

$$d_{md} = \begin{bmatrix} \bar{V}_{ref} & \bar{c}_{P,w} & \bar{c}_{P,l} & \bar{c}_{P,r} & \bar{T}_o & \bar{C}_{r,o} \end{bmatrix}^T_{6\times1}. \tag{7.14d}$$

Concluded from systematical analysis, the pair (A,B) is controllable, the pair (C,A) is observable, and the plant is stable. Thus, the model transformation is accomplished and well prepared for solving of the optimization problem in the predictive control scheme.

7.3.2 Disturbance Model and State Estimation

To achieve offset-free control of the output to their desired targets at steady state, in the presence of plant/model mismatch and/or unmeasured disturbances, the system model expressed in (7.12) is augmented with an integrated disturbance model as proposed in [Pannocchia and Rawlings, 2003] and [Muske and Badgwell, 2002]. The animal heat and contaminant generation partly as a result of function of the number of the animals, are measurable. The parts of the stochastic generation process which in reality affected by various factors, assumed to be unmeasured. The resulting augmented system with process noise n_w and measurement noise n_v is:

$$\tilde{x}(k+1) = \tilde{A}\tilde{x}(k) + \tilde{B}u(k) + \tilde{G}n_w(k), \tag{7.15a}$$

$$y(k) = \tilde{C}\tilde{x}(k) + n_v(k), \tag{7.15b}$$

$$n_w(k) \sim \mathrm{N}(0, Q_w(k)), \tag{7.15c}$$

$$n_v(k) \sim \mathrm{N}(0, R_v(k)), \tag{7.15d}$$

in which the augmented state and system matrices are defined as follows,

$$\begin{aligned} \tilde{x}(k) &= \begin{bmatrix} x(k) \\ x_{umd}(k) \end{bmatrix}_{12\times 1}, \tilde{A} = \begin{bmatrix} A & B_{dumd}C_{dumd} \\ 0 & A_{dumd} \end{bmatrix}_{12\times 12}, \\ \tilde{B} &= \begin{bmatrix} B \\ 0 \end{bmatrix}_{12\times 12}, \tilde{C} = \begin{bmatrix} C & 0 \end{bmatrix}_{6\times 12}, \tilde{G} = \begin{bmatrix} B_{dmd} & 0 \\ 0 & B_{dumd} \end{bmatrix}_{12\times 12}. \end{aligned} \tag{7.16}$$

The full process state $x \in \mathbb{R}^6$ and unmeasurable disturbance state $x_{umd} \in \mathbb{R}^6$ are estimated from the plant measurement y by means of a steady state Kalman filter. The process and measurement noise n_w and n_v are assumed to be uncorrelated zero-mean Gaussian noise sequences with covariance Q_w and R_v. The measurable deterministic disturbance $d_{md} \in \mathbb{R}^{12}$ is assumed to remain unchanged within the prediction horizon and equal to the constant at the last measured value, namely $d_{dmd}(k) = d_{dmd}(k+1/k) = \cdots = d_{dmd}(k+H_p-1/k)$. The detectability of the augmented system in 7.15 is guaranteed when the following condition holds:

$$Rank \begin{bmatrix} (I-A) & -G \\ C & 0 \end{bmatrix} = n + s_d, \tag{7.17}$$

in which, n is the number of the process states, s_d is the number of the augmented disturbance states. This condition ensures a well-posed target tracking problem. For detailed explanation about the proof refer to [Rawlings, 2000] and [Rao and Rawlings, 1999].

7.3.3 Target Calculation

We now formulate the target tracking optimization as the quadratic program formulation in (7.18), in which the steady state target of output, state and input vector (z_s, x_s, u_s) can be determined from the solution of the following computation when tracking a nonzero output reference z_t and the desired input u_t, where $z_s = Cx_s$.

$$\min_{[x_s,u_s]^T} \Psi = (u_s - u_t)^T R_s (u_s - u_t) \tag{7.18a}$$

$$s.t. \begin{cases} \begin{bmatrix} I-A & -B \\ C & 0 \end{bmatrix} \begin{bmatrix} x_s \\ u_s \end{bmatrix} = \begin{bmatrix} B_{dumd}\hat{d}_{umd,k/k} + B_{dmd}d_{md} \\ z_t \end{bmatrix} \\ u_{\min} \le u_s \le u_{\max} \end{cases} \tag{7.18b}$$

In this quadratic program, $R_s \in \mathbb{R}^{9\times 9}$ is a positive definite weighting matrix for the deviation of the input vector from u_t. $\hat{d}_{umd,k/k}$ is the current estimation of the unmeasured state disturbance. The equality constraints in (7.18) guarantee a steady-state solution and offset free tracking of the target vector.

7.3.4 Constrained Receding Horizon Regulation

Given the calculated steady state, the constrained optimization problem is formulated as (7.19) by a quadratic cost function on finite horizon, subjected to the following linear equality and inequalities formed by the system dynamics (7.12) and constraints on the controlled and manipulated variables.

$$\begin{aligned} \min_{u^N} \Phi_k = {} & \hat{w}_{k+N}^T \bar{Q}_N \hat{w}_{k+N} + \Delta v_{k+N}^T S_N \Delta v_{k+N} + \\ & + \sum_{j=0}^{N-1} \left[\hat{w}_{k+j}^T C^T Q C \hat{w}_{k+j} + v_{k+j}^T R v_{k+j} + \Delta v_{k+j}^T S \Delta v_{k+j} \right] \end{aligned} \tag{7.19a}$$

$$s.t. \begin{cases} w_{k+j} = x_{k+j} - x_s, \\ v_{k+j} = u_{k+j} - u_s, \\ w_{k+j+1} = A w_{k+j} + B v_{k+j}, \\ y_{\min} - y_s \le C w_{k+j} \le y_{\max} - y_s, j = 1, 2, \cdots N \\ u_{\min} - u_s \le v_{k+j} \le u_{\max} - u_s, j = 0, 1, \cdots N-1 \\ \Delta u_{\min} \le \Delta v_{k+j} \le \Delta u_{\max}, j = 0, 1, \cdots N \end{cases} \tag{7.19b}$$

where, Φ is the performance index to be minimized by penalizing the deviations of the predictive state $\hat{x}_{k+j}$, control input u_{k+j} and the rate of change Δu_{k+j}, at time j, from the desired steady states. $Q \in \mathbb{R}^{6\times 6}$ and $S \in \mathbb{R}^{12\times 12}$ are symmetric positive semi-definite penalty matrices for process states and rate of input change, $R \in \mathbb{R}^{12\times 12}$ is a symmetric positive definite penalty matrix. It is commonly taken that Q comprises terms of the form $C^T C$ where $r_{k+j} - y_{k+j} = C(x_s - x_{k+j})$. The vector u^N contains the N future open-loop

control moves as shown below

$$u^N = \begin{bmatrix} u_k \\ u_{k+1} \\ \vdots \\ u_{k+N-1} \end{bmatrix}. \tag{7.20}$$

At time $k+N$, the input vector u_{k+j} is set to zero and kept at this value for all $j \geq N$ in the open-loop objective function value calculation. As discussed in the previous section, the plant is stable, therefore, according to [Muske and Rawlings, 1993b], Q_N is defined as the infinite sum: $Q_N = \sum_{i=0}^{\infty} A^{T^i} Q A^i$, which will be determined from the solution of the discrete Lyapunov equation: $Q_N = C^T Q C + A^T Q_N A$. This regulator formulation guarantees nominal stability for all choices of tuning parameters satisfying the conditions outlined above [Muske and Rawlings, 1993b], [Mayne *et al.*, 2000].

The output constraints are applied from time $k+j_1$, $j_1 \geq 1$, through time $k+j_2$, $j_2 \geq j_1$. The value of j_2 is chosen such that feasibility of the output constraints up to time $k+j_2$ implies feasibility of these constraints on the infinite horizon. The value of j_1 is chosen such that the output constraints are feasible at time k. The constrained regulator will remove the output constraints at the beginning of the horizon up to time $k+j_1$ in order to obtain feasible constraints and a solution to the quadratic program. [Muske and Rawlings, 1993b] and [Muske, 1995] explain the existence of finite values for both j_1 and j_2.

Through on-line constrained dynamic optimization, we could obtain a sequence of optimal control signals u^N through a state and disturbance estimator, and the first input value in u^N, u_k, is injected into the plant. This procedure is repeated by using the plant measurements to update the state vector at time k.

7.4 Simulation Results

In order to demonstrate the significant potential of MPC for multi-objective control within constraints, the comparison between the system behaviors performed with and without controller, in the presence of disturbances and noises, are presented. For the following scenario, we assume that the constraint stability of the control system is guaranteed in the infinite horizon when the feasibility of the input constraints is satisfied within the finite horizon N.

Fig. 7.3 is derived based on the nonlinear plant model simulation which is developed from a laboratory livestock stable, where the inlet valve opening is limited within $0(m^2)$-$0.6(m^2)$, the supplied voltage to the fan is limited within $0(V)$-$10(V)$, the entire volume of the laboratory livestock stable is around 2500 (m^3). Because of the slow response of the nonlinear system behavior, the sampling time step is defined to be 2 (*min*), the prediction horizon is $N = 20$. The slew rate of the actuators are very fast compared with the sample time and could be ignored. For animal thermal comfort, the indoor temperature

is limited within $\pm 1.5(^oC)$ around the reference value $21(^oC)$ within the TNZ. For indoor air quality, the indoor air concentration level should be maintained below $700(ppm)$.

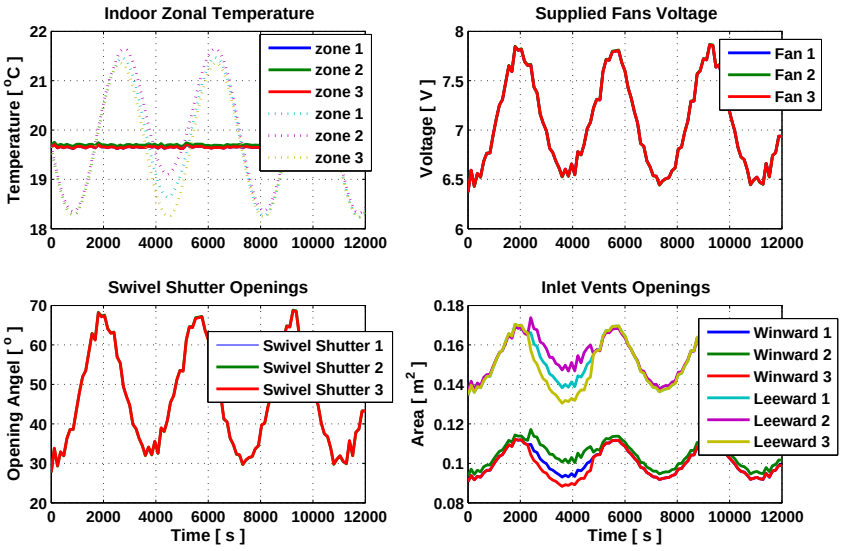

Figure 7.3: Rejection of Deterministic Disturbance: Dynamic Performances of Zonal Temperature with and without MPC; The Response of Control Signals

The nonlinear process behavior performing curves (dashed lines) in Fig. 7.3 demonstrates the thermal system dynamic performances with fixed reference control inputs to the nonlinear system, and clarifies how the imposed disturbances, such as the *sin* curve varying of external temperature, and pulse changes of heating load (adding 2000 (J/s) in the middle zone, and adding 1000 (J/s) in one of the other two zones) influence the system.

The closed loop performance curves (solid lines) illustrates the results with updated optimum control inputs to the nonlinear thermal comfort system. The weights Q on the tracking errors are different according to different requirement of control objective, the weights R on control inputs and weights S on rate of input change are different for inlets and exhaust fans. Through comparing the simulation results, we could recognize that with the application of MPC, the system behavior has been profoundly modified, and the variance of the output has been reduced considerably.

In the same condition of disturbances setting, and with a step change of the reference value for comfortable temperature, Fig. 7.4 (a) and 7.4 (b) show the system performances and actuators behavior. The indoor zonal temperatures keep tracking the reference with slight variations, the carbon dioxide concentration level falls down when the system begin

to react to the increase of external temperature and internal heat sources by controlling the rotating speed of the fans, opening angle of the swivel shutters and the inlet flaps. Thus, the off-set free tracking performances has been achieved by optimizing the steady state value and introducing unmeasurable input disturbance model in terms of integrated white noise. As shown in Fig. 7.4(b), the voltages of the fans and the swivel shutter are immediately raised in response to the onset of the disturbance, and ranged against the constraint, hold the value below the constraint while the disturbance is present, and decrease when the disturbance ceases. The variation of the inlet valve openings on the windward side is smaller than the openings on the leeward side, so that the low pressure (negative internal pressure) ventilation strategy is guaranteed. The nonlinearities of the MPC in handling constraints naturally and flexibly, is manifested through this example.

Through step response analysis and bode plot comparison, we realize that, the plant nonlinearities are not highly significant. By varying the disturbances such as the zonal heat sources which cause the direction change of the inter zonal airflow, and varying the external temperature which are the leading factors of the variation of the indoor thermal comfort, we obtain similar system behaviors with a series of LTI models.

7.5 Conclusion and Future Work

7.5.1 Conclusion

The main achievement of this work is the efficient application of MPC through target calculation, disturbance modeling and receding horizon optimization for multiple objectives: indoor thermal comfort and air quality control. In this paper, an LTI model in terms of state space representation which combined the thermal system and concentration system in connection with the air distribution system is derived. The Offset-free control is achieved and the unmeasured disturbance or model/plant mismatch is compensated. The presented simulation results show the significant advantages of using MPC over linear models for controlled system performance improvement and energy optimization.

7.5.2 Future Work

The Moving Horizon Estimation method will be applied when the unmeasured disturbance constraints are presented and further performance improvement are needed. The weighting matrix on the states of indoor temperature and concentration will be further adjusted in order to achieve a better equilibrium between multiple objectives requirements. The entire control system will be identified through experiments in a real scale livestock barn equipped with hybrid ventilation systems in Syvsten, Denmark, and the result will be compared with those obtained with the currently used controller.

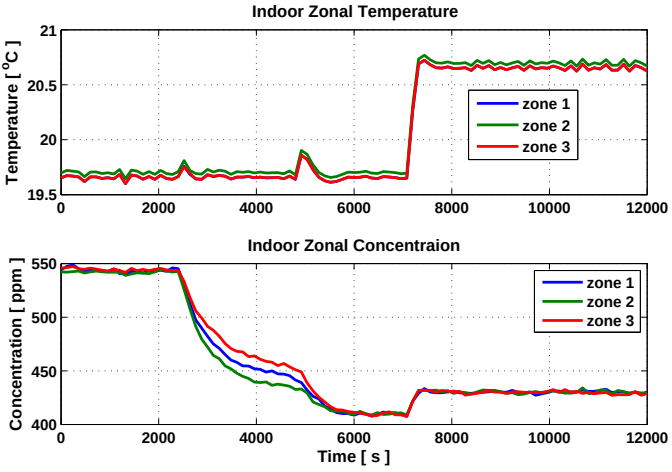

(a)

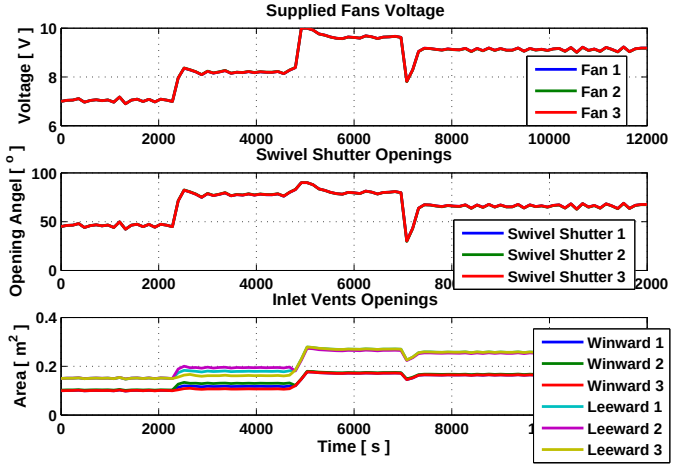

(b)

Figure 7.4: (a) Reference Tracking and Rejection of Deterministic Disturbance. Dynamic Performances of Zonal Temperature and Concentration (b) Optimal Control Signal of Supplied Fans Voltage; Swivel Shutter; Inlet Vents Opening Area

7.6 Acknowledgment

The authors gratefully acknowledge the contribution and financial support from the Danish Ministry of Science and Technology (DMST), and Center for Model Based Control (CMBC) under Grant: 2002-603/4001-93.

Chapter 8

Application of Auto-covariance Least - Squares Method for Model Predictive Control of Hybrid Ventilation in Livestock Stable

Zhuang Wu [1*], Murali R. Rajamani [2], James B. Rawlings [2], Jakob Stoustrup [1]

[1] *Department of Electronic Systems, Aalborg University, Fredrik Bajersvej 7C, 9220 Aalborg East, Denmark*
[2] *Department of Chemical and Biological Engineering, University of Wisconsin, Madison, WI 53706, U.S.A.*

This conference paper was presented at the 26th IEEE American Control Conference (ACC), July, 2007. This paper is reproduced under the conditions of the copyright agreement with the American Automatic Control Council (AACC). The application of Auto-covariance Least Square method is applied in the estimation system for model predictive control of hybrid ventilation system for livestock indoor climate. The purpose is to illustrate the advantages of this method on increasing estimation quality, improving output performance and compensating model/plant mismatch.

Abstract

In this paper, the implementation of a new Auto-covariance Least Square (ALS) technique for livestock hybrid ventilation systems and associated indoor climate with a Model Predictive Control (MPC) strategy is presented. The design is based on thermal comfort parameters for poultry in barns and a combined dynamic model describing the entire system knowledge. Offset-free tracking is achieved with target calculation, moving horizon regulation and disturbance modeling. The unknown noise covariances are diagnosed and corrected by applying the ALS estimator with the closed loop process data. The comparative simulation results show the performance improvement with the ALS estimator in the presence of disturbances and moderate amount of error in the model parameters. The comparison demonstrates the high potential of ALS methods in improving the best practice of process control and estimation.

8.1 Introduction

Environmental control for living systems differs greatly from comparable control for physical systems. Environmental requirements for living systems are typically more complex and nonlinear, and the biological system is likely to have significant and numerous effects on its physical surroundings. The objective of this work is the design of a advanced control system for the hybrid ventilation system and associated indoor environment for livestock barn, where hybrid ventilation systems combine the natural ventilation and mechanical ventilation, and have been widely used for livestock stables. Based on a so called conceptual multi-zone modeling method, the horizontal variation of the indoor temperature and ventilation rate are taken into account and the entire process becomes a strongly coupled Multiple Input and Multiple Output (MIMO) dynamic nonlinear system. The system is exposed to external disturbances with random noises and has actuators with saturation.

As stated in books [Maciejowski, 2002] and [Rossiter, 2003], papers [Mayne *et al.*, 2000], [Rawlings, 2000], [Qin and Badgwell, 2003] and [Pannocchia *et al.*, 2005], Model Predictive Control (MPC) has become the advanced control strategy of choice by industry mainly for the economically important, large-scale, multi-variable processes in the plant. The rationale for MPC in these applications is that it can deal with strong non-linearities, handle constraints and modeling errors, fulfill offset-free tracking, and it is easy to tune and implement. Consequently, applying MPC technology to allow a trade-off between the thermal comfort and energy consumption within constraints is necessary and promising.

The heat dissipation from living animals such as pigs or poultry is one of the major influencing factors to the indoor comfort conditions, and lack of the knowledge about these disturbances makes the implementation of the control algorithm complicated, especially when covariances of the disturbance are unknown. A variety of methods have been proposed to solve this problem. A new Auto-covariance Least-Squares (ALS) method for estimating noise covariances using routine operating data is employed to recover the co-

variances and adaptively determine an optimal kalman filter gain. [Odelson *et al.*, 2007] and [Odelson *et al.*, 2006] have researched and proved the superior advantages of ALS method convincingly through comparing with previous work.

In this paper, the livestock indoor environment and its ventilation control system will be regarded as a feedback loop. Through regulation, target calculation and state estimation, the predictive controller provides the optimal control actions involved with operating the inlet and the exhaust units. The ALS technique is not only expected to give an optimal estimator gain, but also to improve the closed loop performance in the presence of the disturbances and model/plant mismatch. The comparative simulation results derived with the control system with nominal estimator and the ALS method are illustrated.

8.2 Process Dynamic Modeling

The schematic diagram of a large scale livestock barn equipped with hybrid ventilation system analyzed with conceptual multi-zone method is shown in Fig. 8.1(1), 8.1(2) and 8.1(3). The system consists of evenly distributed exhaust units mounted in the ridge of the roof and fresh air inlet openings installed on the walls. From the view of direction A and B, Fig. 8.1(a) and 8.1(b) provide a description of the dominant air flow map of the building including the airflow interaction between each conceptual zone.

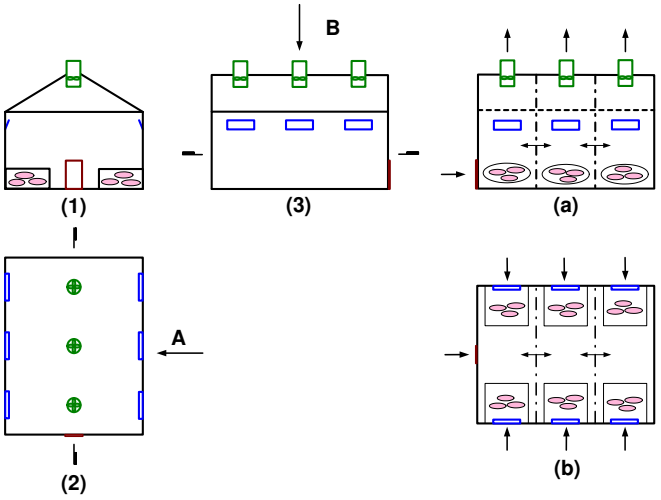

Figure 8.1: Large Scale Livestock Barn and the Dominant Airflow Map of the Barn

As stated in [Wu *et al.*, 2005] and [Wu *et al.*, 2006], the differential algebraic equations governing the sensible heat for indoor thermal comfort is shown in (8.1). The subscript *i*

represents the zone number.

$$M_i c_{p,i} \frac{dT_i}{dt} = \dot{Q}_{i+1,i} + \dot{Q}_{i,i+1} + \dot{Q}_{in,i} + \dot{Q}_{out,i} + \dot{Q}_{transmission,i} + \dot{Q}_{source,i}, \tag{8.1}$$

where, T_i is the zonal air temperature (^oC), $c_{p,i}$ is the specific heat of the air ($J \cdot kg^{-1} \cdot K^{-1}$), M_i is the mass of the air (kg), $\dot{Q}_{i+1,i}$, indicate the heat exchange (J/s) due to the air flow across the conceptual boundary of zone i and zone $i+1$. $\dot{Q}_{in,i}$, $\dot{Q}_{out,i}$ represent the heat transfer (J/s) by air flow through inlet and outlet respectively. The convective heat loss through the building envelope is denoted by $\dot{Q}_{transmission,i}$ (J/s). The heat source $\dot{Q}_{source,i}$ includes the heat gain from animal heat production and heating system.

The volume flow rate through the inlet is calculated by (8.2), where C_d is the discharge coefficient, A is the geometrical opening area (m^2), ΔP is the pressure difference across the opening (Pa) and can be computed by a set of routines solving thermal buoyancy and wind effect as (8.3). The subscript ref stands for the value at reference height, NPL stands for the Neutral Pressure Level (NPL). The internal pressure at a reference height is denoted by P_i.

$$q_{in} = C_d \cdot A_{inlet} \cdot \sqrt{\frac{2 \cdot \Delta P_{inlet}}{\rho_o}}, \tag{8.2}$$

$$\Delta P_{inlet} = \frac{1}{2} C_P \rho_o V_{ref}^2 - P_i + \rho_o g \frac{T_i - T_o}{T_i} (H_{NPL} - H_{inlet}). \tag{8.3}$$

The exhaust unit consists of an axial-type fan and a swivel shutter. We introduce a fan law, as a relationship between the total pressure difference ΔP_{fan}, volume flow rate q_{out}, supplied voltage V_{volt} and the opening angle of swivel shutter θ which can be expressed in (8.4) and (8.5), where the parameters a_0, a_1, a_1, b_0, b_1 and b_2 are empirically determined.

$$\Delta P_{fan} = (b_0 + b_1 \cdot \theta + b_2 \cdot \theta^2) \cdot q_{out}^2 + a_0 \cdot {V_{volt}}^2 + a_1 \cdot q_{out} \cdot V_{volt} + a_2 \cdot q_{out}^2 \tag{8.4}$$

$$\Delta P_{fan} = \frac{1}{2} \rho_o C_{P,r} V_{ref}^2 - P_i - \rho_i g \frac{T_i - T_o}{T_o} (H_{NPL} - H_{fan}). \tag{8.5}$$

For a detailed description and necessary simplifying assumptions of the development of system models, we refer to [Heiselberg, 2004a].

8.3 Model Predictive Control

Model Predictive Control (MPC) refers to a class of control algorithms that compute a sequence of manipulated variable adjustments by utilizing a process model to forecast process behavior and optimize based on a linear or quadratic open-loop performance objective, subject to equality or inequality constraints over a future time horizon.

8.3.1 Model Transformation

We regard the livestock ventilation system as two parts by noting that the overall system consists of a static air distribution system (inlet-exhaust air flow system) and a dynamic thermal system (animal environmental zones). Both of these two systems are mildly nonlinear with MIMO. However, representing or approximating a nonlinear model's dynamic response with some form of linear dynamics is an easy and illuminating way to analyze and solve on-line optimization, and especially, for processes maintained at nominal operating conditions and subject to small disturbances, the potential improvement of using a nonlinear model in MPC would appear small.

Through substitution and multiplication as described in [Wu *et al.*, 2006], the general form of a combined Linear Time Invariant (LTI) state space representation as (8.6) connecting the airflow model with thermal model, and representing the entire system dynamics around the equilibrium point is obtained.

$$x(k+1) = A \cdot x(k) + B \cdot u(k) + B_d \cdot \begin{bmatrix} d_{umd}(k) \\ d_{md}(k) \end{bmatrix}, \tag{8.6a}$$

$$y(k) = C \cdot x(k) + D \cdot u(k) + D_d \cdot \begin{bmatrix} d_{umd}(k) \\ d_{md}(k) \end{bmatrix}, \tag{8.6b}$$

where,

$$B_d = \begin{bmatrix} B_{dumd} & B_{dmd} \end{bmatrix}, D_d = \begin{bmatrix} D_{dumd} & D_{dmd} \end{bmatrix}. \tag{8.7}$$

and, $A \in \Re^{3\times3}$, $B \in \Re^{3\times12}$,$C \in \Re^{3\times}$, $D \in \Re^{3\times12}$,$B_d \in \Re^{3\times8}$,$D_d \in \Re^{3\times8}$ are the coefficient matrices at the equilibrium point. x,y,u,d_{umd},d_{md} denote the sequences of vectors representing deviation variable values of the process state for the indoor temperature of each conceptual zone, the measured output which is equal to the state, the manipulated input which consists of the inlet openings, voltage supplied to the fans and the shutter opening angles, the disturbances of the heat generated from animals and heating system, and the disturbances of external wind speed, wind direction and ambient temperature respectively. y is the measured output, and usually assumed to be same with the controlled output z, $z(k) \equiv y(k)$.

$$x = \begin{bmatrix} \bar{T}_1 & \bar{T}_2 & \bar{T}_3 \end{bmatrix}^T_{3\times1}, \tag{8.8a}$$

$$u = \begin{bmatrix} \bar{A}_{in,i=1\ldots6} & \bar{V}_{volt,j=1\ldots3} & \bar{\theta}_{shutter,j=1\ldots3} \end{bmatrix}^T_{12\times1}, \tag{8.8b}$$

$$d_{umd} = \begin{bmatrix} \bar{\dot{Q}}_1 & \bar{\dot{Q}}_2 & \bar{\dot{Q}}_3 \end{bmatrix}^T_{3\times1}, \tag{8.8c}$$

$$d_{md} = \begin{bmatrix} \bar{V}_{ref} & \bar{c}_{P,w} & \bar{c}_{P,l} & \bar{c}_{P,r} & \bar{T}_o \end{bmatrix}^T_{5\times1}. \tag{8.8d}$$

The pair (A,B) is controllable and the pair (A,C) is observable. The process is stable. Thus, the nonlinear plant model has been transformed into a series of LTI state space models and well prepared for solving the optimization problem in the predictive control scheme.

8.3.2 Disturbance Model and State Estimation

To achieve offset-free control of the output to their desired targets at steady state, in presence of plant/model mismatch and/or un-modeled disturbances, the system model expressed in (8.6) is augmented with an integrated disturbance model according to the general methodology proposed in [Pannocchia and Rawlings, 2003] and [Muske and Badgwell, 2002]. The process performance are influenced by the input disturbances from animal heat production, heating system and external weather condition. The animal productivity heat which is affected by various factors, will be modeled by integrating a random white noise. The resulting augmented system with process noise n_w and measurement noise n_v is:

$$\tilde{x}(k+1) = \tilde{A}\tilde{x}(k) + \tilde{B}u(k) + \tilde{G}n_w(k), \tag{8.9a}$$
$$y(k) = \tilde{C}\tilde{x}(k) + n_v(k), \tag{8.9b}$$
$$n_w(k) \sim \mathrm{N}(0, Q_w(k)), \tag{8.9c}$$
$$n_v(k) \sim \mathrm{N}(0, R_v(k)), \tag{8.9d}$$

in which the augmented state and system matrices are defined as follows,

$$\begin{aligned} \tilde{x}(k) &= \begin{bmatrix} x(k) \\ x_{umd}(k) \end{bmatrix}_{6\times 1}, \tilde{A} = \begin{bmatrix} A & B_{dumd}C_{umd} \\ 0 & A_{umd} \end{bmatrix}_{6\times 6}, \\ \tilde{B} &= \begin{bmatrix} B \\ 0 \end{bmatrix}_{6\times 12}, \tilde{C} = \begin{bmatrix} C & 0 \end{bmatrix}_{3\times 6}, \tilde{G} = \begin{bmatrix} B_{dmd} & 0 \\ 0 & B_{umd} \end{bmatrix}_{8\times 8}. \end{aligned} \tag{8.10}$$

The full process state $x \in \Re^3$ and unmeasurable disturbance state $x_{umd} \in \Re^3$ are estimated from the plant measurement y by means of a steady state Kalman filter. The process and measurement noise n_w and n_v are assumed to be uncorrelated zero-mean Gaussian noise sequences with covariance Q_w and R_v. The determination of these covariances for an optimal filter gain is addressed in the ALS estimator section. The measurable deterministic disturbance $d_{umd} \in \Re^8$ is assumed to remain unchanged within the prediction horizon and equal to the constant at the last measured value, namely $d_{umd}(k) = \hat{d}_{dumd}(k+1/k) = \cdots = \hat{d}_{dumd}(k+H_p-1/k)$. The detectability of the augmented system in (8.9) is guaranteed when the condition holds:

$$Rank\begin{bmatrix} (I-A) & -G \\ C & 0 \end{bmatrix} = n + s_d, \tag{8.11}$$

in which, n is the number of the process states, s_d is the number of the augmented disturbance states. This condition ensures a well-posed target tracking problem. The methods for checking detectability and proofs are provided in [Muske and Badgwell, 2002] and [Pannocchia and Rawlings, 2003].

8.3.3 Target Calculation

We now formulate the target tracking optimization as the quadratic program formulation in (8.12), in which the steady state target of the output, state and input vector (z_s, x_s, u_s) can be determined from the solution of the following computation when tracking the nonzero output reference z_t and the desired input u_t, where $z_s = Cx_s$.

$$\min_{[x_s,u_s]^T} \Psi = (u_s - u_t)^T R_s (u_s - u_t) \tag{8.12a}$$

$$s.t. \begin{cases} \begin{bmatrix} I-A & -B \\ C & 0 \end{bmatrix} \begin{bmatrix} x_s \\ u_s \end{bmatrix} = \begin{bmatrix} 0 \\ z_t \end{bmatrix} \\ u_{\min} \le u_s \le u_{\max} \end{cases} \tag{8.12b}$$

In this quadratic program, R_s is a positive definite weighting matrix for the deviation of the input vector from u_t. The equality constraints guarantee a steady-state solution and offset free tracking of the target vector.

8.3.4 Constrained Receding Horizon Regulation

Given the calculated steady state, the constrained optimization problem for receding horizon regulation is formulated as (8.13a) by a quadratic cost function on finite horizon, subjected to the linear equality and inequalities formed by the system dynamics (8.6) and equipment limitation and the constraints on the controlled variables.

$$\begin{aligned} \min_{u^N} \Phi_k &= \hat{w}_{k+N}^T \bar{Q} \hat{w}_{k+N} + \Delta v_{k+N}^T S \Delta v_{k+N} + \\ &+ \sum_{j=0}^{N-1} \left[\hat{w}_{k+j}^T C^T Q C \hat{w}_{k+j} + v_{k+j}^T R v_{k+j} + \Delta v_{k+j}^T S \Delta v_{k+j} \right] \end{aligned} \tag{8.13a}$$

$$s.t. \begin{cases} w_{k+j} = x_{k+j} - x_s, \\ v_{k+j} = u_{k+j} - u_s, \\ w_{k+j+1} = A w_{k+j} + B v_{k+j}, \\ y_{\min} - y_s \le C w_{k+j} \le y_{\max} - y_s, j = j_1, j_1+1, \cdots j_2 \\ u_{\min} - u_s \le v_{k+j} \le u_{\max} - u_s, j = 0, 1, \cdots N-1 \\ \Delta u_{\min} \le \Delta v_{k+j} \le \Delta u_{\max}, j = 0, 1, \cdots N \end{cases} \tag{8.13b}$$

where, Φ is the performance index to be minimized by penalizing the deviations of the predictive state $\hat{x}_{k+j}$, control input u_{k+j} and the rate of change Δu_{k+j}, at time j, from the desired steady states. $Q \in \Re^{3\times3}$ and $S \in \Re^{12\times12}$ are symmetric positive semi-definite penalty matrices, $R \in \Re^{12\times12}$ is symmetric positive definite penalty matrix. It is commonly taken that Q comprises terms of the form $C^T C$ where $r_{k+j} - y_{k+j} = C(x_s - x_{k+j})$.

The vector u^N contains the N future open-loop control moves as shown below

$$u^N = \begin{bmatrix} u_k \\ u_{k+1} \\ \vdots \\ u_{k+N-1} \end{bmatrix} \tag{8.14}$$

At time $k+N$, the input vector u_{k+j} is set to zero and kept at this value for all $j \geq N$ in the open-loop objective function value calculation. As discussed in previous section, the plant is stable, therefore, according to [Muske and Rawlings, 1993b], Q_N is defined as the infinite sum: $Q_N = \sum_{i=0}^{\infty} A^{T^i} Q A^i$, which will be determined from the solution of the discrete Lyapunov equation: $Q_N = C^T Q C + A^T Q_N A$. This regulator formulation guarantees nominal stability for all choices of tuning parameters satisfying the conditions outlined above ([Muske and Rawlings, 1993a] and [Mayne *et al.*, 2000]).

The output constraints are applied from time $k+j_1$, $j_1 \geq 1$, through time $k+j_2$, $j_2 \geq j_1$. The value of j_2 is chosen such that feasibility of the output constraints up to time $k+j_2$ implies feasibility of these constraints on the infinite horizon. The value of j_1 is chosen such that the output constraints are feasible at time k. The constrained regulator will remove the output constraints at the beginning of the horizon up to time $k+j_1$ in order to obtain feasible constraints and a solution to the quadratic program. [Muske and Rawlings, 1993a] and [Muske, 1995] explain the existence of finite values for both j_1 and j_2.

Through on-line constrained dynamic optimization, we could obtain a sequence of optimal control signals u^N through a state and disturbance estimator, and the first input value in u^N: u_k, is injected into the plant. This procedure is repeated by using the plant measurements to update the state vector at time k.

8.4 ALS Estimator

The technique described in this section is originated in [Odelson *et al.*, 2007] and [Odelson *et al.*, 2006]. Consider the LTI discrete-time model of the augmented system as (8.9), estimates of the states of the system are constructed using the standard Kalman filter as (8.15)

$$\hat{x}_{k+1/k} = A\hat{x}_{k/k-1} + Bu_k + AL_k(y_k - C\hat{x}_{k/k-1}). \tag{8.15}$$

The estimate error is defined as $\varepsilon_k = x_k - \hat{x}_{k/k-1}$, with covariance $P_{k/k-1}$. This covariance $P_{k/k-1} = E\left[\varepsilon_k \varepsilon_k^T\right]$ is the solution to the *Riccati* equation (8.16)

$$\begin{aligned} P_{k+1/k} = {} & AP_{k/k-1}A^T + GQ_wG^T \\ & - AP_{k/k-1}C^T\left[CP_{k/k-1}C^T + R_v\right]^{-1} CP_{k/k-1}A^T, \end{aligned} \tag{8.16}$$

and the Kalman gain L_k is defined as (8.17)

$$L_k = P_{k/k-1}C^T\left[CP_{k/k-1}C^T + R_v\right]^{-1}. \tag{8.17}$$

Assume we process the y_k to obtain state estimates using a linear filter with gain L, which is not necessarily the optimal L for the system. The state estimation error ε_k evolves according to (8.18)

$$\varepsilon_{k+1} = (A - ALC)\varepsilon_k + \begin{bmatrix} G & -AL \end{bmatrix}\begin{bmatrix} w_k \\ v_k \end{bmatrix}. \tag{8.18}$$

The state space model of the innovations $\mathscr{Y} = y_k - C\hat{x}_{k/k-1}$ is defined as (8.19)

$$\varepsilon_{k+1} = \bar{A}\varepsilon_k + \bar{G}\bar{w}_k, \tag{8.19a}$$

$$\mathscr{Y}_k = C\varepsilon_k + v_k, \tag{8.19b}$$

in which,

$$\bar{A} = \left[A - ALC\right]_{n\times n}, \bar{G} = \begin{bmatrix} G & -AL \end{bmatrix}_{n\times(g+p)}, \bar{w} = \begin{bmatrix} w_k \\ v_k \end{bmatrix}_{(g+p)\times 1}. \tag{8.20}$$

n is the number of states in (8.9), p is the number of outputs, g is the number of independent noises. (A,C) is detectable, $\bar{A} = A - ALC$ is stable, the initial estimate error is distributed with mean m_0 and covariance P_0^-. We choose k sufficiently large so that the effects of the initial condition can be neglected, or equivalently, we choose the steady-state distribution as the initial condition:

$$E(\varepsilon_0) = m_0 = 0, \mathrm{cov}(\varepsilon_0) = P_0^- = P^-. \tag{8.21}$$

Now we consider the Auto-covariance which is defined as the expectation of the data with some lagged version of itself [Jenkins and Watts, 1968]

$$\mathscr{C}_j = E\left[\mathscr{Y}_k\mathscr{Y}_{k+1}^T\right], \tag{8.22}$$

and the symmetric Auto-Covariance Matrix (ACM) is then defined as (8.23)

$$\mathscr{R}(N_a) = \begin{bmatrix} \mathscr{C}_0 & \cdots & \mathscr{C}_{N_a-1} \\ \vdots & \ddots & \vdots \\ \mathscr{C}_{N_a-1}^T & \cdots & \mathscr{C}_0 \end{bmatrix}, \tag{8.23}$$

where, N is the user-defined number of lags used in ACM. Accordingly, an ACM of the innovations can be written as follows:

$$\begin{aligned} [\mathscr{R}(N_a)]_s = &\left[(\mathscr{O}\otimes\mathscr{O})(I_{n^2} - \bar{A}\otimes\bar{A})^{-1} + (\Gamma\otimes\Gamma)\mathscr{I}_{n,N_a}\right](G\otimes G)(Q_w)_s \\ &+ \left\{\left[(\mathscr{O}\otimes\mathscr{O})\left(I_{n^2} - \bar{A}\otimes\bar{A}\right)^{-1} + (\Gamma\otimes\Gamma)\mathscr{I}_{n,N_a}\right](AL\otimes AL)\right. \\ &\left. + \left[\Psi\oplus\Psi + I_{p^2{N_a}^2}\right]\mathscr{I}_{p,N_a}\right\}(R_v)_s, \end{aligned} \tag{8.24}$$

in which

$$\mathscr{O} = \begin{bmatrix} C \\ C\bar{A} \\ \vdots \\ C\bar{A}^{N_a-1} \end{bmatrix}, \Psi = \Gamma \begin{bmatrix} \overset{N_a}{\underset{j=1}{\oplus}} (-AL) \end{bmatrix}, \Gamma = \begin{bmatrix} 0 & 0 & 0 & 0 \\ C & 0 & 0 & 0 \\ \vdots & \ddots & \vdots & \vdots \\ C\bar{A}^{N_a-2} & \cdots & C & 0 \end{bmatrix}. \tag{8.25}$$

$\mathscr{I}_{n,N}$ is a permutation matrix that converts the direct sum to a vector, i.e. $\mathscr{I}_{n,N_a}$ is the $(pN_a)^2 \times p^2$ matrix of zeros and ones satisfying

$$\begin{pmatrix} \overset{N_a}{\underset{i=1}{\oplus}} R_v \end{pmatrix}_s = \mathscr{I}_{p,N_a} (R_v)_s, \tag{8.26}$$

where, the subscript s denotes the outcome of applying the *vec* operator. Practically, the estimate of the auto-covariance from real data is computed as

$$\hat{\mathscr{C}}_j = \frac{1}{N_d - j} \overset{N_d-j}{\underset{i=1}{\sum}} \mathscr{Y}_i \mathscr{Y}_{i+j}^T, \tag{8.27}$$

where, N_d is the sample size. Therefore, the estimated ACM $\hat{\mathscr{R}}(N_a)$ is analogously defined using the computed $\hat{\mathscr{C}}_j$.

We define the ALS estimate as

$$\hat{x} = \left[(\hat{Q}_w)_s^T (\hat{R}_v)_s^T \right]^T = \arg\min_x \left\| \mathscr{A} \cdot \hat{x} - \hat{\mathscr{R}}(N_A)_s \right\|_2^2, \tag{8.28}$$

and the solution for estimating Q_w, R_v is the well-known

$$\hat{x} = (\mathscr{A}^T \mathscr{A})^{-1} \mathscr{A}^T \cdot \hat{b}, \tag{8.29}$$

where, $\mathscr{A}$ indicates the left hand side matrix to the least square problem, and

$$\mathscr{A} = \left[D(G \otimes G) \quad D(AL \otimes AL) + \left[\Psi \oplus \Psi + I_{p^2N^2} \right] \mathscr{I}_{p,N_a} \right], \tag{8.30}$$

$$D = \left[(\mathscr{O} \otimes \mathscr{O})(I_{n^2} - \bar{A} \otimes \bar{A})^{-1} + (\Gamma \otimes \Gamma) \mathscr{I}_{n \times N_A} \right], \tag{8.31}$$

$$x = \begin{bmatrix} (Q_w)_s^T & (R_v)_s^T \end{bmatrix}^T, b = \mathscr{R}(N_a)_s. \tag{8.32}$$

The uniqueness of the estimate is a standard result of least-squares estimation [Lawson and Hanson, 1995]. The covariance can be found uniquely when the matrix $\mathscr{A}$ has full column rank. However, in the augmented system as (8.9), the dimension of the driving noise is $w \in \Re^{11}$, according to [Odelson *et al.*, 2007] and [Odelson *et al.*, 2006], it is unlikely to find unique estimates of the covariance (Q_w, R_v), and the solution may not be positive semi-definite. In order to avoid leading to any meaningless solution, adding the

semi-definite constraint directly to the estimation problem to maintain a convex program as (8.33) will ensure uniqueness of the covariance estimation.

$$V = \min_{Q_w, R_v} \left\| \mathscr{A} \begin{bmatrix} (Q_w)_s \\ (R_v)_s \end{bmatrix} - \hat{b} \right\|_2^2 \tag{8.33a}$$

$$s.t. \begin{cases} Q_w \geq 0 \\ R_v \geq 0 \end{cases} \tag{8.33b}$$

The constraints in (8.33) are convex, and the optimization is in the form of a semi-definite programming (SDP) problem, which can be solved efficiently with Newton's method [Nocedal and Wright, 1999].

8.5 Simulation Results

In order to demonstrate the benefits of applying MPC scheme with ALS estimator, the comparison of the control system behavior between using ALS and the nominally tuned estimator are presented. Since we have introduced an integrated white noise model for the input disturbance which could account for the model/plant mismatch, the following simulation results are derived in the presence of a step change of deterministic un-modeled output disturbance. We assume that the state noise covariance $Q_w = 0.01$ and measurement noise $R_v = 0.001$. The data set used for computation is collected from the open loop nonlinear plant simulation. Let $N_d = 200$ and $N_a = 12$. The first 30 points are used as the training set, and the rest are used as a validation set. For the control system, the sampling time step is $T_s = 120(s)$, the prediction horizon is $H_N = 20$.

The estimator gain determined from the known covariances is conventionally regarded as a good tuning choice. However, as demonstrated in Fig. 8.2, in the presence of a step increase of output disturbance, there are some visiable contrasts in the closed loop output performances between using the ALS estimator (solid curves) and the nominal estimator. Using the ALS estimator, the regulator is able to reject the disturbances, tracking the reference faster and further reduce the steady state variances. The frequency distribution for the actuator's changes are shown in Fig. 8.3. The changing frequency of the six inlet openings and supplied voltages for three fans are about the same. It proves that the improved closed loop performance does not require more aggressive manipulated inputs with ALS estimator.

The covariance estimation techniques are based on the properties of the process innovations. Implementing ALS has high potential for improving the quality of estimation in comparison with the original estimator. This may be illustrated as Fig. 8.4 by comparing the frequency distribution of the innovations $\mathscr{Y} = y_k - C\hat{x}_{k/k-1}$ for ALS with that of an nominal estimator.

In conclusion, the normal tuning approach for estimator gain is time consuming and probably prone to failure especially when the real covariances are unknown. The predictive controller combined with the ALS estimator is able to not only achieve off-set free

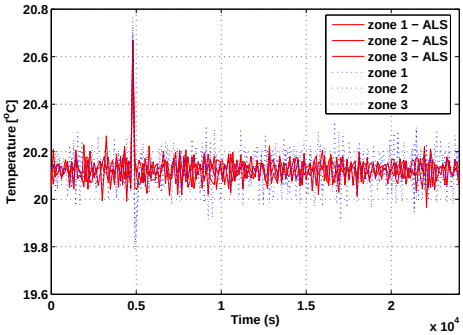

Figure 8.2: Comparison of Closed loop Performances for Set-point Tracking with ALS and Nominal Estimator

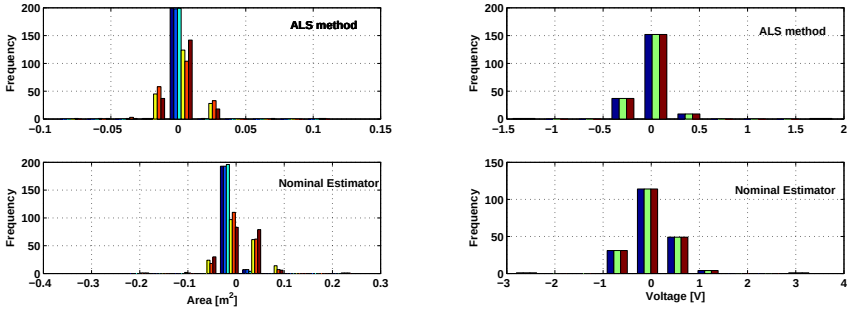

Figure 8.3: Histogram of the Changes in Manipulated Inputs - (a) Inlet Vent Openings (b) Supplied Fan Voltages

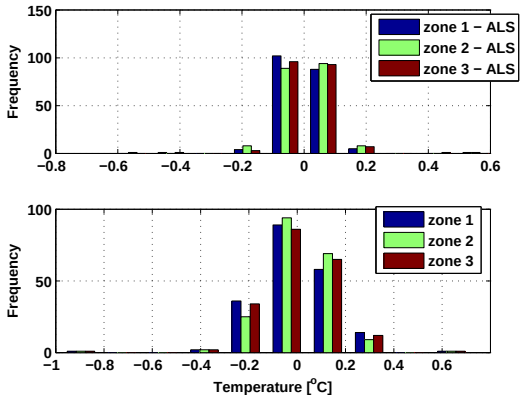

Figure 8.4: Histogram of the Innovations with ALS method and Nominal Estimator

tracking, but also design an optimal estimator to compensate model/plant mismatch and un-modeled disturbances without sacrificing more control actions.

8.6 Conclusion and Future Work

8.6.1 Conclusion

The main achievement of this work is the efficient application of the ALS method to design an adaptive estimation filter for Model Predictive Control of livestock ventilation systems. Through linearization of the nonlinear system, an LTI model in terms of state space representation which connected the thermal system and air distribution system is derived. The process model is augmented by the integrated white noise disturbance model to achieve offset-free control. The presented simulation results show the significant advantages and performance improvement when using MPC over linear models for control and ALS method for estimation.

8.6.2 Future Work

The capability of the proposed estimation method for compensating model/plant mismatch or un-modeled disturbances need further investigations. The theoretical proof and related research could refer to [Rajamani and Rawlings, 2007]. The entire control and estimation system will be implemented and identified in a real scale livestock barn equipped with hybrid ventilation systems in Syvsten, Denmark. The result will be compared with those obtained with the currently used control and estimation system.

8.7 Acknowledgement

The authors gratefully acknowledge the contribution and financial support from the Danish Ministry of Science and Technology (DMST) and Center for Model Based Control (CMBC) with Grant number: 2002-603/4001-93.

Chapter 9

Moving Horizon Estimation and Control of Livestock Ventilation Systems and Indoor Climate

Zhuang Wu [1*], John Bagterp Jorgensen [2], Jakob Stoustrup [1]

[1] *Department of Electronic Systems, Aalborg University, Fredrik Bajersvej 7C, 9220 Aalborg East, Denmark*
[2] *Department of Informatics and Mathematical Modeling, Technical University of Denmark, Kongens Lyngby, 2800 Copenhagen, Denmark*

This conference paper was presented at the 17^{th} *Triennial Event of International Federation of Automatic Control (IFAC) World Congress, June, 2008. This paper is reproduced under the conditions of the copyright agreement with The International Federation of Automatic Control (IFAC). This paper presents the implementation of finite horizon Moving Horizon Estimation and Control scheme with infinite horizon approximation method through online optimization computation. Actuator redundancy strategy is designed to enhance the system resilience to the high frequency wind speed variation and save energy consumption.*

Abstract

In this paper, a new control strategy involves exploiting actuator redundancy in a multi-variable system is developed for rejecting the covariance of the high frequency disturbances and pursuing optimum energy solution. This strategy enhances the resilience of the control system to disturbances beyond its bandwidth and reduce energy consumption through on-line optimization computation. The moving horizon estimation and control (also called predictive control) technology is applied and simulated. The design is based on a coupled mathematical model which combines the hybrid ventilation system and the associated indoor climate for poultry in barns. The comparative simulation results illustrate the significant potential and advancement of the moving horizon methodologies in estimation and control for nonlinear Multiple Input and Multiple Output system with unknown noise covariance and actuator saturation.

9.1 Introduction

The design objective of this work is to design a control strategy to improve the performance of a hybrid ventilation control system for livestock indoor climate. The hybrid ventilation system combines the natural ventilation and mechanical ventilation ([Heiselberg, 2004b]). As shown in Fig. 9.1, the full scale livestock ventilation system consists of evenly distributed exhaust units mounted in the ridge of the roof and fresh air inlet openings installed on the side walls. From the view of direction A and B, Fig. 9.1(a) and 9.1(b) provide a description of the dominant air flow map of the building including the airflow interaction between each conceptual zones.

Traditionally, the livestock ventilation system has been controlled using classical SISO controllers through single zone analysis. The challenge of this work is to introduce a more efficient and comprehensive multi-variable control scheme based on the conceptual multi-zone modeling method to allow a better trade off between the optimum performances of indoor climate and energy consumption saving. The controller mainly focuses on minimizing the variation of the indoor temperature and concentration level, keeping both variables within the Thermal Neutral Zone (TNZ) ([der Hel *et al.*, 1986] and [Geers *et al.*, 1991]) in the presence of actuator saturation, random noise, and disturbances at different frequencies.

Dynamic optimization implemented in moving horizon estimation and control has successfully been applied to a number of industrial processes in order to realize the ambitions of lowering production costs, increasing asset utilization, and improving product quality by reducing the variability of key process quality indicators ([Jorgensen, 2005]). The applications are mainly for the economically important, large-scale, multi-variable processes, and the rationale is that this optimization formulated control algorithm can deal with strong non-linearities, handle constraints and modeling errors, fulfill offset-free tracking, and is easy to tune and implement ([Maciejowski, 2002], [Rossiter, 2003], [Qin and Badgwell, 2003] and [Pannocchia *et al.*, 2005]).

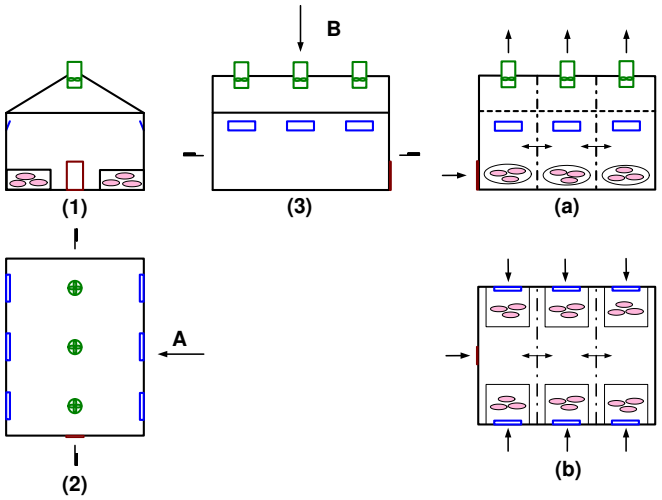

Figure 9.1: Synoptic of Full-scale Livestock Barn

An actuator redundancy is exploited to accommodate the limitation of the bandwidth of the closed-loop system as well as pursuit of an optimum energy solution through on-line optimization computation. By assigning different weights in the objective function which is based on energy consumption considerations, according to the covariance of the high frequency disturbances, the modified optimal control command are reassigned to the actuators. Through exploring the nonlinearities of the axial type fan and swivel shutter in the exhaust unit for passive disturbance attenuation, this strategy enhances the resilience of the predictive control system to disturbances beyond its bandwidth and further reduces energy consumption.

The comparative simulation results derived from the control system with dynamic optimization of moving horizon implementation and the nominal control method are illustrated. Most importantly, the output performances with and without actuator redundancy in the presence of disturbances are demonstrated. The proposed control technique in this paper proved to be fruitful for its high potential and advanced advantages on improving system performance and increasing system utilization.

9.2 Process Dynamic Model

Based on the so called conceptual multi-zone modeling method, the livestock building is compartmentalized into several macroscopic homogeneous conceptual zones horizontally so that the nonlinear differential equations governing the thermal comfort and indoor air quality can be derived based on the energy balance equation for each zone. The inlet

system provides variable airflow directions and controls the amount of incoming fresh air by adjusting the bottom hanged flaps. In the exhaust unit, the airflow capacity is controlled by adjusting the r.p.m. of the fan impeller and the opening angle of swivel shutter. Basically, the zone partition is according to the number of the operating exhaust units. For a detailed description for developing, simplifying and coupling of the models and significant dynamic parameters estimation, we refer to [Wu *et al.*, 2005], [Wu *et al.*, 2007b] and [Wu *et al.*, 2008a].

We regard the livestock ventilation system as consisting of two parts by noting that the overall system consists of a static air distribution system (inlet-exhaust air flow system) and a dynamic environmental system (thermal comfort and indoor air quality). The two parts are interconnected through air flow rate. This strongly coupled Multiple Input and Multiple Output (MIMO) dynamic nonlinear system is expressed as a Linear Time Invariant (LTI) state space representation around the equilibrium point

$$x(k+1) = A \cdot x(k) + B \cdot u(k) + B_d \cdot \begin{bmatrix} d_{umd}(k) \\ d_{md}(k) \end{bmatrix}, \tag{9.1a}$$

$$y(k) = C \cdot x(k) + D \cdot u(k) + D_d \cdot \begin{bmatrix} d_{umd}(k) \\ d_{md}(k) \end{bmatrix}, \tag{9.1b}$$

where, $A \in \mathbb{R}^{6\times6}$, $B \in \mathbb{R}^{6\times12}$, $C \in \mathbb{R}^{6\times6}$, $D \in \mathbb{R}^{6\times12}$, $B_d \in \mathbb{R}^{6\times12}$, $D_d \in \mathbb{R}^{6\times12}$ are the coefficient matrices. The disturbance transient matrices B_d and D_d are formulated as (9.2) corresponding to the unmeasured d_{umd} and measured d_{md} disturbances.

$$B_d = \begin{bmatrix} B_{dumd} & B_{dmd} \end{bmatrix}, D_d = \begin{bmatrix} D_{dumd} & D_{dmd} \end{bmatrix}. \tag{9.2}$$

x, y, u, d_{umd}, d_{md} denote the sequences of vectors representing the deviation variable values of the process state of zonal temperature x_T and carbon dioxide concentration x_C, the measured output, the manipulated input which consists of the inlet valve opening areas, voltages supplied to the fans and the swivel shutter opening angles, the unmeasurable disturbances of animal heat and carbon dioxide generation, the measurable disturbances as the wind speed, wind direction, ambient temperature and concentration level. Assuming that $z(k) \equiv y(k)$, which means that the controlled output z is always same with the measured output y. The representation of these vectors is shown in (9.3)

$$x = \begin{bmatrix} \bar{T}_1 & \bar{T}_2 & \bar{T}_3 & \bar{C}_{r,1} & \bar{C}_{r,2} & \bar{C}_{r,3} \end{bmatrix}^T_{6\times1}, \tag{9.3a}$$

$$u = \begin{bmatrix} \bar{A}_{in,i=1\ldots6} & \bar{V}_{volt,j=1\ldots3} & \bar{\theta}_{shutter,j=1\ldots3} \end{bmatrix}^T_{12\times1}, \tag{9.3b}$$

$$d_{umd} = \begin{bmatrix} \bar{\dot{Q}}_1 & \bar{\dot{Q}}_2 & \bar{\dot{Q}}_3 & \bar{G}_1 & \bar{G}_2 & \bar{G}_3 \end{bmatrix}^T_{6\times1}, \tag{9.3c}$$

$$d_{md} = \begin{bmatrix} \bar{V}_{ref} & \bar{c}_{P,w} & \bar{c}_{P,l} & \bar{c}_{P,r} & \bar{T}_o & \bar{C}_{r,o} \end{bmatrix}^T_{6\times1}. \tag{9.3d}$$

Concluded from the systematical analysis for the developed process model, the pair (A,B) is controllable, the pair (C,A) is observable, and the plant is stable.

9.3 Moving Horizon Estimation and Control

Moving horizon estimation and control is implemented through dynamic optimization calculations. These calculations are conducted on-line and repeated each time when new information such as process measurements become available, the horizon of the estimator and the regulator are shifted one sample forward. At each time, the dynamic optimization considers a fixed window backward of the past measurements to estimate the current state of the system, then the estimated state is used in the process model to forecast the process behavior within a fixed window forward. The dynamic optimization computes the optimal sequence of manipulable variables (control inputs) so that the predicted process behavior is as close to the desired setting reference as possible subject to the physical and operational constraints of the system. Only the first element in the sequence of optimal manipulable variables is implemented on the process.

9.3.1 Target Calculation

As discussed in [Rao and Rawlings, 1999] and [Rawlings, 2000], the target tracking optimization could be formulated as (9.4) with a least-square objective function subjected to the constraints, in which the steady state target of input and state vector u_s and x_s can be determined from the solution of the following computation when tracking a nonzero target vector z_t. The objective of the target calculation is to find the feasible triple (z_s, x_s, u_s) such that z_s and u_s are as close as possible to z_t and u_t, where u_t is the desired value of the input vector at steady state, and, $z_s = Cx_s$. The system has 12 inputs and 3 outputs, therefore, the optimization computation will generate the best combination of the inputs to satisfy the output target at steady state.

$$\min_{[x_s,u_s]^T} \Psi = (u_s - u_t)^T R_s (u_s - u_t) \tag{9.4a}$$

$$s.t. \begin{cases} \begin{bmatrix} I-A & -B \\ C & 0 \end{bmatrix} \begin{bmatrix} x_s \\ u_s \end{bmatrix} = \begin{bmatrix} 0 \\ z_t \end{bmatrix} \\ u_{\min} \leq u_s \leq u_{\max} \end{cases} \tag{9.4b}$$

In this quadratic program, R_s is a positive definite weighting matrix for the deviation of the input vector from u_t. The equality constraints guarantee a steady-state solution and offset free tracking of the target vector. In order to guarantee the uniqueness of the solution through the target calculation, assuming the feasible region is nonempty, the system must be detectable which is also a necessary condition for the nominal stability of the regulator as discussed in the following section [Rao and Rawlings, 1999]. The methods for checking detectability are provided in [Muske and Badgwell, 2002] and [Pannocchia and Rawlings, 2003].

9.3.2 Moving Horizon Control

Constrained Optimization

In [Muske and Rawlings, 1993b], the moving horizon control is formulated as (9.5) by a quadratic cost function on finite horizon, subjected to the following linear equality and inequalities formed by the system dynamics (9.1) and constraints on the controlled and manipulated variables are proposed. [Rao and Rawlings, 1999] and [Rawlings, 2000] discuss the feasibility issues by relaxing the problem in an l_1/l_2^2 optimal sense in the target calculation. The following optimization problem with the exact soft constraints is proposed in [Scokaert and Rawlings, 1999].

$$\begin{aligned}\min_{u^N}\Phi_k^N = &\sum_{j=1}^{N}\frac{1}{2}\left\|z_{k+j}-r_{k+j}\right\|_{Q_z}^2+\frac{1}{2}\|\eta_k\|_{S_\eta}^2+s_\eta'\eta_k\\ &+\frac{1}{2}\sum_{j=0}^{N-1}\left\|\Delta u_{k+j}\right\|_S^2+\left\|u_{k+j}-u_s\right\|_R^2,\end{aligned} \tag{9.5a}$$

$$s.t.\begin{cases} x_{k+j+1}=Ax_{k+j}+Bu_{k+j}+B_d d_{k+j}\\ z_{k+j}=Cx_{k+j}\\ z_{\min}\le z_{k+j}\le z_{\max}, j=1,2,\cdots N\\ u_{\min}\le u_{k+j}\le u_{\max}, j=0,1,\cdots N-1\\ \Delta u_{\min}\le \Delta u_{k+j}\le \Delta u_{\max}, j=0,1,\cdots N-1\end{cases} \tag{9.5b}$$

where, Φ is the performance index to be minimized by penalizing the deviations of the output $\hat{z}_{k+j}$ from the reference r_{k+j}, the slew rate of actuator Δu_{k+j} and the control input u_{k+j} from the desired steady states u_s at time j. The steady state input vector u_s can be determined from the solution of target calculation. $Q_z \in \mathbb{R}^{6\times 6}$ and $S \in \mathbb{R}^{9\times 9}$ are symmetric positive semi-definite penalty matrices for process states and rate of input change, $R \in \mathbb{R}^{9\times 9}$ is a symmetric positive definite penalty matrix. η_k is a slack variable introduced in both the quadratic and linear terms with coefficient S_η and s_η to relax output constraints and avoid infeasible mathematical programs ([Scokaert and Rawlings, 1999]). The vector u^N contains the N future open-loop control moves as shown below

$$u^N = \begin{bmatrix} u_k \\ u_{k+1} \\ \vdots \\ u_{k+N-1}\end{bmatrix}. \tag{9.6}$$

At time $k+N$, the input vector u_{k+j} is set to zero and kept at this value for all $j \ge N$ in the optimization calculation. Since the plant is stable, according to the parametrization method proposed in [Muske and Rawlings, 1993b], the end prediction $z_{k+1} = CAx_k$, implies $z_k = CA^{k-N}x_N$ for $k \ge N$ such that

$$\sum_{k=N}^{\infty} z_k^T Q z_k = x_N^T\left(\sum_{k=N}^{\infty}\left(CA^{k-N}\right)^T QCA^{k-N}\right)x_N = x_N^T Q_N x_N, \tag{9.7}$$

in which, Q_N may be computed from the Lyapunov equation

$$Q_N = \sum_{k=N}^{\infty} \left(CA^{k-N}\right)^T QCA^{k-N} = \sum_{j=0}^{\infty} \left(CA^j\right)^T QCA^j = C^T QC + A^T Q_N A. \tag{9.8}$$

It proved to be clear that the solution generated from the finite horizon optimization formulation with a terminal equality constraint is the approximate solution to the infinite horizon linear quadratic optimal control problem for stable systems. The selection of horizon N has been subject of extensive research ([Muske and Rawlings, 1993a], [Rawlings and Muske, 1993], [Scokaert and Rawlings, 1998], and [Mayne *et al.*, 2000]).

Unconstrained Optimization

The feedback gain of moving horizon control derived from the unconstrained linear quadratic optimization, together with the estimator gain derived from Kalman Filter provide the framework for analyzing properties such as the stability and bandwidth of the system in frequency domain. The formulation of finite horizon quadratic programming without constraint has been discussed in [Rawlings and Muske, 1993] for stability analysis and briefly described as follows:

$$\min_{u^N} \Phi_k^N = \frac{1}{2} u^{NT} H u^N + g^T u^N \tag{9.9}$$

in which, $H = \Gamma^T Q_z \Gamma + H_S$ is the hessian matrix, $g = M_{x_0} x_0 + M_R R + M_{u_{-1}} u_{-1} + M_D D$, $M_{x_0} = \Gamma^T Q_z \Phi$, $M_R = -\Gamma^T Q_Z$, $M_D = \Gamma^T Q_z \Gamma_D$

$$\begin{aligned}
\Phi &= \begin{bmatrix} C_z A \\ C_z A^2 \\ \vdots \\ C_z A^N \end{bmatrix}, \Gamma = \begin{bmatrix} H_1 & 0 & 0 & \cdots & 0 \\ H_2 & H_1 & 0 & \cdots & 0 \\ H_3 & H_2 & H_1 & & 0 \\ \vdots & \vdots & \vdots & \ddots & \vdots \\ H_N & H_{N-1} & H_{N-2} & \cdots & H_1 \end{bmatrix} \\
\Gamma_D &= \begin{bmatrix} H_{1,d} & 0 & 0 & \cdots & 0 \\ H_{2,d} & H_{1,d} & 0 & \cdots & 0 \\ H_{3,d} & H_{2,d} & H_{1,d} & & 0 \\ \vdots & \vdots & \vdots & \ddots & \vdots \\ H_{N,d} & H_{N-1,d} & H_{N-2,d} & \cdots & H_{1,d} \end{bmatrix}, \\
H_S &= \begin{bmatrix} 2S & -S & & \cdots & 0 \\ -S & 2S & -S & \cdots & \vdots \\ & & \ddots & & \\ \vdots & \cdots & -S & 2S & -S \\ 0 & \cdots & & -S & S \end{bmatrix}, M_{u_{-1}} = - \begin{bmatrix} S \\ 0 \\ 0 \\ 0 \\ 0 \end{bmatrix},
\end{aligned} \tag{9.10}$$

where,$H_i = CA^{i-1}B, H_{i,d} = CA^{i-1}B_d$, for $1 \leq i \leq N$. The optimal u^N could be found by taking gradient of Φ_k and set it to zero. The first control move u_k at current time k will be applied to the plant.

$$u_k = K_{MPC} \cdot \begin{bmatrix} x_0 \\ R \\ u_{-1} \\ D_d \end{bmatrix} \tag{9.11}$$

where, S_H is the square root of the hessian matrix $H = {S_H}^T S_H$

$${S_H}^T S_H K_{x0} = -M_{x0}, \tag{9.12a}$$

$${S_H}^T S_H K_R = -M_R, \tag{9.12b}$$

$${S_H}^T S_H K_{u-1} = -M_{u-1}, \tag{9.12c}$$

$${S_H}^T S_H K_D = -M_D, \tag{9.12d}$$

therefore,

$$K_{full} = \begin{bmatrix} K_{x0} & K_R & K_{u-1} & K_D, \end{bmatrix} \tag{9.13}$$

and,

$$K_{MPC} = K_{full}(1 : \ell, :). \tag{9.14}$$

Figure 9.2 demonstrates the structure of the entire feedback control system with estimator and the control law described in 9.11 with derived feedback gain 9.13.

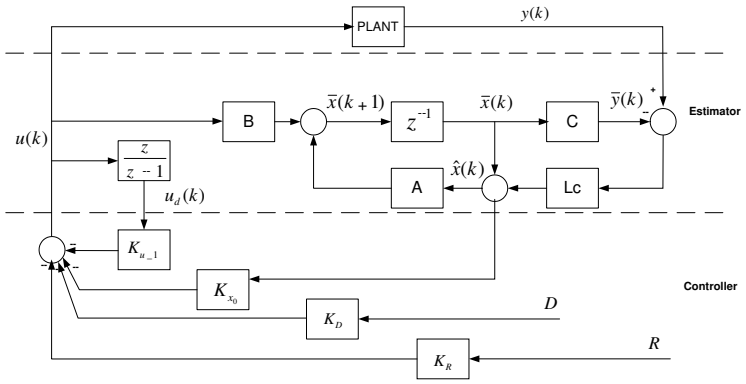

Figure 9.2: Structure of the Feedback Control System

9.3.3 Moving Horizon Estimation

The linear Moving Horizon Estimation (MHE) solves the constrained linear least square problem is expressed as the constrained linear quadratic optimization (9.15). This formu-

lation of MHE was first proposed by [Muske *et al.*, 1993] and [Robertson *et al.*, 1996].

$$\begin{aligned}\min_{\left[\hat{x}_{k-N/k},\hat{w}^N\right]} \Psi_k^N &= \frac{1}{2}\left\|\hat{x}_{k-N/k}-\bar{x}_{k-N/k-N-1}\right\|^2_{P^{-1}_{k-N/k-N-1}} \\ &+\frac{1}{2}\sum_{j=k-N}^{k-1}\left\|w_{j/k}\right\|^2_{Q_w^{-1}}+\left\|v_{j/k}\right\|^2_{R_v^{-1}},\end{aligned} \tag{9.15a}$$

$$s.t.\begin{cases} x_{k+j+1}=Ax_{k+j}+Bu_{k+j}+B_d d_{k+j}+Gw_{k+j} \\ z_{k+j}=Cx_{k+j}+v_{k+j} \\ x_{\min}\le\hat{x}_{k-N/k}\le x_{\max} \\ w_{\min}\le\hat{w}_k\le w_{\max} \\ z_{\min}\le z_k\le z_{\max}\end{cases} \tag{9.15b}$$

The estimator selects the state $x_{(k-N/k)}$, a sequence of process noise $\left\{w_{j/k}\right\}_{j=k-N}^{k}$ and a sequence of measurement noise $\left\{v_{j/k}\right\}_{j=k-N}^{k}$ such that the agreement with the measurement $\left\{y_{j/k}\right\}_{j=k-N}^{k}$ is as good as possible while still respecting the process dynamics, the output relation, and the constraints. The process and measurement noise n_w and n_v are assumed to be uncorrelated zero-mean Gaussian noise sequences with covariance Q_w and R_v. Q_w, R_v and $P_{k-N/k-N-1}$ are assumed to be symmetric and positive definite. The initial condition is as (9.17):

$$\begin{bmatrix} w \\ v \end{bmatrix} \sim \mathrm{N}\left(\begin{bmatrix} 0 \\ 0 \end{bmatrix}, \begin{bmatrix} Q_w & 0 \\ 0 & R_v \end{bmatrix} \right) \tag{9.16}$$

$$x_{k-N/k-N-1} \sim \mathrm{N}\left(\bar{x}_{k-N/k-N-1}, \quad P_{k-N/k-N-1} \right) \tag{9.17}$$

The inverse of the weighting matrices R_v^{-1}, Q_w^{-1} and P_{k-N}^{-1} are quantitative measures of our confidence in the output model, the dynamic system model and the initial estimate, respectively. As described in [Rao and Rawlings, 2000], [Rao, 2000], [Tenny and Rawlings, 2002], and [Rao and Rawlings, 2002], the covariance $P_{k-N/k-N-1}$ is derived by the solution of the Lyapunov Equation $P_{k-N/k-N-1}=\bar{A}^T P_{k-N/k-N-1}\bar{A}+\bar{G}^T\bar{Q}\bar{G}$, in which,

$$\bar{A}=\begin{bmatrix}A-ALC\end{bmatrix}, \bar{G}=\begin{bmatrix}G & -AL\end{bmatrix}, \bar{Q}=\begin{bmatrix}Q_w & 0 \\ 0 & R_v\end{bmatrix}. \tag{9.18}$$

To achieve offset-free control of the output to their desired targets at steady state, in the presence of plant/model mismatch and/or unmeasured disturbances, the system model expressed in (9.1) is augmented with an integrated disturbance model as proposed in [Muske and Badgwell, 2002] and [Pannocchia and Rawlings, 2003] to form an augmented moving horizon estimator. The dynamics of the disturbance model will be the stochastic generation process of animal heat and contaminant gas. The resulting augmented system

with process noise n_w and measurement noise n_v is

$$\tilde{x}(k+1) = \tilde{A}\tilde{x}(k) + \tilde{B}u(k) + \tilde{G}n_w(k), \tag{9.19a}$$
$$y(k) = \tilde{C}\tilde{x}(k) + n_v(k), \tag{9.19b}$$
$$n_w(k) \sim \mathrm{N}(0, Q_w(k)), \tag{9.19c}$$
$$n_v(k) \sim \mathrm{N}(0, R_v(k)), \tag{9.19d}$$

in which the augmented state and system matrices are defined as follows,

$$\begin{aligned} \tilde{x}(k) &= \begin{bmatrix} x(k) \\ x_{umd}(k) \end{bmatrix}_{12\times 1}, \tilde{A} = \begin{bmatrix} A & B_{dumd}C_{dumd} \\ 0 & A_{dumd} \end{bmatrix}_{12\times 12}, \\ \tilde{B} &= \begin{bmatrix} B \\ 0 \end{bmatrix}_{12\times 12}, \tilde{C} = \begin{bmatrix} C & 0 \end{bmatrix}_{6\times 12}, \tilde{G} = \begin{bmatrix} B_{dmd} & 0 \\ 0 & B_{dumd} \end{bmatrix}_{12\times 12}. \end{aligned} \tag{9.20}$$

In this model, the original process state $x \in \mathbb{R}^6$ is augmented with the integrated unmeasurable disturbance state $x_{umd} \in \mathbb{R}^6$. The measurable deterministic disturbance $d_{md} \in \mathbb{R}^{12}$ is assumed to remain unchanged within the prediction horizon and equal to the constant at the last measured value, namely $d_{dmd}(k) = d_{dmd}(k+1/k) = \cdots = d_{dmd}(k+N-1/k)$. The detectability of the augmented system in (9.20) is guaranteed when the condition holds:

$$Rank\begin{bmatrix} (I-\tilde{A}) & -\tilde{G} \\ \tilde{C} & 0 \end{bmatrix} = n + s_d, \tag{9.21}$$

in which, n is the number of the process states, s_d is the number of the augmented disturbance states. This condition ensures a well-posed target tracking problem. $(\tilde{A}, \tilde{Q}^{1/2})$ is stabilizable. For detailed explanation about the proof refer to [Pannocchia and Rawlings, 2003].

The structure of the moving horizon estimation and control is as Fig. 9.3.

9.4 Actuator Redundancy

An actuator redundancy strategy is developed through exploring the nonlinearities of the manipulators which possess redundancy and solving a convex optimization. A constrained nonlinear optimization is formulated as (9.22), with a stage cost in terms of the quadratic function with quadratic terms and the equality constraints from the nonlinear algebraic equation of the exhaust unit.

$$\min_{[V,\theta]^T} \mathrm{E}_k = \|V_k\|^2_{Q_V} + \|\theta_k\|^2_{\sigma\cdot R_\theta} \tag{9.22a}$$

$$s.t. \begin{cases} \Delta P_k = (b_0 + b_1\theta_k + b_2\theta_k^2)q_k^2 + a_0V_k^2 + a_1q_kV_k + a_2q_k^2 \\ V_{\min} \le V_k \le V_{\max} \\ \theta_{\min} \le \theta_k \le \theta_{\max} \end{cases} \tag{9.22b}$$

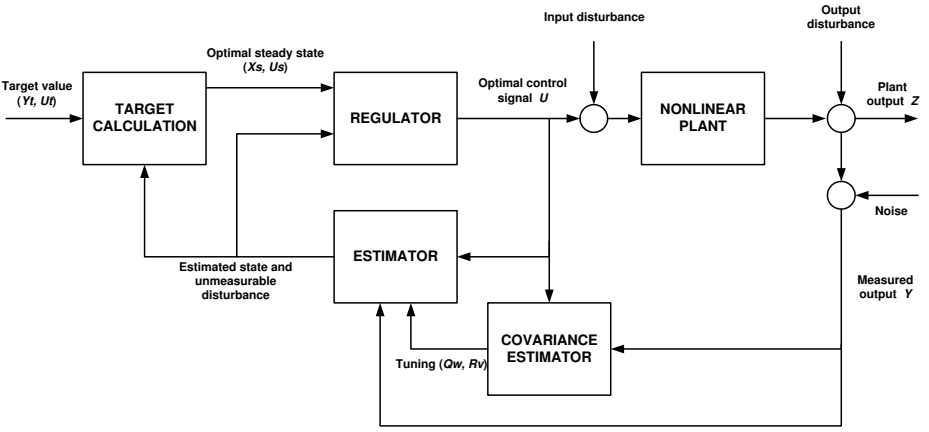

Figure 9.3: Moving Horizon Estimation and Control for Nonlinear Plant

where, Q_V and R_θ are symmetric positive definite matrices. σ is the variance of the covariance of the high frequency wind speed signal which is processed through digital filters. σ is the adjusting factor for assigning different penalties on the energy associated decision variable: the supplied voltage V_k and the swivel shutter opening angle θ_k, in order to attain the demand ventilation rate and attenuate the wind gusts. The cost function and the nonlinear characteristic curve of the exhaust unit are demonstrated in Fig. 9.4. The optimum point searching trajectory is moving along the different flow rate contour lines at the constant pressure surface.

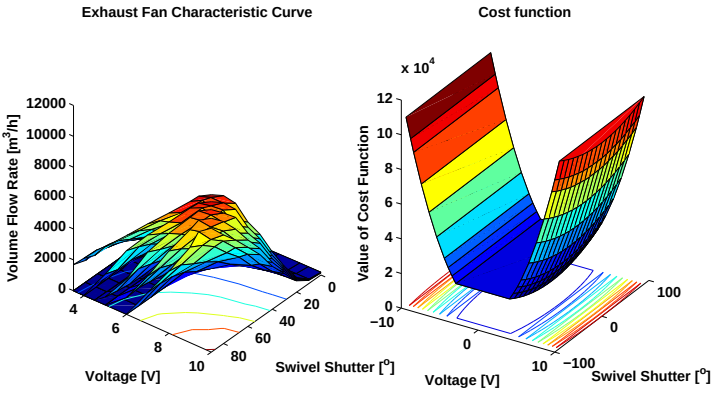

Figure 9.4: Nonlinear Equality Constraints and Cost Function

The overview of the designed entire control structure for the livestock indoor climate system is shown in Fig. 9.5. The research focuses have been mainly on the actuator redundancy and dynamic controller design, where the dynamic controller is the moving horizon control and estimation computed through the dynamic optimization. The developed redundancy optimization is integrated with the model predictive control and implemented in a feed-forward approach. This strategy enhances the resilience of the control system to disturbances beyond its bandwidth, passively attenuate the disturbances, and reduces energy consumption through on-line optimization computation.

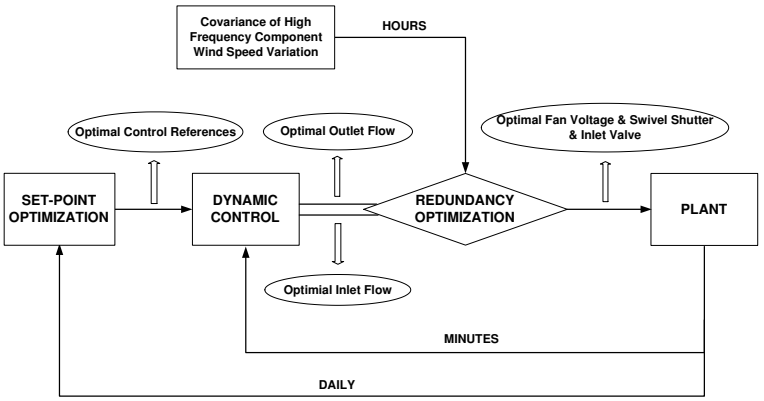

Figure 9.5: Structure of the Entire Control System with Moving Horizon Control and Actuator Redundancy

9.5 Simulation Results

The nonlinear developed plant model is used for simulation. The hard constraints on the inlet valve opening is $0(m^2)$-$0.6(m^2)$, on the supplied fan voltage is $0(V)$-$10(V)$ and on the swivel shutter is $0(^o)$-$90(^o)$. The entire volume of the stable is around 2500 (m^3). The weights Q on the tracking errors are different according to different requirement of the control objective. For animal thermal comfort, the indoor temperature is limited around the reference value $21(^oC)$ within the TNZ. For indoor air quality, the indoor air concentration level should be maintained below $700(ppm)$. The sampling time step is defined to be 2 (*min*), the prediction horizon is $N = 20$. For the following simulation scenarios, we assume that the constraint stability of the control system is guaranteed in the infinite horizon when the feasibility of the input constraints is satisfied within the finite horizon.

9.5.1 Off-set free tracking

In order to demonstrate the benefits of moving horizon estimation and control in handling constraints and fulfilling off-set free tracking for multi-variable system, the system performances for indoor zonal temperature and concentration level are presented. As shown in Fig. 9.6, the simulation results are derived in the presence of pulse and step changes of mean value of external weather condition such as the temperature and wind speed variation with large covariances, and different zonal heat production. Fig. 9.7 shows the corresponding actuator behaviors.

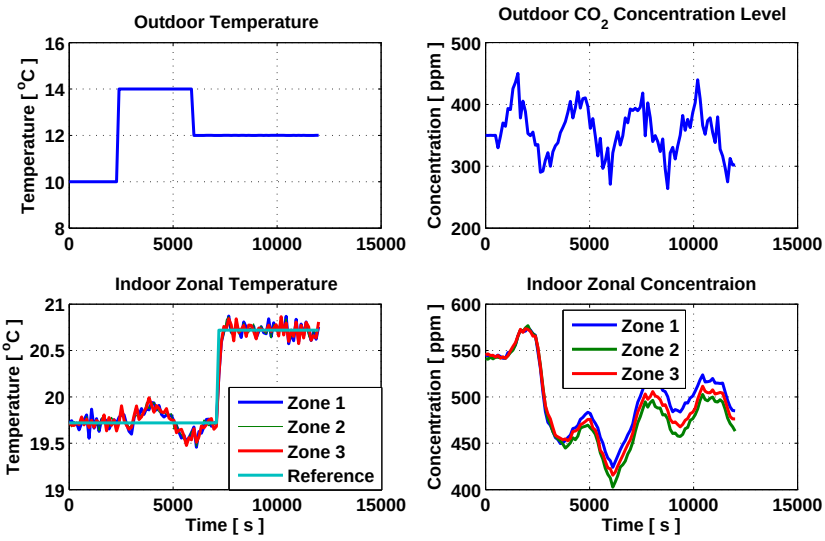

Figure 9.6: Reference Tracking and Rejection of Deterministic Disturbance. Dynamic Performances of Zonal Temperature and Concentration

With a step change of the reference value for comfortable temperature, the indoor zonal temperatures keep tracking the reference with slight variations, the zonal concentration level vary with the change of the actuators and stay below the limitation. Viewed from Fig. 9.7, the voltage and swivel shutter in the exhaust unit rise and fall in response to the onset and cease of the disturbances. The inlet valve opening areas on the windward and leeward side are adjusted differently according to the local zonal disturbance variations. The actuator behavior of exhaust unit in each zone is similar, thus only one of them is picked up for demonstration. The comparison of the control signals for exhaust unit manifests the improvement of the operating behavior derived from the redundancy optimization, on pursuing optimum energy consumption and attenuating the high frequency wind speed variation.

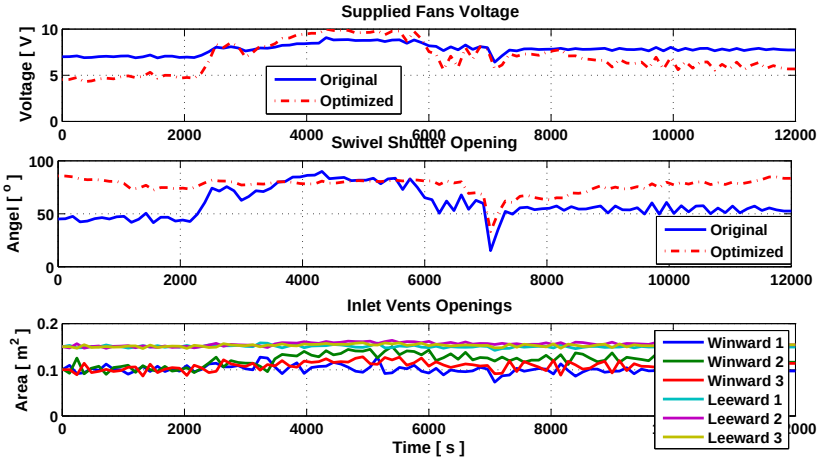

Figure 9.7: Optimal Control Signals. Solid line (Dynamic Control without Actuator Redundancy); Dashed dot line (with Actuator Redundancy)

9.5.2 Exhaust System Energy Optimization

Fig. 9.8 depicts the effect of actuator redundancy in exhaust unit based on the energy consumption consideration, and the analysis of covariance of the high frequency change of wind speed. Fig. 9.8 (a) shows the wind speed disturbances and its low and high frequency component. Fig. 9.8 (b) shows the comparison of the exhaust unit operating behavior with and without the actuator redundancy.

9.5.3 Comparison of Kalman Filter and MHE

As shown in Fig. 9.9, the simulation results have convincingly proved the advantages of applying moving horizon method for estimation and control compared with the controller using a nominal Kalman Filter in rejecting the unmeasured disturbances and lowering the output variation.

Through demonstration and comparison both for output performances and actuators behaviors, we could recognize that with the application of dynamic optimization in a moving horizon matter, the system behavior has been profoundly modified, and the variance of the output has been reduced considerably. With the designed redundancy optimization scheme, the system resilience to disturbances is enhanced, the efficiency of actuator utilization is increased, and the optimal solution of energy consumption is also pursued.

Through step response analysis and bode plot comparison, we realize that, the plant nonlinearities are not highly significant. By varying the disturbances such as the zonal

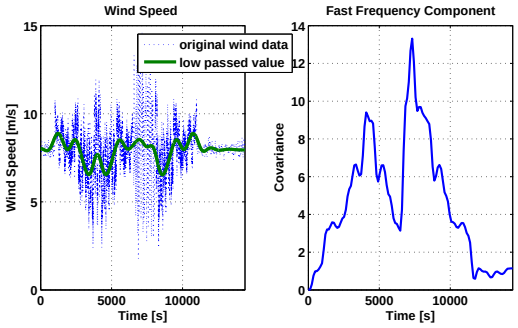

(a)

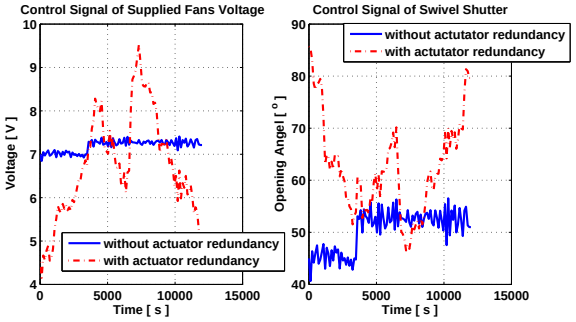

(b)

Figure 9.8: (a)Wind Speed Disturbance and the Amplitude of its High Frequency Components (covariance) (b) Comparison of the Control Signal of Exhaust Fan System

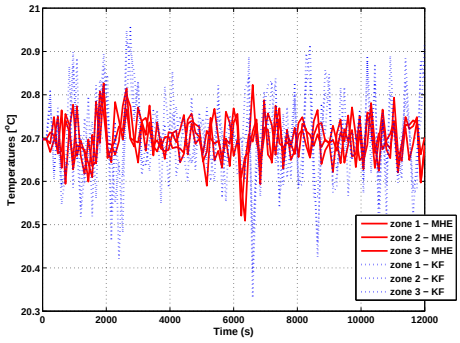

Figure 9.9: Comparison of the System Performances with MHE technique vs. Nominal Kalman Filter Method

heat sources which cause the direction change of the inter zonal airflow, and varying the external temperature which are the leading factors of the variation of the indoor thermal comfort, we obtain similar system behaviors with a series of LTI models.

9.6 Conclusion and Future Work

9.6.1 Conclusion

The main achievement of this work is the control performance improvement and energy consumption optimization. The offset-free control is achieved with moving horizon estimation and control, and the optimum energy using solution is derived through applying actuator redundancy.

9.6.2 Future Work

MHE together with ALS method will be further investigated for compensating the model/plant mismatch and the un-modeled disturbance, such as the zonal heat source changes due to the animals ransom distribution. The issue of comfort air movement around the animals and minimum ventilation rate will be included into optimization computations, and the actuator redundancy will be applied for the inlet system in order to protect against wind gust and reduce draft. The feasibility and efficiency of the control system will be validated through experiments in the real-scale livestock building.

9.7 Acknowledgement

The authors gratefully acknowledge the support from the Danish Ministry of Science and Technology.

Chapter 10

Parameter Estimation of Dynamic Multi-zone Models for Livestock Indoor Climate Control

Zhuang Wu [1*], Per Heiselberg [2], Jakob Stoustrup [1]

[1] *Department of Electronic Systems, Aalborg University, Fredrik Bajersvej 7C, 9220 Aalborg East, Denmark*
[2] *Department of Building Technology and Structural Engineering, Aalborg University, Sohngaardsholmsvej 57, 9000 Aalborg, Denmark*

This conference paper was presented at the 29th Air Infiltration and Ventilation Center (AIVC) Conference on Advanced Building Ventilation and Environmental Technology for Addressing Climate Change Issues, 2008. This paper is reproduced under the conditions of the copyright agreement with the International Network for Information on Ventilation and Energy Performance (INIVE) of European Economic Interest Grouping (EEIG). The developed livestock hybrid ventilation and indoor climate models are verified as well as other employed important parameters. The experiments are carried out in a real-scale poultry stable located in Denmark.

Abstract

In this paper, a multi-zone modeling concept is proposed based on a simplified energy balance formulation to provide a better prediction of the indoor horizontal temperature variation inside livestock building. The developed mathematical models reflect the influences from the weather, the livestock, the ventilation system and the building on the dynamic behavior of the indoor climate. Some significant parameters employed in the livestock ventilation system and indoor climate models as well as the airflow interaction between each conceptual zones are identified with the use of experimental time series data collected during summer and winter in a laboratory livestock building of Denmark. The obtained comparative simulation results between the measurements and the prediction, confirm that a very simple multi-zone model can capture the salient dynamical features of the climate dynamics, which are needed for control purposes.

Nomenclature

T	Temperature
C_r	Air Contaminant gas concentration
$\dot{Q}$	Heat transfer rate
g	Gravitational acceleration
M	Air mass
V	Volume
A	Area
H	Height
ρ	Density
U	Heat transfer coefficient of building construction material
c_p	Heat capacity at constant pressure
$\dot{m}$	Mass flow rate
$\dot{q}$	Air volume flow rate
$\dot{n}$	Air exchange rate
$\dot{G}$	Contaminant generation rate from animals
P	Pressure
ΔP	Pressure difference
C_d	Discharge coefficient of inlet system
P_i	Internal Pressure at reference height
C_p	Surface pressure coefficient
V_{ref}	Wind speed at reference level

Subscript

i	Indoor zonal numbers

o	Outdoor
in	Input to the building
out	Output from the building
wall	Building envelope
transmission	Heat transfer through convection, conduction and radiation
source	Production or generation source
inlet	Inlet vent
fan	The exhaust unit
NPL	Neutral Pressure Level

10.1 Introduction

Livestock environmental control plays crucial role in alleviation of thermal strain and the maintenance of a good indoor air quality, preserving animal health and welfare and improving the efficiency of animal production. The investigations in this respect ([Cunha *et al.*, 1997], [Gates *et al.*, 2001], [Pasgianos *et al.*, 2003], [Taylor *et al.*, 2004], [Soldatos *et al.*, 2005], [Arvanitis *et al.*, 2007]) have shown the indispensability for control and perspective for future research.

Indoor climate model of livestock building are essential for improving environmental performances and control efficiencies. The aim of this work is to identify the developed models, that should unite the simplicity on the parameter level and a correct description of the zone based indoor climate that are important for multi-variable control studies.

Concerning the indoor climate and energy consumption for the large scale livestock building, the actual indoor environment at any controlling sensors (especially when the sensors are located horizontally) will depend on the air flow distribution that is usually depicted as a map of the dominant air paths. Therefore, neglecting the horizontal variations could obviously result in the significant deviations from the optimal environment for the sensitive pigs or chickens in the livestock barn. On the other hand, the ventilation has become an important part of the energy consumption of buildings, so it is necessary to study more specifically the compartmentalized local climate and the associated airflow interaction, in order to control more specifically the heating and ventilating systems.

Traditional multi-zone modeling method are often appropriate for average size buildings, since intra-room mixing is usually orders of magnitude faster than inter-room air exchange and physical walls act as partitions for each zone, so that each room may act like a well-mixed compartment. However, for partition-less livestock building with localized ventilation and source locations, with persistent spatial temperature/concentration gradient, the single well-mixed compartment approach is inappropriate ([Sohn and Small, 1999],[O'Neill, 1991]). Instead of using Computer Fluid Dynamic (CFD) codes, though proves to give detailed inter-zonal flow and temperature distribution, and higher order model approach like Active Mixing Volume (AMV) described in [Young *et al.*, 2000] and [L. Price, 1999], we suggest a so-called conceptual multi-zone method to satisfy the necessary precision for evaluating local climate within various zones of a building. This

approach is similar with the zonal model principle as proposed in [Gagneau and Allard, 2001], [Haghighat *et al.*, 2001] and [Riederer *et al.*, 2002], that consists in breaking up the entire indoor air volume into macroscopic homogeneous conceptual zones in which mass and energy conservation must obeyed. This method maintains the simplicity of the first order model, yet captures the major heterogeneity in the room to reach the desired controlling objectives.

10.2 Laboratory Livestock Building in Denmark

The livestock building located in Syvsten, Denmark, is a large scale concrete building which used to be a broiler house, with floor area of $753m^2$, length of $64.15m$, width of $11.95m$, and approximate volume of $2890m^3$, see Fig. 10.1. In order to control the indoor climate, hybrid ventilation system ([Heiselberg, 2004a]) is equipped, necessary actuators and sensors were installed and connected to an acquisition and control system based on an PC positioned in the monitor room. The detailed explanation of the positioning, numbering and function of the installed equipment in the test stable are described in both graphical and tabular format as shown in Fig. 10.2, 10.3, 10.4 and Table 10.3, 10.4.

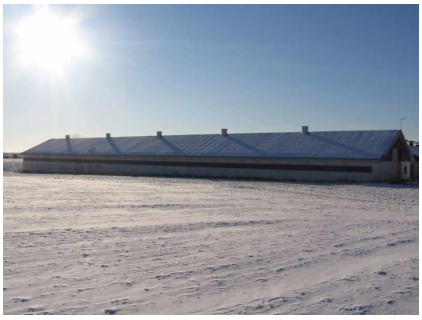

Figure 10.1: A Full Scale Poultry Stable Located in Syvsten, Denmark

The installed actuators are five exhaust units evenly distributed on the ridge of the roof with the maximum flow rate of $17.8m^3/h$, totally sixty-two inlet units controlled by winch motors mounted on the long windward and leeward side walls with the whole maximum opening area of $6.45m^2$. Through the inlet system, the incoming fresh cold air mixes with indoor warm air, and then drops down to the animal environmental zones slowly in order to satisfy the zonal comfort requirement. In winter, when the outdoor temperature is much lower than the animal comfort temperature, the inlet valve opening area will be decreased to lead the cold air directly towards the ceiling, to protect against the intrude of the cold air to the animal living zone by slowing the down the mixing procedure, and vice versa in summer. Axial type fan and the integrated swivel shutter of the exhaust unit are adjusted to provide appropriate ventilation rate and guarantee a low pressure ventilation strategy.

Both the shutter in the exhaust unit and the bottom-hanged flaps in inlet system are used to attenuate the effect of wind gust.

The heating system consists of two major heat sources, one for heating up the indoor temperatures through the steel pipes with length of $400m$, diameter of $0.04m$ installed on each side of the wall under the inlet system, and the other for physically simulating the animal heat production with six water heating radiators equipped near the floor with the range of supplied heating water temperature from 15^oC to 55^oC. They are both coupled to an oil furnace placed in the monitor room. The connections are as shown in Fig. 10.3, where, BV represents the Ball Valve, P represents the Pump, FS and TS denote the water flow sensor and surface temperature sensor.

The inside and outside air temperatures are measured with temperature sensors which are positioned around one meter above the floor. The flow sensors and position sensors are mounted in the exhaust unit and inlet valve openings, in order to measure the exhaust flow rate and inlet flap opening positions. The pressure sensors are mounted on the side walls to measure the pressure difference across the inlet unit.

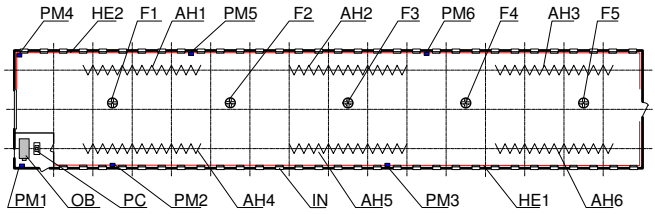

Figure 10.2: Overview of the Hardware Equipped in the Stable

Symbol	Function
AH1 - AH6	Heat Sources Simulator for Animal Heat Production
SH1 - SH2	Heat Sources Simulator for Stable Heating System
IN	Inlet
OB	Oil Furnace
PC	System Computer
PM1 - PM6	Winch Motor
F1 - F5	Axial Exhaust Fan

Table 10.3: Hardware Equipped in The Livestock Building

The control computer in the stable is a Commercial Off-The shelf System (COTS). The server is a standard computer with PCI I/O cards from National Instruments which is used to connect to the sensors and actuators in the stable. The computer runs Linux as the operating system and uses Comedi as an open source library to connect to the I/O cards. Fig. 10.5 shows these connections as well as how the sensor values and actuator

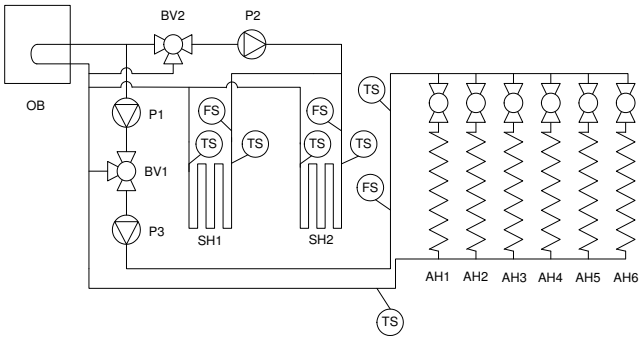

Figure 10.3: The Complete Heating System in the Stable

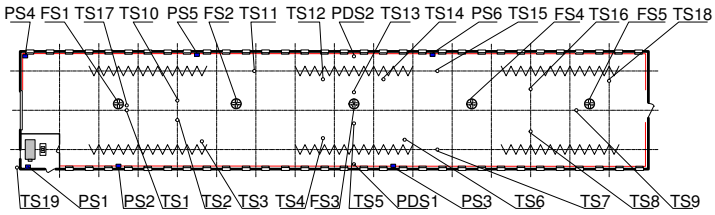

Figure 10.4: Overview of the Sensors Mounted inside the Stable

demands are accessed from a client, through a network interface card (NIC) over the Internet or a local area network (LAN) to a web browser. The computer is running an SSH server, which makes it possible to upload and run programs remotely. The more detailed description of the hardware inside the livestock building and the COTS system is given in [Jessen *et al.*, 2006a] and [Jessen *et al.*, 2006b].

Symbol	Function
FS1 - FS5	Flow Sensors (outlet)
PDS1 - PDS2	Pressure Difference Sensors
TS1 - TS19	Temperature Sensors (air)
PS1 - PS6	Position Sensors (inlet)

Table 10.4: Sensors Installed in The Livestock Building

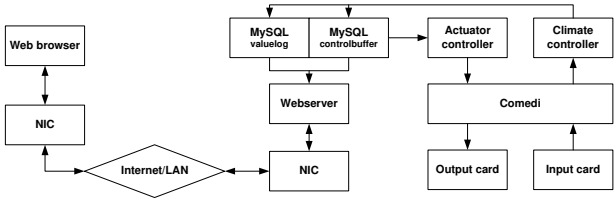

Figure 10.5: Overview of the Connections When Viewing Data from the Server

10.3 Process Models

The block diagram of the process which is composed of actuator and climate models are shown in Fig. 10.6.

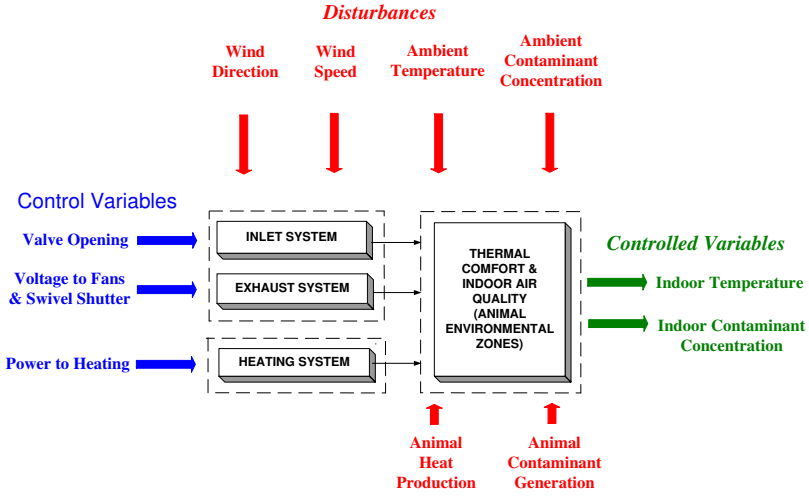

Figure 10.6: Block Diagram of Process Models

10.3.1 Inlet Unit Model

The inlet system provides variable airflow directions and controls the amount of incoming fresh air by adjusting the bottom hanged flaps. The volume flow rate through the inlet is calculated by (10.1). The pressure difference ΔP across the opening can be computed by a set of routines solving thermal buoyancy and wind effect as (10.2). The value of wind induced pressure coefficient C_P changes according to the wind direction, the building

surface orientation and the topography and roughness of the terrain in the wind direction.

$$\cdot q_{in} = C_d \cdot A_{inlet} \cdot \sqrt{\frac{2 \cdot \Delta P_{inlet}}{\rho_o}}, \tag{10.1}$$

$$\Delta P_{inlet} = \frac{1}{2} C_P \rho_o V_{ref}^2 - P_i + \rho_o g \frac{T_i - T_o}{T_i} (H_{NPL} - H_{inlet}). \tag{10.2}$$

10.3.2 Exhaust Unit Model

In the exhaust unit, the airflow capacity is controlled by adjusting the r.p.m. of the fan impeller and the opening angle of the shutter. We introduce a fan law, as a relationship between the total pressure difference ΔP_{fan}, volume flow rate q_{out}, supplied voltage V_{volt} and the shutter opening angle θ, which can be approximated in a nonlinear static equation (10.3), where the parameters a_0, a_1, a_1, b_0, b_1, b_1 are empirically determined from experiments made by SKOV A/S in Denmark. As shown in (10.4), the total pressure difference across the unit is the difference between the wind pressure on the roof and the internal pressure at the entrance of the unit which considers the pressure distribution calculated upon the internal pressure at Neutral Pressure Level (NPL) denoted by P_i.

$$\Delta P_{fan} = (b_0 + b_1 \cdot \theta + b_2 \cdot \theta^2) \cdot q_{out}^2 + a_0 \cdot {V_{volt}}^2 + a_1 \cdot q_{out} \cdot V_{volt} + a_2 \cdot q_{out}^2 \tag{10.3}$$

$$\Delta P_{fan} = \frac{1}{2} \rho_o C_{P,r} V_{ref}^2 - P_i - \rho_i g \frac{T_i - T_o}{T_o} (H_{NPL} - H_{fan}). \tag{10.4}$$

10.3.3 Multi-zone Climate Model

By applying a conceptual multi-zone modeling method, the building is compartmentalized into several macroscopic homogeneous conceptual zones horizontally. The nonlinear differential equation relating the zonal temperature can be derived for each zone as (10.5). The following energy transfer terms appear in the zonal model: the convective inter-zonal heat exchange $\dot{Q}_{i+1,i}$ and $\dot{Q}_{i,i+1}$; the heat transfer by mass flow through inlet and outlet $\dot{Q}_{in,i}$ and $\dot{Q}_{out,i}$; the transmission of heat loss through building envelope by convection and radiation $\dot{Q}_{conve,i}$; the heat source in the zone $\dot{Q}_{source,i}$.

$$M_i c_{p,i} \frac{dT_i}{dt} = \dot{Q}_{i+1,i} + \dot{Q}_{i,i+1} + \dot{Q}_{in,i} + \dot{Q}_{out,i} + \dot{Q}_{transmission,i} + \dot{Q}_{source,i} \tag{10.5}$$

in which,

$$\dot{Q}_{transmission,i} = U \cdot A_{wall,i} \cdot (T_i - T_o), \tag{10.6}$$

$$\dot{Q}_{i,i+1} = c_{p,i} \cdot \rho_i \cdot \dot{q}_{i,i+1} \cdot T_i. \tag{10.7}$$

where the inter-zonal mass flow rate $\dot{m}_{i,i+1}$ is the sum of several different flow elements, such as the airflow interaction $\dot{m}_{i,i+1,V}$ caused by the extracted fans, the airflow zonal

crossing $\dot{m}_{i,i+1,\cdot IN}$ resulted from the inlet jet trajectory, and the airflow mixing $\dot{m}_{i,i+1,T}$ due to the inter-zonal convective phenomena for example the convective flows at surface, thermal plume and so on. We propose $k_{i,i+1} \cdot \Delta T_{i,i+1}$ to compute $\dot{m}_{i,i+1,T}$, where $k_{i,i+1}$ is the inter-zonal airflow mixing parameter and could be determined through experiment calibration with e.g. the gas tracer method. Obeying the principle of conservation of mass, there are 4 patterns (*I*,*II*,*III* and *IV*) of airflow interaction (see Fig. 2.7(a)) computed through the differentiate of ventilation rate, where part of the amount accounts for the well-mixed zone air interaction by fans, and the other part of the amount accounts for the external air interaction by the inlet jet. The major elements of the zonal convective heat transfer is shown in Fig. 2.7 (b). The different airflow patterns play important effects on the system nonlinearities and determine the different operating conditions.

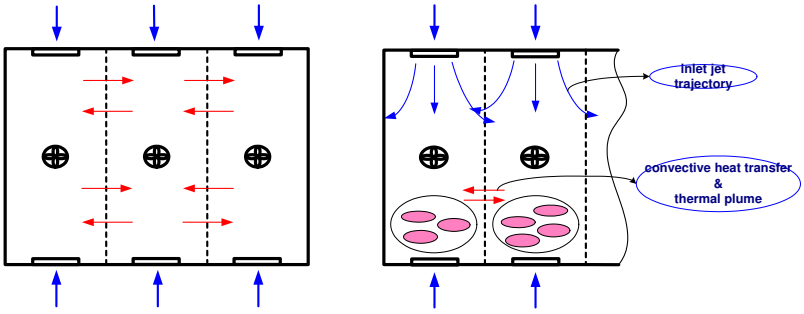

Figure 10.7: The two mode of intern zonal-flow pattern

10.4 Parameter Estimation

The dynamic models of the actuator and the multi-zone indoor climate system are expressed nonlinearly with respect to some dynamic parameters, which then can be estimated by using constrained nonlinear least square techniques based on the data-set collected from experiments. This algorithm is a subspace trust region method and is based on the interior-reflective *Newton* method. Each iteration involves the approximate solution of a large linear system using the method of Preconditioned Conjugate Gradients (PCG). This constrained nonlinear least square method not only yields consistent positive estimates of the parameter values, but also exhibits close to optimum performance in the analyzed models. The constraints to the optimization routines are the non-negativity for all of the parameters.

The coefficient C_d for the inlet system, varies considerably with the inlet type, opening area, as well as incoming air temperature and flow rate. However, for simplifying

the computation, we use a constant value which is determined through experiment for all openings, even though it might lead to over/under-prediction of airflow capacity and thereby larger openings than necessary. Fig. 10.8 demonstrates the comparison of the characteristic curve of the air volume flow rate through the inlet opening obtained from the measurement and the simulation model, corresponding to negative pressure differences range from 5 to 40 Pa. The colorful curves represent different opening percentages.

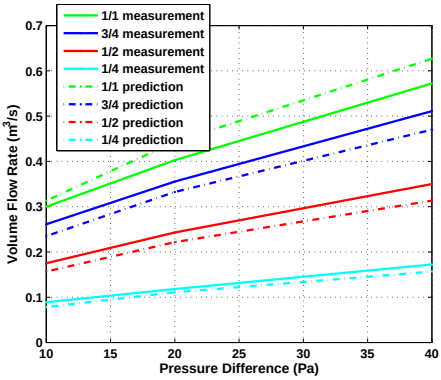

Figure 10.8: Inlet Characteristic Curve

Fig. 10.9 illustrates the performances of the exhaust fan at a specific swivel shutter opening with the measurement data and the validation data. The surface represents the character of the fan with pressure-voltage-flow data, and is approximated by the quadratic equation (10.3), in which the parameters are determined empirically from the experiments as listed in Table 10.5.

coefficients	C_d	a_0	a_1	a_2
values	0.7415	-0.2714	-5.4001	82.6241
coefficients	b_0	b_1	b_2	
values	86.6241	-3.4072	0.0198	

Table 10.5: Numerical Values of Model Coefficients Determined from Parameter Estimation

The above estimation is based on the experimental data set collected through the individual tests on the equipment made in the company's laboratory. The parameters employed in the multi-zone climate model, such as the effective volume, the inter-zonal mixing coefficient, the air flow rate (the absolute value), and the heat transfer coefficient of the building envelopes, are identified from the experiments conducted in the real scale

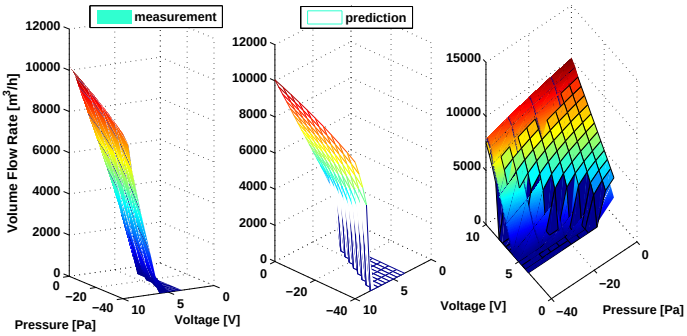

Figure 10.9: Comparison of Exhaust Fan Characteristic Curve

livestock stable, located in Syvsten, Denmark. The ventilation strategy applied in the stable is low pressure ventilation, which uses the exhaust units to pull out the indoor air to mechanically generate a relatively low internal pressure compared to the external pressure, thus let the outdoor fresh air into the building. In mild weather countries such as Denmark, the outdoor air temperature is almost always lower than the indoor air temperature. Thus hybrid ventilation will always be used as a cooling source for buildings.

Two scenarios, one in summer and one in winter, with various external temperatures and mild wind level have been used for demonstration. In the experiments, the data were obtained from dynamic experiments with sampling rate 30 seconds. The time constant of the axial type fan is around 10 seconds, the swivel shutter is around 52 seconds, the inlet valve is around 75 seconds and the heating system is around 1 hour. The following figures depict the experimental cases: One in summer (case No. 1) with constant actuators setting for ventilation rate $4.8m^3/s$, inlet opening area $1.46m^2$ and input water temperature for the heating system 55^oC; the second one is in winter (case No. 2) with a Pseudo-Random Digital Signal (PRDS) as the ventilation actuators inputs setting to the indoor climate system. The ventilation rate varies between $3.4m^3/s$ to $4.4m^3/s$, inlet opening area varies between $1.1m^2$ to $2.1m^2$, and the heating power is maintained constant. These two scenarios are thought to represent typical but not the only two cases encountered in the steady state and the dynamic behavior of the model for parameter estimation of the livestock building comprised of three partition-less conceptual zones. All of these experiments are made when wind is mild and stay below $3m/s$, which means that there are no wind gust exits and the pressure difference across the inlets on windward wall and leeward wall are possibly kept to be positive. The fan's rotating speed, shutter and inlet opening position are indicated with voltage which is generated by the analog output card $(0-10VDC)$ corresponding to the minimum and maximum of the flow rate and opening area.

Validation are carried out with the input signals which were not used in the estimation

processes and then the output of model was compared with the measured results. Fig. 10.10 and 10.11 show the comparison between measured temperature and the simulated temperature. It is observed that the average temperatures are in reasonably accord, with the exception of the unignorable steady state fluctuations.

coefficients	case No.1	case No.2	Units
k_{12}	1.04	0.12	$\frac{m^3}{s \cdot K}$
k_{21}	1.02	0.08	$\frac{m^3}{s \cdot K}$
k_{23}	0.76	0.12	$\frac{m^3}{s \cdot K}$
k_{32}	0.80	0.18	$\frac{m^3}{s \cdot K}$
q_{12}	1.13	0.19	$\frac{m^3}{s}$
q_{21}	0.91	0	$\frac{m^3}{s}$
q_{23}	1.02	0.99	$\frac{m^3}{s}$
q_{32}	1.01	0.82	$\frac{m^3}{s}$
$q_{in,1}$	1.53	1.48	$\frac{m^3}{s}$
$q_{in,2}$	1.17	1.42	$\frac{m^3}{s}$
$q_{in,3}$	1.33	1.13	$\frac{m^3}{s}$
V_1	6135.04	31186.95	m^3
V_2	6913.57	34044.13	m^3
V_3	18154.01	46750.56	m^3
$UA_{wall,1}$	3780.20	31788.58	$\frac{J}{s \cdot K}$
$UA_{wall,2}$	3757.23	36963.98	$\frac{J}{s \cdot K}$
$UA_{wall,3}$	3700.32	30602.88	$\frac{J}{s \cdot K}$

Table 10.6: Numerical Values of Model Coefficients Determined from Parameter Estimation

Table 10.6 summarize the estimated parameter values for each scenario that resulted from the optimization computation. The discrepancy between the identified and the realistic parameter values deserve further research and investigations, for example the estimated effective zonal volume is around 10 order magnitude bigger than the geometrical values.

However, these phenomena could be explained by the fact that we neglect some influencing factors and the existence of unpredictable airflow path like the shot-circuiting and stagnant zones in ventilated spaces ([Soldatos *et al.*, 2005], [Daskalov, 1997]), uncertainties such as the heat capacity of the construction material, the latent heat loss through evaporation, the degree of air mixing, building leakage and wind effect. Further more, the heat transfer coefficient has a close relationship with air-flow pattern and the resulting air velocity, and most importantly, the effect of the slow dynamics of the building materials.

The most important phenomena, represented in the proposed model are manifested experimentally and by detailed simulation. From this analysis, a further understanding for the development of the conceptual multi-zone models is obtained. The model is appropriate for capturing the salient dynamics of indoor climate in large, heterogeneous, partition-less buildings, for the purpose of measurement and control.

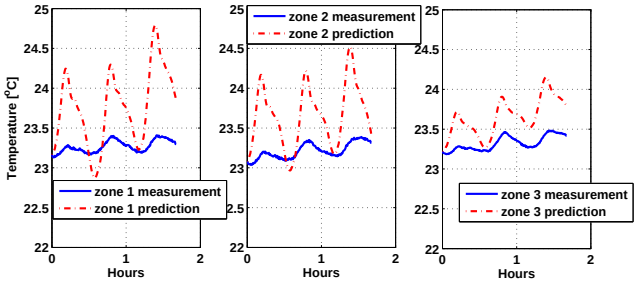

(a)

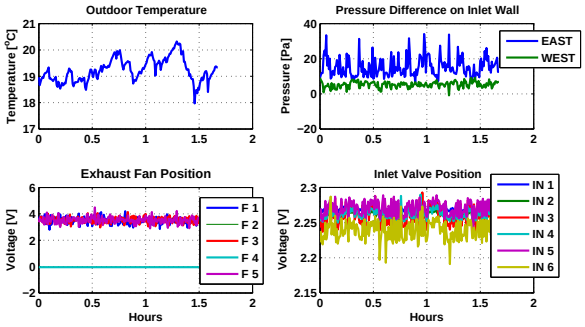

(b)

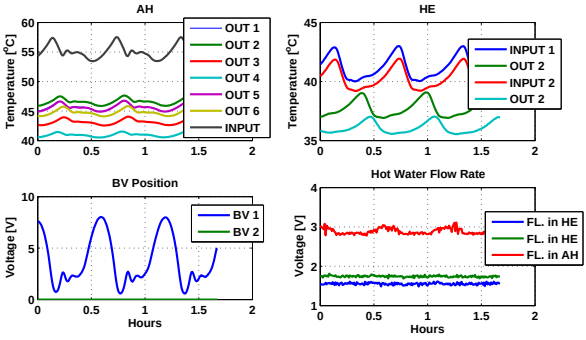

(c)

Figure 10.10: Case No. 1 (a) Comparison of Indoor Zonal Air Temperatures (b) Outdoor Weather Condition and Actuators Action (c) Heat Exchanger and Radiator

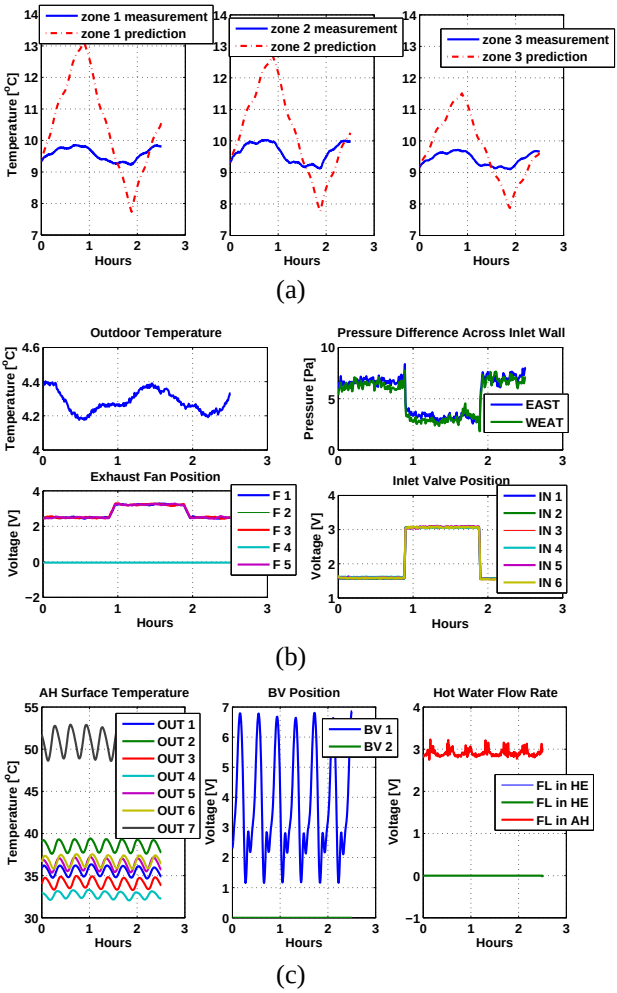

Figure 10.11: Case No. 3 (a) Comparison of Indoor Zonal Air Temperatures (b) Outdoor Weather Condition and Actuators Action (c) Heat Exchanger and Radiator

10.5 Conclusions and Future Work

10.5.1 Conclusion

The comparative results between the measured data and the simulated output confirm the value of conceptual multi-zone approach in simulating the indoor climate behavior of the large scale partition-less livestock buildings, show the potential of applying model-based multi-variable control purposes.

10.5.2 Future Work

The dynamic model of the heat convection and radiation from heating source and the heat transmission of construction material could be integrated into the climate model to enhance its coherence. The inter-zonal flow interaction will be further calibrated with advanced tools, e.g. gas-tracer method. The pressure coefficient which has been assumed to be constant will be identified through experiment and regarded as time variant disturbance entering the system.

10.6 Acknowledgement

The authors gratefully acknowledge the financial support from SKOV A/S, the technical support from Master students and their supervisor from Aalborg University, Esbjerg.

Part III

Appendixes

In this part the supplementary work are stated, including the applied equations and matrices in computations. Finally the bibliographic list of the thesis is given.

Appendix A

A Multi-zone Climate and Ventilation Equipment Model Equations

In this appendix the equations and matrices used for simulation and linearization are presented. The combination of dynamic indoor climate model with the static airflow distribution model are evolved. The model scaling is presented.

A.1 Nonlinear Plant Models

The full nonlinear coupled algebraic dynamic equation for indoor zonal temperatures is

$$\rho_i \cdot V_1 \cdot c_p \frac{dT_1}{dt} = \dot{M}_{21} \cdot c_p \cdot T_2 - \dot{M}_{12} \cdot c_p \cdot T_1 + \dot{M}_{in,1} \cdot c_p \cdot T_o + \dot{M}_{in,4} \cdot c_p \cdot T_o - \dot{M}_{out,1} \cdot c_p \cdot T_1 - UA_1(T_1 - T_o) + \dot{Q}_{animal,1} + \dot{Q}_{heat,1}, \tag{A.1a}$$

$$\rho_i \cdot V_2 \cdot c_p \frac{dT_2}{dt} = -\dot{M}_{21} \cdot c_p \cdot T_2 + \dot{M}_{12} \cdot c_p \cdot T_1 + \dot{M}_{32} \cdot c_p \cdot T_3 - \dot{M}_{23} \cdot c_p \cdot T_2 + \dot{M}_{in,2} \cdot c_p \cdot T_o + \dot{M}_{in,5} \cdot c_p \cdot T_o - \dot{M}_{out,2} \cdot c_p \cdot T_2 - UA_2 \cdot (T_2 - T_o) + \dot{Q}_{animal,2} + \dot{Q}_{heat,2}, \tag{A.1b}$$

$$\rho_i \cdot V_3 \cdot c_p \frac{dT_3}{dt} = -\dot{M}_{32} \cdot c_p \cdot T_3 + \dot{M}_{23} \cdot c_p \cdot T_2 + \dot{M}_{in,3} \cdot c_p \cdot T_o + \dot{M}_{in,6} \cdot c_p \cdot T_o - \dot{M}_{out,3} \cdot c_p \cdot T_3 - UA_3 \cdot (T_3 - T_o) + \dot{Q}_{animal,3} + \dot{Q}_{heat,3}. \tag{A.1c}$$

The equations and matrices for simulation of nonlinear model A.1 is

$$\begin{bmatrix} T_1 \\ T_2 \\ T_3 \end{bmatrix}^{k+1} - \begin{bmatrix} T_1 \\ T_2 \\ T_3 \end{bmatrix}^{k} = \begin{bmatrix} A_{11} & A_{12} & 0 \\ A_{21} & A_{22} & A_{23} \\ 0 & A_{32} & A_{33} \end{bmatrix} \cdot \begin{bmatrix} T_1 \\ T_2 \\ T_3 \end{bmatrix}^{k} + \Delta t \cdot \frac{T_o}{\rho_i V_i} \cdot \begin{bmatrix} \dot{M}_{in,1} + \dot{M}_{in,4} \\ \dot{M}_{in,2} + \dot{M}_{in,5} \\ \dot{M}_{in,3} + \dot{M}_{in,6} \end{bmatrix}$$
$$+ \Delta t \cdot \frac{1}{\rho_i V_i c_p} \cdot \begin{bmatrix} \dot{Q}_{animal,1} + \dot{Q}_{heating,1} \\ \dot{Q}_{animal,2} + \dot{Q}_{heating,2} \\ \dot{Q}_{animal,3} + \dot{Q}_{heating,3} \end{bmatrix} + \Delta t \cdot \frac{T_o}{\rho_i V_i c_p} \cdot \begin{bmatrix} UA_1 \\ UA_2 \\ UA_3 \end{bmatrix}. \quad \text{(A.2)}$$

where, the matrices are defined as following

$$A_{11} = \left[-\Delta t \cdot \frac{\dot{M}_{12}}{\rho_i V_1} - \Delta t \frac{UA_1}{\rho_i V_1 c_p} - \Delta t \frac{\dot{M}_{out,1}}{\rho_i V_1} \right], A_{12} = \left[\Delta t \cdot \frac{\dot{M}_{21}}{\rho_i V_1} \right]$$
$$A_{21} = \left[\Delta t \frac{\dot{M}_{12}}{\rho_i V_2} \right], A_{22} = \left[-\Delta t \frac{\dot{M}_{21}}{\rho_i V_2} - \Delta t \frac{\dot{M}_{23}}{\rho_i V_2} - \Delta t \frac{UA_2}{\rho_i V_2 c_p} - \Delta t \frac{\dot{M}_{out,2}}{\rho_i V_2} \right], A_{23} = \left[\Delta t \frac{\dot{M}_{32}}{\rho_i V_2} \right]$$
$$A_{32} = \left[\Delta t \frac{\dot{M}_{23}}{\rho_i V_3} \right], A_{33} = \left[-\Delta t \frac{\dot{M}_{32}}{\rho_i V_3} - \Delta t \frac{UA_3}{\rho_i V_3 c_p} - \Delta t \frac{\dot{M}_{out,3}}{\rho_i V_3} \right].$$

The full nonlinear coupled algebraic dynamic equation for indoor zonal concentration is

$$\frac{dC_{r,1}}{dt} = -C_{r,1} \cdot \dot{N}_{out,1} - C_{r,1} \cdot \dot{N}_{1,2} + C_{r,2} \cdot \dot{N}_{2,1} + C_{in} \cdot \dot{N}_{in,1} + C_{in} \cdot \dot{N}_{in,4} + \frac{G_1}{V_1}, \quad \text{(A.3a)}$$
$$\frac{dC_{r,2}}{dt} = -C_{r,2} \cdot \dot{N}_{out,2} - C_{r,2} \cdot \dot{N}_{2,1} - C_{r,2} \cdot \dot{N}_{2,3} + C_{r,1} \cdot \dot{N}_{1,2} + C_{r,3} \cdot \dot{N}_{3,2} + C_{in} \cdot \dot{N}_{in,2} + C_{in} \cdot \dot{N}_{in,5} + \frac{G_2}{V_2}, \quad \text{(A.3b)}$$
$$\frac{dC_{r,3}}{dt} = -C_{r,3} \cdot \dot{N}_{out,3} - C_{r,3} \cdot \dot{N}_{3,2} + C_{r,2} \cdot \dot{N}_{2,3} + C_{in} \cdot \dot{N}_{in,3} + C_{in} \cdot \dot{N}_{in,6} + \frac{G_3}{V_3}. \quad \text{(A.3c)}$$

The equations and matrices for simulation of the nonlinear model of A.3 is

$$\begin{bmatrix} C_{r,1} \\ C_{r,2} \\ C_{r,3} \end{bmatrix}^{n+1} = \begin{bmatrix} A_{11} & A_{12} & 0 \\ A_{21} & A_{22} & A_{23} \\ 0 & A_{32} & A_{33} \end{bmatrix} \cdot \begin{bmatrix} C_{r,1} \\ C_{r,2} \\ C_{r,3} \end{bmatrix}^{n} + \Delta t \cdot C_{in} \cdot \begin{bmatrix} \dot{N}_{in,1} + \dot{N}_{in,4} \\ \dot{N}_{in,2} + \dot{N}_{in,5} \\ \dot{N}_{in,3} + \dot{N}_{in,6} \end{bmatrix} + \Delta t \cdot \frac{1}{V_i} \cdot \begin{bmatrix} G_1 \\ G_2 \\ G_3 \end{bmatrix}. \quad \text{(A.4)}$$

where, the matrices are defined as following

$$A_{11} = \left[1 - (\dot{N}_{out,1} + \dot{N}_{1,2}) \cdot \Delta t \right], A_{12} = \left[\dot{N}_{2,1} \cdot \Delta t \right],$$
$$A_{21} = \left[\dot{N}_{1,2} \cdot \Delta t \right], A_{22} = \left[1 - (\dot{N}_{out,2} + \dot{N}_{2,1} + \dot{N}_{2,3}) \cdot \Delta t \right], A_{23} = \left[\dot{N}_{3,2} \cdot \Delta t \right],$$
$$A_{32} = \left[\dot{N}_{2,3} \cdot \Delta t \right], A_{33} = \left[1 - (\dot{N}_{out,3} + \dot{N}_{3,2}) \cdot \Delta t \right].$$

The full nonlinear steady state equation for ventilation components include the equations for exhaust unit as A.5, and the equations for inlet system as A.6.

$$\Delta P_m = (b_0 + b_1\theta + b_2\theta^2) q_m^2 + a_0 \left(V_{voltage} \right)^2 + a_1 q_m \left(V_{voltage} \right) + a_2 q_m^2, \quad \text{(A.5a)}$$
$$\Delta P_m = P_e - P_i = \frac{1}{2} \rho_o C_{P,r} V_{ref}^2 - P_i - \rho_i g (\frac{T_i}{T_o} - 1)(H_r - H_m). \quad \text{(A.5b)}$$

$$\Delta P_{in} = \frac{\rho_o}{2} \cdot \frac{q_{in}^2}{(C_d A_{in})^2}, \quad \text{(A.6a)}$$
$$\Delta P_{in} = \frac{1}{2} C_P \rho_o V_{ref}^2 - P_i + \rho_o g (1 - \frac{T_o}{T_i})(H_r - H_{in}). \quad \text{(A.6b)}$$

A.2 Model Linearization and Combination

The matrices of linearized zonal temperature model is

$$A_{sT} = \begin{bmatrix} -\frac{UA_1}{\rho V c_p} - \frac{\dot{M}_{12,o}}{\rho V} - \frac{\dot{M}_{out,1,o}}{\rho V} & \frac{\dot{M}_{21,o}}{\rho V} & 0 \\ \frac{\dot{M}_{12,o}}{\rho V} & -\frac{UA_2}{\rho V c_p} - \frac{\dot{M}_{21,o}}{\rho V} - \frac{\dot{M}_{23,o}}{\rho V} - \frac{\dot{M}_{out,2,o}}{\rho V} & \frac{\dot{M}_{32,o}}{\rho V} \\ 0 & \frac{\dot{M}_{23,o}}{\rho V} & -\frac{UA_3}{\rho V c_p} - \frac{\dot{M}_{32,o}}{\rho V} - \frac{\dot{M}_{out,3,o}}{\rho V} \end{bmatrix}_{3\times 3}, \tag{A.7}$$

$$B_{sdT} = \begin{bmatrix} \frac{1}{\rho V c_p} & & (\frac{UA_1}{\rho V c_p} + \frac{\dot{M}_{in,1,o}}{\rho V} + \frac{\dot{M}_{in,4,o}}{\rho V}) \\ & \frac{1}{\rho V c_p} & (\frac{UA_2}{\rho V c_p} + \frac{\dot{M}_{in,2,o}}{\rho V} + \frac{\dot{M}_{in,5,o}}{\rho V}) \\ & \frac{1}{\rho V c_p} & (\frac{UA_3}{\rho V c_p} + \frac{\dot{M}_{in,3,o}}{\rho V} + \frac{\dot{M}_{in,6,o}}{\rho V}) \end{bmatrix}_{3\times 4}, \tag{A.8}$$

$$B_{sT,I} = \begin{bmatrix} [\frac{T_{o,o}}{\rho V} - \frac{T_{2,o}}{\rho V}] & 0 & 0 & [\frac{T_{o,o}}{\rho V} - \frac{T_{2,o}}{\rho V}] & 0 & 0 & [-\frac{T_{1,o}}{\rho V} + \frac{T_{2,o}}{\rho V}] & 0 & 0 \\ 0 & [\frac{T_{o,o}}{\rho V} - \frac{T_{2,o}}{\rho V}] & 0 & 0 & [\frac{T_{o,o}}{\rho V} - \frac{T_{2,o}}{\rho V}] & 0 & 0 & 0 & 0 \\ \frac{T_{2,o}}{\rho V} & \frac{T_{2,o}}{\rho V} & \frac{T_{o,o}}{\rho V} & \frac{T_{2,o}}{\rho V} & \frac{T_{2,o}}{\rho V} & \frac{T_{o,o}}{\rho V} & -\frac{T_{2,o}}{\rho V} & -\frac{T_{2,o}}{\rho V} & -\frac{T_{3,o}}{\rho V} \end{bmatrix}_{3\times 9}, \tag{A.9}$$

$$B_{sT,II} = \begin{bmatrix} [\frac{T_{o,o}}{\rho V} - \frac{T_{2,o}}{\rho V}] & 0 & 0 & [\frac{T_{o,o}}{\rho V} - \frac{T_{2,o}}{\rho V}] & 0 & 0 & [-\frac{T_{1,o}}{\rho V} + \frac{T_{2,o}}{\rho V}] & 0 & 0 \\ [\frac{T_{2,o}}{\rho V} - \frac{T_{3,o}}{\rho V}] & [\frac{T_{o,o}}{\rho V} - \frac{T_{3,o}}{\rho V}] & 0 & [\frac{T_{2,o}}{\rho V} - \frac{T_{3,o}}{\rho V}] & [\frac{T_{o,o}}{\rho V} - \frac{T_{3,o}}{\rho V}] & 0 & [-\frac{T_{2,o}}{\rho V} + \frac{T_{3,o}}{\rho V}] & [-\frac{T_{2,o}}{\rho V} + \frac{T_{3,o}}{\rho V}] & 0 \\ \frac{T_{3,o}}{\rho V} & \frac{T_{3,o}}{\rho V} & \frac{T_{o,o}}{\rho V} & \frac{T_{3,o}}{\rho V} & \frac{T_{3,o}}{\rho V} & \frac{T_{o,o}}{\rho V} & -\frac{T_{3,o}}{\rho V} & -\frac{T_{3,o}}{\rho V} & -\frac{T_{3,o}}{\rho V} \end{bmatrix}_{3\times 9}, \tag{A.10}$$

$$B_{sT,III} = \begin{bmatrix} [\frac{T_{o,o}}{\rho V} - \frac{T_{1,o}}{\rho V}] & 0 & 0 & [\frac{T_{o,o}}{\rho V} - \frac{T_{1,o}}{\rho V}] & 0 & 0 & 0 & 0 & 0 \\ [\frac{T_{1,o}}{\rho V} - \frac{T_{3,o}}{\rho V}] & [\frac{T_{o,o}}{\rho V} - \frac{T_{3,o}}{\rho V}] & 0 & [\frac{T_{1,o}}{\rho V} - \frac{T_{3,o}}{\rho V}] & [\frac{T_{o,o}}{\rho V} - \frac{T_{3,o}}{\rho V}] & 0 & [-\frac{T_{1,o}}{\rho V} + \frac{T_{3,o}}{\rho V}] & [-\frac{T_{2,o}}{\rho V} + \frac{T_{3,o}}{\rho V}] & 0 \\ \frac{T_{3,o}}{\rho V} & \frac{T_{3,o}}{\rho V} & \frac{T_{o,o}}{\rho V} & \frac{T_{3,o}}{\rho V} & \frac{T_{3,o}}{\rho V} & \frac{T_{o,o}}{\rho V} & -\frac{T_{3,o}}{\rho V} & -\frac{T_{3,o}}{\rho V} & -\frac{T_{3,o}}{\rho V} \end{bmatrix}_{3\times 9}, \tag{A.11}$$

$$B_{sT,IV} = \begin{bmatrix} [\frac{T_{o,o}}{\rho V} - \frac{T_{1,o}}{\rho V}] & 0 & 0 & [\frac{T_{o,o}}{\rho V} - \frac{T_{1,o}}{\rho V}] & 0 & 0 & 0 & 0 & 0 \\ [\frac{T_{1,o}}{\rho V} - \frac{T_{2,o}}{\rho V}] & [\frac{T_{o,o}}{\rho V} - \frac{T_{2,o}}{\rho V}] & 0 & [\frac{T_{1,o}}{\rho V} - \frac{T_{2,o}}{\rho V}] & [\frac{T_{o,o}}{\rho V} - \frac{T_{2,o}}{\rho V}] & 0 & [-\frac{T_{1,o}}{\rho V} + \frac{T_{2,o}}{\rho V}] & 0 & 0 \\ \frac{T_{2,o}}{\rho V} & \frac{T_{2,o}}{\rho V} & \frac{T_{o,o}}{\rho V} & \frac{T_{2,o}}{\rho V} & \frac{T_{2,o}}{\rho V} & \frac{T_{o,o}}{\rho V} & -\frac{T_{2,o}}{\rho V} & -\frac{T_{2,o}}{\rho V} & -\frac{T_{3,o}}{\rho V} \end{bmatrix}_{3\times 9}. \tag{A.12}$$

The matrices for linearized zonal concentration model is

$$A_{sC} = \begin{bmatrix} (-\dot{N}_{12,o} - \dot{N}_{out,1,o}) & \dot{N}_{21,o} & 0 \\ \dot{N}_{12,o} & (-\dot{N}_{21,o} - \dot{N}_{23,o} - \dot{N}_{out,2,o}) & \dot{N}_{32} \\ 0 & \dot{N}_{23} & (-\dot{N}_{32,o} - \dot{N}_{out,3,o}) \end{bmatrix}, \tag{A.13}$$

$$B_{sdC} = \begin{bmatrix} \frac{1}{V_1} & 0 & 0 & \dot{N}_{in,1,o} + \dot{N}_{in,4,o} \\ 0 & \frac{1}{V_2} & 0 & \dot{N}_{in,2,o} + \dot{N}_{in,5,o} \\ 0 & 0 & \frac{1}{V_3} & \dot{N}_{in,3,o} + \dot{N}_{in,6,o} \end{bmatrix}, \tag{A.14}$$

$$B_{sC,I} == \begin{bmatrix} [C_{in,o} - C_{r,2,o}] & 0 & 0 & [C_{in,o} - C_{r,2,o}] & 0 & 0 & [-C_{r,1,o} + C_{r,2,o}] & 0 & 0 \\ 0 & [C_{in,o} - C_{r,2,o}] & 0 & 0 & [C_{in,o} - C_{r,2,o}] & 0 & 0 & 0 & 0 \\ C_{r,2,o} & C_{r,2,o} & C_{in,o} & C_{r,2,o} & C_{r,2,o} & C_{in,o} & -C_{r,2,o} & -C_{r,2,o} & -C_{r,3,o} \end{bmatrix}_{3\times 9}, \tag{A.15}$$

$$B_{sC,II} = \begin{bmatrix} [C_{in,o} - C_{r,2,o}] & 0 & 0 & [C_{in,o} - C_{r,2,o}] & 0 & 0 & [-C_{r,1,o} + C_{r,2,o}] & 0 & 0 \\ [C_{r,2,o} - C_{r,3,o}] & [C_{in,o} - C_{r,3,o}] & 0 & [C_{r,2,o} - C_{r,3,o}] & [C_{in,o} - C_{r,3,o}] & 0 & [-C_{r,2,o} + C_{r,3,o}] & [-C_{r,2,o} + C_{r,3,o}] & 0 \\ C_{r,3,o} & C_{r,3,o} & C_{in,o} & C_{r,3,o} & C_{r,3,o} & C_{in,o} & -C_{r,3,o} & -C_{r,3,o} & -C_{r,3,o} \end{bmatrix}_{3\times 9}, \tag{A.16}$$

$$B_{sC,III} = \begin{bmatrix} [C_{in,o} - C_{r,1,o}] & 0 & 0 & [C_{in,o} - C_{r,1,o}] & 0 & 0 & 0 & 0 & 0 \\ [C_{r,1,o} - C_{r,3,o}] & [C_{in,o} - C_{r,3,o}] & 0 & [C_{r,1,o} - C_{r,3,o}] & [C_{in,o} - C_{r,3,o}] & 0 & [-C_{r,1,o} + C_{r,3,o}] & [-C_{r,2,o} + C_{r,3,o}] & 0 \\ C_{r,3,o} & C_{r,3,o} & C_{in,o} & C_{r,3,o} & C_{r,3,o} & C_{in,o} & -C_{r,3,o} & -C_{r,3,o} & -C_{r,3,o} \end{bmatrix}_{3\times 9}, \tag{A.17}$$

$$B_{sC,IV} = \begin{bmatrix} [C_{in,o} - C_{r,1,o}] & 0 & 0 & [C_{in,o} - C_{r,1,o}] & 0 & 0 & 0 & 0 & 0 \\ [C_{r,1,o} - C_{r,2,o}] & [C_{in,o} - C_{r,2,o}] & 0 & [C_{r,1,o} - C_{r,2,o}] & [C_{in,o} - C_{r,2,o}] & 0 & [-C_{r,1,o} + C_{r,2,o}] & 0 & 0 \\ C_{r,2,o} & C_{r,2,o} & C_{in,o} & C_{r,2,o} & C_{r,2,o} & C_{in,o} & -C_{r,2,o} & -C_{r,2,o} & -C_{r,3,o} \end{bmatrix}_{3\times 9}. \tag{A.18}$$

where, the subscript I,II,III and IV correspond to the four inter-zonal airflow patterns, which have been explained in Fig. 2.7 in Chapter 2.

The linearized model for exhaust unit is derived as

$$\begin{aligned}\Delta\tilde{P}_m &= (a_1 V_{voltage,o} + 2a_2 q_{m,o} + 2b_0 q_{m,o} + 2b_1\theta_o q_{m,o} + 2b_2\theta_o^2 q_{m,o})\tilde{q}_m \\ &\quad + (2a_0 V_{voltage,o} + a_1 q_{m,o})\tilde{V}_{voltage} + (b_1 q_{m,o}^2 + 2b_2 q_{m,o}^2\theta_o)\tilde{\theta}, \qquad \text{(A.19)}\\ \Delta\tilde{P}_m &= \tilde{P}_e - \tilde{P}_i = (C_{P,r,o}\rho_o V_{ref,o})\tilde{V}_{ref} + (\frac{1}{2}\rho_o V_{ref,o}^2)\tilde{c}_{P,r} - \tilde{P}_i \\ &\quad + \rho_i g(H_r - H_m)\frac{T_{i,o}}{T_{o,o}^2}\tilde{T}_o - \rho_i g(H_r - H_m)\frac{1}{T_{o,o}}\tilde{T}_i. \qquad \text{(A.20)}\end{aligned}$$

The linearized model for inlet system is derived as

$$\begin{aligned}\Delta\tilde{P}_{in} &= \left[\frac{\rho_o}{C_d^2 A_{in,o}^2} q_{in,o}\right]\tilde{q}_{in} + \left[-\frac{\rho_o}{C_d^2 A_{in,o}^3} q_{in,o}^2\right]\tilde{A}_{in}, \qquad \text{(A.21)}\\ \Delta\tilde{P}_{in} &= (C_{P,o}\rho_o V_{ref,o})\tilde{V}_{ref} + (\frac{1}{2}\rho_o V_{ref,o}^2)\tilde{c}_P - \tilde{P}_i \\ &\quad - \rho_o g(H_r - H_{in})\frac{1}{T_{i,o}}\tilde{T}_o + \rho_o g(H_r - H_{in})\frac{T_{o,o}}{T_{i,o}^2}\tilde{T}_i. \qquad \text{(A.22)}\end{aligned}$$

Combining the linearized exhaust unit equation A.20 and inlet system equation A.22, together with the mass balance equation which has been defined in 6.7 in Chapter 6 generate the followings:

$$E\bar{q} + Fu + Gw + Kx_T = 0 \qquad \text{(A.23)}$$

where,

$$\bar{q} = \begin{bmatrix} \tilde{q}_{in,1} \\ \tilde{q}_{in,2} \\ \tilde{q}_{in,3} \\ \tilde{q}_{in,4} \\ \tilde{q}_{in,5} \\ \tilde{q}_{in,6} \\ \tilde{q}_{m,1} \\ \tilde{q}_{m,2} \\ \tilde{q}_{m,3} \\ \tilde{P}_i \end{bmatrix}_{10\times 1}, u = \begin{bmatrix} \tilde{A}_{in,1} \\ \tilde{A}_{in,2} \\ \tilde{A}_{in,3} \\ \tilde{A}_{in,4} \\ \tilde{A}_{in,5} \\ \tilde{A}_{in,6} \\ \tilde{V}_{voltage,1} \\ \tilde{V}_{voltage,2} \\ \tilde{V}_{voltage,3} \\ \tilde{\theta}_1 \\ \tilde{\theta}_2 \\ \tilde{\theta}_3 \end{bmatrix}_{12\times 1}, w = \begin{bmatrix} \tilde{V}_{ref} \\ \tilde{c}_{P,w} \\ \tilde{c}_{P,l} \\ \tilde{c}_{P,r} \\ \tilde{T}_o \end{bmatrix}_{5\times 1}, x_T = \begin{bmatrix} \tilde{T}_1 \\ \tilde{T}_2 \\ \tilde{T}_3 \end{bmatrix}_{3\times 1}. \qquad \text{(A.24)}$$

where the matrices are

$$E=\begin{bmatrix} E_{in,1} & & & & & & & & & -1\\ & E_{in,2} & & & & & & & & -1\\ & & E_{in,3} & & & & 0 & & & -1\\ & & & E_{in,4} & & & & & & -1\\ & & & & E_{in,5} & & & & & -1\\ & & & & & E_{in,6} & & & & -1\\ & & 0 & & & & E_{out,1} & & & -1\\ & & & & & & & E_{out,2} & & -1\\ & & & & & & & & E_{out,3} & -1\\ \rho_o & \rho_o & \rho_o & \rho_o & \rho_o & \rho_o & -\rho_i & -\rho_i & -\rho_i & 0 \end{bmatrix}_{10\times 10}, \tag{A.25}$$

$$E_{in,i}=-\left[2e_c q_{in,o}+\frac{\rho_o}{C_d^2 A_{in,i,o}^2}q_{in,i,o}\right], E_{out,i}=-(a_1 V_{voltage,o}+2a_2 q_{m,o}+2b_0 q_{m,o}+2b_1\theta_o q_{m,o}+2b_2\theta_o^2 q_{m,o})$$

$$F=\begin{bmatrix} F_{in,1} & & & & & & & & & & & \\ & F_{in,2} & & & & & & & & & & \\ & & F_{in,3} & & & & & & 0 & & & \\ & & & F_{in,4} & & & & & & & & \\ & & & & F_{in,5} & & & & & & & \\ & & & & & F_{in,6} & & & & & & \\ & & 0 & & & & F_{out,v,1} & & & F_{out,\theta,1} & & \\ & & & & & & & F_{out,v,2} & & & F_{out,\theta,2} & \\ & & & & & & & & F_{out,v,3} & & & F_{out,\theta,3}\\ 0 & 0 & 0 & 0 & 0 & 0 & 0 & 0 & 0 & 0 & 0 & 0 \end{bmatrix}_{10\times 12}, \tag{A.26}$$

$$F_{in,i}=-\left[-\frac{\rho_o}{C_d^2 A_{in,i,o}^3}q_{in,i,o}^2\right], F_{out,v,i}=-(2a_0 V_{voltage,o}+a_1 q_{m,o}), F_{out,\theta,i}=-(b_1 q_{m,o}^2+2b_2 q_{m,o}^2\theta_o)$$

$$G=\begin{bmatrix} G_{wind,w} & G_{CP,w} & 0 & 0 & G_{To,in}\\ G_{wind,w} & G_{CP,w} & 0 & 0 & G_{To,in}\\ G_{wind,w} & G_{CP,w} & 0 & 0 & G_{To,in}\\ G_{wind,l} & 0 & G_{CP,l} & 0 & G_{To,in}\\ G_{wind,l} & 0 & G_{CP,l} & 0 & G_{To,in}\\ G_{wind,l} & 0 & G_{CP,l} & 0 & G_{To,in}\\ G_{wind,r} & 0 & 0 & G_{CP,r} & G_{To,out}\\ G_{wind,r} & 0 & 0 & G_{CP,r} & G_{To,out}\\ G_{wind,r} & 0 & 0 & G_{CP,r} & G_{To,out}\\ 0 & 0 & 0 & 0 & 0 \end{bmatrix}_{10\times 5}, \tag{A.27}$$

$$G_{wind}=C_P\rho_o V_{ref,o}, G_{CP}=(\frac{1}{2}\rho_o V_{ref,o}^2), G_{To,in}=-\frac{\rho_o g(H_r-H_{in})}{T_{i,o}}, G_{To,out}=\rho_i g(H_r-H_m)\frac{T_{i,o}}{T_{o,o}^2}$$

$$K=\begin{bmatrix} K_{Iin,1} & 0 & 0\\ 0 & K_{in,2} & 0\\ 0 & 0 & K_{in,3}\\ K_{in,4} & 0 & 0\\ 0 & K_{in,5} & 0\\ 0 & 0 & K_{in,6}\\ K_{out,1} & 0 & 0\\ 0 & K_{out,2} & 0\\ 0 & 0 & K_{out,3}\\ 0 & 0 & 0 \end{bmatrix}_{10\times 3}, \tag{A.28}$$

$$K_{in,i}=\rho_o g(H_r-H_{in})\frac{T_{o,o}}{T_{i,o}^2}, K_{out,j}=-\rho_i g(H_r-H_m)\frac{1}{T_{o,o}}.$$

The manipulated variable of the finalized state space representation denoted by u is derived by conversion

$$u = \begin{bmatrix} I_{9\times 9} & 0_{9\times 1} \end{bmatrix} \cdot \bar{q} = \begin{bmatrix} I_{9\times 9} & 0_{9\times 1} \end{bmatrix} \cdot \left[-E^{-1}(Fu + Gw + Kx_T)\right]. \tag{A.29}$$

and the internal pressure P_i is expressed as

$$\tilde{P}_i = \begin{bmatrix} 0_{1\times 9} & I_{1\times 1} \end{bmatrix} \cdot \bar{q} = \begin{bmatrix} 0_{1\times 9} & I_{1\times 1} \end{bmatrix} \cdot \left[-E^{-1}(Fu + Gw + Kx_T)\right]. \tag{A.30}$$

Substitute the equation A.29 into the state space thermal model as described in 7.8 in Chapter 7, the finalized transforming matrices for zonal temperature model are

$$A_T = A_{sT} + B_{sT} \cdot \rho \cdot \begin{bmatrix} I_{9\times 9} & 0 \end{bmatrix} \cdot (-E^{-1}) \cdot K, \tag{A.31}$$

$$B_T = B_{sT} \cdot \rho \cdot \begin{bmatrix} I_{9\times 9} & 0 \end{bmatrix} \cdot (-E^{-1}) \cdot F, \tag{A.32}$$

$$B_{dwT} = B_{sT} \cdot \rho \cdot \begin{bmatrix} I_{9\times 9} & 0 \end{bmatrix} \cdot (-E^{-1}) \cdot G, \tag{A.33}$$

$$B_{dQT} = B_{sTd}. \tag{A.34}$$

For zonal concentration model 7.9 in Chapter 7, the finalized matrices are

$$A_C = A_{sC}, \tag{A.35}$$

$$B_C = B_{sC} \cdot \frac{3600}{V} \cdot \begin{bmatrix} I_{9\times 9} & 0_{9\times 1} \end{bmatrix} \cdot (-E^{-1}) \cdot F, \tag{A.36}$$

$$B_{dX_TC} = B_{sC} \cdot \frac{3600}{V} \cdot \begin{bmatrix} I_{9\times 9} & 0_{9\times `1} \end{bmatrix} \cdot (-E^{-1}) \cdot K, \tag{A.37}$$

$$B_{dwC} = B_{sC} \cdot \frac{3600}{V} \cdot \begin{bmatrix} I_{9\times 9} & 0_{9\times `1} \end{bmatrix} \cdot (-E^{-1}) \cdot G, \tag{A.38}$$

$$B_{dGC} = B_{sCd}. \tag{A.39}$$

A.3 Model Scaling

The unscaled linear model transfer function of the process in deviation variables is

$$y_{us} = G_{us}u + G_{d,us}d, \tag{A.40}$$

$$e_{us} = y_{us} - r_{us}. \tag{A.41}$$

In order to make the variable less than one in magnitude, each variable will be divided by its maximum expected or allowed change.

$$d_s = D_d^{-1} d_{us}, D_d^{-1} = d_{us,\max}, \tag{A.42}$$

$$u_s = D_u^{-1} u_{us}, D_u^{-1} = u_{us,\max}, \tag{A.43}$$

$$y_s = D_e^{-1} y_{us}, D_e^{-1} = e_{us,\max}, \tag{A.44}$$

$$e_s = D_e^{-1} e_{us}, D_e^{-1} = e_{us,\max}. \tag{A.45}$$

$$\tag{A.46}$$

Substitute A.3 into A.3, we derive

$$y_s = G_s u + G_{d,s} d, \tag{A.47}$$

$$e_s = y_s - r_s. \tag{A.48}$$

the scaled transfer function become:

$$G_s = D_e^{-1} G_{us} D_u, G_{d,s} = D_e^{-1} G_{d,us} D_d. \tag{A.49}$$

The scaled reference $r_s = R\tilde{r}$, where, $R = D_e^{-1} D_r = r_{us,\max} / e_{us,\max}$.

Appendix B

Matrices used for Moving Horizon Estimation and Control

In this appendix the matrices used for quadratic programming of moving horizon estimation and control are presented.

The quadratic programming is formulated as:

$$\min \phi = \frac{1}{2} U^T H U + f^T U \tag{B.1}$$

$$s.t. \begin{cases} AU \leq b \\ lb \leq U \leq ub \end{cases} \tag{B.2}$$

The target calculation is:

$$\min_{[x_s, u_s]^T} \Psi = (u_s - u_t)^T R_s (u_s - u_t) + (y_s - y_t)^T Q_s (y_s - y_t) \tag{B.3}$$

$$s.t. \begin{cases} \begin{bmatrix} I - A & -B \\ C & 0 \end{bmatrix} \begin{bmatrix} x_s \\ u_s \end{bmatrix} = \begin{bmatrix} B_{dum} \hat{d}_{umd} + B_{dm} d_{md} \\ y_s \end{bmatrix} \\ u_{\min} \leq u_s \leq u_{\max} \end{cases} \tag{B.4}$$

where,

$$\begin{aligned} &H = \begin{bmatrix} C^T Q_s C & 0 \\ 0 & R_s \end{bmatrix}, f = - \begin{bmatrix} Q_s C \cdot y_t \\ R_s \cdot u_t \end{bmatrix}, \\ &A = \begin{bmatrix} I - A & -B \\ A - I & B \end{bmatrix}, b = \begin{bmatrix} B_{dum} \hat{d}_{umd} + B_{dm} d_{md} \\ -B_{dum} \hat{d}_{umd} - B_{dm} d_{md} \end{bmatrix}, lb = \begin{bmatrix} x_{\min} \\ u_{\min} \end{bmatrix}, ub = \begin{bmatrix} x_{\max} \\ u_{\max} \end{bmatrix}. \end{aligned} \tag{B.5}$$

The Receding Horizon Regulation is:

$$\min_{u^N} \Phi_k^N = \frac{1}{2}\sum_{k=0}^{N} \|z_k - r_k\|_{Q_z}^2 + \frac{1}{2}\sum_{k=0}^{N-1} \|\Delta u_k\|_S^2 + \|u_k - u_s\|_{S_u}^2 \tag{B.6}$$

$$s.t. \begin{cases} x_{k+j+1} = Ax_{k+j} + Bu_{k+j} + B_d d_{k+j} \\ z_{k+j} = Cx_{k+j} \\ z_{\min} \le z_{k+j} \le z_{\max}, j = 1,2,\cdots N \\ u_{\min} \le u_{k+j} \le u_{\max}, j = 0,1,\cdots N-1 \\ \Delta u_{\min} \le \Delta u_{k+j} \le \Delta u_{\max}, j = 0,1,\cdots N-1 \end{cases} \tag{B.7}$$

where,

$$H = \Gamma_U^T Q_Z \Gamma_U + H_S + S_U,$$
$$f = M_{x_0} x_0 + M_R R + M_{u_{-1}} u_{-1} + M_D D + M_{U_s} U_s,$$
$$M_{x_0} = \Gamma_U^T Q_Z \Phi, M_R = -\Gamma_U^T Q_Z, M_D = \Gamma_U^T Q_Z \Gamma_D, M_{U_s} = S_U$$

$$H_S = \begin{bmatrix} 2S & -S & & \cdots & \\ -S & 2S & -S & \cdots & \\ & -S & 2S & -S & \\ \vdots & \vdots & -S & 2S & -S \\ & & & -S & S \end{bmatrix}, M_{u_{-1}} = \begin{pmatrix} -\begin{bmatrix} S \\ 0 \\ 0 \\ 0 \\ 0 \end{bmatrix} \end{pmatrix},$$

$$\Phi = \begin{bmatrix} C_z A \\ C_z A^2 \\ C_z A^3 \\ \vdots \\ C_z A^N \end{bmatrix}, \Gamma_U = \begin{bmatrix} C_z B & 0 & 0 & \cdots & 0 \\ C_z AB & C_z B & 0 & \cdots & 0 \\ C_z A^2 B & C_z AB & C_z B & & 0 \\ \vdots & \vdots & \vdots & & \vdots \\ C_z A^{N-1} B & C_z A^{N-2} B & C_z A^{N-3} B & \cdots & C_z B \end{bmatrix}, \tag{B.8}$$

$$\Gamma_D = \begin{bmatrix} C_z E & 0 & 0 & \cdots & 0 \\ C_z AE & C_z E & 0 & \cdots & 0 \\ C_z A^2 E & C_z AE & C_z E & & 0 \\ \vdots & \vdots & \vdots & & \vdots \\ C_z A^{N-1} E & C_z A^{N-2} E & C_z A^{N-3} E & \cdots & C_z E \end{bmatrix},$$

$$A = \begin{bmatrix} \Lambda \\ -\Lambda \\ \Gamma \\ -\Gamma \end{bmatrix}, b = \begin{bmatrix} \Delta U_{\max} \\ -\Delta U_{\min} \\ Z_{\max} - \Phi x_0 - \Gamma_d D \\ -Z_{\min} + \Phi x_0 + \Gamma_d D \end{bmatrix},$$

$$\Lambda = \begin{bmatrix} -I & I & & & \\ & -I & I & & \\ & & -I & I & \\ & & & -I & I \end{bmatrix}, lb = U_{\min}, ub = U_{\max}.$$

The Moving Horizon Estimation is:

$$\min_{\left[\hat{x}_{k-N/k},\hat{w}^N\right]} \Psi_k^N = \frac{1}{2}\left\|\hat{x}_{k-N/k} - \bar{x}_{k-N/k-N-1}\right\|^2_{P_{k-N}^{-1}} + \frac{1}{2}\sum_{j=k-N}^{k-1}\left\|w_{j/k}\right\|^2_{Q_w^{-1}} + \left\|v_{j/k}\right\|^2_{R_v^{-1}} \tag{B.9}$$

$$s.t. \begin{cases} x_{k+j+1} = Ax_{k+j} + Bu_{k+j} + B_d d_{k+j} + Gw_{k+j} \\ z_{k+j} = Cx_{k+j} + v_{k+j} \\ x_{\min} \le \hat{x}_{k-N/k} \le x_{\max} \\ w_{\min} \le \hat{w}_k \le w_{\max} \\ z_{\min} \le z_k \le z_{\max} \end{cases} \tag{B.10}$$

where,

$$\begin{aligned} H &= \begin{bmatrix} P_{k-N}^{-1} & 0 \\ 0 & Q_W^{-1}, \end{bmatrix} + a^T R_V^{-1} a, \\ f &= \left(-\begin{bmatrix} P_{k-N}^{-1} \\ 0 \end{bmatrix} \bar{x}_{k-N/k-N-1}^T\right) + \left(-a^T R_V^{-1} b\right), \\ b &= Y - \Gamma_U U - \Gamma_D D, \\ a &= \begin{bmatrix} \Phi & \Gamma_W \end{bmatrix} \\ \Gamma_W &= \begin{bmatrix} 0 & 0 & 0 & \cdots & \cdots & 0 \\ C_z G & 0 & 0 & \cdots & \cdots & 0 \\ C_z AG & C_z G & 0 & 0 & \cdots & 0 \\ \vdots & \vdots & \vdots & \vdots & \vdots & \vdots \\ C_z A^{N-1} G & C_z A^{N-2} G & \cdots & C_z AG & C_z G & 0 \end{bmatrix}, \\ A &= \begin{bmatrix} \Phi & \Gamma_W \\ -\Phi & -\Gamma_W \end{bmatrix}, b = \begin{bmatrix} \bar{\eta}_{\max} - (\Gamma_U U + \Gamma_D D) \\ -\bar{\eta}_{\min} + (\Gamma_U U + \Gamma_D D) \end{bmatrix}, \\ lb &= \begin{bmatrix} x_{\min} \\ W_{\min} \end{bmatrix}, ub = \begin{bmatrix} x_{\max} \\ W_{\max} \end{bmatrix}. \end{aligned} \tag{B.11}$$

Bibliography

[Andersen, 2007] Palle Andersen. *Optimal Control*. Department of Electronic Systems, Aalborg University, 2007. Lecture Note.

[Arvanitis *et al.*, 2007] K. G. Arvanitis, G. D. Pasgianos, P. I. Daskalov, S. Vougioukas, and N. A. Sigrimis. A nonlinear pi controller for climate control of animal buildings. *Proceedings of the European Control Conference*, pages 5851 – 5857, 2007.

[Baldwin and Ingram, 1967] B. A. Baldwin and D. L. Ingram. Behavioural thermoregulation in pigs. *Physiology and Behavior*, 2(1):15 – 20, 1967.

[Barber and Feddes, 1994] E. M. Barber and J. J. R. Feddes. Environmental control technology for cold-climate livestock housing. *Pig News and Information*, 15(1):25 – 30, 1994.

[Beattie *et al.*, 2000] V. E. Beattie, N. E. O'Connell, and B. W. Moss. Influence of environmental enrichment on the behavior, performance and meat quality of domestic pigs. *Livestock Production Science*, 65:71 – 79, 2000.

[Berckmans *et al.*, 1993] D. Berckmans, M. de Moor, and B. de Moor. Linking physical models to system identification in micro-environment control. *Automatic Control. World Congress 1993. Proceeding of the 12th Triennial World Congress of the International Federation of Automatic Control*, 4:1143 – 1146, 1993.

[Bjerg *et al.*, 2000] B. Bjerg, K. Svidt, G. Zhang, and S. Morsing. The effect of pen partitions and thermal pig simulators on airflow in a livestock test room. *Journal of Agricultural Engineering Research*, 77(3):317 – 326, 2000.

[Brecht *et al.*, 2005] A. Van Brecht, S. Quanten, T. Zerihundesta, and D. Berckmans. Indoor air climate control. In *26th AIVC Conference Ventilation in Relation to the Energy Perofrmance of Buildings*, pages 271 – 286, Brucels, Belgium, 2005. International Energy Agency, Air Infiltration and Ventilation Center, Operating Agent and Management, INIVE EEIG.

[Carpenter, 1981] G. A. Carpenter. *Environmental aspects of housing for animal production*, chapter Ventilation Systems, pages 331 – 350. Butterworth Heinemann, England, 1981.

[Chao and Gates, 1996] K. Chao and R. S. Gates. Design of switching control systems for ventilated greenhouses. *Transaction of ASAE*, 39(4):1513 – 1523, 1996.

[Chao *et al.*, 2000] K. Chao, R. S. Gates, and N. Sigrimis. Fuzzy logic controller design for staged heating and ventilating systems. *Transactions of the ASAE*, 43(6):1885 – 1894, 2000.

[Clark, 1981] J. A. Clark. *Environmental aspects of housing for animal production*. Butterworth Heinemann, England, 1981.

[Colbaugh and Glass, 1992] R. Colbaugh and K. Glass. On controlling robots with redundancy. *Robotics and Computer-Integrated Manufacturing*, 9(2):121 – 135, 1992.

[Cunha *et al.*, 1997] J. B. Cunha, C. Couto, and A. E. Ruano. Real-time parameter estimation of dynamic temperature models for greenhouse environmental control. *Control Engineering Practice*, 5(10):1473 – 1481, 1997.

[Cutler and Ramaker, 1980] C. R. Cutler and B. L. Ramaker. Dynamic matrix control - a computer control algorithm. In *Proceedings of Joint American Control Conference*, San Francisco, 1980.

[Daskalov *et al.*, 2006] P. I. Daskalov, K. G. Arvanitis, G. D. Pasgianos, and N. A. Sigrimis. Non-linear adaptive temperature and humidity control in animal buildings. *Biosystems Engineering*, 93(1):1 – 24, 2006.

[Daskalov, 1997] P. I. Daskalov. Prediction of temperature and humidity in a naturally ventilated pig building. *Journal of Agricultural Engineering Research*, 68:329 – 339, 1997.

[der Hel *et al.*, 1986] W. Van der Hel, R. Duijghuisen, and M. W. A. Verstegen. The effect of ambient temperature and activity on the daily variation in heat production of growing pigs kept in groups. *Journal of Agricultural Science*, 34:173 – 184, 1986.

[Ferreira *et al.*, 2002] P. M. Ferreira, E. A. Faria, and A. E. Ruano. Neural network models in greenhouse air temperature prediction. *Neurocomputing*, 43:51 – 75, 2002.

[Gagneau and Allard, 2001] S. Gagneau and F. Allard. About the construction of autonomous zonal models. *Energy and Buildings*, 33:245 – 250, 2001.

[Gates *et al.*, 2001] R. S. Gates, K. Chao, and N. Sigrimis. Identifying design parameters for fuzzy control of staged ventilation control systems. *Computers and Electronics in Agriculture*, 31:61 – 74, 2001.

[Geers *et al.*, 1991] R. Geers, H. Ville, and V. Goedseels. Environmental temperature control by the pig's comfort behavior through image processing. *Transaction of ASAE*, 34(6):2583 – 2586, 1991.

[Haghighat *et al.*, 2001] F. Haghighat, Y. Li, and A. C. Megri. Development and validation of a zonal model - poma. *Building and Environment*, 36:1039 – 1047, 2001.

[Harral and Boon, 1997] B. B. Harral and C. R. Boon. Comparison of predicted and measured air flow patterns in a mechanically ventilated livestock building without animals. *Journal of Agricultural Engineering Research*, 66:221 – 228, 1997.

[Heiselberg and Nielsen, 1996] P. Heiselberg and P. V. Nielsen. *Flow Element Models*. Indoor environmental technology, paper no. 65. Instituttet for Bygningsteknik, Aalborg University, Denmark, 1996.

[Heiselberg, 1996] P. Heiselberg. *Analysis and Prediction Techniques*. Indoor environmental technology, paper no. 64. Instituttet for Bygningsteknik, Aalborg University, Denmark, 1996.

[Heiselberg, 2004a] P. Heiselberg. *Natural and Hybrid Ventilation*. Aalborg University, Denmark, 2004. Lecture Note.

[Heiselberg, 2004b] P. Heiselberg, editor. *Principle of Hybrid Ventilation, Annex 35: Hybrid Ventilation in New and Retrofitted Office Buildin*, Denmark, 2004. International Energy Agency, Energy Conservation in Buildings and Community Systems, Aalborg University.

[Ingram and Legge, 1974] D. L. Ingram and K. F. Legge. Effects of environmental temperature on food intake in growing pigs. *Comparative Biochemistry and Physiology – Part A: Physiology*, 48(3):573–581, 1974.

[Ingram, 1974] D. L. Ingram. *Heat loss from animals and man*. Butterworths, London, 1974.

[Jenkins and Watts, 1968] G. Jenkins and D. Watts. *Spectral Analysis and Its Applications*. Holden-Day, San Francisco, CA, 1968.

[Jessen *et al.*, 2006a] J. J. Jessen, J. F. D. Nielsen, and H. Schioeler. Cots technologies for internet based monitoring of livestock buildings. In *Proceedings of the 10th IASTED International Conference on Internet and Multimedia Systems and Applications*, pages 10 – 15, 2006.

[Jessen *et al.*, 2006b] J. J. Jessen, H. Schioeler, J. F. D. Nielsen, and M. R. Jensen. Cots technologies for integrating development environment, remote monitoring and control of livestock stable climate. In *Proceedings of 2006 IEEE International Conference on System, Man, and Cybernetics*, 2006.

[Jessen, 2007] J. J. Jessen. *Embedded Controller Design for Pig Stable Ventilation Systems*. PhD thesis, Aalborg University, Aalborg, Denmark, 2007.

[Jorgensen, 2005] J. B. Jorgensen. *Moving Horizon Estimation and Control*. PhD thesis, Department of Chemical Engineering, Technical University of Denmark, Denmark, 2005.

[K. Janssens, 2004] T. Z. Desta C. Boonen D. Berckmans K. Janssens, A. V. Brecht. Modeling the internal dynamics of energy and mass transfer in an imperfectly mixed ventilated airspace. *Indoor Air*, 14, 2004.

[Kvasnica *et al.*, 2004] M. Kvasnica, P. Grieder, and M. Baotić. Multi-Parametric Toolbox (MPT), 2004.

[L. Price, 1999] D. Berckman K. Janssens J. Taylor L. Price, P. Young. Data-based mechanistic modelling (dbm) and control of mass and energy transfer in agricultural buildings. *Anual Reviews In Control*, 23:71 – 82, 1999.

[Lawson and Hanson, 1995] C. L. Lawson and R. J. Hanson. *Solving Least Squares Problems*. SIAM, Philadelphia, PA, 1995.

[Linker *et al.*, 1997] R. Linker, P. O. Gutman, and I. Seginer. Robuts simutaneous control of temperature and co_2 concentration in greenhouses. *IFAC Mathematical and Control Application in Agriculture and Horticulture*, 1997.

[Maciejowski, 2002] J. M. Maciejowski. *Predictive Control with Constraints*. Prentice-Hall, England, 2002.

[Mayne and Michalska, 1990] D. Q. Mayne and H. Michalska. Receding horizon control of constrained nonlinear ssytems. *IEEE Transaction of Automation and Control*, 35:814 – 824, 1990.

[Mayne *et al.*, 2000] D. Q. Mayne, J. B. Rawlings, C. V. Rao, and P. O. M. Scokaert. Constrained model predictive control: Stability and optimality. *Automatica*, 36:789 – 814, 2000.

[Milgen *et al.*, 1997] J. Van Milgen, J. Noblet, S. Dobois, and J. F. Bemier. Dynamic aspects of oxygen consumption and carbon dioxide production in swine. *British Journal of Nutrition*, 78:397 – 410, 1997.

[Moor and Berckmans, 1996a] M. De Moor and D. Berckmans. Building a grey box model to model the energy and mass transfer in an imperfectly mixed fluid by using experimental data. *Mathematics and Computers in Simulation*, 42:233 – 244, 1996.

[Moor and Berckmans, 1996b] M. De Moor and D. Berckmans. Building a grey box model to model the energy and mass transfer in an imperfectly mixed fluid by using experimental data. *Mathematics and Computers in Simulation*, 42:233 – 244, 1996.

[Morari and Lee, 1999] M. Morari and J. H. Lee. Model predictive control: past, present and future. *COmputers and Chemical Engineering*, 23:667 – 682, 1999.

[Muske and Badgwell, 2002] K. R. Muske and T. A. Badgwell. Disturbance modeling for offset-free linear model predictive control. *Journal of Process Control*, 12:617 – 632, 2002.

[Muske and Rawlings, 1993a] K. R. Muske and J. B. Rawlings. Linear model predictive control of unstable processes. *Journal of Process Control*, 3(2):85 – 96, 1993.

[Muske and Rawlings, 1993b] K. R. Muske and J. B. Rawlings. Model predictive control with linear models. *AIChE Journal*, 39(2):262 – 287, 1993.

[Muske *et al.*, 1993] K. R. Muske, J. B. Rawlings, and J. H. Lee. Receding horizon recursive state estimation. *Proceeding of 1993 American Control Conference*, pages 900 – 905, 1993.

[Muske, 1995] K. R. Muske. *Linear Model Predictive Control of Chemical Process*. PhD thesis, The University of Texas at Austin, United States, 1995.

[Nakamura and Ghodoussi, 1989] Y. Nakamura and M. Ghodoussi. Dynamics computation of closed-link robot mechanisms with nonredundant and redundant actuators. *IEEE Transanctions on Robotics and Automation*, 5(3):294 – 302, 1989.

[Nielsen and Madsen, 1996] B. Nielsen and H. Madsen. Predictive control of air temprature in greenhouses. In *Prodeeding of 13th IFAC World Congress*, pages 399 – 404, San Francisco, USA, 1996.

[Nielsen and Madsen, 1998] B. Nielsen and H. Madsen. Identification of a linear continuous time stochastic model of the heat dynamics of a greenhouse. *Journal of Agricultural Engineering Researcj*, 71:249 – 256, 1998.

[Nocedal and Wright, 1999] J. Nocedal and S. J. Wright. *Numerical Optimization*. Springer Series in Operations Research. Springer - Verlag, New York, 1999.

[Odelson *et al.*, 2006] B. J. Odelson, M. R. Rajamani, and J. B. Rawlings. A new autocovariance least - squares method for estimating noise covariances. *Automatica*, 42:303 –308, 2006.

[Odelson *et al.*, 2007] B. J. Odelson, A. Lutz, and J. B. Rawlings. The autocovariance least-sqaure method for estimating covariances: Application to model - based control of chemical reactors. *IEEE Transactions on Control Systems Technology*, 14(3):532 – 540, 2007.

[Odelson, 2003] B. J. Odelson. *Estimating Disturbance Covariances From Data For Improved Control Performance*. PhD thesis, University of Wisconsin, Madison, 2003.

[Ohta *et al.*, 2004] K. Ohta, M. M. Svinin, Z. W. Luo, S. Hosoe, and R. Laboissiere. Opitmal trajectory formation of constrained human arm reaching movements. *Journal of Biological Cybernetics*, 91:23 – 36, 2004.

[O'Neill, 1991] P. J. O'Neill. Identification of flow and volume parameters in multizone systems using a single-gas tracer technique. *ASHRAE Transactions*, 97(1):49 – 54, 1991.

[Panagakis and Axaopoulos, 2004] P. Panagakis and P. Axaopoulos. Comparison of two modeling methods for the prediction of degree-hours and heat-stress likelihood in a swine building. *Transactions of the ASAE*, 47(2):585 – 590, 2004.

[Pannocchia and Rawlings, 2003] G. Pannocchia and J. B. Rawlings. Disturbance models for offset-free model predictive control. *AIChE Journal*, 49(2):426 – 437, 2003.

[Pannocchia *et al.*, 2005] G. Pannocchia, N. Laachi, and J. B. Rawlings. A candidate to replace pid control: Siso-constrained lq control. *AIChE Journal*, 51:1178 – 1189, 2005.

[Pasgianos *et al.*, 2003] G. D. Pasgianos, K. G. Arvanitis, P. Polycarpou, and N. Sigrimis. A nonlinear feedback technique for greenhouse environmental control. *Computers and Electronics in Agriculture*, 40:153 – 177, 2003.

[Pedersen and Sallvik, 1984] S. Pedersen and K. Sallvik. *Report of Working Group on Climatization of Animal Houses*. International Commission of Agricultural Engineering, Section II. Scottish Farm Building Investigation Unit, Craibstone, Aberdeen, Scotland, UK, 1984.

[Pedersen and Sallvik, 2002] S. Pedersen and K. Sallvik. *4th Report of Working Group on Climatization of Animal Houses. Heat and Moisture production at animal and house levels*. International Commission of Agricultural Engineering, Section II. Research Center Bygholm, Danish Institute of Agricultural Sciences, Horsens, Denmark, 2002.

[Pedersen *et al.*, 1998] S. Pedersen, H. Takai, J. O. Johnsen, J. H. M. Metz, P. W. G. Groot Koerkamp, G. H. Uenk, V. R. Phillips, M. R. Holden, R. W. Sneath, J. L. Short, R. P. White, J. Hartung, J. Seedorf, M. Schrder, K. H. H. Linkert, and C. M. Wathes. A comparison of three balance methods for calculating ventilation rates in livestock buildings. *Journal of Agricultural Engineering Research*, 70(1):25 – 37, 1998.

[Poulsen and Pedersen, 2005] H. Poulsen and S. Pedersen. *Klimateknik, Ventilation, Isolering og Opvarmning*. Landbrugsforlaget, Denmark, 4 edition, 2005.

[Qin and Badgwell, 2003] S. J. Qin and T. A. Badgwell. A survey of industrial model predictive control technology. *Control Engineering Practice*, 11:733 – 746, 2003.

[Rajamani and Rawlings, 2007] M. R. Rajamani and J. B. Rawlings. Estimation of the disturbance structure from data using semidefinite programming and optimal weighting. *Automatica*, 2007. to be published.

[Rajamani, 2007] M. R. Rajamani. *Data-based Techniques to Improve State Estimation in Model Predictive Control*. PhD thesis, University of Wisconsin, Madison, 2007.

[Rao and Rawlings, 1999] C .V. Rao and J. B. Rawlings. Steady states and constraints in model predictive control. *AIChE Journal*, 45(6):1266 – 1278, 1999.

[Rao and Rawlings, 2000] C. V. Rao and J. B. Rawlings. *Nonlinear Moving Horizon State Estimation*. Nonlinear Model Predictive Control. Birkhauser, Basel, 2000.

[Rao and Rawlings, 2002] C. V. Rao and J. B. Rawlings. Constrained process monitoring: Moving-horizon approach. *AIChE Journal*, 48(1):97 – 109, 2002.

[Rao, 2000] C. V. Rao. *Moving Horizon Strategies for the constrained Monitoring and Control of Nonlinear Discrete-Time Systems*. PhD thesis, University of Wisconsin-Madison, United States, 2000.

[Rawlings and Muske, 1993] J. B. Rawlings and K. R. Muske. The stability of constrained receding horizon control. *IEEE Transactions on Automatic Control*, 38(10):1512–1516, 1993.

[Rawlings, 2000] J. B. Rawlings. *Tutorial Overview of Model Predictive Control*. Special section, Industrial Process Control. IEEE Control Systems Magazine, 2000.

[Richalet *et al.*, 1978] J. Richalet, A. Rault, J. L. Testud, and J. Papon. Model pedictive heuristic control: application to industrial processes. *Automatica*, 14:413 – 428, 1978.

[Riederer *et al.*, 2002] P. Riederer, D. Marchio, J. C. Visier, A. Husaunndee, and R. Lahrech. Room thermal modelling adapted to the test of hvac control systems. *Building and Environment*, 37:777 – 790, 2002.

[Rinaldo *et al.*, 2000] D. Rinaldo, J. Le Dividich, and J. Noblet. Adverse effects of tropical climate on voluntary feed intake and performance of growing pigs. *Livestock Production Science*, 66:223 – 234, 2000.

[Robertson *et al.*, 1996] D. G. Robertson, J. H. Lee, and J. B. Rawlings. A moving horizon-based approach for least-squares estimation. *AIChE Journal*, 42(8):2209 – 2224, 1996.

[Rossiter, 2003] J. A. Rossiter. *Model-based Predictive Control, A Practical Approach*. CRC Press, Florida, 2003.

[Schauberger *et al.*, 2000] G. Schauberger, M. Piringer, and E. Petz. Steady-state balance model to calculate the indoor climate of livestock buildings, demonstrated for finishing pigs. *International Journal of Biometerorology*, 43:154 – 162, 2000.

[Scokaert and Rawlings, 1998] P. O. M. Scokaert and J. B. Rawlings. Constrained linear quadrautic regulation. *IEEE Transaction on Automatic Control*, 43:1163 – 1169, 1998.

[Scokaert and Rawlings, 1999] P. O. M. Scokaert and J. B. Rawlings. Feasibility issues in linear model predictive control. *AIChE Journal*, 45:1649 – 1659, 1999.

[Scokaert, 1997] P. O. M. Scokaert. Infinite horizon generalized predictive control. *International Journal of Control*, 66:161 – 175, 1997.

[Skogestad and Postlethwaite, 1996] S. Skogestad and I. Postlethwaite. *Multivariable Feedback Control: Analysis and Design*. New York: Wiley, 1996.

[Sohn and Small, 1999] M. D. Sohn and M. J. Small. Parameter estimation of unknown air exchange rates and effective mixing volumes from tracer gas measurements for complex multizone indoor air models. *Journal of Building and Environment*, 34:293 – 303, 1999.

[Soldatos *et al.*, 2005] A. G. Soldatos, K. G. Arvanities, P. I. Daskalov, G. D. Pasgianos, and N. A. Sigrimis. Nonlinear robust temperature-humidity control in livestock buildings. *Journal of Computers and Electronics in Agriculture*, 49:357 – 376, 2005.

[Svidt and Bjerg, 1996] K. Svidt and B. Bjerg. Computer prediction of air quality in livestock buildings. *Department of Building Technology and Structure Engineering, Aalborg University*, 1996.

[Svidt *et al.*, 1998] K. Svidt, G. Zhang, and B. Bjerg. Cfd simulation of air velocity distribution in occupied livestock buildings. *Department of Building Technology and Structure Engineering, Aalborg University*, 1998.

[Tauson *et al.*, 1998] A. H. Tauson, A. Chwaliborg, J. Ludvigsen andK. Jakobsen, and G. Throbek. Effect of short-term exposure to high ambient temperatures on gas exchange and heat production in boars of different breeds. *Animal Science*, 66:431 – 440, 1998.

[Taylor *et al.*, 2004] C. J. Taylor, P. Leigh, L. Price, P .C. Young, E. Vranken, and D. Berckmans. Proportional-integral-plus (pip) control of ventilation rate in agricultureal buildings. *Control Engineering Practice*, 12:225 – 233, 2004.

[Tchamitchian and Tantau, 1996] M. Tchamitchian and H. J. Tantau. Optimal control of the daily greenhouse climate: physical approach. In *Proceeding of IFAC 13th Triennial World Congress*, San Franciscon, USA, 1996.

[Tenny and Rawlings, 2002] M. J. Tenny and J. B. Rawlings. Efficient moving horizon estimation and nonlinear model predictive control. In *Proceedings of the American Control Conference*, pages 4475 – 4480, Ancorage, 2002.

[Tenny, 2002] M. J. Tenny. *Computational Strategies for Nonlinear Model Predictive Control*. PhD thesis, University of Wisconsin, Madison, 2002.

[Timmons *et al.*, 1995] M. B. Timmons, R. S. Gates, R. W. Bottcher, T. A. Carter, J. Brake, and M. J. Wineland. Simulation analysis of a ne temperature control method for poultry housing. *Journal of Agricultural Engineering Research*, 62:237 – 245, 1995.

[Wachenfelt *et al.*, 2001] E. V. Wachenfelt, S. Pedersen, and G. Gustafsson. Release of heat, moisture and carbon dioxide in an aviary system for laying hens. *British Poultry Science*, 42:171 – 179, 2001.

[Wagenberg *et al.*, 2005] A. V. Van Wagenberg, J. M. Aerts, A. Van Brecht, E. Vranken, T. Leroy, and D. Berckmans. Climate control based on temperature measurement in the animal-occupied zone of a pig room with ground channel ventilation. *Transactions of the ASAE*, 48(1):355 – 365, 2005.

[Wu *et al.*, 2005] Z. Wu, P. Heiselberg, and J. Stoustrup. Modeling and control of livestock ventilation systems and indoor environments. In *26th AIVC Conference on Ventilation in Relation to the Energy Perofrmance of Buildings*, pages 335 – 340, Brussels, Belgium, September 2005. International Energy Agency, Air Infiltration and Ventilation Center, Operating Agent and Management, INIVE EEIG.

[Wu *et al.*, 2006] Z. Wu, M. R. Rajamani, J. B. Rawlings, and J. Stoustrup. Model predictive control of the hybrid ventilation for livestock. In *Proceedings of 45th IEEE Conference on Decision and Control*, pages 1460 – 1465, San Diego, United States, December 2006.

[Wu *et al.*, 2007a] Z. Wu, M. R. Rajamani, J. B. Rawlings, and J. Stoustrup. Application of autocovariance least - squares method for model predictive control of hybrid ventilation in livestock stable. In *Proceedings of 26th IEEE American Control Conference*, pages 3630 – 3635, New York, United States, June 2007.

[Wu *et al.*, 2007b] Z. Wu, M. R. Rajamani, J. B. Rawlings, and J. Stoustrup. Model predictive control of thermal comfort and indoor air quality in livestock stable. In *Proceedings of IEEE European Control Conference*, pages 4746 – 4751, Kos, Greece, July 2007.

[Wu *et al.*, 2008a] Z. Wu, J. Stoustrup, and P. Heiselberg. Parameter estimation of dynamic multizone models for livestock indoor climate control. In *29th AIVC Conference on advanced building ventilation and environmental technology for addressing climate change issues*, Kyoto, Japan, October 2008. International Energy Agency, Air Infiltration and Ventilation Center, Operating Agent and Management, INIVE EEIG.

[Wu *et al.*, 2008b] Z. Wu, J. Stoustrup, and J. B. Joerngensen. Moving horizon estimation and control of livestock ventilation systems and indoor climate. In *Proceedings of 17th Triennial Event of International Federation of Automatic Control World Congress*, Seoul, Korea, July 2008.

BIBLIOGRAPHY

[Xin, 1999] H. Xin. Assessing swine thermal comfort by image analysis of postural behaviors. *American Society of Animal Science and American Dairy Science Association*, 1999.

[Y. Zhang, 1992] S. Sokhansanj Y. Zhang, E. M. Barber. A model of the dynamic thermal environment in livestock buildings. *Journal of Agricultural Engineering Researcj*, 53:103 – 122, 1992.

[Young *et al.*, 2000] P. C. Young, L. Price, D. Berckmans, and K. Janssens. Recent developments in the modelling of imperfectly mixed airspaces. *Computers and Electronics in Agriculture*, 26:239 – 254, 2000.

[Zhang and Barber, 1995] Y. Zhang and E. M. Barber. An evaluation of heating and ventilation control strategies for livestock buildings. *Journal of Agricultural Engineering Research*, 60:217 – 225, 1995.